UNIVERSITY OF BIRMINGHAM

Interlocked Structures

Based on H-bonded Barbiturate Complexes

Peter James Thornton

A thesis submitted to the University of Birmingham for the degree of Doctor of Philosophy

School of Chemistry

College of Engineering and Physical Sciences

The University of Birmingham

October 2014

Abstract

The work contained within this thesis concerns the synthesis and characterisation of novel [2]-rotaxanes, mediated via H-bonded templation. The template in question is based upon the barbiturate receptor as developed by A. D. Hamilton which up until now had not been utilised in the synthesis of interlocked structures.

The initial approaches centred on the use of long appendages of the barbiturate towards a threading, and subsequent clipping approach; however a lack of initial threading event prevented formation of the pseudorotaxane. In an attempt to overcome these difficulties, the synthesis of more rigid, dumbbell-barbiturates, were applied towards a receptor-based clipping approach, but the steric bulk acquired from the rigid spacer groups appeared to hinder any cyclisation.

To overcome the problem of threading, shorter appendages were utilised and the threading was observed via a crystal structure of the complex. Subsequent stoppering of the azide-terminated appendages in a CuAAC reaction afforded the first Hamilton Receptor based [2]-rotaxane. Further studies involving bichromophoric, anthracene-terminated receptors were then utilised with these barbiturate guests in the synthesis of a [2]-rotaxane via a novel light-induced photodimerisation.

Acknowledgements

Firstly I would like to thank my supervisor, Prof James H.R. Tucker, for not only giving me the opportunity to undertake this project, but also for his fantastic support and guidance throughout. A very big thank you to our collaborators Dr N McClenaghan and Arnuad Tron in Bordeaux for their help, guidance and work towards this project. It really wouldn't have been possible without them.

I would like to thank all past and present members of the Tucker group, especially Huy for his constant support over the 5 years we've worked together. The group really are an outstanding group of people and I feel privileged to have worked alongside them. I wish them all the very best in their future careers.

A special thank you to Neil spencer and all the analytical and support staff here at the University who have done a fantastic job throughout my time here and have made this thesis possible.

Throughout my PhD, I would not have been able to achieve anything were it not for the unending support of my friends and family. So a special thank you to Mom, Dad, Roz and my extended family. Thanks also to my grandparents for all their support and especially to my Nan, who unfortunately was unable to see me finish. Thanks to all my friends here at Birmingham, both in and out of Uni and to EYP – past and present members. A special thank you to Mr Bill, who kept me going through the trickiest of times and a final, and very special thank you to my girlfriend Jaz, for her eternal faith in me and for making the past three years my happiest so far.

Table of Contents

List of Abbreviations

A	Absorption
A	Hydrogen bond acceptor
alk	Alkyl
Anth	Anthracene singals (NMR spectra)
aq.	Aqueous
Ar	Aromatic
br.	In NMR spectra: broad peak
C	Concentration, $moldm^{-3}$
CuAAC	Copper catalysed azide alkyne cycloaddition
d	In NMR spectra: doublet peak
δ( )	Chemical shift, ppm
D	Hydrogen bond donor
DCM	Dichloromethane
DMAP	*N,N*-Diisopropylethylamine
DMF	*N,N*-Dimethylformamide
DMSO	Dimethyl Sulfoxide
$ES^{+/-}$	Electrospray mass spectrometry (+ve or –ve mode)
G	Guest
H	Host
H:G	Host guest complex
hh	head to head (anthracene dimer)
ht	head to tail (anthracene dimer)
IR	Infrared Spectrometry; infrared spectrum
J	Coupling constant, Hz
K	Binding Constant

λ	Wavelength, nm
$\lambda\nu_x$	photon of x nm
m	In NMR spectra: multiplet
M	Molar, $mol.L^{-1}$
mp	melting point
ν	wave number, cm^{-1}
NMR	Nuclear magnetic resonance spectroscopy
PMB	paramethoxy benzyl
ppm	Part per million
pyr	pyridine signals (NMR spectra)
q	In NMR spectra: quadruplet
quint.	In NMR spectra: quintuplet
s	In NMR spectra: singlet
t	In NMR spectra: triplet
TBAF	Tetra-n-butylammonium flouride
THF	Tetrahydrofuran
UV-Vis	UV-Visible spectrometry

1. Introduction

1.1 Supramolecular chemistry

Supramolecular chemistry is a field best described by Nobel Laureate J-M Lehn as *'chemistry beyond the molecule'*.[1] This neatly ties in the concept that supramolecular chemistry is not concerned with the classical bonds of chemistry, but rather the intermolecular forces *between* the covalent molecules themselves. The concepts of supramolecular chemistry, or more specifically the host-guest interaction, were first described by Hermann Emil Fischer in 1894. He proposed the enzyme-substrate interaction being one of molecular recognition, where the substrate (guest) and enzyme (host) have a complementary size match. He coined the phrase 'lock and key' to emphasise the specificity and complementarity of these interactions, stabilised by intermolecular forces such as electrostatics, hydrogen bonding and π-π stacking. Aside from the enzyme-substrate interaction, other biological phenomena which exemplify the concepts of supramolecular chemistry include protein folding, and DNA helices, displaying the properties of preorganisation, recognition and reversibility.

The natural world has had time on its side to enhance and modify supramolecular interactions to provide powerful biological catalysts for numerous functions within the metabolic processes of life. Chemists on the other hand, have had to probe and elucidate these interactions in order to recreate them in the laboratory. It is not surprising therefore, that supramolecular chemistry has had a heavy biological influence in terms of inspiration and emulation. With the discovery and description of the hydrogen bond in the early 20th

century, chemists were developing the knowledge to be able to understand these intermolecular interactions at the molecular level, but it was not until the 1960's that synthetic supramolecular chemistry first emerged. Since then it has seen vast growth in terms of the templates, motifs and architectures available, with a growing wealth of real-world applications.

In its simplest form, supramolecular chemistry may be regarded as *host-guest chemistry*, a process of *molecular recognition*, resulting in the formation of a *supramolecular complex*, as demonstrated in **Figure 1.1**. As observed in enzymes, the guest substrate is bound to the cavity via intermolecular bonds in a complementary fashion and chemists have found many varied motifs employing this lock (H) and key (G) interaction. The interaction is a reversible one, with the thermodynamics of binding determined by the strengths and number of interactions present.[2] Attachment of various reporter groups to these host species can result in supramolecular devices.

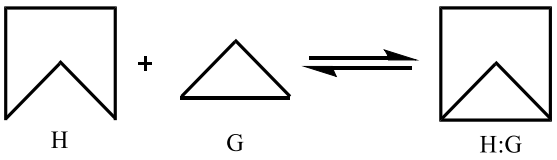

Figure 1.1 – Formation of a Host:Guest (H:G) complex from its substituents.

A fundamental aspect of supramolecular chemistry is that of *preorganisation* and *self-assembly* and these were demonstrated in the first examples of simple supramolecular architectures, given by Charles John Pedersen[3] (and earning him recognition through the award of a Nobel prize in 1987 along with Jean-Marie Lehn and Donald J. Cram). He reported the synthesis of cyclic polyethers without the use of high dilution techniques.

These compounds were made by exploiting the host-guest interaction between the cyclic polyether and a group 1 metal cation. The metal cation is stabilised within the ring via ion-dipole interactions between the metal cation and oxygen atoms of the ring and it is this interaction that allows the polyether chain to adopt the conformations required for cyclisation, as shown in **Figure 1.2**. This concept gives rise to what is known as known as the *macrocyclic effect*.

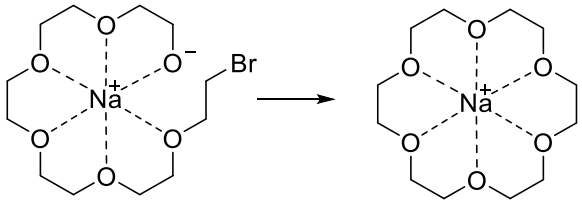

Figure 1.2 – Demonstration of the *Macrocyclic Effect* from a H:G interaction.

1.1.1 Intermolecular Forces

Due to the fact that supramolecular chemistry is concerned with intermolecular interactions 'beyond the molecule', classical covalent and ionic bonds are not necessarily observed. What are present between molecules are a series of non-covalent interactions of varying strengths, depending on the functional groups and substituents present between two or more interacting species. These interactions can be subdivided into five groups, in order of their relative strengths; electrostatics, H-Bonding, π-π interactions, van der Waals forces and hydrophobic/solvatophobic effects. Bearing in mind that typical covalent bonds are of the order of 300-900 $kJmol^{-1}$, these interactions are somewhat weaker and in some cases considerably so. However, when added together over entire arrays, relatively stable structures may be formed.

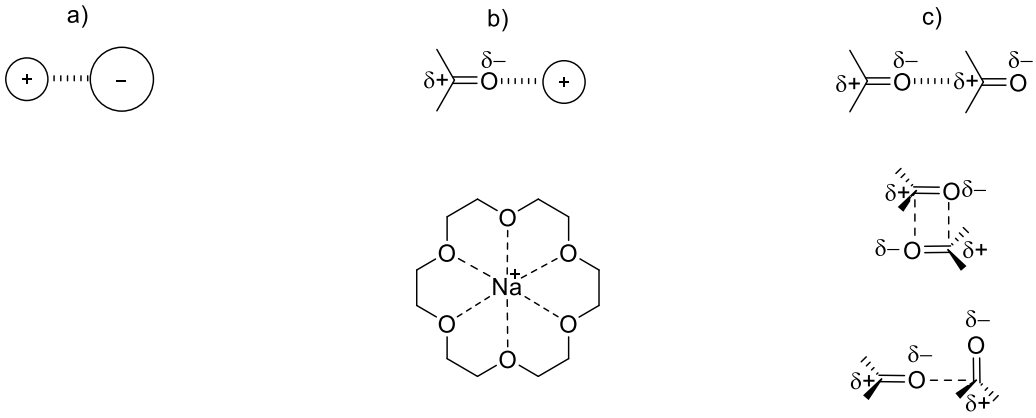

Figure 1.3 - Electrostatic interactions of ion-ion (a), ion-dipole (b) and dipole-dipole (c).

Electrostatic interactions arise due to the close proximity of formal or partial charges and are summarised in **Figure 1.3**. These include ion-ion interactions (a) (an ionic bond), ion-dipole (50-200 kJmol^{-1}) and dipole-dipole (5-50 kJmol^{-1}) interactions.[4] Due to their relative strengths, they can be applied towards the design of supramolecular architectures and have seen widespread use. Ion-dipole interactions (b) have been utilised in supramolecular structures such as the crown ether complexes for the encapsulation of group 1 and 2 metal cations as described above. The dipoles present are a direct result of an imbalance of charge in a bond due to the relative electronegativities of the atoms present. In such complexes, the lone pairs of the oxygen donor atoms are attracted to the positive charge of the metal cation. Application of this concept has resulted in the development of a whole host of supramolecular sensors, devices and logic gates based on crown ethers. Dipole-dipole interactions, such as those between carbonyl compounds (c), despite a degree of directionality, are generally weaker than ion-dipole interactions and are easily overcome in solution.

Hydrogen bonding (4-120 kJmol^{-1})[4] may be considered as a specific type of dipole-dipole interaction. The nature of an H-bond is determined by electrostatics, repulsive and dispersion forces, induced dipoles as well charge transfer and typically involves an interaction between a hydrogen atom attached to an electronegative atom (the donor, **D**) and another electronegative atom (the acceptor, **A**). This arises due to the electronegative nature of the donor atom, whereby electron density is withdrawn from the hydrogen atom, creating a relatively large positive charge density.[2] This is attracted to a lone pair belonging to an atom of a nearby molecule, resulting in a relatively strong and highly directional interaction, shown in **Figure 1.4.a**.

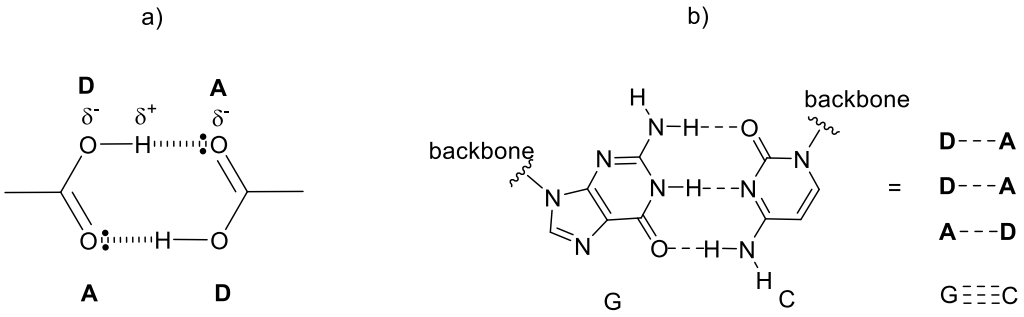

Figure 1.4 – An example of H-bonding (a) and complementary base-pairing of C and G bases in DNA (b).

Due to its high level of directionality and absence of any formal charges, H-bonding has seen extensive use in natural and synthetic supramolecular structures, with the most widely known being the base pairing of DNA, a G-C base pair is shown in **Figure 1.4.b**. As mentioned previously, the interactions alone are relatively weak; however, they experience a cumulative effect when present throughout the whole DNA strand, which results in a highly ordered and stable structure. H-bonding also plays a significant role in protein folding.

When designing H-bonding supramolecular structures, aside from the donor-acceptor arrays already discussed, it is important to consider the secondary effects of H-bonding. This concept was developed through computational studies carried out by Jorgensen and Pranata[5] in their study of triply hydrogen bonded complexes, **Figure 1.5**.

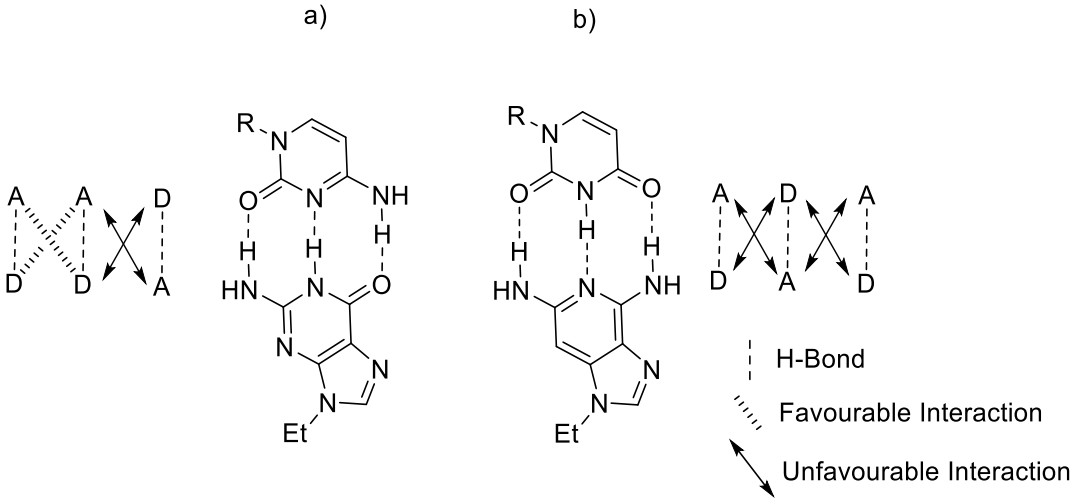

Figure 1.5 – Examples of secondary effects present in H-bonding structures.

The two component complexes in question have identical H-bonding motifs in terms of their donor and acceptor parts, (two NH--OC and one NH--N H-bonds) but their association constants differ considerably. The association constant of complex (a) was found to be 10^4-10^5 M^{-1} in $CHCl_3$, whereas complex (b) in $CHCl_3$ was found to be only 170 M^{-1}.[6] This variation was attributed to the arrangement of the three H-bonds present. In an H-bonding array, centres of like charge repel and as such ADA-DAD complexes experience unfavourable secondary interactions, and so considering the structures above, (a) contains an extra favourable interaction with respect to (b) which results in a stronger binding constant.

π-π stacking occurs between systems containing aromatic rings, with the two most stable forms being either face-to-face (parallel displaced) or edge-to-face, **Figure 1.6**. The

interactions arise due to the inherent quadropole moment present within benzene rings. Due to the delocalisation of charge and arrangement of orbitals, there is a negative charge above and below the plane of the ring and by adopting a parallel or T-shaped configuration, unfavourable interactions are minimised.[4]

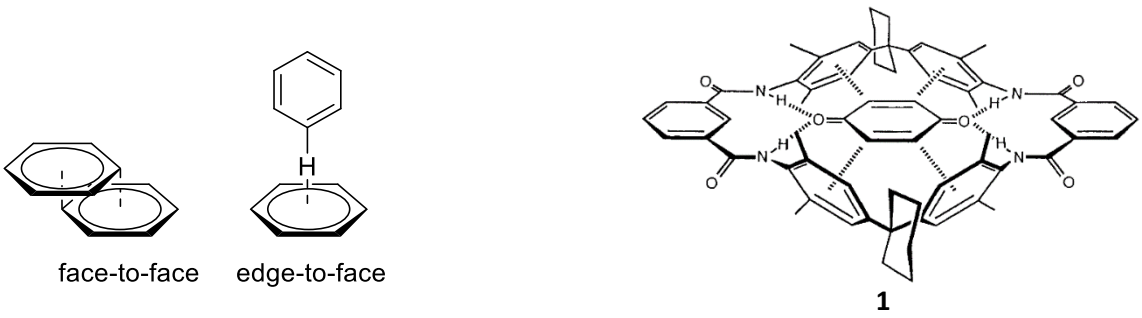

Figure 1.6 – Common forms of π-π stacking and a supramolecular host, **1**, bearing π-π stacking stabilisations encapsulating benzoquinone.[7]

These interactions have been employed in the use of receptor **1** towards the recognition of benzoquinone by Hunter, in an attempt to mimic the features of quinone binding domains in bacterial photosynthetic reaction centres.[7] The receptor binds benzoquinone via 4 H-bonds, but the binding is enhanced upon by the presence of π-π interactions.

Hydrophobic/solvatophobic effects may not necessarily be considered interactions per se, but more of a 'driving force' towards the association of apolar components in aqueous media or vice-versa. There are entropic and enthalpic components present in this association which should be addressed. For example, in the case of calix[n]arenes, a hydrophobic pocket is present within the internal walls of the molecular cyclinder. An entropic driving force exists whereby small organic molecules will sit within the cavity, excluding water molecules and increasing the entropy of the system. The enthalpic term

arises from the stabilisation of water molecules originally within the cavity. Once free from the relatively poor polar-apolar interactions within the cavity, the water molecules are able to re-establish H-bonding with the bulk solvent and as a result, their overall energy and that of the system is reduced.[4] As well as this, there are also additional van der Waals and π-π stacking interactions experienced by the encapsulated molecule, which serve to lower the energy. This was first demonstrated by Koga et al.[8] with the encapsulation of durene in a cyclophane receptor, **2**, in acidic aqueous media, shown in **Figure 1.7**.

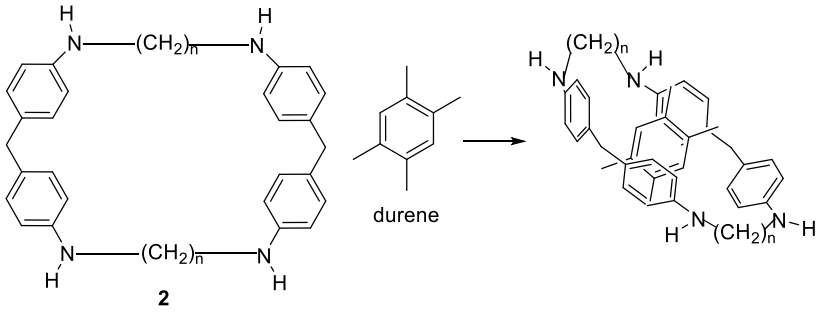

Figure 1.7 – Encapsulation of durene within an apolar cavity.

The final interaction to be considered, although not strictly supramolecular, is the *coordinate* or *dative bond*, where an electron pair is donated from a ligand to a metal centre. Despite this technically being a covalent bond, this concept sees wide use in supramolecular chemistry due to its reversibility and its application in the formation of self-assembled structures. The precise geometries of the metal centre/complex, and the reversibility of the assembly processes have given rise to the formation of some elaborate molecular topologies.

1.1.2 Design of neutral guest binders

In the design of neutral guest binders there are certain factors to consider including the optimal functional groups for binding, the spatial requirements and rigidity vs flexibility of the host/guest. As discussed previously, the most critical aspect is one of a size-match complementarity. The example shown in **Figure 1.8,** developed by Hamilton and co-workers, is a relatively simple motif, **3**, displaying H-bond mediated 'recognition' of glutaric acid.[9] Noting the presence of unfavourable secondary interactions, the amidopyridine motif was replaced by a urea motif, **4**, resulting in a marked increase in the binding constant, with the H:G complex stable even in highly competitive solvents.[10]

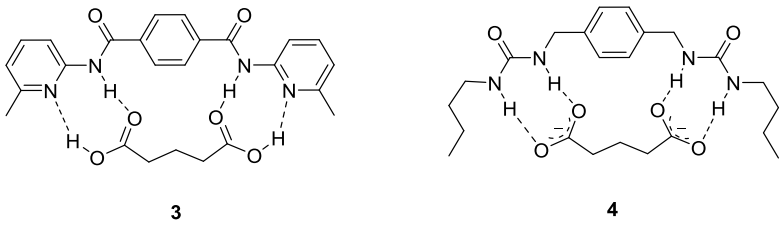

Figure 1.8 – Optimisation of binding through functional group changes.

Highlighting the importance of a size-match fit is the exemplary example shown by Julius Rebek.[11] Shown below in **Figure 1.9** are two highly selective receptors for diketopipirazines and barbiturates. In the case of **5**, the dilactam receptor forms a complex with cyclo(L-leucine)$_2$, which showed a >2.5 kcalmol^{-1} higher stability than its enantiomer. The meso form of the receptor, **6**, showed selectivity for barbiturates but the corresponding diimide receptors showed no selectivity for either guest species.

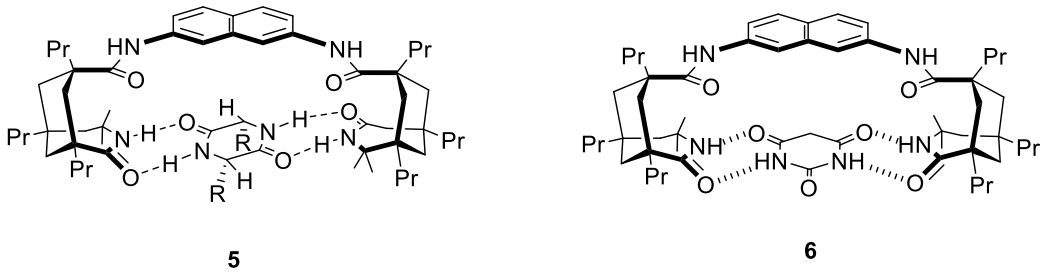

5 **6**

Figure 1.9 – Structurally similar receptors for diketopipirazines (**5**) and barbiturates (**6**).

The concept of a preorganisation effect was also highlighted by the same group through the synthesis of molecular clefts, **Figure 1.10**. By incorporating intramolecular H-bonds, the primary structure of **7** adopted is one suitable for binding, requiring no further organisation of the molecule. This is analogous to the secondary structure adopted by proteins in positioning their functional groups for optimal substrate binding.

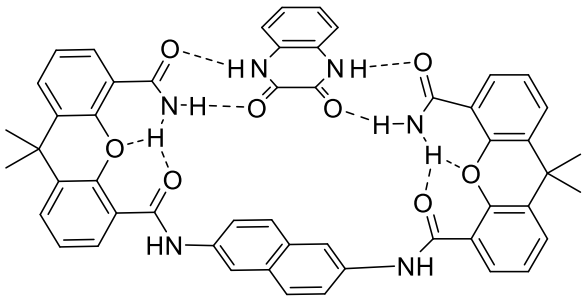

7

Figure 1.10 – Preorganisation of binding sites used to enhance binding.

1.2 Interlocked Structures

1.2.1 History, Nomenclature and Approaches

Synonymous with the field of supramolecular chemistry is that of interlocked structures. By definition, these are structures which consist of two or more independent components which are not connected via classical chemical bonds, but instead are bound via a

'mechanical bond'. This means that the components cannot be separated without breaking a covalent bond. Classical examples include rotaxanes, catenanes and knots, the former of which is the basis of this thesis. The name rotaxane comes from the latin words *rota*, meaning wheel and *axis*, meaning axle, and was first proposed by Schill and Zollkopf.[12] A rotaxane consists of at least one threaded macrocycle around an axle, with large stopper groups capping the end and preventing dissociation of the macrocycle. The word catenane derives from the latin word *caten*a, meaning chain, and are structures consisting of two interlocked molecular rings which cannot be separated without breaking either ring, analogous to chain links. The simplest structures of both forms of interlocked structures are shown below in **Figure 1.11**.

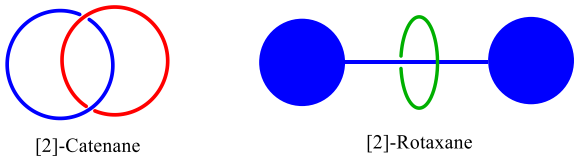

Figure 1.11 – Simplest topologies of classic catenanes and rotaxanes.

The nomenclature surrounding interlocked structures is fairly trivial, with the schematic diagrams above showing the simplest topologies of two interlocked components. The number in square brackets denotes the number of interlocked components present within the structure and a selection of other topologies are demonstrated in **Figure 1.12**.

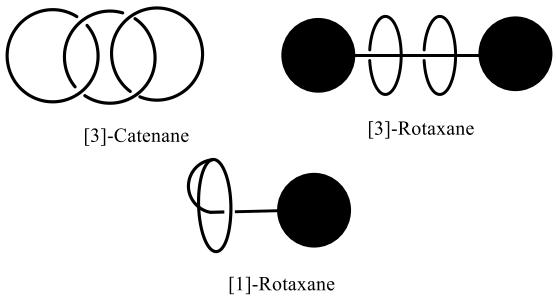

Figure 1.12 – More elaborate topologies of interlocked structures.

Catenanes were the first interlocked structures to be proposed as far back as 1912, but it wasn't until 1960 that the first catenane was able to be synthesised, as reported by by E. Wasserman.[13] He highlighted that the limitations of what could be achieved were down to the synthetic tools and protocols available. The catenane, **8,** shown in **Figure 1.13**, relied on a statistical synthetic approach for its formation, in that the acyclic component was observed to thread through the macrocycle and cyclise purely by chance, with the process not mediated/preorganised by any intermolecular interaction.

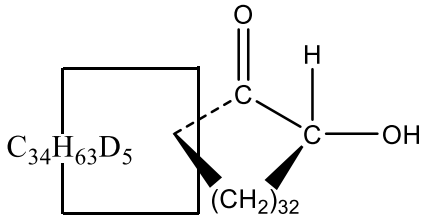

8

Figure 1.13 – The first characterised catenane produced via a statistical approach.

Diethyl tetratriacontanedioate was first cyclised and subsequently reduced using zinc with deuterated HCl. The cyclisation was again carried out, but this time in the presence of the reduced deuterated macrocycle. Once purified, the fraction containing the acyloin ring was observed to contain C-D stretches in its I.R. spectrum, indicating the presence of the interlocked deuterated macrocycle. A statistical approach essentially relies on the

probability of the linear molecule penetrating the macrocycle and then being cyclised itself, trapping the catenane. The yields for the catenane were therefore very low, far less than 1%, so improved strategies were required. The concept of threading using a statistical approach was then demonstrated in the synthesis of the first rotaxane, by Harrison and Harrison in 1967 using resin bound macrocycles (**Figure 1.14**).[14]

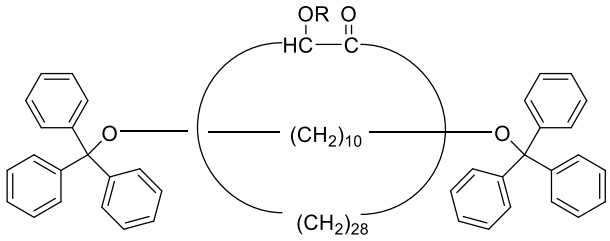

9

Figure 1.14 – Synthesis of a [2]-rotaxane via the use of resin bound macrocycles.

A directed-strategy was subsequently proposed by G. Schill and A. Luttringhaus.[15] Their method, shown in **Figure 1.15**, consisted of a 'directed synthesis' whereby through a careful connection/disconnection strategy, they used the central phenyl group as a scaffold on which to construct the catenane, **10**, over several synthetic steps.

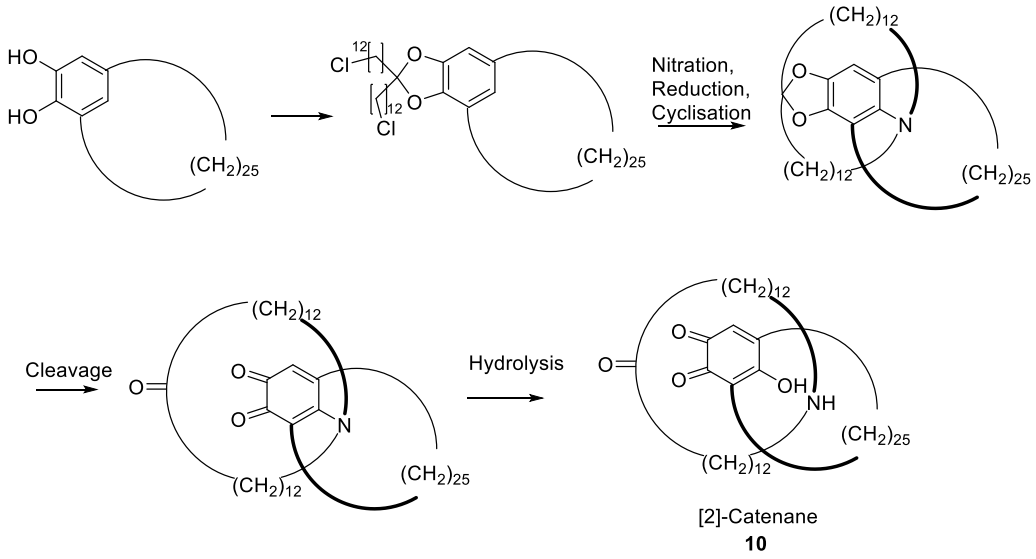

Figure 1.15 – Directed synthesis of a [2]-Catenane.

Despite improving upon the yields of Wasserman, this strategy involved up to 10 steps and it was not until the exploitation of supramolecular chemistry and the concept of pre-organisation that the synthesis of these interlocked structures could be realised in a few simple synthetic steps.

What followed on from these classical approaches was the application of supramolecular chemistry towards the formation of interlocked structures utilising metal ions,[16] donor-acceptor motifs,[17] and hydrophobic interactions.[18] This meant that there was no longer a need for rather convoluted syntheses or low probabilities of threading; instead the strategies employed the use of intermolecular interactions to pre-organise the components into the desired conformation for forming interlocked structures.[19]

In applying supramolecular approaches to the synthesis of rotaxanes, several methods for their synthesis can be found in the literature, as summarised in **Figure 1.16**.

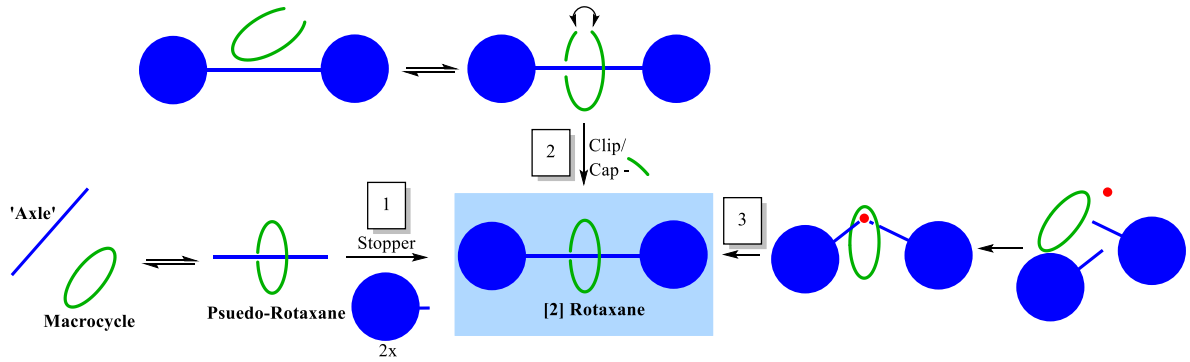

Figure 1.16 – Approaches towards rotaxane formation, showing stoppering (1), clipping (2) and active templation (3).

The first method shown, known as 'capping' or 'stoppering',[20] involves the formation of a pseudo-rotaxane where a linear molecule threads through the macrocycle, a process driven by favourable supramolecular interactions. Once the complex is formed, the macrocycle is mechanically trapped with appropriately sized stopper groups, preventing it from dissociating. The second is a 'clipping' approach and involves the use of a pre-stoppered thread.[21] Again utilising supramolecular interactions, the macrocycle precursor is assembled around the axle and then either clipped together or capped with a suitable reacting group to form the rotaxane. The third example shown is known as an 'active template' approach, a more recent development, first achieved by Leigh and co-workers,[22] and involves a metal centre that has a dual function. The metal centre is templated within the macrocycle via coordination, whereby the active site of catalysis is then located within the macrocycle itself. Any subsequent metal-catalysed bond formation between the two complementary stoppers then results in the formation of a rotaxane. Due to the nature and position of the bond forming process, with the stopper groups in excess, all the macrocycle molecules can be converted into the interlocked product, achieving very high yields over traditional approaches.

1.2.2 H-bond-Templated Interlocked Structures

Due to the nature of the work contained within this thesis, the primary focus of discussion relates to H-bonding and its use in the synthesis of interlocked architectures. As a route to pre-organisation, H-bonds offer very attractive attributes towards the synthesis of structures with well-defined geometries. Despite being relatively weak, they have enhanced directionality and specificity over some other intermolecular forces. Therefore out of the various template strategies available for the pre-organisation of host and guest components towards the formation of interlocked structures, H-bonding has found its own niche in the vast array of template directed synthesis.

1.2.2.1 Neutral Guests

The first example of the use of H-bonds in the templation towards interlocked structures was demonstrated by Hunter in 1992.[23] In attempts towards improving the yields of his recent benzoquinone receptor shown previously in **Figure 1.6**, a modified strategy was proposed which involved 'capping' towards a macrocycle rather than synthesis via high dilution. Due to the nature of the H-bonding groups present, the synthesis of a [2]-catenane by-product in 34 % yield was achieved. Later, the concept of H-bonding templation was applied towards the synthesis of rotaxanes by Vögtle et al. using these same receptors. Rather than capping an internalised unit as in the case shown by Hunter, the approach was to stopper a threaded and bound diisophthaloyl chloride component, resulting in a [2]-rotaxane. Extension of this work within the same group led to improvements of the threading moiety through the receptor using olefinic diacid dichloride as the template.[24] What was gained from this study was an understanding of how a dual stoppering event of a

threaded component is not necessarily the most facile route towards rotaxanes, and the stoppering of mono-stoppered, threaded complexes can be more efficient.

One of the most efficient and high yielding H-bond templates to date is the fumaramide system developed by the Leigh group,[25] which serves to highlight the importance of preorganisation (**Figure 1.17**). When comparing to the already reported peptide based binding motif, **11**,[26] the fumaramide site, **12**, has considerably less rotational degrees of freedom and as such, locks the binding site in a conformation ideal for macrocycle binding and subsequent clipping. Excellent yields of 97% were reported for the rotaxane, compared to the good yields of 30-60% obtained with peptide forms.

Due to the well-known chemistry and H-bonding geometry of benzylic amide macrocycles, as used in the examples above, they have been used to template around many different H-bond accepting motifs as shown in **Figure 1.17**. These include squarine complexes (**13**)[27], azodicarboxylates (**14**)[28] and phosphinic (**15**)[29] moieties.

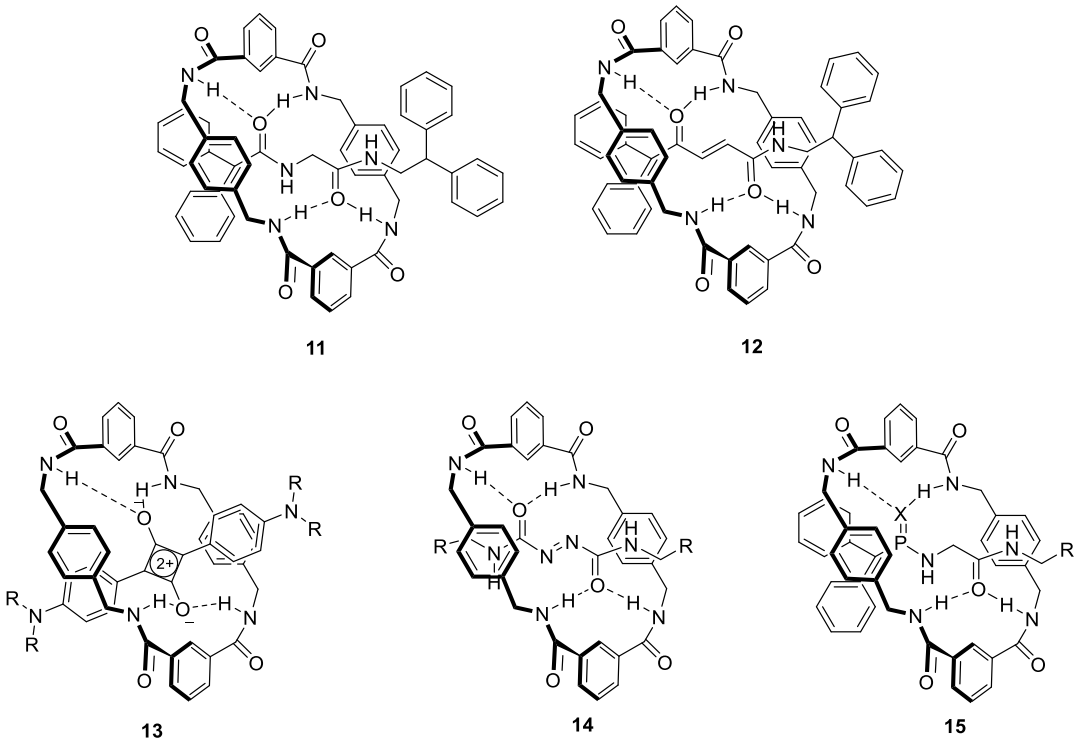

Figure 1.17 – A selection of H-bonded rotaxanes of benzylic-amide macrocycles bearing different functional binding groups.

1.2.2.2 Cationic Guests

Cationic H-bond template motifs include the combination of secondary dialkylammonium centres and crown ethers, which also utilise ion-dipole interactions, and were first used for the synthesis of rotaxane **16** in 1996 by Stoddart, **Figure 1.18**.[30]

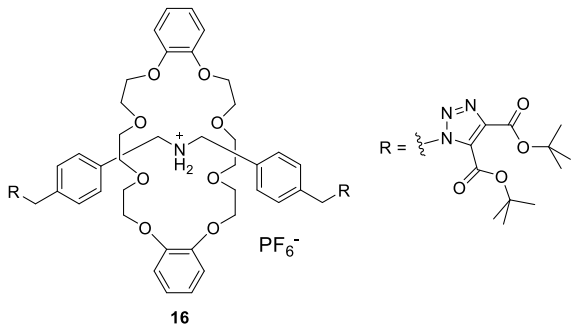

Figure 1.18 – Stoddart's dialkylammonium template rotaxane.

Interlocked structures bearing this binding unit have been synthesised via stoppering reactions,[31] pre-rotaxanes[32] and clipping,[33] and have also been used to achieve higher order, [3]-rotaxanes.[34]

1.2.2.3 Anionic Guests

Anion templation, stabilised through the use of H-bond donors has also found use within the templation of interlocked structures. The first example of this was displayed by Vögtle and co-workers and involved the templation of a phenolate anion using the isophtalamide-type macrocycles already shown in **Figure 1.6** and **Figure 1.17**.

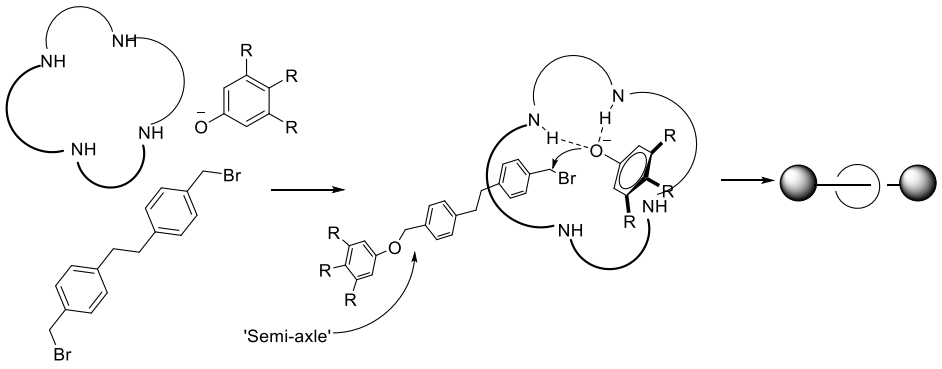

Scheme 1.1 - Vögtle's anion template rotaxane.

As shown in **Scheme 1.1**, initially the dibromide reacts to form a 'semi-axle'. This then reacts with the bound phenolate-macrocycle complex, acting as a supramolecular nucleophile. This method can produce rotaxanes in excellent yields of 95%. This method, whilst high yielding, does however involve reaction of the anionic template for the formation of a rotaxane, and therefore does not 'live on' in the interlocked structure. In order to probe the possible function of anion templation, such as that of sensing, the conservation of an anionic template is required.

The conservation of an anionic template was first demonstrated by the group of Paul Beer.[35] Aside from the H-bonding present, the motif in **Figure 1.19** also employs electrostatics from the pyridinium cation and a degree of π-π stacking to improve the efficacy of the template. Once the anion had templated the stoppered thread, the host could be cyclised via Grubbs' metathesis forming the [2]-rotaxane, **17**, in 47% yield. Anion exchange, followed by comparison studies between the pyridinium•PF_6 thread and the rotaxane•PF_6 showed the rotaxane to have enhanced selectivity towards chloride ions, clearly due to the binding site created between the diamide units of the macrocycle and thread within the rotaxane. Larger anions must either displace the pyridinium from the macrocycle or sit above the plane of the binding site, which in either case would weaken the binding interaction.

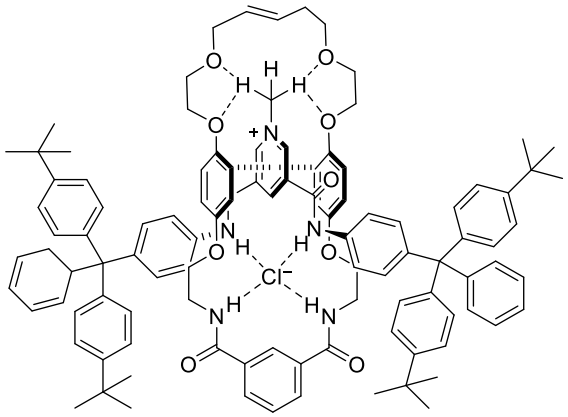

17

Figure 1.19 – Beer's anion template rotaxane.

1.2.2.4 Molecular Motion and Applications

With the methods for the synthesis of these topologically interesting structures developed, the advancement of their potential applications has also been investigated,

primarily focussing on the mimicry of components of machinery from the macroscopic world. One of the earliest examples was shown by Stoddart in the synthesis of switchable molecular shuttles,[36] and whilst not H-bonding in nature, the scope of concepts drawn from this example make it worthy of mention. Using their previously developed π-donor-acceptor motif of benzidine stations and cyclophane macrocycles, by extending the thread and incorporating a second station of biphenol, a two-station thread, **18**, was made as shown in **Figure 1.20**. At room temperature, the macrocycle moved between stations at a rate comparable to the NMR timescale and as such, only broad, indistinct signals are observed. However, upon cooling to 229 K, the macrocycle was observed to be located at either of the two distinct stations whereby station exchange was no longer comparable to the NMR timescale.

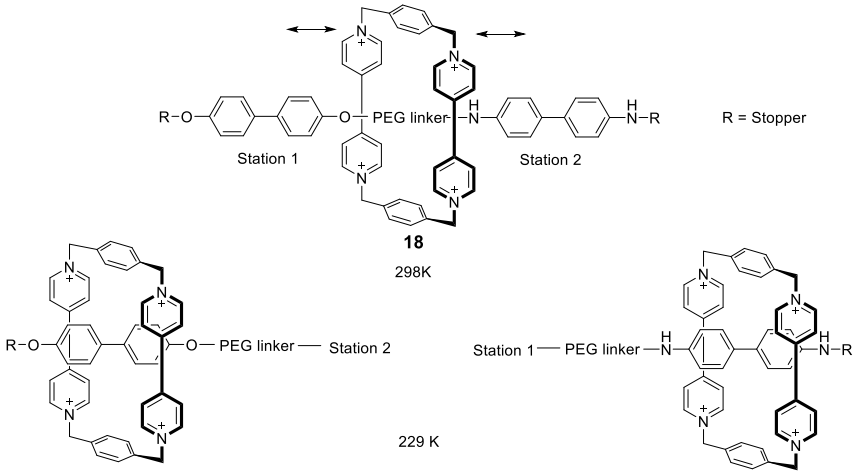

Figure 1.20 – Temperature dependent molecular shuttling based on biaryl stations.

The concept of shuttling has been extending to the realm of H-bonded interlocked structures and was first demonstrated by Leigh and co-workers[37] in a similar manner to that of Stoddart. By taking their already developed system of peptide-based H-bonding templates and applying a further station, they too were able to locate the H-bonding

benzylic amide macrocycle at both stations, as observed via variable temperature NMR experiments. They were also able to lock the macrocycle at one station through functionalisation of the thread to block translation, as shown in **Figure 1.21**.

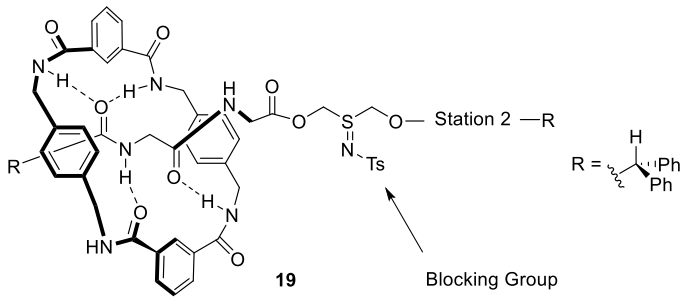

Figure 1.21 – Translational motion between stations is restricted by the NTs group.

Rather than rely on the temperature to control the location at a particular station, it is desirable to have an input such as light to drive the motion. As such, an event of controlled dynamic motion occurs where a particular station may be occupied following the application of a certain input or stimulus. Again, via the use of H-bonding, Leigh and co-workers were able to show fast and reversible translational motion of a molecular shuttle, **20**, via a photo-induced process, shown in **Figure 1.22**.[38]

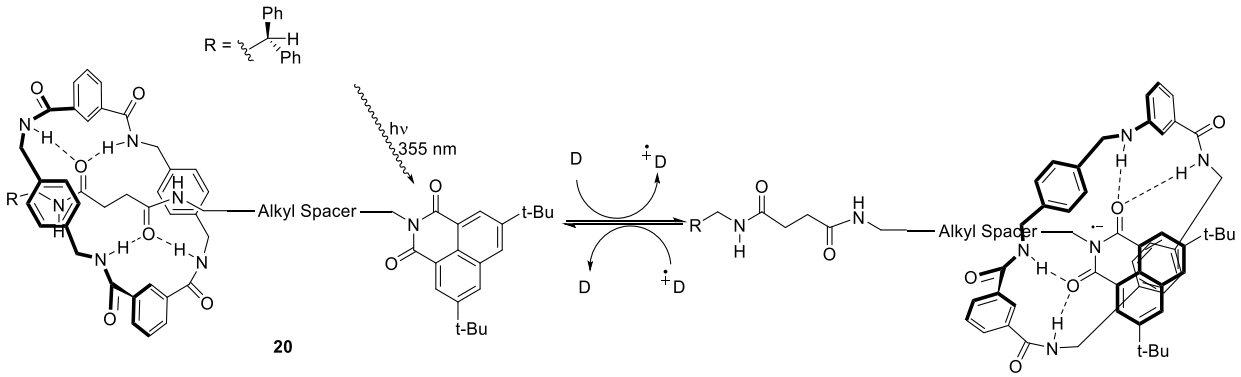

Figure 1.22 – Photo-induced molecular shuttling.

Prior to the 355 nm laser pulse, the shuttle is located at the succinamide station, due to the poor H-bonding nature of the napthalimide group. After photo-reduction of this unit

by an external donor, D, the napthalimide group becomes an excellent H-bond acceptor and the shuttle moves from one station to the other. This reversible shuttling process occurred at a rate of 10^4 times per second. Leigh and co-workers have also extended their H-bonded motifs towards pH controlled systems.[39]

The concept of using interlocked structures to perform various functions, employing the concept of bottom-up construction, has been shown recently in the transport of protons,[40] the synthesis of molecular lifts[41] and muscles,[42] as well as the sequence specific synthesis of small peptides[43] and applications in potential drug delivery using 'nano-valves'.[44]

1.3 Barbiturates

1.3.1 History, background and uses

The first and simplest of all barbiturates, barbituric acid, was synthesised in 1864 by the German chemist Adolf von Baeyer via the condensation of urea with diethyl malonate (**Scheme 1.2**). Being biologically inactive the long historical use of this family of compounds as a sedative was not fully realised until the synthesis of its derivative 5,5-diethylbarbituric acid, **21**, in 1884, and its subsequent discovery as an hypnotic in 1903 by Emil Fischer.[45] What followed was a vast array (more than 2500)[46] of substituted barbiturates classified according to their biological activity, ranging from short to long lasting effects, and finding use as anxiolytics, anticonvulsants, analgesics and hypnotics. A sample of various functionalised barbiturates, **22**-**24**, are shown in **Figure 1.23**, highlighting how various substitutions at the 5-5' position allows control of their activity. Due to their active dose

being relatively close to their overdose threshold and coupled with their addictive nature, barbiturates were phased out of clinical use in favour of benzodiazepines; however some still find use in medicine in the treatment of epilepsy and owing to their lethal properties, in lethal injections and euthanasia.

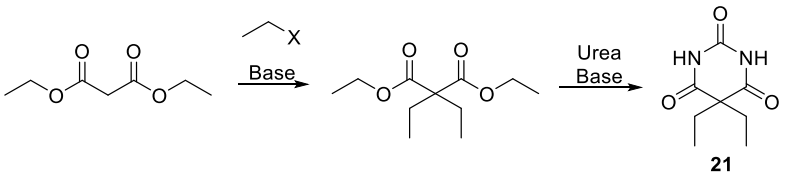

Scheme 1.2 – Classical synthesis of substituted barbiturates.

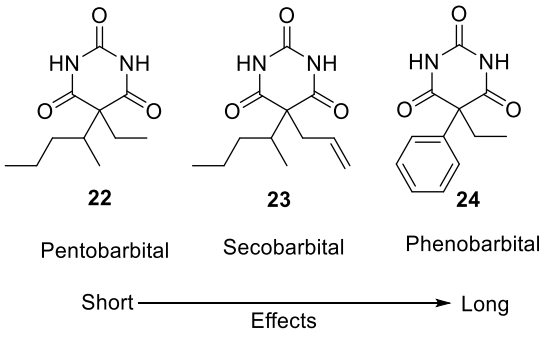

Figure 1.23 - Highlighting the difference in biological effect based on functionalisation.

Aside from their interesting biological activity, barbiturates also possess an interesting supramolecular property in that the symmetrical imide groups provide a H-bonding motif of the order ADA, which forms H-bonds with groups containing the corresponding DAD motif. This was first utilised by Feibush in the development of chiral separation protocols towards heterocyclic drugs by HPLC,[47] and involved the attachment of 2,6-diamino pyridine units to the stationary phase. The concept of complementarily binding barbital using artificial receptor molecules was then expanded upon by the Hamilton group.[48]

1.3.2 Hamilton receptors

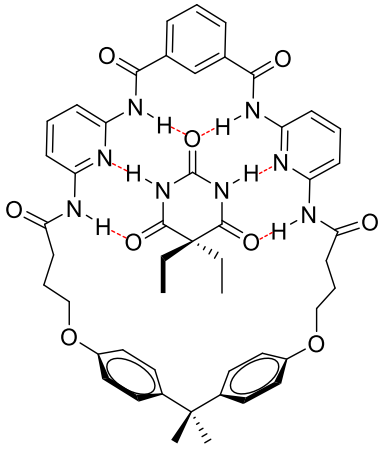

25:**21**

Figure 1.24 – Hamilton's receptor for barbiturates.

Shown in **Figure 1.24** is the barbiturate receptor, **25**, designed by Hamilton. The receptor comes in two parts, the main binding site, or 'bridge', and the variable lower unit linking the two terminal amines. Through the use of an appropriate isophthaloyl spacer, the two 2,6-diamino pyridine units form a binding cavity capable of binding barbital, **21**, via six complementary H-bonds. Binding is enhanced relative to acyclic receptors via cyclisation of the receptor due to the macrocyclic effect, shown by a 100 fold difference in binding constant. These receptors gave high binding constants to various barbiturate derivatives in non-competitive solvents, the highest of which was with barbital, with a value of 1.37×10^6 M^{-1} at 25^o C in $CDCl_3$.

1.3.3 Applications

Since the discovery of these highly successful barbiturate receptors, they have seen a number of applications. Known as the Pauling principle, enzyme catalysis depends upon substrate complexation and transition state stabilization and Hamilton applied these

concepts towards the construction of artificial enzymes. As a result Hamilton was able to display rate accelerations of phosphoryl-transfer reactions,[49] and was also able to mimic the action of protease enzymes.[50] An optimal proximity and position of the H-bonded barbiturate relative to a functionalised receptor was identified. By placing the nucleophile and substrate in the correct proximity and orientation, and thereby mimicking the transition state, a large acceleration in the rate of transacylation reactions was achieved. The analytical capabilities of these receptors was also demonstrated in the enhanced extraction of phenobarbital from a 20 μM phenobarbital solution in human control serum.[51] The group then went on to develop the receptor further, through the attachment of redox and photo-active chromophores, as shown in **Figure 1.25**.[52]

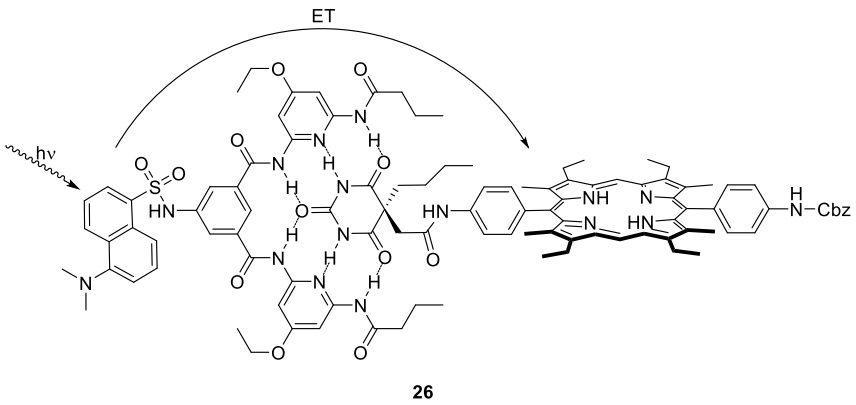

Figure 1.25 – ET via Barbiturate mediated binding.

Quenching of fluorescence was observed due to energy transfer to the H-bonded barbiturate group. This 'self-assembly' strategy was a general one, allowing for many choices in the chromophore components used. This family of photoreceptors and barbiturates were again used in an attempt to mimic the natural processes of the enzyme Cytochrome P450.[53]

Other groups have utilised the specificity of the Hamilton receptor in various ways. Building upon the analytical approach demonstrated by Hamilton, Li and co-workers were able to demonstrate micro-extractions of barbital and its derivatives using receptor doped films.[54] Later, the work of San-Qi Zhang demonstrated the use of receptors when bound to solid supports for applications of column chromatography.[55] The groups of Tucker and Bassani have used an anthracene tagged Hamilton receptor to demonstrate photo-switched binding.[56] The bridge of the receptor was functionalised at the 6-amino position with alkyl chains terminated with anthracene units. In the open form, the receptor bound barbital with a high binding constant. Upon anthracene dimerization, a head-to-tail photodimer was formed and this conformation impacted strongly on the binding site of the receptor. As can be seen in **Figure 1.26**, the ortho-xylene units protrude into the cavity and the 4 N-H bonds no longer point towards the centre of the cavity, due to the distortion of the macrocycle. The barbital was thus removed from the binding site upon formation of the photo-dimer and shows weak binding with the dimerised receptor. It should be noted that the binding is not fully inhibited when using longer alkyl chains, an important aspect with regards to this thesis.

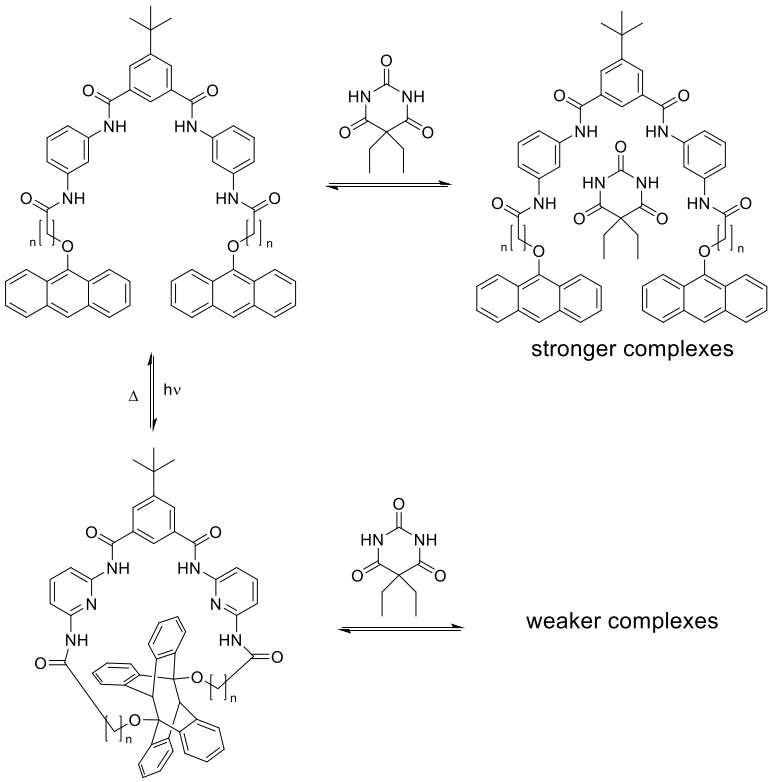

Figure 1.26 - Photo-switched binding of barbital using anthracene tagged Hamilton receptors.

1.4 Key Reactions

1.4.1 Grubbs Metathesis

Metathesis, derived from the greek word meaning 'change of position' has, over the past few decades, had a profound impact on synthetic organic chemistry. The first developments in the field came from the ring-opening metathesis polymerisation (ROMP) of norbornene via titanium catalysis[57] and was later developed upon, and extended to other cycloalkenes through the use of organometallic iridium and ruthenium compounds.[58] The history then moves through one of development, from multi, to single component catalytic systems and despite efforts to improve upon this family of catalysts, they still required harsh reaction conditions and showed limited functional group tolerance and sensitivity towards oxygen and moisture. The series showing the development of Grubbs' catalysts is

shown in **Figure 1.27**. With the advent of Grubbs' initial ruthenium akylidene complex ,**27** ,[59] which showed slightly reduced metathesis activity (relative to current ROMP catalysts of the time), but with improvements over functional group tolerance, the first synthetically useful ruthenium based metathesis catalyst, with regards to ring-opening metathesis polymerization of highly strained cyclic olefins was obtained. In order to gain further control over the utility of these catalysts with regards to other forms of metathesis, further modification of the ruthenium ligands was required. By substitution of the triphenylphosphine ligands with better σ-donating alkylphosphines, **28**, new and improved metathesis activity was accomplished and the first ruthenium complex active towards acyclic olefins was achieved.[60] The final modification of this complex towards establishing a catalyst with high activity came with the replacement of the vinylalkylidene, with a benzylidene ligand, **29**, to afford Grubbs' 1st generation catalyst.[61]

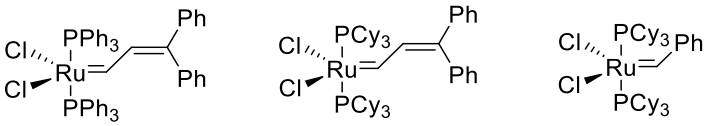

27 **28** **29**

Figure 1.27 – Development of ruthenium catalysts towards Grubbs' 1st gen. catalyst, **29**.

There are three main types of metathesis reaction, as summarised in **Figure 1.28**. Ring-opening metathesis polymerisation (ROMP) involves the polymerization of monomers containing strained, unsaturated rings, with the driving force being one of ring-strain release. Ring-closing metathesis (RCM) is the intramolecular metathesis of terminal olefins, resulting in a cyclic structure. The major driving force in this process is entropic, due to the formation of two molecules from one substrate. One of the two molecules is typically

ethene, a gaseous molecule making the reaction essentially irreversible and driving the reaction to completion. Cross metathesis (CM) involves the transalkylidenation of two terminal alkenes producing a new C-C bond between the two motifs.[62]

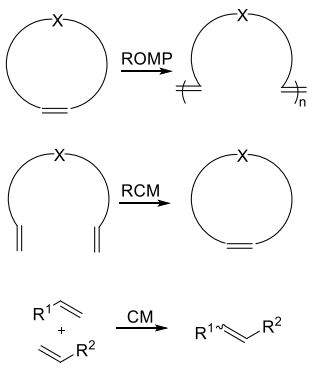

Figure 1.28 – Common forms of Ru catalysed metathesis.

The mechanism for this metathesis reaction was first proposed by Herisson and Chauvin in 1971 and is shown below in **Figure 1.29**.[63] The metal carbene undergoes an initiation step with an olefin to form a metallocyclobutane intermediate (a). Collapse of this structure to release ethene (b) in a [2+2] cycloaddition occurs to leave the olefin as now part of the metal carbene complex. Subsequent addition of the second olefin (c) again forms a metallocyclobutane intermediate and collapse of this (d) regenerates the metal carbene catalyst and the metathesis product. The difference in stereoisomers occurs as a result of the geometry of addition and free rotation prior to forming the metallocyclobutane intermediate, shown in square brackets.

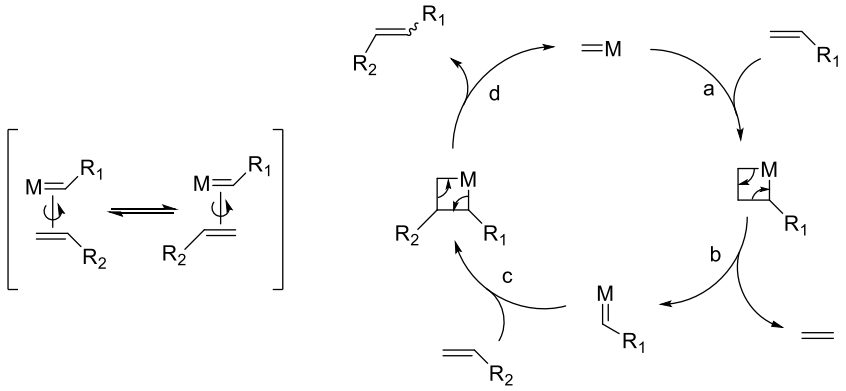

Figure 1.29 – Chauvin's mechanism for olefin metathesis.

Owing to the highly selective and successful nature of olefin metathesis, it is not surprising that it has found great use in synthetic chemistry,[64] and due to metathesis of large ring sizes being possible, this includes the formation of interlocked structures. Only a few years after the discovery of these catalysts, the group of Sauvage was able to apply their Cu(I) template approach and capture the [2]-catenane, **30**, in excellent yields, via RCM between the terminal olefins of the complexed thread, shown in **Figure 1.30**.[65]

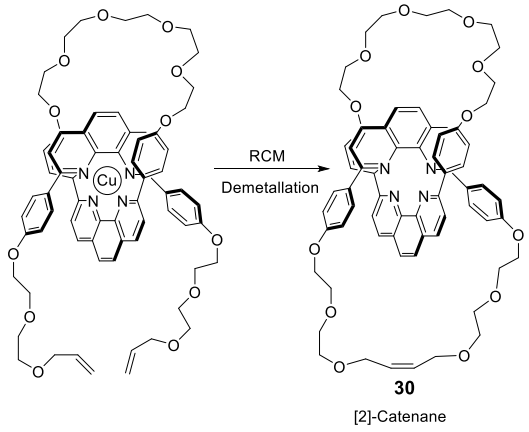

Figure 1.30 – Sauvage's Cu(I) template approach coupled with RCM to from catenanes.

This concept of clipping via RCM has since been expanded upon by numerous groups to include multicomponent architectures using various H:G preorganisation motifs.[66]

1.4.2 Cycloaddition Reactions

Cycloaddition reactions have played an integral role in the synthesis of interlocked structures, including those found within this thesis, in part due to their reliability and high selectivity for the functional groups involved. The latter part of this thesis concerns the use of photo-induced dimerization via a photo-induced cycloaddition, which will be covered in greater detail in chapter 4. Although the use of this specific approach has not yet been utilised in the capture event of an interlocked structure, there are many other cycloaddition reactions present in the literature that have been applied towards their synthesis as outlined below.

The [3+2] cycloaddition between fullerene and an azomethine ylide, as developed by Prato et al.[67] was later applied towards the synthesis of rotaxanes, employing the fullerene moiety as a stopper group as shown in **Scheme 1.3**.[68] However, this was not involved in the capture event of the interlocked structure and subsequent clipping of a benzylic amide macrocycle around the fumaramide template, as developed by the Leigh group,[25] achieved the [2]-rotaxane.

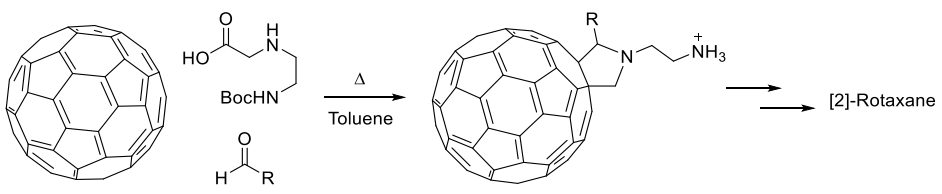

Scheme 1.3 - Attachment of a fullerene stopper group via a [3+2] cycloaddition.

The use of a cycloaddition reaction to capture an interlocked species has been shown by the group of Yuliang Li.[69] Again through the use of a bis-amide binding motif, a pseudo-rotaxane, **31**, was formed, and stoppered via a [2+2] cycloaddition between a terminal bisaryl alkyne and tetracyanoquinodimethane forming **32**, as shown in **Scheme 1.4**. This method of stoppering was chosen over other more widely used cycloadditions in order to circumvent the need for any metal catalyst.

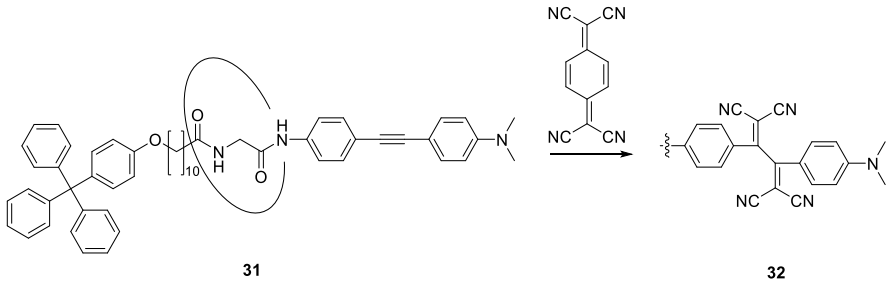

31 32

Scheme 1.4 – Stoppering event utilising a [2+2] cycloaddition between TCNQ and a bisarylalkyne.

Another approach regarding the synthesis of interlocked structures via cycloaddition reactions was shown by the Leigh group, **Scheme 1.5**.[70] By employing Zn(II) lewis acids in an active-template approach, the metal ion would be coordinated within the macrocycle cavity in an ideal geometry for substrate binding. Once the stoppered dieneophile was coordinated to the bound metal, the double bond would protrude through the macrocycle and be available for subsequent Zn(II) catalysed Diels-Alder cycloaddition with the stoppered diene, affording **33**.

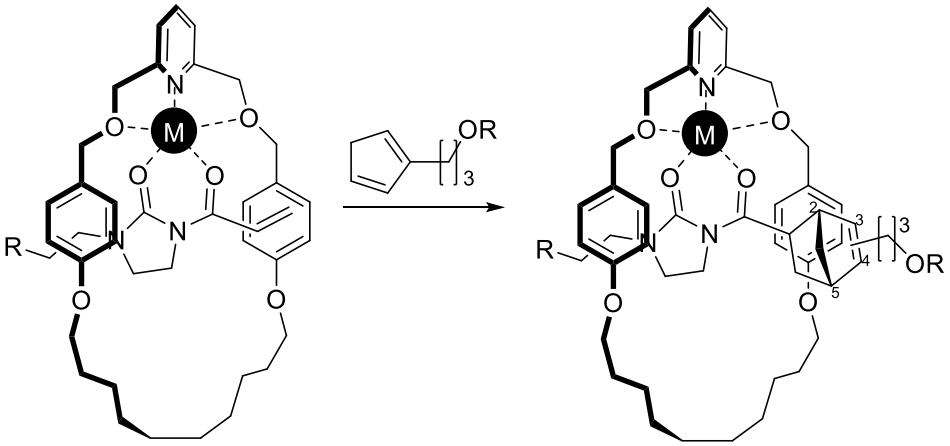

33

Scheme 1.5 – Synthesis of a [2]-Rotaxane via [4+2] cycloaddition.

Interestingly, only the 2-substituted isomer of the diene was found to react to form the rotaxane, with 90% of the rotaxane being the 1,4-isomer, whereas all four isomers were observed when using an acyclic ligand. In contrast to usual active template methods, which involve a 'passive' metal ion, in this case the template site was incorporated into the rotaxane and the metal-ligand interaction 'lived on' in the interlocked structure allowing the synthesis of metal-chelated molecular shuttles.

1.4.2.1 Huisgen 1,3-Dipolar Cycloaddition

Of these cycloaddition reactions, probably the most prevalent in the literature, and now synonymous with the term 'click chemistry', is the formation of 1,2,3-triazoles using the Huisgen 1,3-dipolar cycloaddition. The term 'click reaction' was coined by Sharpless in 2001, to describe reactions which, amongst other attributes, must be modular, high yielding, wide in scope and stereospecific. As well as these features, the reaction must possess certain characteristics which include simple reaction conditions and product isolation.[71] The azide-alkyne Huisgen 1,3-dipolar cycloaddition satisfies many of the

required attributes. However, the thermal reaction fails in this respect owing to elevated temperatures and a mixture of regioisomers. It was not until this reaction was expanded upon by the groups of Meldal[72] and Sharpless,[73] through the introduction of Cu(I) catalysis, that high yielding, regiospecific reactions were achieved at ambient temperatures and in a variety of solvents including water. From here on, this reaction will be referred to as a click or CuAAC reaction. The proposed mechanism is shown below in **Scheme 1.6**.[74]

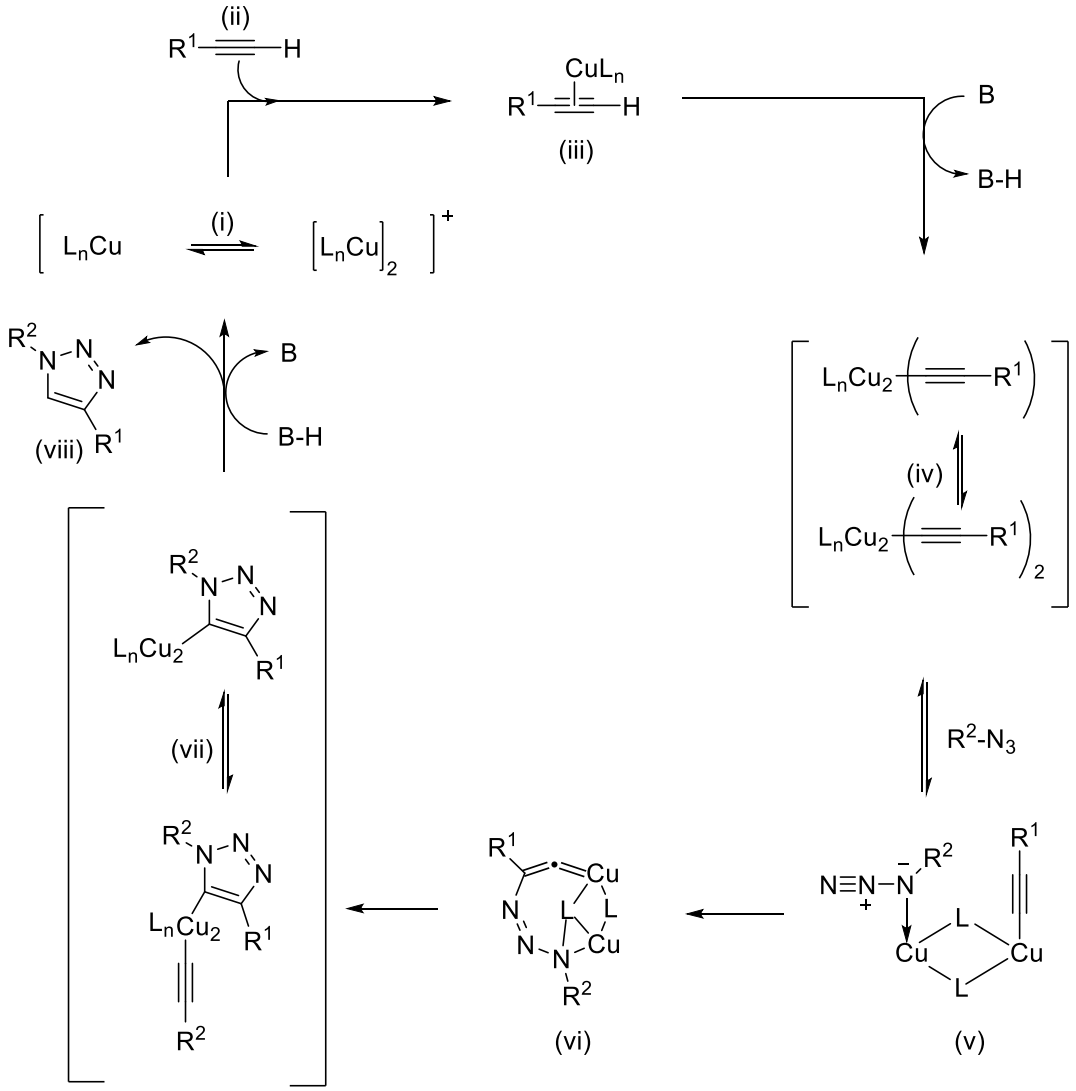

Scheme 1.6 – Proposed outline of species involved in the catalytic cycle.

The initial step involves formation of the copper(I) acetylide (iii). From DFT calculations, it was deduced that the process is not a concerted [2+3] cycloaddition, but a stepwise mechanism, with the rate of the catalytic process being second order with respect to copper.[75] The role of the second copper atom appears to be activation of the azide moiety (v). Complexation of the azide activates it towards nucleophilic attack of the acetylide to the azide (vi). This metallocycle positions the bound azide for subsequent ring contraction (vii) followed by protonation and dissociation to afford the product.

Triazole-bearing psuedorotaxane **34** was produced by Mock,[79] in their attempts towards catalysis using cucurbit[6]uril, CB[6]. This method did not use a Cu(I) catalyst and was reliant on the Pauling principle of catalysis, via the encapsulation of the reactants within the hydrophobic pocket, holding the reactive groups in close proximity as shown in **Figure 1.31 (a)**.[80] This work was expanded upon towards interlocked structures in the late 90's by Steinke[81] towards the formation of catalytically self-threading polyrotaxanes. This concept utilised 2 bi-functional monomers, which once cyclised within the cucurbituril, form a perfect mainchain polyrotaxane, **35**.

a)

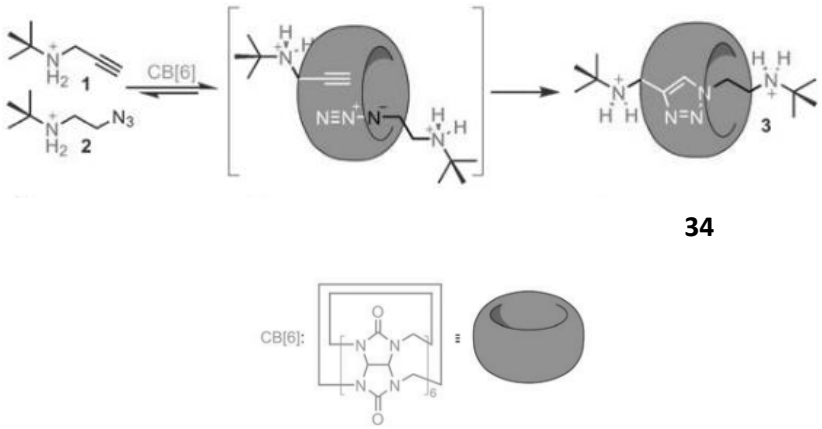

b)

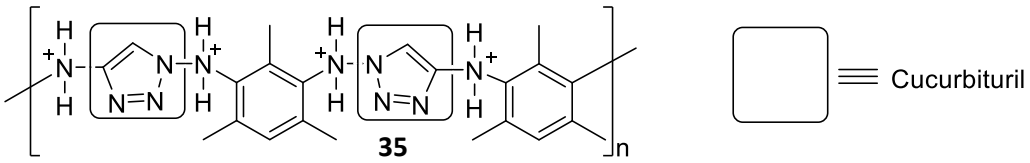

Figure 1.31 – a) The Pauling principle of catalysis as demonstrated by Mock and b) The repeating unit of the polyrotaxane.

With the advent of the CuAAC reaction, it is not surprising that, owing to the high utility and specificity of this reaction, it has seen wide and varied use in a whole host of reactions to form interlocked structures. However, not only has it seen use in the synthesis of building blocks and the covalent capture of the structures themselves, but due the stability towards the functional groups involved, it has found use in the formation of triazole rings which can function as ligands in controlling structure dynamics, as well as in post-synthetic functionalisation.

The CuAAC reaction was first applied towards the synthesis of interlocked structures by the group of Sauvage.[20] By using their 'passive', Cu(I)-directed approach originally developed for targeting catenanes and knots,[76] and by combining the preorganisation of a phenanthroline macrocycle and an azide-functionalised bypyridine 'thread', the formation

of a pseudo-rotaxane was possible, shown in **Scheme 1.7**. This was then followed by using the CuAAC reaction to cap the complex, affording a [2]-Rotaxane, **36**, in 62% yield.

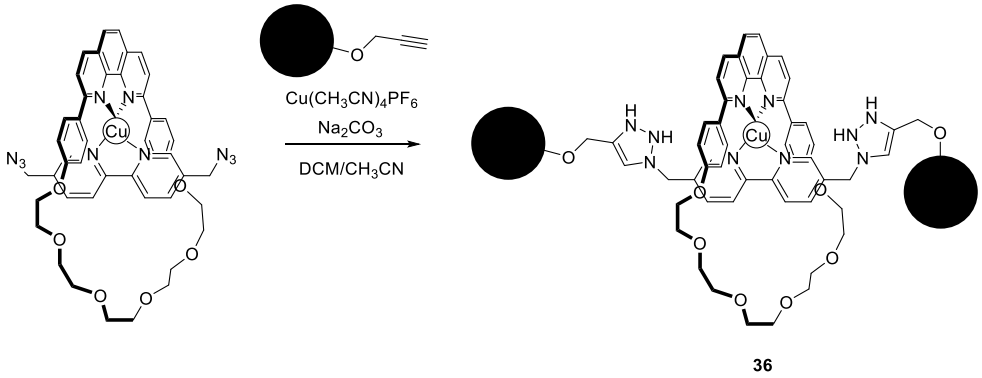

Scheme 1.7 – Stoppering of a pseudo-rotaxane via CuAAC reaction.

By far the most elegant use of this reaction was to apply a strategy of 'active' templation. Building upon the template strategy of Sauvage, this was first demonstrated by the Leigh group, who were able to produce excellent yields of rotaxane using substoichiometric amounts of Cu(I).[22] By employing the tetrahedral geometry of a Cu(I) atom, and coordinating this at a pyridine site within a macrocycle, this metal centre served the dual purpose of locating reacting species within the macrocycle as well as catalysing the reaction itself. Once the Cu(I) was bound within the macrocyle, the reacting azide and alkyne groups would bind with the Cu(I) catalyst either side of the plane of the macrocycle and a subsequent CuAAC reaction would form the rotaxane, **37**. **Scheme 1.8** shows the key step in the catalytic cycle at which both azide and alkyne components bind to the Cu atom either side of the macrocycle, due to its inherent tetrahedral geometry. This method has since been extensively expanded and adapted upon by others.

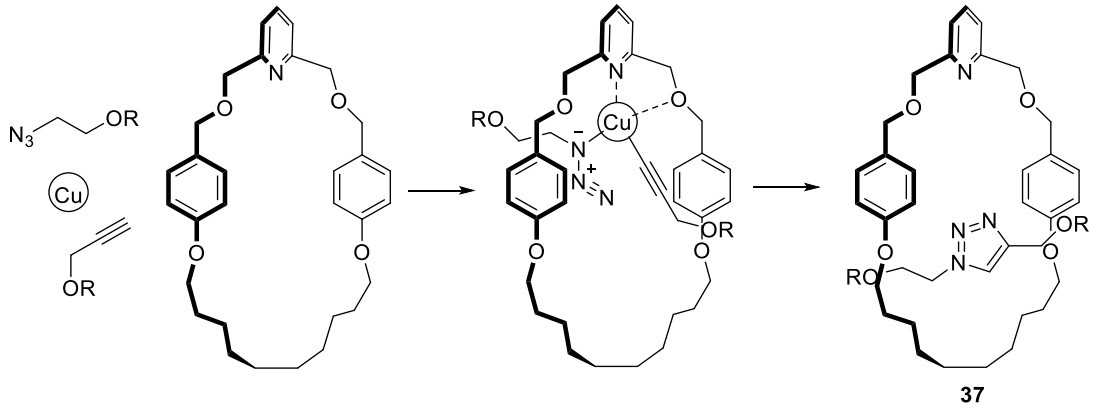

Scheme 1.8 – Active-template approach employing the CuAAC reaction where R = Bulky stopper.

As mentioned in **Section 1.2**, the work of Paul Beer's group in the field of interlocked structures has centred on the use of anion templation.[21, 77] Their work was extended to incorporate the triazole group in this anion template approach, **Scheme 1.9**.[66b] The C(5)-H bond of the triazole group is slightly polar. However, no anion binding was observed and conversion of the triazole unit, via methylation, to the triazolium cation was shown to greatly enhance anion binding. In utilising this anion binding, the triazolium cation was employed in their anion-templated RCM synthesis of [2]-rotaxane **38**.

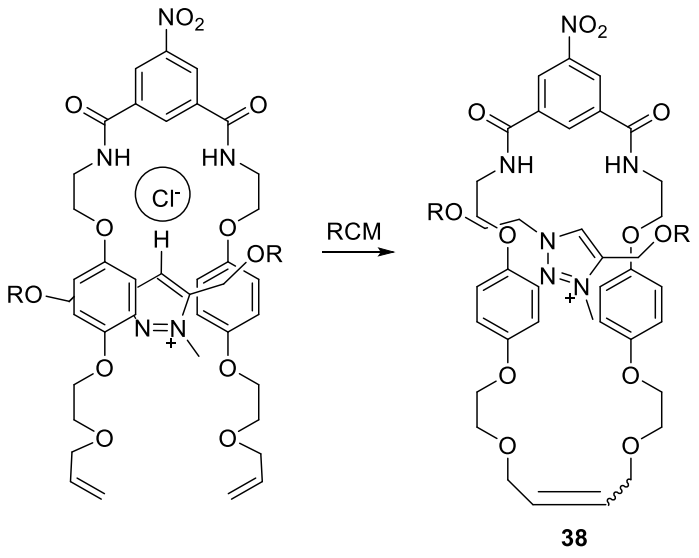

Scheme 1.9 – Capture of an interlocked structure via preorganisation of an anion-triazolium complex.

This motif exhibited stronger binding with Br^- compared to Cl^-, with association constants of 907 M^{-1} and 90 M^{-1}, respectively (in $CDCl_3$/MeOD 1:1). This was a different result to what was expected since typically, these systems are selective for Cl^- in mixed solvent systems.[77] The rotaxane synthesis was then repeated using Br^- as the templating ion and an increased yield of rotaxane was observed, which was attributed to the enhanced binding affinity and preorganisation of Br^-. This highlights a significant improvement in the size-shape match for Br^- over Cl^- in this particular system.

1.5 Introduction to the project

1.5.1 Description and aims

Despite the current and very successful approaches to interlocked structures, there are relatively few templates in use, relative to the wide scope of their diverse structures and applications. It is the aim of this thesis to build upon the current understanding of templating techniques and add to the number of template motifs available towards the synthesis of interlocked structures. The concept is to utilise the specific interaction of Hamilton receptors and their barbiturate guests to allow a new template towards interlocked structures to be realised.

This receptor binding motif is particularly attractive towards interlocked structure formation due to its high level of complementarity with barbiturate guests. One key structural aspect of this interaction is that of the sp^3 carbon at the 5-position of the barbiturate. A crystal structure produced by the Hamilton group[78] (**Figure 1.32**), shows that when barbital is bound to a planar, Hamilton macrocycle, this sp^3 carbon allows the

ethylene groups to protrude above and below the plane of the macrocycle. It can be envisaged, that with suitable extension and functionalisation of the groups attached at this position, an interlocked structure can be realised.

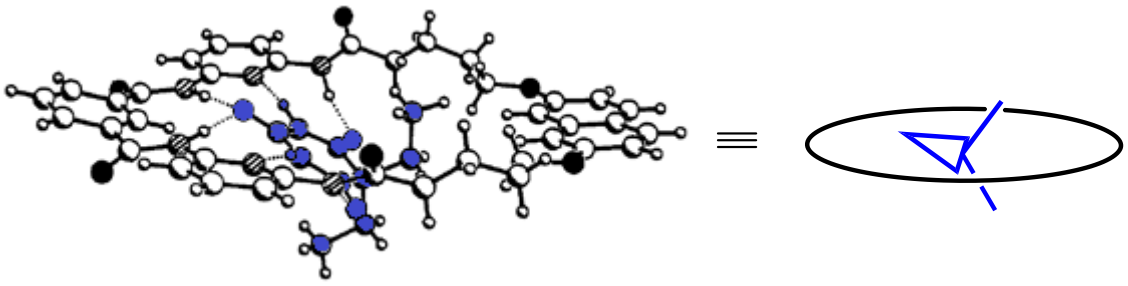

Figure 1.32 – Crystal structure of a H:G complex consisting of Hamilton's receptor and barbital and the corresponding schematic to highlight the threaded appendages.

1.5.2 Hosts and Guests

During this project, a series of different forms of Hamilton receptor have been synthesised, along with a range of complementary barbiturates, as summarised in **Figure 1.33** and **1.34**. The Hamilton receptors consist of both cyclic and acyclic forms, with the methods towards formation and the particular type of interlocked structures that result, dependent on the specific combination of host and guest.

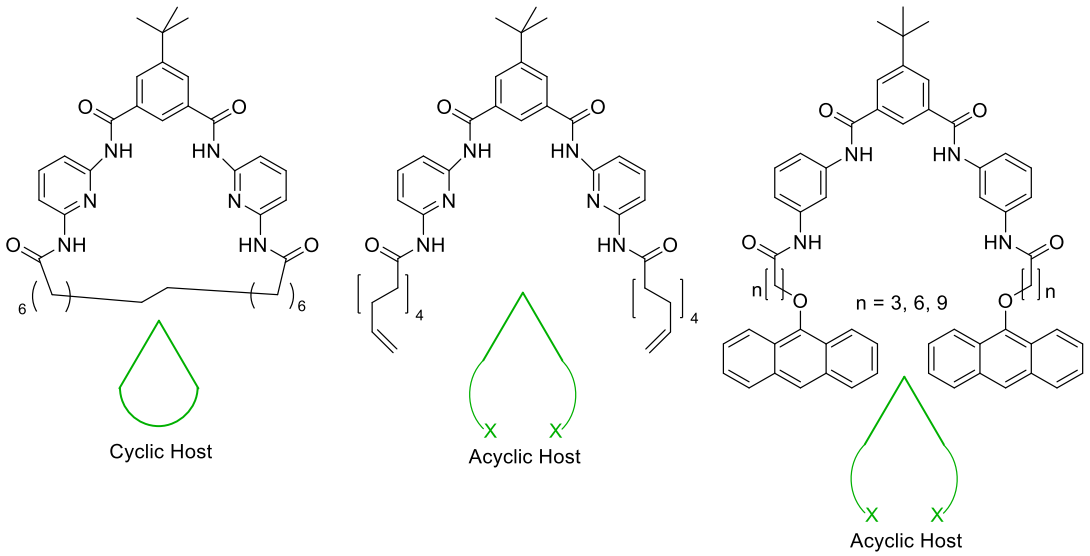

Figure 1.33 – Acyclic and cyclic Hamilton receptors for various approaches towards interlocked structures.

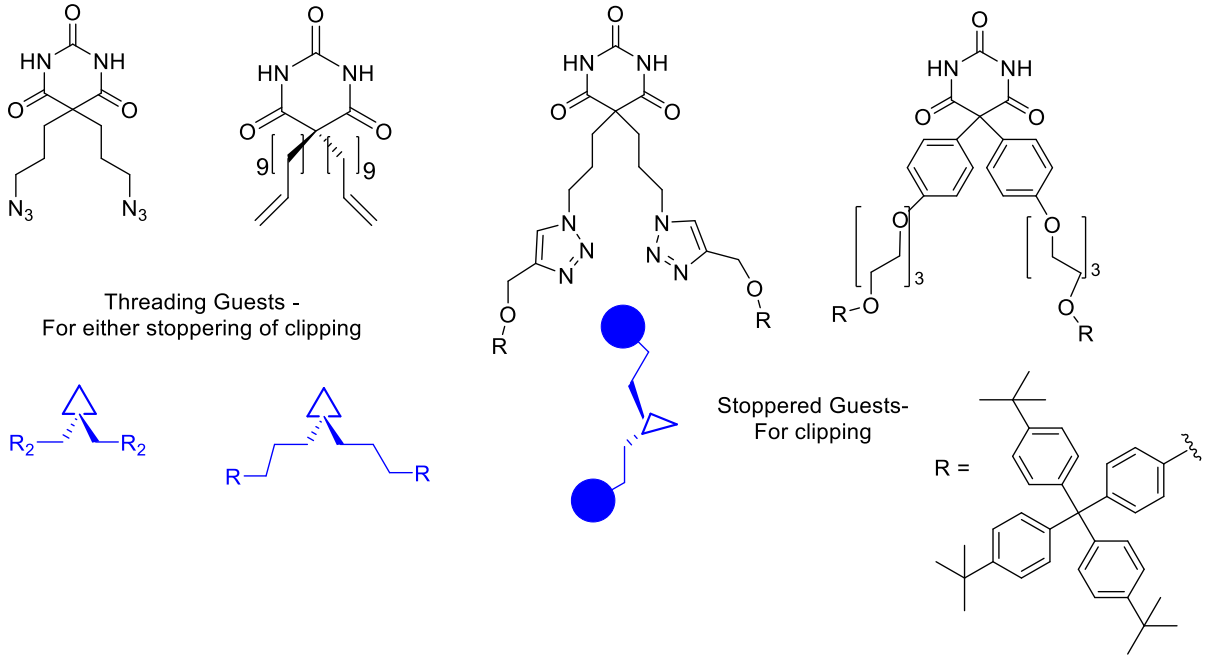

Figure 1.34 – Barbiturate guests for various approaches towards interlocked structures.

Firstly, considering the acyclic receptors, a 'dumbbell-shaped' barbiturate with stopper groups pre-attached may be bound within the receptor. If the receptor is appropriately functionalised with pendant arms and terminated with reactive groups, then

an interlocked structure may be formed using a clipping approach. Of the many reactive groups available to terminate the receptor two groups were chosen for this project: (I) olefin groups for a Grubbs metathesized ring closing reaction and (II) anthracene groups for photo-dimerization. This second method was particularly interesting because if successful, it would be the first known example of the formation of an interlocked structure using a photo-chemical reaction. The clipping approach towards interlocked structures using acyclic Hamilton receptors are shown below in **Figure 1.35**.

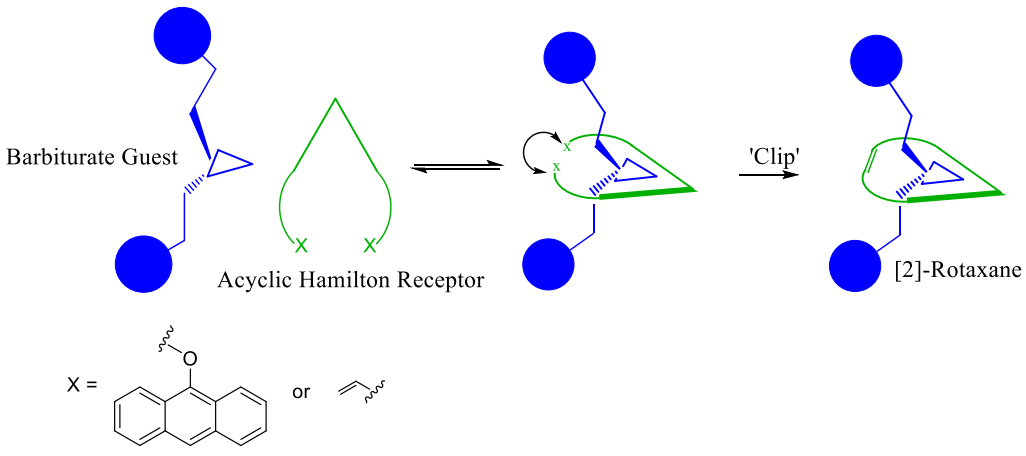

Figure 1.35 - Route towards interlocked structures using acyclic Hamilton receptors.

The second approach involved the use of a Hamilton macrocycle. The barbiturate was expected to thread through the macrocycle and once bound in the cavity, the pendant arms could be used to form an interlocked structure. Depending on the type of functionalisation of the barbiturate pendant arms, either catenane or rotaxane formation could be possible. With regards to a clipping reaction, Grubbs metathesis would again be used in this approach when the terminal groups of the barbiturate arms were olefins. This would build upon the work of a previous PhD student on the project, Mathias Rocher,[79] which was focussed on catenane formation. For a stoppering approach, the terminal groups

of the thread and stopper would be an alkyne-azide pair, enabling the use of a copper catalysed azide-alkyne 1,3-dipolar cycloaddition. The processes involved using macrocyclic Hamilton receptors are summarised in **Figure 1.36**.

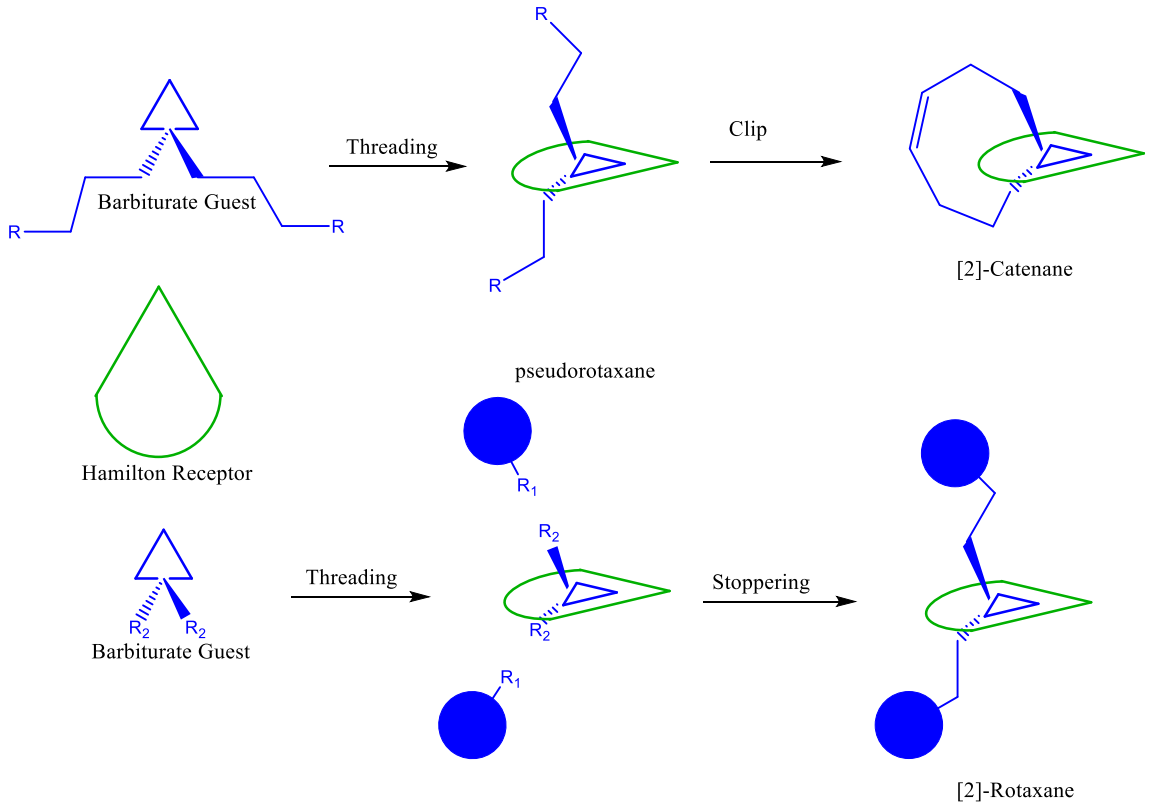

Figure 1.36 – Routes towards interlocked structures using macrocyclic Hamilton receptors.

1.6 References

1. Lehn, J.-M., Supramolecular Chemistry—Scope and Perspectives Molecules, Supermolecules, and Molecular Devices (Nobel Lecture). *Angew. Chem. Int. Ed.* **1988,** *27* (1), 89-112.

2. Beer, P. D.; Gale, P. A.; Smith, D. K., *Supramolecular Chemistry*. Oxford University Press: Oxford, 1999.

3. Pedersen, C. J., Cyclic polyethers and their complexes with metal salts. *J. Am. Chem. Soc.* **1967,** *89* (26), 7017-7036.

4. Steed, J. W.; Atwood, J. L., *Supramolecular Chemistry*. Wiley: Oxford, 2009.

5. Jorgensen, W. L.; Pranata, J., Importance of secondary interactions in triply hydrogen bonded complexes: guanine-cytosine vs uracil-2,6-diaminopyridine. *J. Am. Chem. Soc.* **1990,** *112* (5), 2008-2010.

6. (a) Kyogoku, Y.; Lord, R.; Rich, A., *Biochim. Biophys. Acta* **1969,** *179*, 10; (b) Kyogoku, Y.; Lord, R. C.; Rich, A., The effect of substituents on the hydrogen bonding of adenine and uracil derivatives. *Proc. Natl. Acad. Sci.* **1967,** *57* (2), 250-257.

7. Hunter, C. A., Molecular recognition of p-benzoquinone by a macrocyclic host. *Chem. Commun.* **1991,** (11), 749-751.

8. Odashima, K.; Itai, A.; Iitaka, Y.; Koga, K., Host-guest complex formation between a water-soluble polyparacyclophane and a hydrophobic guest molecule. *J. Am. Chem. Soc.* **1980,** *102* (7), 2504-2505.

9. Garcia-Tellado, F.; Goswami, S.; Chang, S. K.; Geib, S.; Hamilton, A. D., *J. Am. Chem. Soc* **1990,** *112* (7393).

10. Fan, E.; Van Arman, S. A.; Kincaid, S.; Hamilton, A. D., Molecular recognition: hydrogen-bonding receptors that function in highly competitive solvents. *J. Am. Chem. Soc.* **1993,** *115* (1), 369-370.

11. Rebek, J., Molecular recognition and biophysical organic chemistry. *Acc. Chem. Res.* **1990,** *23* (12), 399-404.

12. Schill, G.; Zollkopf, H., *Nachr. Chem. Techn.* **1967,** *15*, 149.

13. Wasserman, E., The preparation of interlocking rings: A Catenane. *J. Am. Chem. Soc.* **1960,** *82* (16), 4433-4434.

14. Harrison, I. T.; Harrison, S., Synthesis of a stable complex of a macrocycle and a threaded chain. *J. Am. Chem. Soc.* **1967,** *89* (22), 5723-5724.

15. Schill, G.; Lüttringhaus, A., The Preparation of Catena Compounds by Directed Synthesis. *Angew. Chem. Int. Ed.* **1964,** *3* (8), 546-547.

16. Chambron, J.-C.; Harriman, A.; Heitz, V.; Sauvage, J.-P., *J. Am. Chem. Soc.* **1993,** *115*, 7419.

17. Cordova, E.; Bissell, R. A.; Spencer, N.; Ashton, P. R.; Stoddart, J. F.; Kaifer, A. E., Novel rotaxanes based on the inclusion complexation of biphenyl guests by cyclobis(paraquat-p-phenylene). *J. Org. Chem.* **1993,** *58* (24), 6550-6552.

18. Isnin, R.; Kaifer, A. E., A new approach to cyclodextrin-based rotaxanes. *Pure Appl. Chem.* **1993,** *65*, 495.

19. Ashton, P. R.; Goodnow, T. T.; Kaifer, A. E.; Reddington, M. V.; Slawin, A. M. Z.; Spencer, N.; Stoddart, J. F.; Vicent, C.; Williams, D. J., A [2] Catenane Made to Order. *Angew. Chem. Int. Ed.* **1989,** *28* (10), 1396-1399.

20. Mobian, P.; Collin, J.-P.; Sauvage, J.-P., Efficient synthesis of a labile copper(I)-rotaxane complex using click chemistry. *Tetrahedron Lett.* **2006,** *47* (28), 4907-4909.

21. Ng, K.-Y.; Cowley, A. R.; Beer, P. D., Anion templated double cyclization assembly of a chloride selective [2]catenane. *Chem. Commun.* **2006,** (35), 3676-3678.

22. Aucagne, V.; Hänni, K. D.; Leigh, D. A.; Lusby, P. J.; Walker, D. B., Catalytic "Click" Rotaxanes: A Substoichiometric Metal-Template Pathway to Mechanically Interlocked Architectures. *J. Am. Chem. Soc.* **2006,** *128* (7), 2186-2187.

23. Hunter, C. A., Synthesis and structure elucidation of a new [2]-catenane. *J. Am. Chem. Soc.* **1992,** *114* (13), 5303-5311.

24. Jäger, R.; Baumann, S.; Fischer, M.; Safarowsky, O.; Nieger, M.; Vögtle, F., Non-Ionic Template Synthesis of Amide-Linked Rotaxanes: Olefinic and Aliphatic Axle Building Blocks. *Liebigs Ann.* **1997,** *1997* (11), 2269-2273.

25. Gatti, F. G.; Leigh, D. A.; Nepogodiev, S. A.; Slawin, A. M. Z.; Teat, S. J.; Wong, J. K. Y., Stiff, and Sticky in the Right Places: The Dramatic Influence of Preorganizing Guest Binding Sites on the Hydrogen Bond-Directed Assembly of Rotaxanes. *J. Am. Chem. Soc.* **2001,** *123* (25), 5983-5989.

26. Johnston, A. G.; Leigh, D. A.; Murphy, A.; Smart, J. P.; Deegan, M. D., The Synthesis and Solubilization of Amide Macrocycles via Rotaxane Formation. *J. Am. Chem. Soc.* **1996,** *118* (43), 10662-10663.

27. Xiao, S.; Fu, N.; Peckham, K.; Smith, B. D., Efficient Synthesis of Fluorescent Squaraine Rotaxane Dendrimers. *Org. Lett.* **2009,** *12* (1), 140-143.

28. Berná, J.; Alajarín, M.; Orenes, R.-A., Azodicarboxamides as Template Binding Motifs for the Building of Hydrogen-Bonded Molecular Shuttles. *J. Am. Chem. Soc.* **2010,** *132* (31), 10741-10747.

29. Ahmed, R.; Altieri, A.; D'Souza, D. M.; Leigh, D. A.; Mullen, K. M.; Papmeyer, M.; Slawin, A. M. Z.; Wong, J. K. Y.; Woollins, J. D., Phosphorus-Based Functional Groups as Hydrogen Bonding Templates for Rotaxane Formation. *J. Am. Chem. Soc.* **2011,** *133* (31), 12304-12310.

30. Aston, P. R.; Glink, P. T.; Stoddart, J. F.; Tasker, P. A.; White, A. J. P.; Williams, D. J., Self-assembling [2]- and [3]Rotaxanes from Secondary Dialkylammonium Salts and Crown Ethers. *Chem. Eur. J.* **1996,** *2* (6), 729-736.

31. Kawasaki, H.; Kihara, N.; Takata, T., High Yielding and Practical Synthesis of Rotaxanes by Acylative End-Capping Catalyzed by Tributylphosphine. *Chem. Lett.* **1999,** *28* (10), 1015-1016.

32. Hirose, K.; Nishihara, K.; Harada, N.; Nakamura, Y.; Masuda, D.; Araki, M.; Tobe, Y., Highly Selective and High-Yielding Rotaxane Synthesis via Aminolysis of Prerotaxanes Consisting of a Ring Component and a Stopper Unit. *Org. Lett.* **2007,** *9* (16), 2969-2972.

33. Kilbinger, A. F. M.; Cantrill, S. J.; Waltman, A. W.; Day, M. W.; Grubbs, R. H., Magic Ring Rotaxanes by Olefin Metathesis. *Angew. Chem. Int. Ed.* **2003,** *42* (28), 3281-3285.

34. G. Kolchinski, A.; A. Roesner, R.; H. Busch, D.; W. Alcock, N., Molecular riveting: high yield preparation of a [3]-rotaxane. *Chem. Commun.* **1998,** (14), 1437-1438.

35. Wisner, J. A.; Beer, P. D.; Drew, M. G. B.; Sambrook, M. R., Anion-Templated Rotaxane Formation. *J. Am. Chem. Soc.* **2002,** *124* (42), 12469-12476.

36. Bissell, R. A.; Cordova, E.; Kaifer, A. E.; Stoddart, J. F., A chemically and electrochemically switchable molecular shuttle. *Nature* **1994,** *369* (6476), 133-137.

37. Lane, A. S.; Leigh, D. A.; Murphy, A., Peptide-Based Molecular Shuttles. *J. Am. Chem. Soc.* **1997,** *119* (45), 11092-11093.

38. Brouwer, A. M.; Frochot, C.; Gatti, F. G.; Leigh, D. A.; Mottier, L. c.; Paolucci, F.; Roffia, S.; Wurpel, G. W. H., Photoinduction of Fast, Reversible Translational Motion in a Hydrogen-Bonded Molecular Shuttle. *Science* **2001,** *291* (5511), 2124-2128.

39. Keaveney, C. M.; Leigh, D. A., Shuttling through Anion Recognition. *Angew. Chem. Int. Ed.* **2004,** *43* (10), 1222-1224.

40. Hesseler, B.; Zindler, M.; Herges, R.; Luning, U., A Shuttle for the Transport of Protons Based on a 2 Rotaxane. *Eur. J. Org. Chem.* **2014,** *2014* (18), 3885-3901.

41. Badjić, J. D.; Balzani, V.; Credi, A.; Silvi, S.; Stoddart, J. F., A Molecular Elevator. *Science* **2004,** *303* (5665), 1845-1849.

42. Liu, Y.; Flood, A. H.; Bonvallet, P. A.; Vignon, S. A.; Northrop, B. H.; Tseng, H.-R.; Jeppesen, J. O.; Huang, T. J.; Brough, B.; Baller, M.; Magonov, S.; Solares, S. D.; Goddard, W. A.; Ho, C.-M.; Stoddart, J. F., Linear Artificial Molecular Muscles. *J. Am. Chem. Soc.* **2005,** *127* (27), 9745-9759.

43. Lewandowski, B.; De Bo, G.; Ward, J. W.; Papmeyer, M.; Kuschel, S.; Aldegunde, M. J.; Gramlich, P. M. E.; Heckmann, D.; Goldup, S. M.; D'Souza, D. M.; Fernandes, A. E.; Leigh, D. A., Sequence-Specific Peptide Synthesis by an Artificial Small-Molecule Machine. *Science* **2013,** *339* (6116), 189-193.

44. Nguyen, T. D.; Leung, K. C. F.; Liong, M.; Pentecost, C. D.; Stoddart, J. F.; Zink, J. I., Construction of a pH-Driven Supramolecular Nanovalve. *Org. Lett.* **2006,** *8* (15), 3363-3366.

45. Fischer, E.; Dilthey, A., Ueber C-Dialkylbarbitursäuren und über die Ureïde der Dialkylessigsäuren. *Liebigs Ann. Chem.* **1904,** *335* (3), 334-368.

46. López-Muñoz, F.; Ucha-Udabe, R.; Alamo, C., *Neuropsychiatr Dis Treat.* **2005,** *1*, 329.

47. Feibush, B.; Figueroa, A.; Charles, R.; Onan, K. D.; Feibush, P.; Karger, B. L., Chiral separation of heterocyclic drugs by HPLC: solute-stationary phase base-pair interactions. *J. Am. Chem. Soc.* **1986,** *108* (12), 3310-3318.

48. Chang, S. K.; Hamilton, A. D., Molecular recognition of biologically interesting substrates: synthesis of an artificial receptor for barbiturates employing six hydrogen bonds. *J. Am. Chem. Soc.* **1988,** *110* (4), 1318-1319.

49. Tecilla, P.; Chang, S. K.; Hamilton, A. D., Transition-state stabilization and molecular recognition: acceleration of phosphoryl-transfer reactions by an artificial receptor. *J. Am. Chem. Soc.* **1990,** *112* (26), 9586-9590.

50. Tecilla, P.; Hamilton, A. D., Molecular recognition and catalysis; acceleration of acyl transfer reactions by a hydrogen-bonding receptor. *Chem. Commun.* **1990,** (18), 1232-1234.

51. Valenta, J. N.; Dixon, R. P.; Hamilton, A. D.; Weber, S. G., Enhanced Extraction of Phenobarbital from Serum with a Designed Artificial Receptor. *Anal. Chem.* **1994,** *66* (14), 2397-2403.

52. Tecilla, P.; Dixon, R. P.; Slobodkin, G.; Alavi, D. S.; Waldeck, D. H.; Hamilton, A. D., Hydrogen-bonding self-assembly of multichromophore structures. *J. Am. Chem. Soc.* **1990,** *112* (25), 9408-9410.

53. Hamilton, A.; Slobodkin, G.; Fan, E., *New J. Chem.* **1992,** *16*, 643.

54. Li, S.; Sun, L.; Chung, Y.; Weber, S. G., Artificial Receptor-Facilitated Solid-Phase Microextraction of Barbiturates. *Anal. Chem.* **1999,** *71* (11), 2146-2151.

55. Zhang, S.-Q.; Fukase, K.; Izumi, M.; Fukase, Y.; Kusumoto, S., Synthesis Based on Affinity Separation (SAS): Separation of Products Having Barbituric Acid Tag from Untagged Compounds by Using Hydrogen Bond Interaction. *Synlett* **2001,** *2001* (05), 0590-0596.

56. Molard, Y.; Bassani, D. M.; Desvergne, J.-P.; Horton, P. N.; Hursthouse, M. B.; Tucker, J. H. R., Photorelease of an Organic Molecule in Solution: Light-Triggered Blockage of a Hydrogen-Bonding Receptor Site. *Angew. Chem. Int. Ed.* **2005,** *44* (7), 1072-1075.

57. Truett, W. L.; Johnson, D. R.; Robinson, I. M.; Montague, B. A., Polynorbornene by Coördination Polymerization1. *J. Am. Chem. Soc.* **1960,** *82* (9), 2337-2340.

58. Porri, L.; Rossi, R.; Diversi, P.; Lucherini, A., Ring-Opening polymerization of cycloolefins with catalysts derived from ruthenium and iridium. *Die Makromolekulare Chemie* **1974,** *175* (11), 3097-3115.

59. Nguyen, S. T.; Johnson, L. K.; Grubbs, R. H.; Ziller, J. W., Ring-opening metathesis polymerization (ROMP) of norbornene by a Group VIII carbene complex in protic media. *J. Am. Chem. Soc.* **1992,** *114* (10), 3974-3975.

60. Nguyen, S. T.; Grubbs, R. H.; Ziller, J. W., Syntheses and activities of new single-component, ruthenium-based olefin metathesis catalysts. *J. Am. Chem. Soc.* **1993,** *115* (21), 9858-9859.

61. Schwab, P.; Grubbs, R. H.; Ziller, J. W., Synthesis and Applications of RuCl2(CHR')(PR3)2: The Influence of the Alkylidene Moiety on Metathesis Activity. *J. Am. Chem. Soc.* **1996,** *118* (1), 100-110.

62. Vougioukalakis, G. C.; Grubbs, R. H., Ruthenium-Based Heterocyclic Carbene-Coordinated Olefin Metathesis Catalysts†. *Chem. Rev.* **2009,** *110* (3), 1746-1787.

63. Jean-Louis Hérisson, P.; Chauvin, Y., Catalyse de transformation des oléfines par les complexes du tungstène. II. Télomérisation des oléfines cycliques en présence d'oléfines acycliques. *Makromol. Chem.* **1971,** *141* (1), 161-176.

64. Grubbs, R. H.; Chang, S., Recent advances in olefin metathesis and its application in organic synthesis. *Tetrahedron* **1998,** *54* (18), 4413-4450.

65. Weck, M.; Mohr, B.; Sauvage, J.-P.; Grubbs, R. H., Synthesis of Catenane Structures via Ring-Closing Metathesis. *J. Org. Chem.* **1999,** *64* (15), 5463-5471.

66. (a) Iwamoto, H.; Itoh, K.; Nagamiya, H.; Fukazawa, Y., Convenient synthesis of [3]catenane by olefin metathesis dimerizations. *Tetrahedron Lett.* **2003,** *44* (31), 5773-5776; (b) Mullen, K. M.; Mercurio, J.; Serpell, C. J.; Beer, P. D., Exploiting the 1,2,3-Triazolium Motif in Anion-Templated Formation of a Bromide-Selective Rotaxane Host Assembly. *Angew. Chem. Int. Ed.* **2009,** *48* (26), 4781-4784; (c) Dasgupta, S.; Wu, J., Template-directed synthesis of kinetically and thermodynamically stable molecular necklace using ring closing metathesis. *Org. Biomol. Chem.* **2011,** *9* (9), 3504-3515.

67. Maggini, M.; Scorrano, G.; Prato, M., Addition of azomethine ylides to C60: synthesis, characterization, and functionalization of fullerene pyrrolidines. *J. Am. Chem. Soc.* **1993,** *115* (21), 9798-9799.

68. Mateo-Alonso, A.; Prato, M., Synthesis of a soluble fullerene–rotaxane incorporating a furamide template. *Tetrahedron* **2006,** *62* (9), 2003-2007.

69. Zhou, W.; Xu, J.; Zheng, H.; Liu, H.; Li, Y.; Zhu, D., Charge Transfer Chromophore-Stopped [2]Rotaxane through [2 + 2] Cycloaddition. *J. Org. Chem.* **2008,** *73* (19), 7702-7709.

70. Crowley, J. D.; Hänni, K. D.; Leigh, D. A.; Slawin, A. M. Z., Diels−Alder Active-Template Synthesis of Rotaxanes and Metal-Ion-Switchable Molecular Shuttles. *J. Am. Chem. Soc.* **2010,** *132* (14), 5309-5314.

71. Kolb, H. C.; Finn, M. G.; Sharpless, K. B., Click Chemistry: Diverse Chemical Function from a Few Good Reactions. *Angew. Chem. Int. Ed.* **2001,** *40* (11), 2004-2021.

72. Tornøe, C. W.; Christensen, C.; Meldal, M., Peptidotriazoles on Solid Phase: [1,2,3]-Triazoles by Regiospecific Copper(I)-Catalyzed 1,3-Dipolar Cycloadditions of Terminal Alkynes to Azides. *J. Org. Chem.* **2002,** *67* (9), 3057-3064.

73. Rostovtsev, V. V.; Green, L. G.; Fokin, V. V.; Sharpless, K. B., A Stepwise Huisgen Cycloaddition Process: Copper(I)-Catalyzed Regioselective "Ligation" of Azides and Terminal Alkynes. *Angew. Chem. Int. Ed.* **2002,** *41* (14), 2596-2599.

74. Bock, V. D.; Hiemstra, H.; van Maarseveen, J. H., CuI-Catalyzed Alkyne–Azide "Click" Cycloadditions from a Mechanistic and Synthetic Perspective. *Eur. J. Org. Chem.* **2006,** *2006* (1), 51-68.

75. Rodionov, V. O.; Fokin, V. V.; Finn, M. G., Mechanism of the Ligand-Free CuI-Catalyzed Azide–Alkyne Cycloaddition Reaction. *Angew. Chem. Int. Ed.* **2005,** *44* (15), 2210-2215.

76. Dietrich-Buchecker, C. O.; Sauvage, J.-P., A Synthetic Molecular Trefoil Knot. *Angew. Chem. Int. Ed.* **1989,** *28* (2), 189-192.

77. Beer, P. D.; Sambrook, M. R.; Curiel, D., Anion-templated assembly of interpenetrated and interlocked structures. *Chem. Commun.* **2006,** (20), 2105-2117.

78. Chang, S. K.; Van Engen, D.; Fan, E.; Hamilton, A. D., Hydrogen bonding and molecular recognition: synthetic, complexation, and structural studies on barbiturate binding to an artificial receptor. *J. Am. Chem. Soc.* **1991,** *113* (20), 7640-7645.

79. Rocher, M. Towards Interlocked Structures Based on H-Bonded Barbiturate Complexes. University of Birmingham, Birmingham, 2010.

2 Synthesis of the precursor components of non-photoactive Interlocked Structures

As mentioned in the introduction, this thesis focuses on a number of different approaches towards H-bonded interlocked structures containing barbiturate components. As such, a number of different Hamilton-type receptors and barbiturates have been synthesised. Concerning the different types of receptor required, both cyclic and acyclic forms have been synthesised as well as a range of barbiturate guest compounds in order to fully investigate various strategies i.e. clipping/stoppering. A summary of the compounds which were synthesised is shown below in **Figure 2.1**.

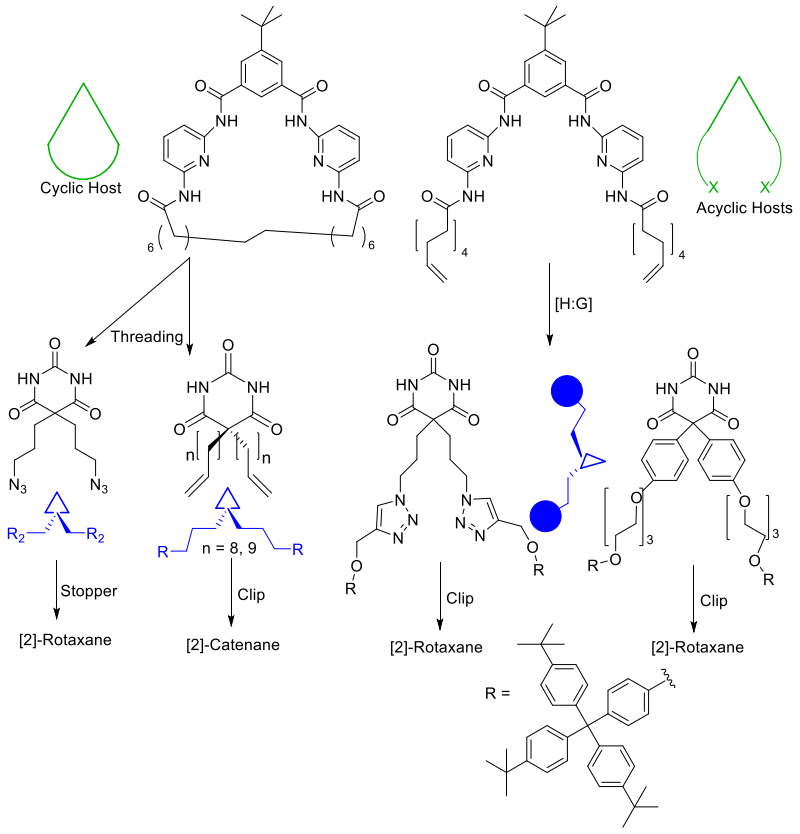

Figure 2.1 – Receptor and guest target compounds contained within Chapter 2, with method of capture shown.

Contained within this chapter are some studies carried out by our collaborators in Bordeaux. These include a ^{1}H NMR comparison (**Figure 2.19**), Job plot (**Figure 2.16**) and binding study (**Figure 2.18**) between host **45** and guest **83** as well as obtaining a crystal structure of the pseudo-rotaxane complex (**Figure 2.17**). A binding study between host **45** and guest **85** (**Figure 2.21**) was also carried out in Bordeaux.

2.1 Synthesis of Hamilton-Receptor Host molecules

Before any deviation in the synthesis with regards to which type of receptor was to be used, the bridge of the receptor first had to be synthesised.[1] The first step in the synthesis involved the formation of isophthaloyl chloride in quantitative yield from isophthalic acid using oxalyl chloride and catalytic DMF in DCM. Upon removal of the volatile component of the reaction mixture, the diacid chloride, **39**, was then used as obtained and reacted with excess 2,6-diamino pyridine using triethylamine as a base to form the binding site of the receptor, **40**, **Scheme 2.1** . The bridging component of the receptor was isolated via column chromatography in 75% yield and characterised by ^{1}H NMR spectroscopy.

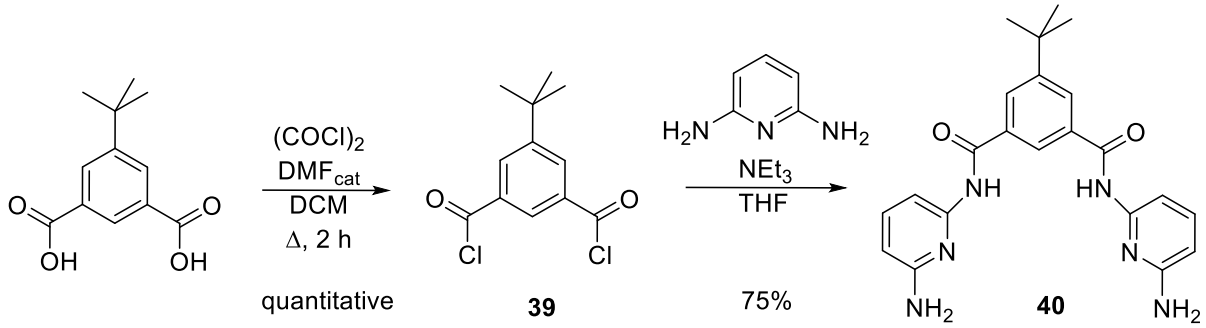

Scheme 2.1 – Synthesis of 'Bridge' Receptor **40**.

2.1.1 Acyclic Receptors:

Once the bridge of the receptor had been synthesised, the synthetic route could then deviate to accommodate the various strategies proposed with the bridge functionalised accordingly. The first target was the acyclic receptor with an 8-carbon linker. The starting material undecenoyl chloride was commercially available. The formation of the acyclic receptors was then carried out by reacting the bridge receptor **40** with the desired olefin terminated acid chloride, **Scheme 2.2**. After work up, the receptor **41** could be isolated via column chromatography or addition of hexane to the crude mixture and was obtained in fairly good yields. This acyclic receptor could now be applied towards a clipping strategy via complexation with stopper-terminated barbiturates (Chapter 3) as well as towards the synthesis of macrocyclic precursors, as outlined in the following section.

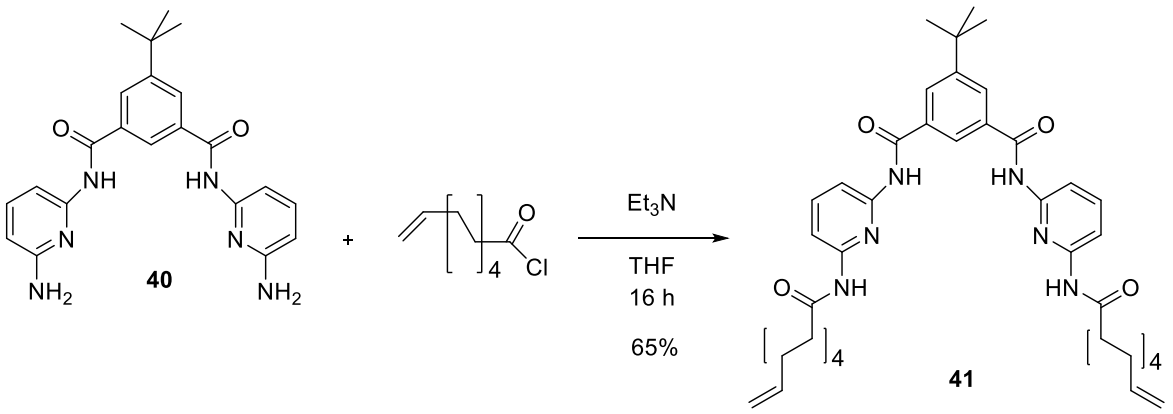

Scheme 2.2 – Synthesis of acyclic receptor **41**.

2.1.2 Cyclic Receptors

To obtain the cyclised forms of the receptor, for application towards a threading/stoppering strategy, two routes were identified as outlined below; firstly via Grubbs metathesis of **41** and secondly via direct cyclisation of bis-amine **40**. As already

mentioned, there is the possibility to cyclise the acyclic receptors using a Grubbs catalyst, followed by subsequent reduction of the double bond.

2.1.2.1 Via Grubbs Metathesis:

Following **Scheme 2.3**, the acyclic receptor **41** was dissolved in DCM and after the addition of 10 mol% Grubbs (I) catalyst, the solution was refluxed for 2-3 hours. The reaction was monitored via TLC and once the cyclisation was complete, the solvents were removed and the crude was purified via column chromatography. Yields for the reaction varied, ranging from 85-95%. The double bond could then be reduced using $Pd(OH)_2$ on carbon. The ring-closed receptor was dissolved in EtOAc and an excess of palladium catalyst was added. A balloon was used to supply the hydrogen over the 16 h period. After several unsuccessful attempts varying solvent, temperature and H_2 source, the reduction was finally accomplished through the addition of a few drops of NEt_3 to the reaction mixture. The addition of NEt_3 results in the formation of a trialkyliminium–palladium hydride complex, which acts as the H_2 source in this reaction.[2] The success of this approach could be due to the homogeneity of **42** and the hydrogen source. The work up consisted of filtration through a plug of silica and washing with EtOAc, affording the reduced product in near quantitative yields.

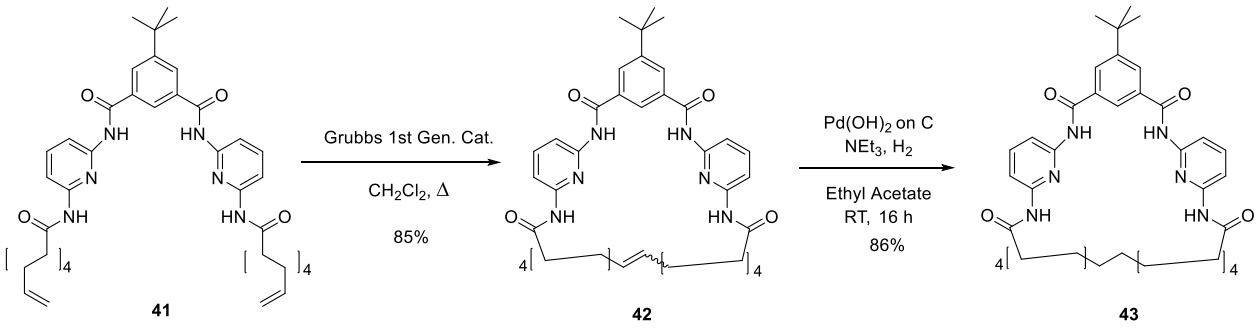

Scheme 2.3 - Synthesis of cyclic receptors via Grubbs catalysis.

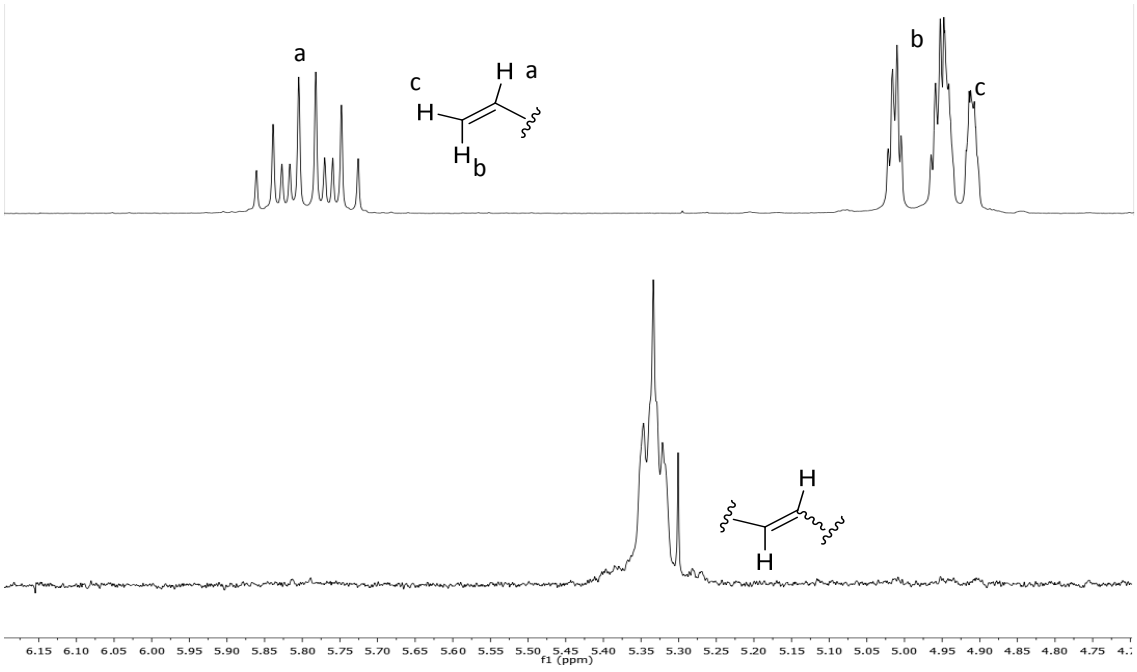

Figure 2.2 – ^{1}H NMR comparing the allyl regions before and after metathesis.

The ^{1}H NMR spectra in **Figure 2.2** show the allyl region of the acyclic receptor **41** before and after metathesis. The terminal olefin gives two peaks at 4.95 and 4.79 in the acyclic form and after metathesis a single peak at 5.33 is observed. Concerns with this metathesis method towards a clipping approach were the possible lack of H-bonded complexation between host and guest at the reflux temperature required for the reaction and also a potential adverse effect on the reaction when carried out in the presence of a

barbiturate thread. Therefore, the feasibility of this cyclisation under alternative conditions was investigated. All reactions were carried out in DCM with a receptor concentration of 4.5 mM. 10 mol% Grubbs catalyst was used at room temperature. The progress of each reaction was monitored via TLC.

Table 2.1 – The yields of various Grubbs catalysed metathesis reactions of **41** at room temperature.

Catalyst	Additive	Yield
Grubbs (I)	-	70%
Grubbs (I)	Barbital (1 equiv.)	82%
Grubbs (II)	-	70%

After periodically monitoring the conversion over 4 hours, there was still starting material remaining and so the reactions were left overnight. Each was then worked up in identical fashion to the original method and the yields are shown in **Table 2.1**. It appears that the reaction of **41** suffers a slight decrease in yield when conducted at room temperature compared to the yield obtained under reflux (85%) and that there appears to be no discernible difference between the Grubbs (I) and (II) catalysts. Interestingly, the reaction yield was observed to increase upon the addition of 1 equivalent of barbital. This is probably due to some degree of preorganistion, whereby the receptor, when bound to barbital, positions the terminal olefin groups in a more favourable position for metathesis/cyclisation to occur. An important consequence of this addition was the fact that it was not possible to obtain the pure, cyclised receptor from this reaction and only a H:G complex was obtained when purifying the reaction mixture via column chromatography, and methanol was then used as a competitive solvent to obtain the pure product. This has important implications with regards to any detection/purification of interlocked structures since the H:G complexes may elute together, regardless of their interlocked nature. Further

competition studies would therefore be required to confirm the interlocked nature of a H:G complex.

2.1.2.2 Direct Cyclisation:

The second method towards cyclic receptors consisted of a cyclisation reaction between the bridge receptor and the desired diacid chloride, **Scheme 2.4**. The diacid chloride, **44**, was synthesised from the commercially available hexadecanedioic acid using $(COCl)_2$ with DMF catalyst in DCM. As before, the diacid chloride was used as obtained and reacted with **40** in THF, with NEt_3 as a base in a high-dilution, macrocyclisation reaction. This method involved the simultaneous and slow addition of receptor and acid chloride to the reaction vessel via the use of syringe pumps over a period of two hours. This serves to minimise the intermolecular side reactions, and any subsequent polymerisation inherent in cyclisation reactions. After stirring overnight, the volatiles were removed and the crude was purified via column chromatography giving the pure macrocycle, **45**, in 33% yield. The yield for this reaction, despite being low, is fairly typical for this type of cyclisation.

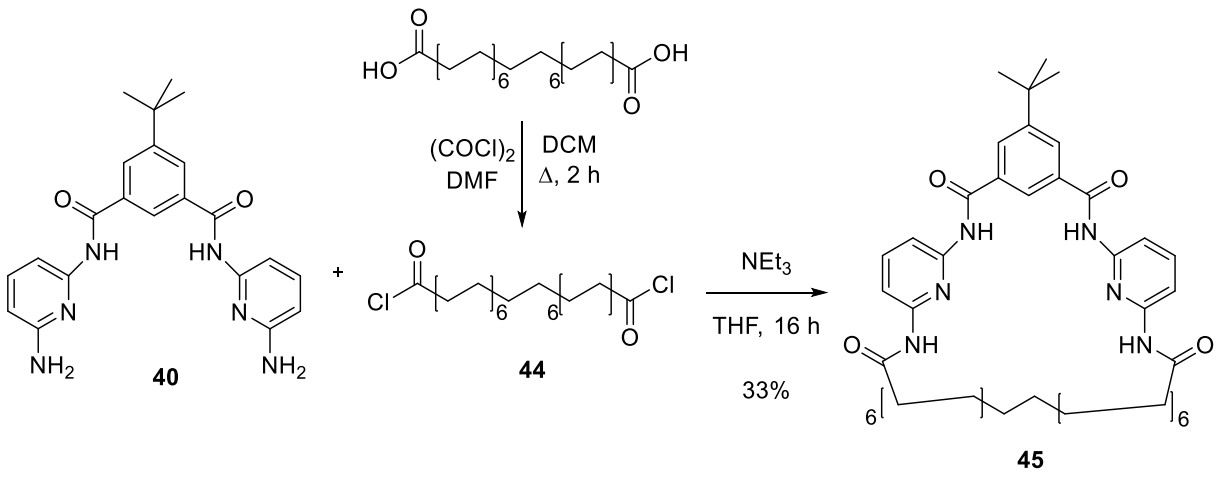

Scheme 2.4 – Synthesis of **45**, via macrocyclisation.

2.2 Synthesis of the Stopper Group

The stopper group chosen for these sets of interlocked compounds was the bulky 4-(tris(4-(tert-butyl)phenyl)methyl)phenol, **48**. Following the literature procedure set out by Stoddart,[3] the synthesis was fairly trivial, with high yielding reaction steps (**Scheme 2.5**).

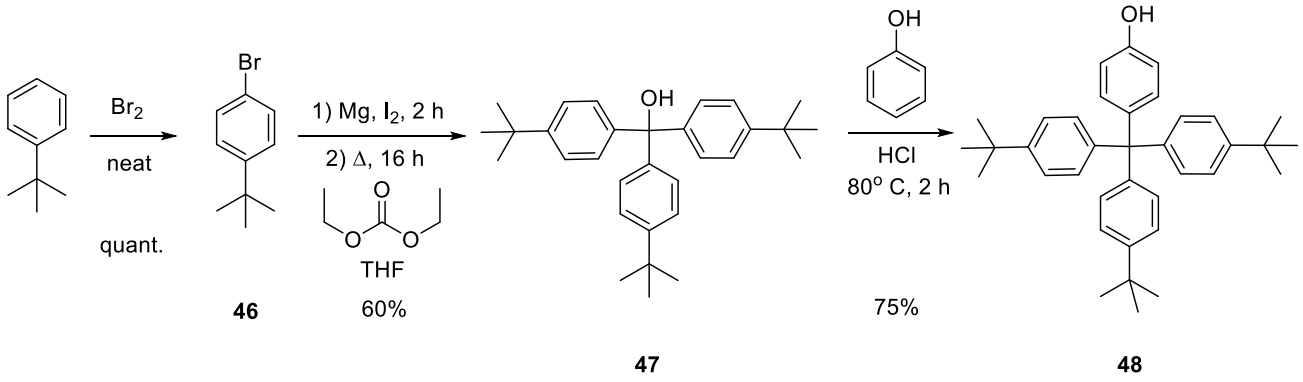

Scheme 2.5 – Synthesis of the stopper group, **48**.

The first step was a bromination of *tert*-butyl benzene, giving the bromobenzene, **46**, which was then used as obtained to form a Grignard reagent, using magnesium with catalytic iodine. The following reaction involved a threefold attack of the Grignard reagent on diethyl carbonate, which upon quenching, formed tris(4-(tert-butyl)phenyl)methanol, **47**, which was purified via recrystallization. The final step was a Friedel Crafts reaction of **47** in phenol using HCl as a catalyst. After work up, the crude was again purified via recrystallization affording **48** in a good yield. Depending on the functionalization required, the free OH of **48** could now be derivatized with any number of reacting groups as outlined in the following sections.

2.3 Synthesis of Flexible Barbiturate guests

2.3.1 Concept

These barbiturates are termed 'flexible' due to the type of functionality at the 5-position. The barbiturates are functionalised with CH_2 linkers and as a result, other than the minor directionality imposed by the sp^3 carbon, have an inherent flexibility about this point. The initial target compounds were the synthetically simple, flexible barbiturates to be used in a clipping approach in attempts towards both catenanes and rotaxanes (**Figure 2.3**). The formation of rotaxanes via a clipping method, as in (a), involved using a pre-stoppered barbiturate and an acyclic receptor and obtaining the interlocked structure via Grubbs-catalysed metathesis. A second approach, targeting catenanes as in (b), required the barbiturate to consist of bis-functionalization at the 5 position with long alkyl chains terminating in olefin groups. It was anticipated that these molecules would be able to thread through the macrocycle, forming a pseudo-rotaxane, with subsequent clipping via Grubbs-catalysed metathesis producing the desired interlocked structure.

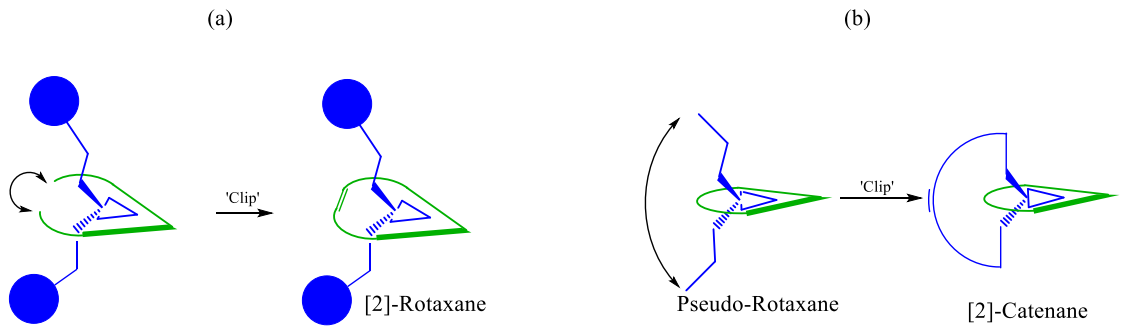

Figure 2.3 – Schematic diagram shows the various Grubbs catalysed clipping methods involving bis-olefins.

2.3.2 Stopper Terminated Barbiturates

The first investigation regarding the synthesis of interlocked structures was towards rotaxanes via the pre-stoppered barbiturate (**Figure 2.3(a)**). The synthesis of these flexible barbiturate guest molecules followed the classical barbiturate synthesis via di-substitution of diethyl malonate. The first step in the synthesis was functionalization of the stopper group with a triethylene glycol linker (**Scheme 2.6**). The bis-iodo compound was used to allow further reaction at the terminus of the linker once it has been attached to the stopper. Although formation of the unwanted, di-substituted product would compromise the yield of product, this side reaction was minimised through the use of a large excess of the bis-iodo compound (10 molar equivalents) compared to **48**. After the addition of K_2CO_3, the suspension was stirred overnight under reflux. The solvent was then removed and the crude product was purified via column chromatography. A moderate yield was obtained but this was considered acceptable given that di-substitution could still occur and that the starting materials could be synthesised in large amounts.

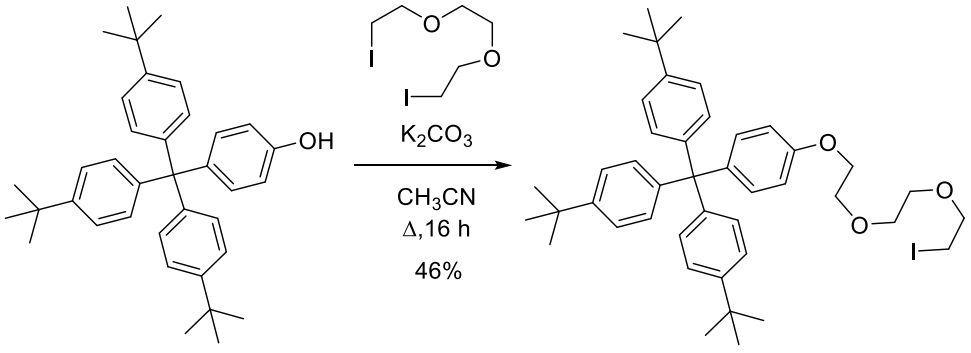

48 **49**

Scheme 2.6 – Synthesis of the stopper group with pendant arm, **49**.

The next step was to attach the stopper group **49** to diethylmalonate for cyclisation (**Scheme 2.7**). Diethyl malonate was added to a suspension of NaH in THF. After stirring for 30 minutes, **49** was added and stirred. However, although the reaction was refluxed over a period of three days, only starting material was recovered after work up and purification.

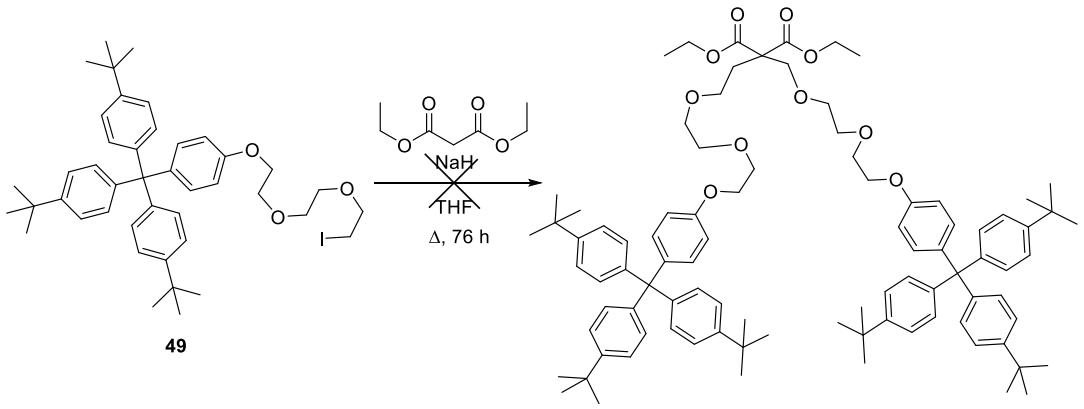

Scheme 2.7 – Unsuccessful attempt towards a di-substituted malonate.

The reason for this reaction being unsuccessful is possibly due to a poor solubility of **49** and steric factors concerning the attachment of two bulky groups to the alpha carbon of the malonate. **49** was recovered from the reaction mixture. Similar reactions have been carried out with a structurally similar trityl stopper and these were only achieved in 9% yield.[4] The trityl group is less bulky than this tris-alkyl analogue and so it may appear that the required di-substitution is not possible with these compounds. To overcome this steric problem, an increase in chain length is possible. However, long chains might hinder the clipping process due to an increase in rotational degrees of freedom, negating the effect of the sp^3 carbon. Also, when considering the final cyclisation of the disubstituted malonate with urea, these reactions have been shown to suffer reduced yields when using bulky substituents, when compared to the previous di-substitution step.[4] For these reasons, the

desired product appeared unattainable and so the synthesis of flexible stoppered barbiturates and the approach of clipping these compounds towards a rotaxane was not investigated further.

2.3.3 Olefin Terminated Barbiturates

The investigation towards interlocked structures then turned towards the clipping approach using olefin terminated barbiturates (**Figure 2.3(b)**). The synthesis followed the same procedure for the unsuccessful stoppered-barbiturate synthesis already outlined, but a related strategy had already been shown to be successful in previous projects.[4]

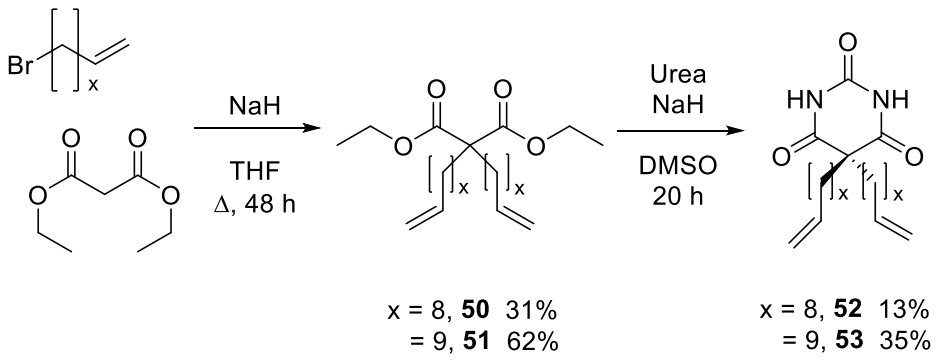

Scheme 2.8 – Synthesis of olefin terminated flexible barbiturates **52** and **53**.

The allyl bromide of desired chain length was first reacted with diethyl malonate in THF with 2.2 equivalents of NaH. The reaction mixture was purified using column chromatography to afford the di-substituted malonates **50** and **51**. These were then cyclised with urea in DMSO and the crude was purified via column chromatography to form the 5,5,bis-substituted barbiturates **52** and **53** (**Scheme 2.8**).

2.3.4 Binding Study of a Flexible Guest

The barbiturate guest, **53**, was then investigated for its binding properties with the Hamilton receptor **45**. A solution of **45** was made up to a concentration of 5.08 x 10^{-3} M (in $CDCl_3$) and then a guest solution, at concentration 5.13 x 10^{-3} M, (in $CDCl_3$) was added to the receptor solution. The host:guest interaction is shown below in **Figure 2.4**.

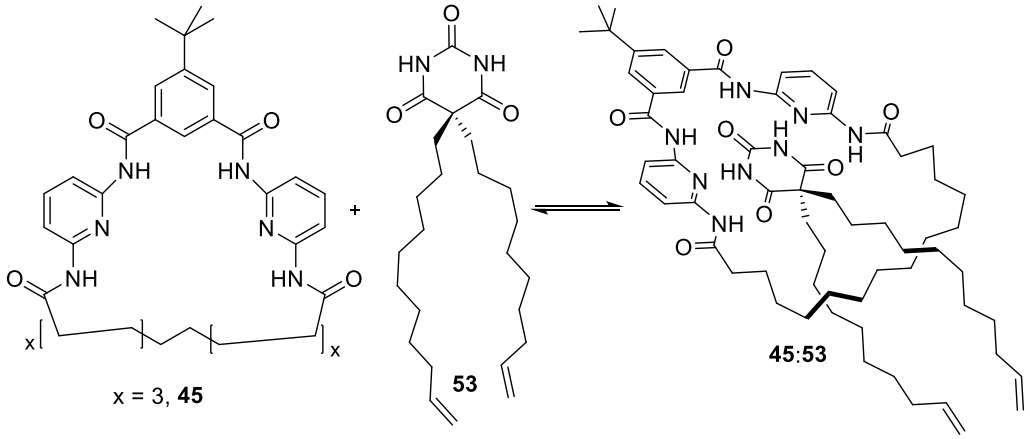

Figure 2.4 – Proposed Host:Guest interaction of **45** with **53**.

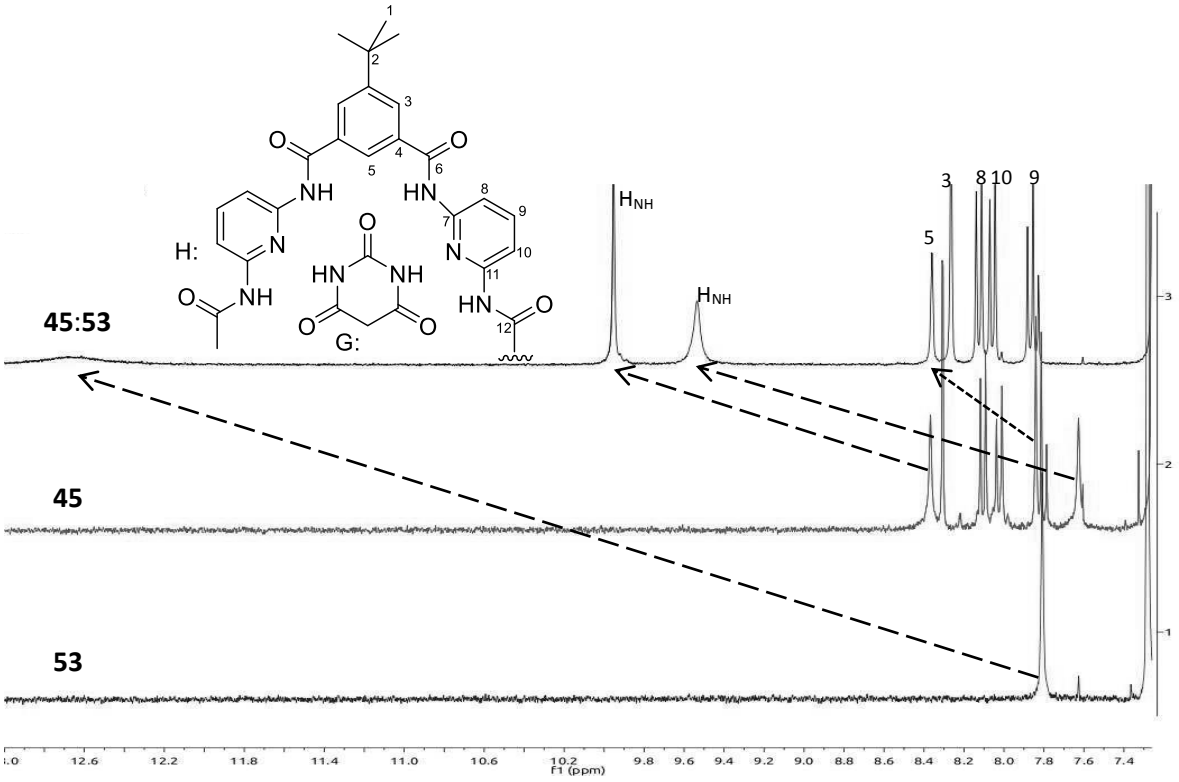

Figure 2.5 - ^{1}H NMR stack showing the aryl region of **45**, **53** and **45**:**53** complex at 289 K in $CDCl_3$ at 5.00 mM. Inset: Schematic of H:G interaction

The ^{1}H NMR spectra in **Figure 2.5** highlight the downfield region of each spectrum and clearly show the downfield shift of the N-H protons of both guest and receptor upon complexation indicating an H-bonded structure. The macrocycle H_{NH} protons experience a downfield shift of 2.11 ppm for the NH closest to the bridging benzene and 1.9 ppm for the second NH proton. A large shift of 4.87 ppm was observed for the barbiturate H_{NH} signal, showing a very strong interaction. Another significant shift noticed was the signal corresponding to the proton at position 5. The orientation of this proton places it in the binding site of the receptor and so a shift upon guest complexation is not unexpected, conversely the protons of the bridge and pyridine units on the exterior of the binding site experience very little shifting. This is strong evidence for the formation and orientation of the desired H:G complexation for barbiturate-templated interlocked structures.

The binding constant for the H:G system was measured via monitoring the H_{NH} shift of the macrocycle during a ^{1}H NMR titration experiment (**Figure 2.6**). This method involved the stepwise addition of known equivalents of guest into a solution of receptor and the addition of guest shifted the signal depending on the concentration and strength of interaction. A stack plot of the experiment clearly shows the gradual shift of the H_{NH} proton of the macrocycle, which moves relative to the concentration of guest added, up to 3.98 equivalents. The experiment was carried out using a concentration of 5.00 mM regarding the macrocycle, using the solvent system $CDCl_3$-5% DMSO. The DMSO was used to achieve full solubility of the macrocycle. However, being a competitive solvent, this will influence the binding constant relative to pure $CDCl_3$.

The experiment was carried out by the stepwise addition of up to 5 equivalents of guest molecule, however no increase in H_{NH} shift was observed after 3.98 equivalents and at this point the guest was considered fully bound to the macrocycle. It is worth noting the initial spectra (bottom) shows a shift in NH peaks relative to the previous example in **Figure 2.5**. This is due to the presence of a competitive solvent, DMSO. The peak shifts were used to assign the binding constant for this particular system and by treating the data using the software WinEQNMR[5] a binding curve (**Figure 2.7**) and subsequent binding constant can be extracted.

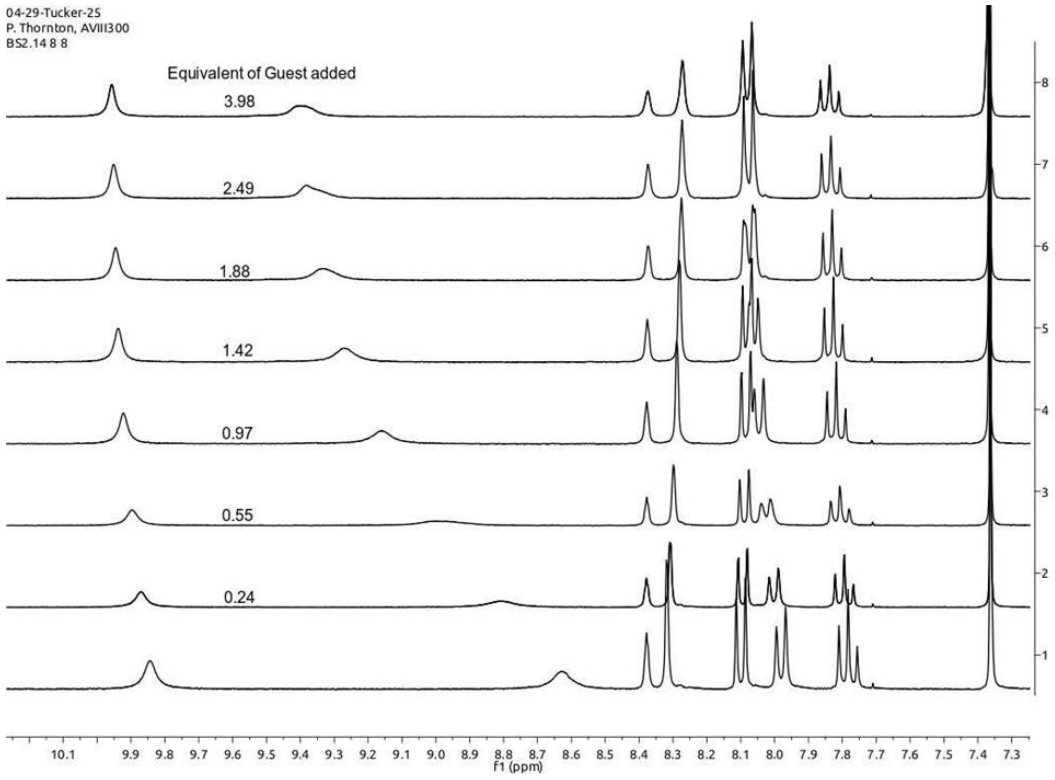

Figure 2.6 - ^{1}H NMR stack showing the aryl region of **45** upon addition of **53** up to and including 3.98 equivalents at 289 K.

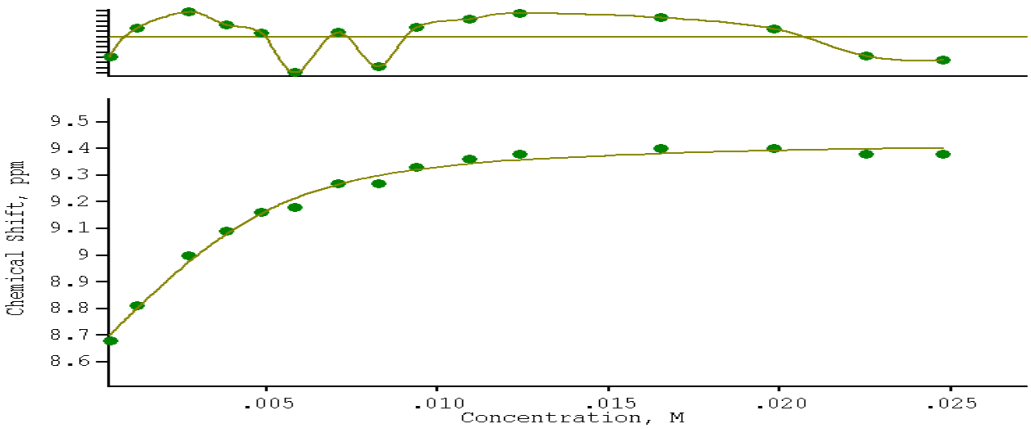

Figure 2.7 - Binding curve obtained via WinEQNMR, also showing deviation from the best fit.

The binding constant was found to be 1.07 x 10^{3} M^{-1} (± 200), giving a log(K) value of 3.03 at 298 K. The relatively large error observed in this value probably arose from the

difficulty in peak picking due to the broad nature of the NH peaks. Comparing the binding constant with the analogous compound, **52**, synthesised by Mathias Rocher, this appears to exhibit weaker binding. For the compound containing an 8-CH_2 linker, the binding constant was obtained using isothermal calorimetry and found to have a log(K) value of 4.62 ± 0.04.[4] This difference can be explained through the use of DMSO in the solvent system, since any competitive binding with solvent molecules would reduce the binding constant between host and guest.

2.4 Rigid Barbiturates

2.4.1 Introduction

Despite the ability of these guests' potential to thread and then cyclise, it was found previously that they may be too flexible. It can be envisaged that shorter lengths would have less degrees of rotation and therefore display more 'rigid-like' behaviour. However, any shorter lengths than those seen with x=8 would form a ring smaller than is found in any known catenane using a clipping approach.[6] So it seems that x=9 is the limit at which the catenane would readily form when using terminal groups in a cyclisation process. However, although sufficient flexibility would be required to ring close around the macrocycle, such inherent flexibility in the barbiturate chains would not particularly favour the initial threading process, with any cyclisation only occurring in a 'perched' conformation. Whilst both host and guest molecules are fairly planar in their own right, from the solid state crystal structure determined by Hamilton, it can be seen that the bound barbiturate and pyridine units, are not co-planar, with the barbiturate sitting out of the plane of the

receptor by 27°.[1] One can therefore imagine the situation where the arms of the barbiturate do not thread but instead form a perched complex as demonstrated in **Figure 2.8**.

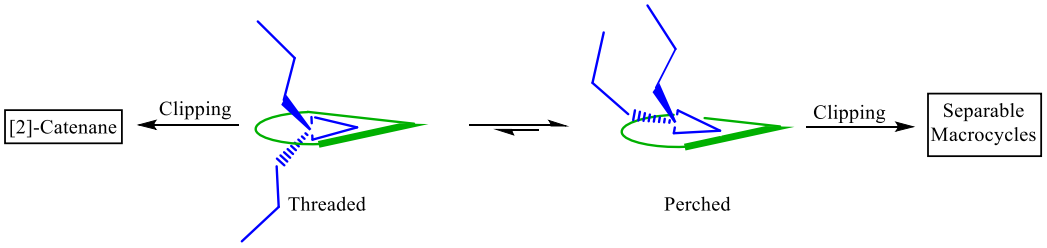

Figure 2.8 – Schematic to show the possible orientation between host and guest giving a 'perched' or 'threaded' complex.

Obviously, any clipping in the perched case would only lead to the recovery of two independent, non-interlocked macrocycles. One idea to circumvent this possible issue would be to synthesise more rigid guest molecules. It was thought that by introducing more rigidity at the 5-position, then the sp^3 directionality at this position could be emphasised and so if the barbiturate were to bind in the binding site, it would have a greater probability of threading through the macrocycle. Similarly, this problem encountered with threading can be applied to the concept of rotaxane formation. In other words, when clipping around the barbiturate dumbbell, if there is not sufficient rigidity or directionality in the spacers between the barbiturate and the stoppers, then there would be less chance of a clipping event occurring around the axle of the dumbbell. To create this rigidity, a phenyl group spacer was proposed (**Figure 2.9**), although this posed a much greater synthetic challenge over the flexible guest molecules.

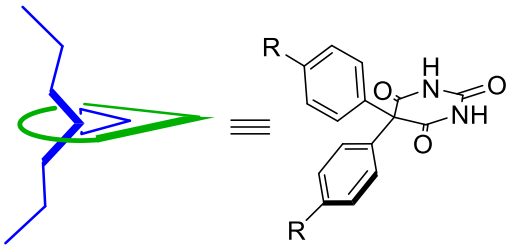

Figure 2.9 - Schematic showing the chemical analogue of a proposed 'rigid' barbiturate.

Previous synthetic procedures found in the literature for the formation of the bis-arylated barbiturate **54** consisted of a Friedel Krafts reaction of alloxon monohydrate (**Scheme 2.9**).[7] However this is only suitable for simple aryl compounds and is not applicable for the longer chains and the types of functionality for an interlocked structure.

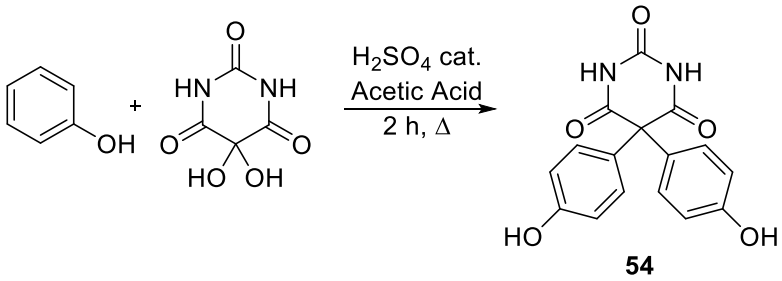

Scheme 2.9 – Classical synthesis of diphenyl barbiturates.

One might propose to simply functionalise the free OH group of the phenol. However this is not possible due to the relative acidity of the imide protons of the barbiturate and so any substitution would occur at this site rather than at the required OH, as shown in **55**, **Scheme 2.10**.

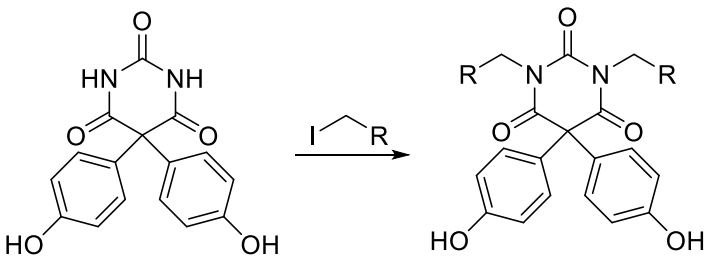

54 **55**

Scheme 2.10 – N-functionalisation rather than at the desired phenol substituent.

It was therefore desirable to find alternative means to achieve the bis-arylation of barbituric acid. A method reported by Kopinski et al.[8] was found, as discussed in detail in the following section.

2.4.2 Arylation Reactions using Organolead(IV) Compounds

A reaction which has proved extremely useful throughout this thesis in the synthesis of new barbiturates is the arylation reaction of aryl lead tricarboxylate compounds. The efficacy of these compounds in the arylation of carbon nucleophiles was first discovered in the mid-70's after the group of Pinhey et al. conducted studies of aryllead(IV) tricarboxylates with TFA[9] and later applied this chemistry towards the synthesis of a series of biaryl compounds.[10, 11] The approach was extended to a wide range of soft carbon nucleophiles such as β-dicarbonyl compounds, **Scheme 2.11**, the motif found within barbiturates, and led to highly substituted quaternary carbons. Incidentally, these additions exhibit higher yields and faster reaction times when $R_1 \neq H$.[12]

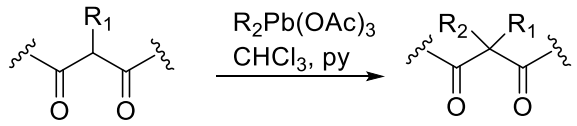

Scheme 2.11 – Arylation of β-dicarbonyl compounds.

The process of generating these aryllead(IV) tricarboxylates can be through either direct plumbation or metal-metal exchange, with the latter being the more widely accepted method. The first example of metal-metal exchange was shown by Kocheshkov[13] in 1952 generating the target compound using mercury(II) acetate. The use of various metal/semimetal centres has since been shown, including the use of mercury, tin and silicon. However, the use of mercury catalysed boron-lead exchange, as explored by Pinhey,[14] displayed a simpler method when compared to mercury or tin exchange, and a greater economy in terms of aryl group transfer. Generation of the active species **56**, to be used in situ, is shown in **Scheme 2.12**.

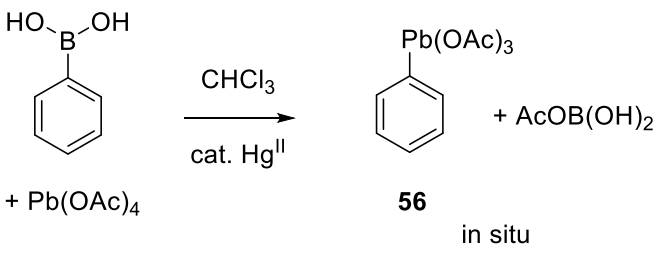

Scheme 2.12 – Formation of the *in situ* organolead species.

The aryllead(IV) tricarboxylates, generated via transmetalation, behave as aryl cation equivalents with their most useful reactions being, but not limited to, those with soft carbon nucleophiles, resulting in *C*-arylation. In general, these reactions proceed with greater yields when more acidic substrates are used. This concept was applied by Pinhey towards barbituric acid in the synthesis of ibuprofen and phenobarbital and showed that diarylation of β-diketones containing two α-hydrogens was possible and that the acyclic precursor diethylmalonate was unreactive.[15]

Despite some reported arylations experiencing steric inhibition, the hindered compounds which can be obtained with this reaction point towards a ligand coupling mechanism as described by Trost and shown below in **Figure 2.10**.[16]

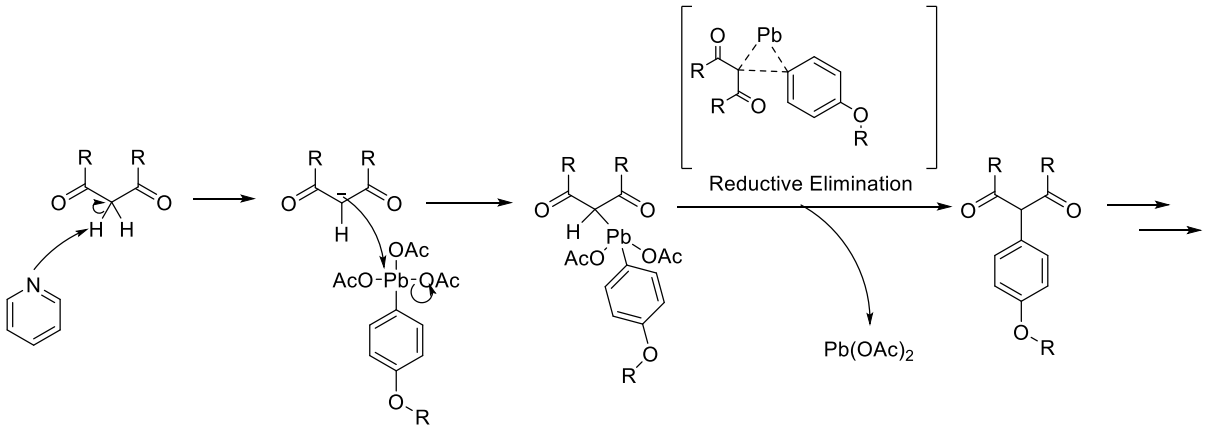

Figure 2.10 – Mechanism of arylation.

The process involves deprotonation of an α-hydrogen, and subsequent attack from this nucleophilic centre to form the organolead intermediate. A reductive elimination step forms the new C-C bond, and a subsequent addition of a second aryl group will afford the diarylated product. Through the use of this lead mediated ligand coupling mechanism, using phenylboronic acid precursors, they were able to functionalise barbituric acid with two para-methoxyphenyl groups, in essence achieving the compound shown above in **Scheme 2.9** (R=Me), but via what could be a more synthetically useful procedure if tolerant to different functionality. Applying this towards rigid guests for interlocked systems, shown in **Scheme 2.13**, the synthesis of these 'rigid' compounds requires forming the boronic acid, and then utilising a boron–lead exchange to form an aryl-lead intermediate. Despite the examples of Pinhey showing the substitution of simple phenyl groups it was hoped to extend the synthesis to the more elaborate groups required for an interlocked structure. For

the purposes of clipping, X can be either olefin terminated groups towards a catenane, or a bulky stopper group for subsequent clipping with a receptor to from a rotaxane.

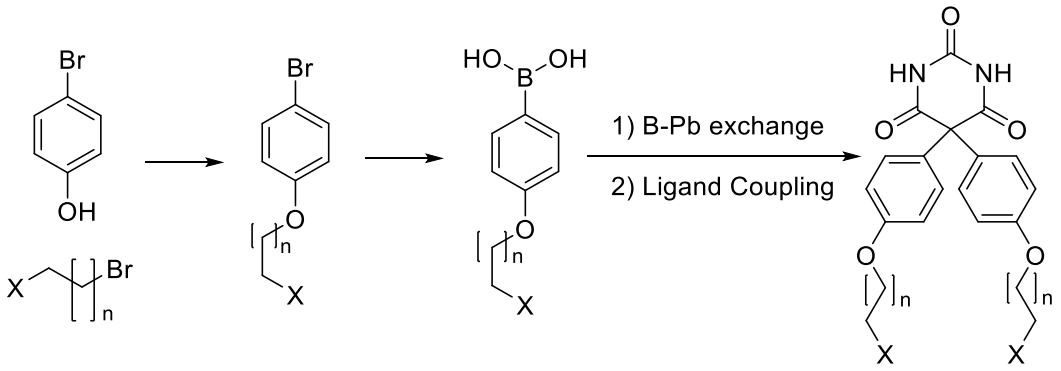

Scheme 2.13 - Proposed synthesis of rigid barbiturates utilising boron/lead exchange.

2.4.3 Synthesis of Rigid Barbiturates - Olefin Terminated Compounds

The initial strategy investigated toward these rigid barbiturates was in aiding the threading process and so the phenyl spacer was appended with an alkyl chain terminated in an olefin group. To test the synthetic strategy in the presence of olefin groups, a test synthesis was first carried out using allyl bromide (x = 1) (**Scheme 2.14**).

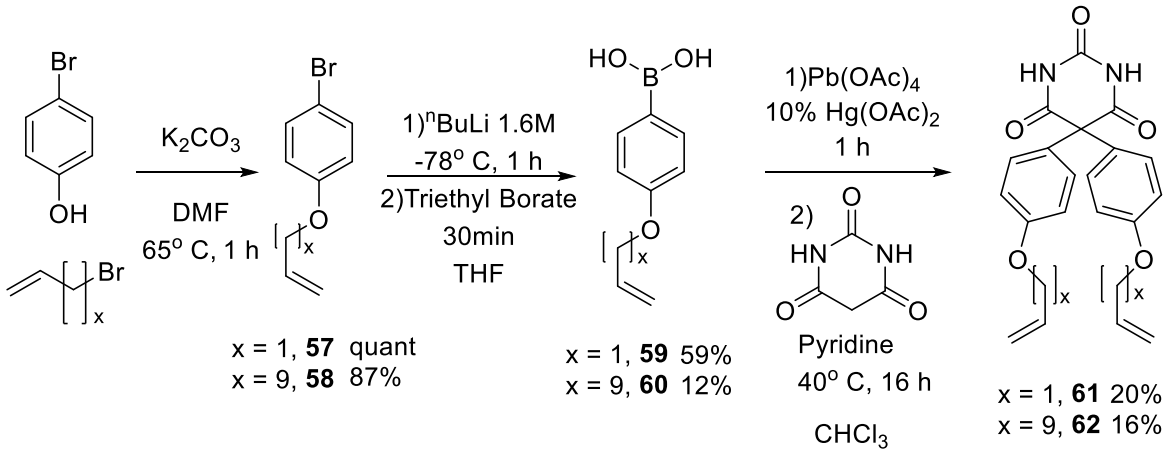

Scheme 2.14 – Synthesis of allyl functionalised phenylboronic acids.

The synthetic strategy began with the funtionalisation of bromo phenol with the required bromo alkene. The allyl bromide was attached via nucleophillic substitution at the phenol OH using K_2CO_3 as a base, and compound **57** was obtained in excellent yield. The next step, formation of the boronic acid, consisted of a lithiation step at -78^o C in THF using ^{n}BuLi. The reaction was then quenched with triethyl borate and formed the boronic acid, **59**, which was purified using recrystallization from water and obtained in good yield.

The following key step was a boron-lead exchange reaction between phenyl boronic acid and $Pb(OAc)_4$ (**Scheme 2.14**). The lead(IV) tetra-acetate was dissolved in dry $CHCl_3$ along with a catalytic amount of mercury(II) acetate and heated to 40^o C. The boronic acid, **59**, was then added under argon flow, via spatula, over a period of 15 minutes. Stirring at 40^o C was maintained for 1 h as the boron-lead exchange occurred. Addition of barbituric acid with molar equivalents of pyridine followed and the suspension was then stirred overnight. After work up, the crude product was purified via column chromatography to obtain the bis-arylated product, **61**. This 'proof of concept' guest molecule highlights the possibilities of introducing and employing a more widely varied library of barbiturate substituents for interlocked structures.

Despite this successful and optimistic synthesis where x=1, when extending the chain to a longer and more useful tether, a number of problems arose. When x=9, the functionalization of bromophenol to form **58** proceeded well and in good yield. However the formation of the boronic acid, **60**, was hindered due to gel formation, almost certainly due to a combination of the low temperature and increased chain length. To overcome this, repeated warming and cooling of the reaction, to reform a solution, was needed and this

will have contributed towards the reduced yield. The boronic acid, once formed, was only able to be purified via column chromatography. However, boronic acids are fairly unstable regarding purification via this method and this will have also contributed towards the reduced yield. Attempts were made towards recrystallization but no suitable method and/or solvent was found. Boronic acid, **60**, was then used in the synthesis of **62** and showed similar yields to the allyl analogue. The more easily isolatable butandiol bromo-ester was synthesised and used in the B-Pb exchange reaction, but despite reports that the boron/lead exchange can occur with both the boronic acid and ester analogues,[8] this also proved unsuccessful and only starting materials were recovered, implying the initial exchange could not occur. Despite observing low, but adequate yields in the final boron-lead exchange step, the process of forming and purifying the olefin-terminated phenylboronic acid, **60**, was deemed too problematic and so another synthetic strategy towards these rigid barbiturates was required.

2.5 Rigid Barbiturates – Stopper Terminated Compounds

Due to the synthetic challenge of olefin terminated rigid barbiturates, and the template effect already observed in the cyclisation of receptor **41,** the most promising route toward an interlocked structure should be clipping the receptor around a dumbbell shaped barbiturate, forming a rotaxane. Previous work has shown this to be difficult with the use of flexible threads[4] and so it would be desirable for the synthesis of dumbbell barbiturates with phenyl spacers.

2.5.1 Trityl Stoppers

The initial approach was to follow the procedure mentioned previously, via the phenyl boronic acid to arrive at the bis-arylated dumbbell (**Scheme 2.14**). However, the synthesis was even more challenging than with the olefin derivatives due to the solubility of **63** and no boronic acid was able to be formed and only the starting material was recovered (**Scheme 2.15**).

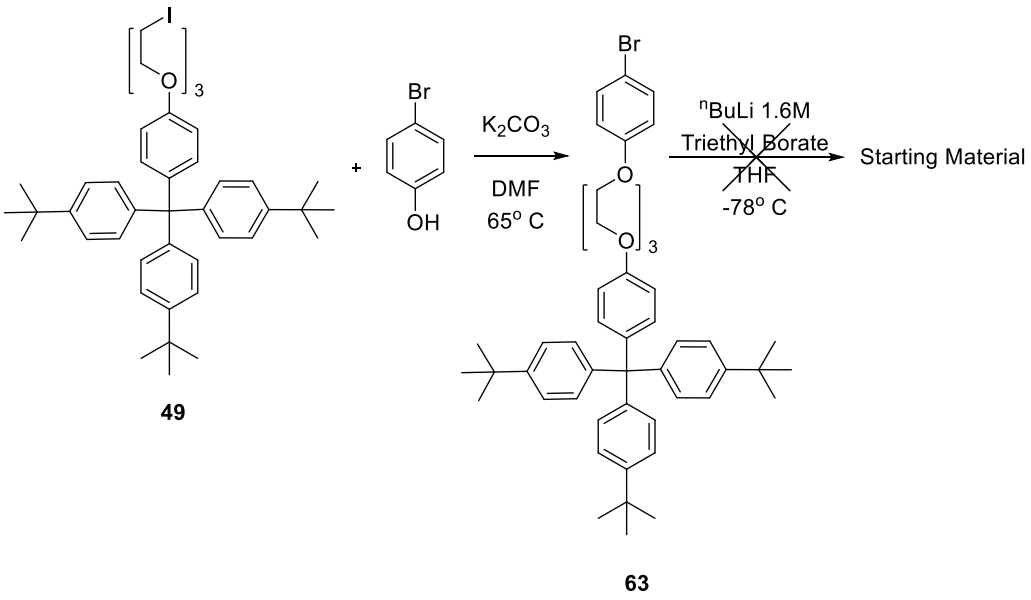

Scheme 2.15 - Unsuccessful attempt toward a stopper derivitised phenyl boronic acid.

2.5.2 Silyl Stoppers

Due to the issue of the solubility of **63**, an alternative silyl group was proposed. The common protecting group *tert*-butyldiphenyl silyl (TBDPS) is a relative bulky group and although somewhat labile, it is the most stable in the silyl protecting group series. A crude 3D model constructed in ChemBio3D Ultra (**Figure 2.11**), shows the relative sizes of the stopper and macrocycle in a space filling display mode showing the stopper is in fact bulky

enough and unable to slip over the ring, however further and more in-depth computational studies would be required to confirm this.

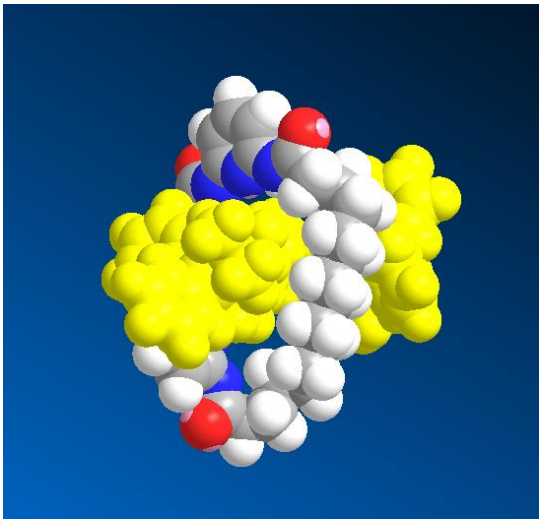

Figure 2.11 - ChemBio3D Ultra model depicting **45** with a TBDPS stoppered thread (yellow).

The synthesis again started from bromophenol and is shown in **Scheme 2.16**. Addition of a triethylene glycol unit via an iodine substituent was achieved using K_2CO_3 and NaI in DMF. The reaction was heated for 24 hours at 110^{o} C and after work up was purified by column chromatography to give **64** in good yield of 70%. The tether was then functionalised with TBDPSCl and **65** was formed in 45% yield. Subsequent formation of the boronic acid was carried out as previously described to give **66**. The compound showed enhanced solubility due to the silyl group and conversion was achieved pure and in quantitative yields, with no column necessary. Unfortunately, the desired product was not formed in the following step and **66** was returned without the boronic acid group. For this reason, the silyl-stopper series of compounds was not investigated further.

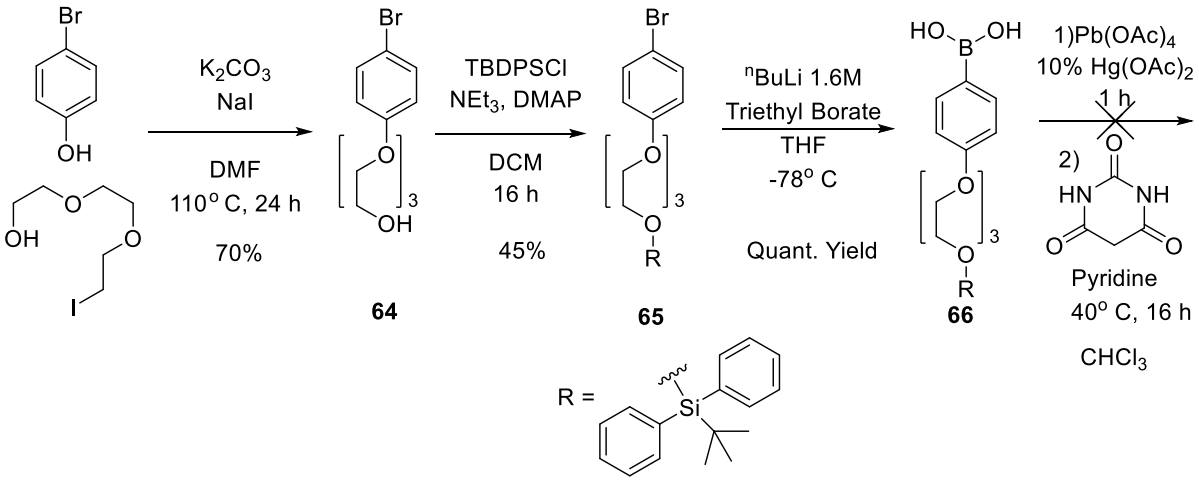

Scheme 2.16 – Synthesis and subsequent failure of the TBDPS stoppered compounds.

2.5.3 'Protect-First' Strategy

Due to the clear problems surrounding the current strategy regarding the synthesis of these bis-arylated barbiturates it seemed necessary to find an alternate route. It was for this reason that a 'protect-first' strategy was proposed. It seems the boron-lead exchange reaction is not feasible with large functional groups and when these are present, the synthetic route can also be problematic when forming the boronic acid. A method involving addition of the aryl groups at as early a stage as possible and then focusing on the functionalisation of these phenyl groups could be the most successful strategy. The target intermediary of the protection strategy is shown below in **Figure 2.12**.

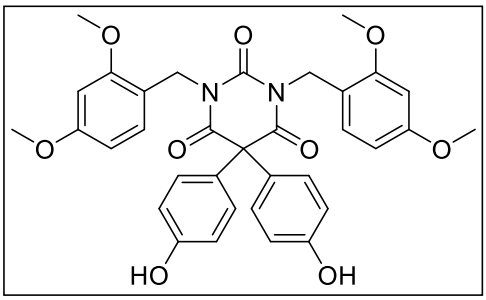

Figure 2.12 – Intermediate target towards dumbbell barbiturates.

Attachment of imide protecting groups allows the required functionalization of the aryl OH groups. The protecting groups were used in order to circumvent the problem of functionalising the imide site over the OH of the aryl group. The protecting group chosen was 2,4-dimethoxy benzyl (2,4-DMB).

2.5.3.1 Synthesis of Benzyl Protected Barbiturates

Before any protection strategies were attempted, the initial protected barbiturate was synthesised. This was achieved in two high yielding steps (**Scheme 2.17**) starting with the formation of a bis protected urea, **67**, using a modified literature procedure.[17] 2-4,dimethoxybenzylamine was dissolved in DCM and cooled to 0^{o} C. The 2-4,dimethoxybenzylisocyanate was then added dropwise resulting in the instantaneous precipitation of the product which was isolated through filtration in quantitative yield. **67** was then cyclised with malonic acid, again using a modified literature procedure[18] via refluxing in acetic anhydride overnight. Subsequent work up afforded a yellow solid of 1,3-bis(2,4-dimethoxybenzyl)Barbituric acid, **68**. ^{1}H NMR analysis showed that the product appeared pure. However subsequent dissolving in DCM and refluxing with charcoal produced a clean, fluffy-white solid which reduced the yield but resulted in an improvement in the yields of subsequent reactions.

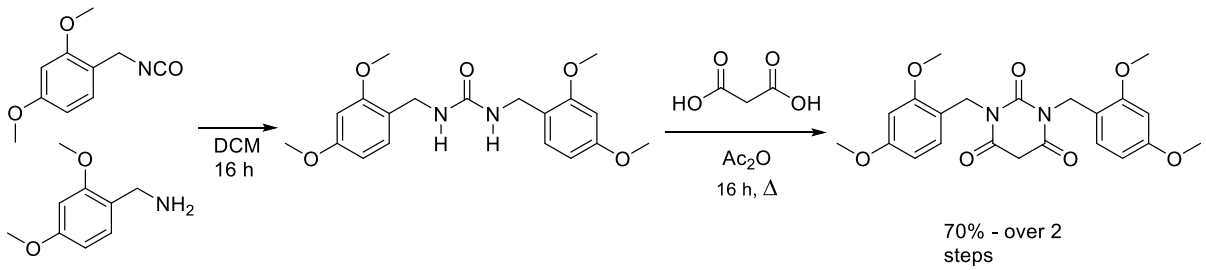

67 **68**

Scheme 2.17– Synthesis of N-protected barbiturates

2.5.4 Protect First Strategy and the Feasibility of Key Reactions

The 'protect first' strategy is shown schematically in **Scheme 2.19** below and begins with the protected barbiturate **68**. The first step was a proposed arylation with a simple boronic acid. Keeping the boronic acid as simple as possible was key towards the success of this route, and allowed a much more feasible addition to the barbiturate compared with the low yields and challenging synthesis seen with more complicated systems. The simplest aryl motifs for this protection strategy are shown below in **Scheme 2.18** where a free OH is present allowing subsequent functionalization. The B-Pb exchange reaction was attempted, but the presence of free OH groups seemed to interfere with the reaction and both attempts were unsuccessful. The starting material **68** was recovered and the boronic acid suffered degredation.

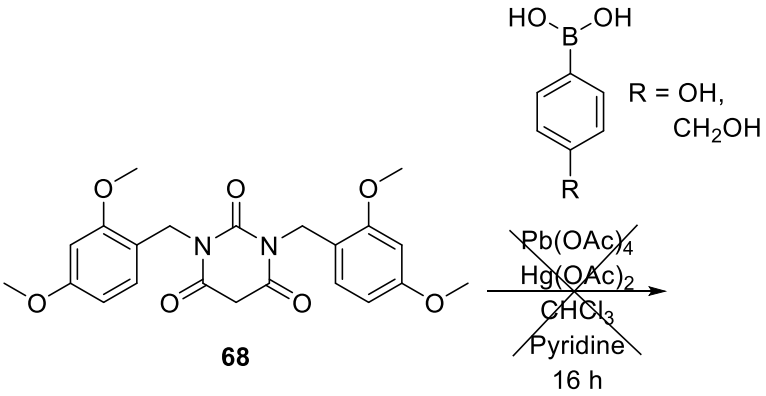

Scheme 2.18 – Attempts towards arylation of **68** using simple phenylboronic acids.

This problem introduced an extra protection/deprotection step into the strategy. Once arylated with an O-protected phenylboronic acid, the steps follow deprotection of the oxygen, then functionalisation to form the thread motif and subsequent N-H deprotection giving the rigid "target dumbbell".

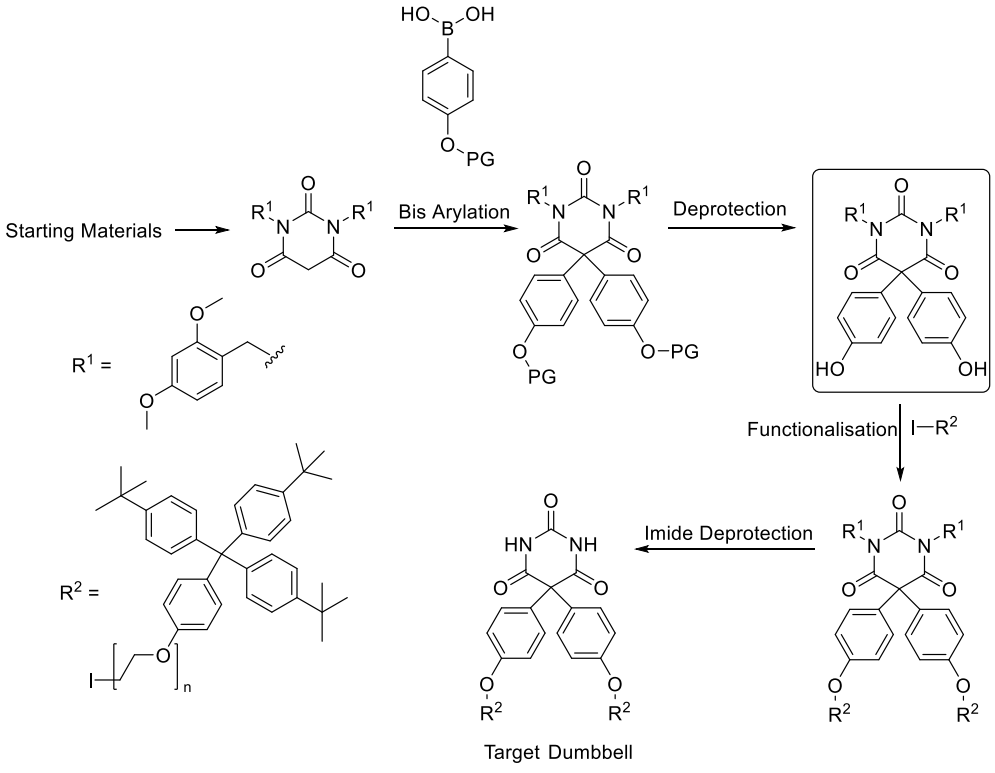

Scheme 2.19 – Modified protection strategy towards rigid barbiturates.

In order to test the feasibility of this protection strategy a series of test reactions of the key steps were first carried out, in some cases on analogues of the desired motifs. The first test was to ensure that the B-Pb exchange reaction will work in the presence of the N-benzyl protecting groups *and* when the phenyl boronic acid is appended with a small protecting group. Initial investigations were first carried out with bis-paramethoxybenzyl barbituric acid, **PMB-BA**, obtained from our collaborators in Bordeaux. The bis-arylation was achieved using the commercially available 3-methoxyphenylboronic acid and **69** was obtained (**Scheme 2.20**). The procedure followed for this step was the same as those mentioned for previous ligand coupling reactions.

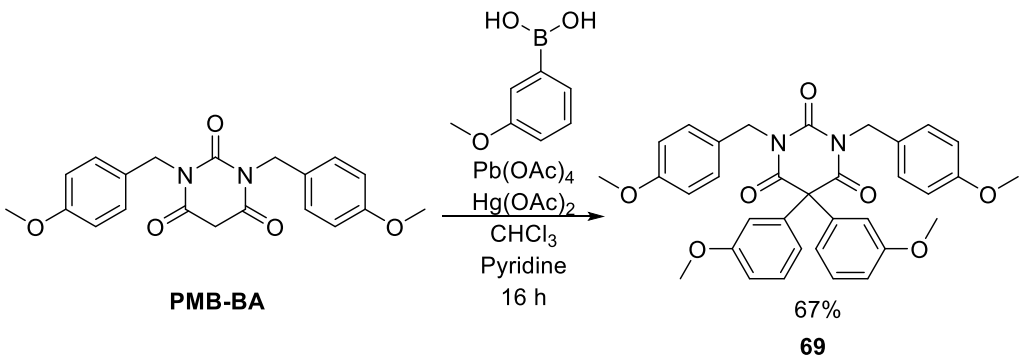

Scheme 2.20 - Synthesis of N-protected diphenyl barbiturate

Owing to this promising result it was important to determine that the newly attached phenyl groups were stable to any subsequent imide deprotection. This compound was then taken through various deprotections in order to determine the best method for removal of the benzyl groups. Reactions with Pd(C) or $Pd(OH)_2$ under H_2 atmosphere were unsuccessful and attempts to form the Boc-protected barbiturate, from **69**, followed by deprotection on work up were also unsuccessful. In each case only the starting material was recovered. Deprotection was found to be successful using ceric(IV) ammonium nitrate

(CAN). CAN is a one electron oxidizing agent which enables oxidative cleavage of protecting groups via an oxonium ion. The generic reaction pathway is shown in **Scheme 2.21**.[19]

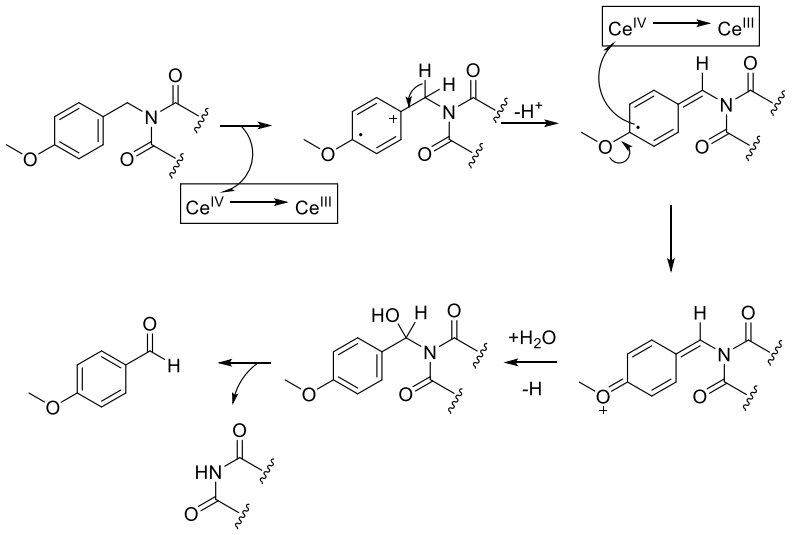

Scheme 2.21 - Mechanism of methoxybenzyl deprotection using CAN.

The protecting group is oxidized and cleaved in a two-step electron transfer process. Cerium is a strong oxidizing agent and two independent Ce(IV) atoms are reduced to Ce(III) in the electron transfer steps. The free amide and corresponding aldehyde are formed, both usefully diagnostic of the cleavage via ^{1}H NMR spectroscopy. The bis-arylated 2,4-DMB protected barbiturate, **69**, was then treated with CAN and left to stir overnight in a 1:3 solvent mix of water/acetonitrile (**Scheme 2.22**). After workup, and purification via column chromatography the product, **70**, was isolated affording the required deprotected barbiturate. Loss of protecting groups was confirmed by ^{1}H NMR spectroscopy and mass spectrometry.

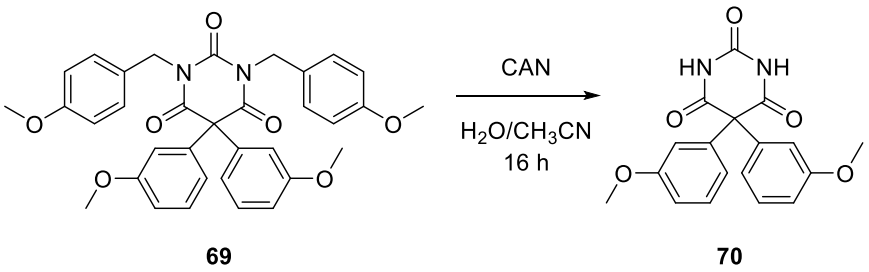

69 **70**

Scheme 2.22 – Synthesis of debenzylated diphenyl barbiturate, **70**.

Despite the success in removal of these protecting groups using CAN, it was decided to use the 2,4-dimethoxybenzyl analogues, as seen in **68**, since these should more labile groups compared with the example above due to extra resonance stabilisation.

2.5.5 Synthesis of Rigid Dumbbell Barbiturates

The protecting group for the O-phenylboronic acid to be used should have good stability during the ligand coupling reaction and be easily removed under conditions which do not remove the 2,4-DMB groups. The protecting group selected was TBDMS. Following **Scheme 2.23**, the TBDMS protected boronic acid, **72**, was synthesised in two steps from bromophenol. The first step involved protection of the OH group, and **71** was isolated in quantitative yields after column chromatography. The second step was formation of the boronic acid using the same method of lithiation and quenching with triethyl borate as seen previously giving **72** in good yield. The purification required the use of column chromatography due to any attempts at recrystallization being unsuccessful, and the isolated yields therefore suffered due to the purification step. **72** was then used in the ligand coupling reaction to form the bis-protected, diarylated barbituric acid, **73**. The boronic acid is required in excess (2.2 equivalents) and affords the product, after purification by column chromatography, in acceptable yields. Subsequent deprotection of

the silyl groups of **73** with TBAF in THF gave the deprotected product, **74**, in excellent yields after purification via column chromatography. As already stressed, **74** is an important intermediate in the synthesis of rigid barbiturates, owing to the fact that any number of different groups relating towards the synthesis of interlocked structures can be attached at a relatively late stage in the synthesis, provided that they are stable to the final CAN deprotection. Once the OH group is appropriately functionalised, all that remains is the final deprotection of the 2,4-DMB groups to achieve the rigid guests.

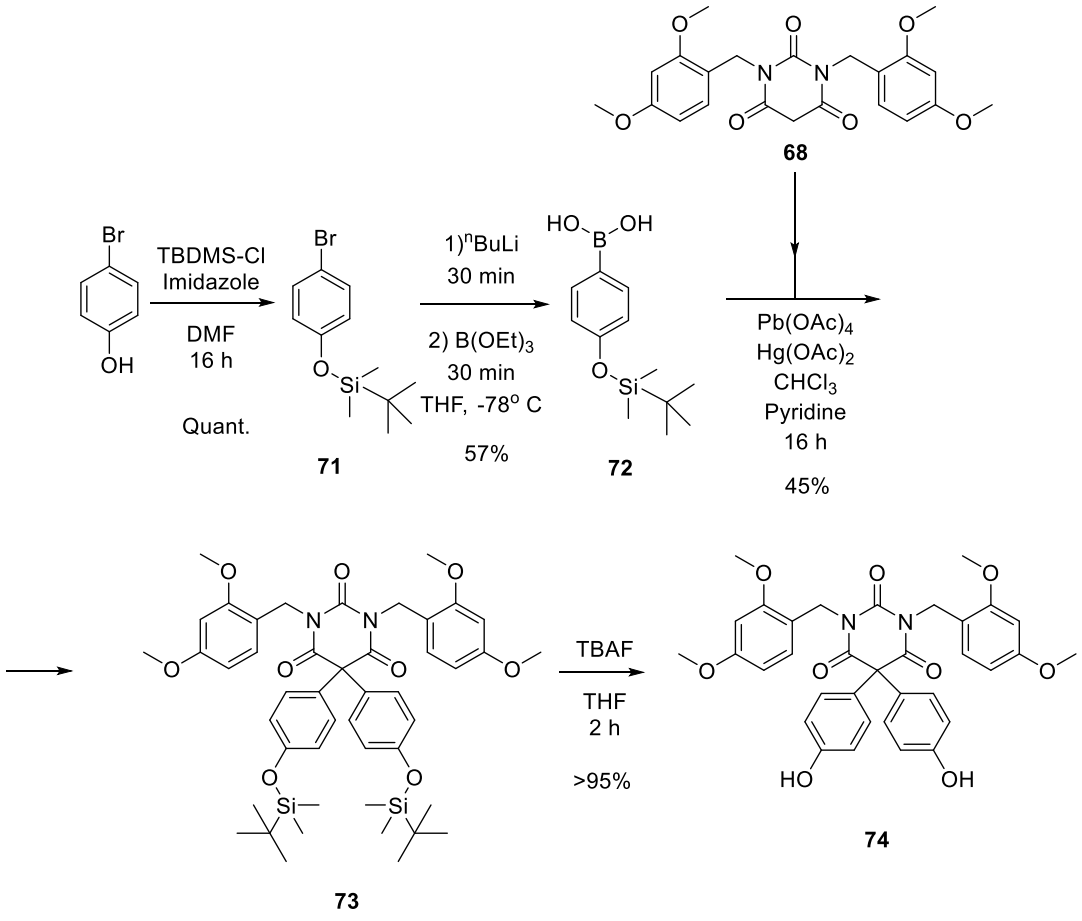

Scheme 2.23 – Synthesis of rigid thread precursor, **74.**

The molecule chosen to functionalise the barbiturate was the trityl phenyl appended with iodo-terminated triethylene glycol linkers (**Scheme 2.24**). Starting from the previously

synthesised compound, **49**, the stopper was attached to **74** by reacting it in excess, in DMF, with Cs_2CO_3 as a base. After work up and purification the stopper-terminated, rigid barbiturate, **75**, was synthesised in good yields of 75%. The next and final step in the synthesis involved deprotection of the 2,4-DMB groups. Due to the inherent issues of solubility found when using these stopper groups, the reported conditions for CAN deprotection (acetone/water)[19] were unacceptable for these series of compounds. A solvent mix of DCM/acetone/water was chosen and this was combined with gentle heating to allow for maximum solubility of the starting material, whilst still allowing the presence of the water required for the reaction. Monitored by TLC, the reaction was complete in only 15 minutes and after purification via column chromatography afforded the rigid, stoppered guest, **76** which was characterised via ^{1}H, ^{13}C and mass spectrometry. A low yield of 22% shows scope for optimisation of this reaction, whether through varying time, temperature or solvent system, but this fell outside the scope of the current investigation. These rigid, dumbbell shaped guest molecules can now be used for a clipping approach with acyclic receptor compounds as outlined in the following chapter.

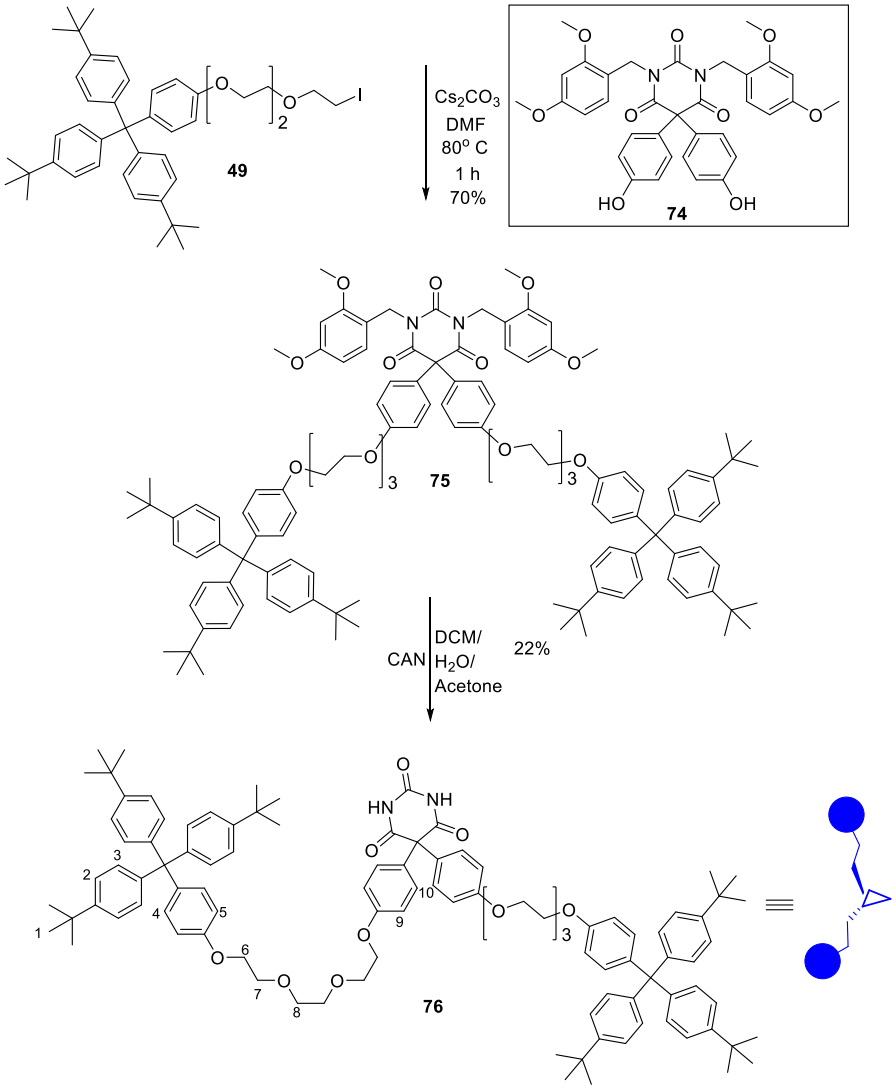

Scheme 2.24 – Synthesis of **76**, via attachment of stopper groups to **74** and subsequent deprotection.

The ^{1}H NMR spectrum of **76**, with assignment of peaks is shown in **Figure 2.13**.

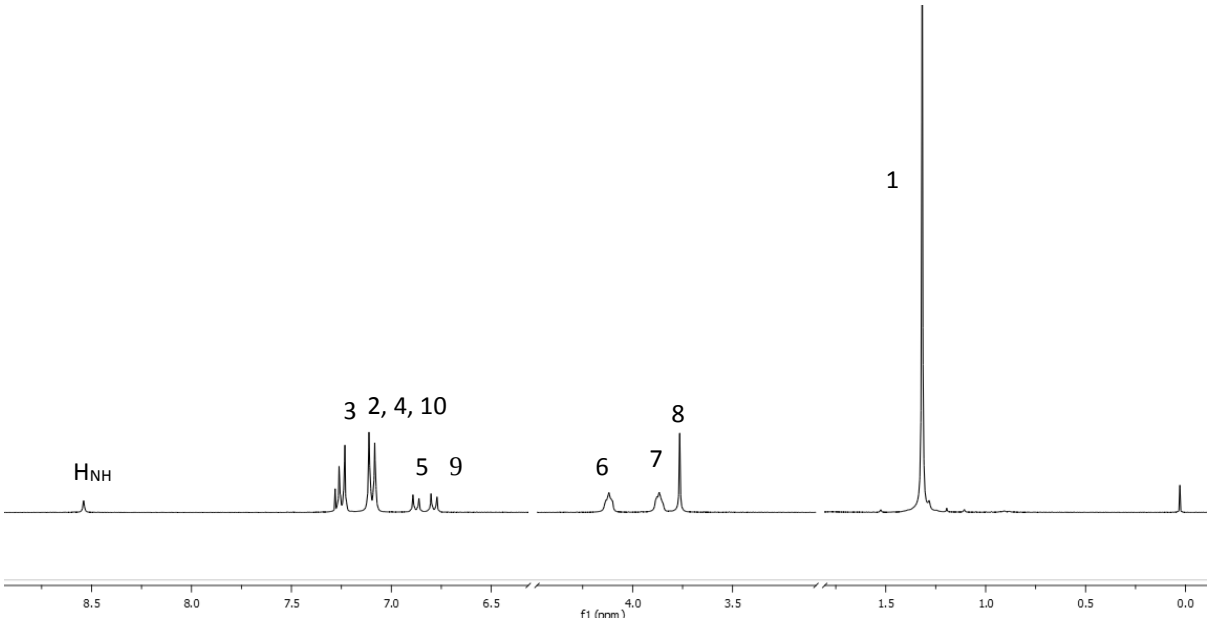

Figure 2.13 - ^{1}H NMR of **76** in $CDCl_3$ at 298 K.

2.5.6 Attempts towards reduced reaction steps.

Despite this successful strategy, due to the number of steps involved, some of which were fairly low yielding, a secondary strategy was proposed. This route attempted to attach the phenyl groups at the α carbon prior to the cyclisation to the barbiturate. The proposed strategy is shown below in **Scheme 2.25** and starts from anisole and a triketone.

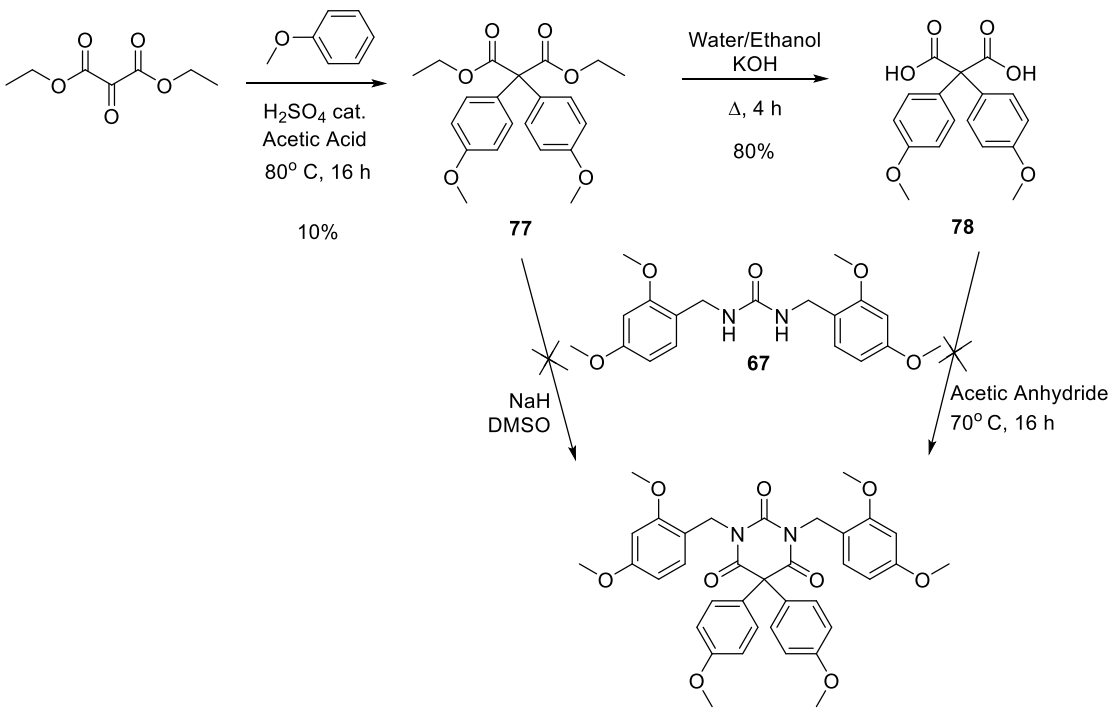

Scheme 2.25 – Attempts towards diphenyl barbiturates

The bisarylated malonate **77** was formed via a Friedel Crafts reaction with ketomalonate and anisole. The reagents were dissolved in acetic acid and a catalytic amount of H_2SO_4 was added. The solution was stirred under reflux for two hours and then stirred at room temperature overnight. After work-up and purification, **77** was isolated in 10% yield. The ester **77** was then converted to the acid **78** by refluxing for four hours in water/ethanol with KOH as a base. The compound was purified via column chromatography and was obtained in 80% yield.

Further cyclisation with a protected urea would form the protected barbiturate with aryl groups attached. However, neither **77** or **78** were unable to be cyclised to the barbiturate and only starting materials were recovered.

2.5.7 Interactions with Receptors 41 and 42

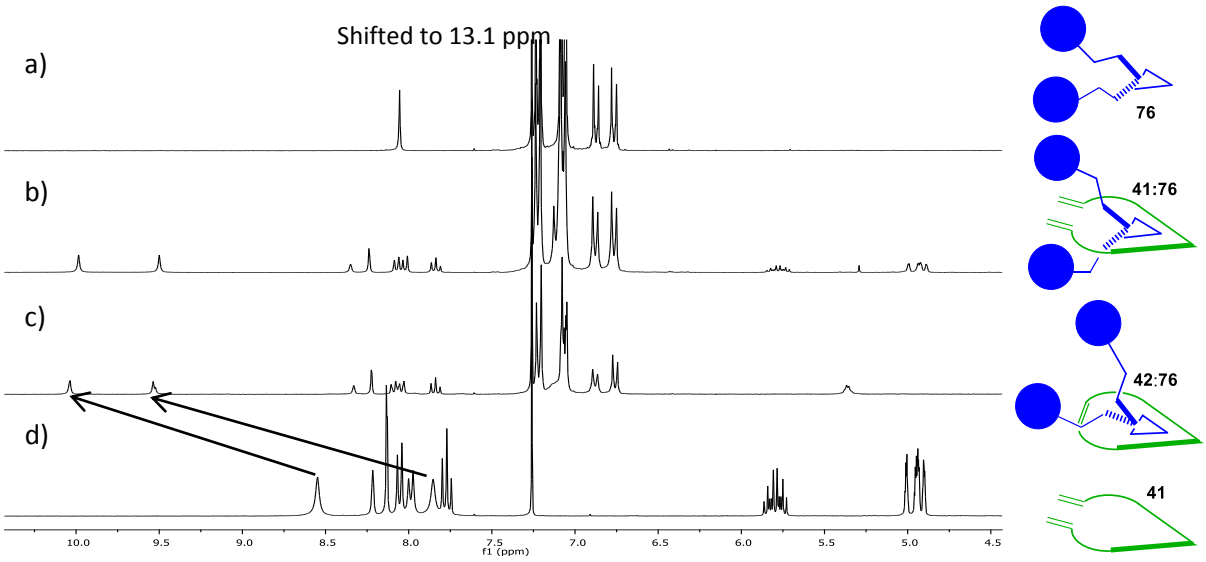

Figure 2.14 – Stacked ^{1}H NMR spectra showing **76** (a), **41:76** (b), **42:76** (c) and **41** (d) in $CDCl_3$ (5 mM) and at 298 K.

Shown in the spectra of **Figure 2.14** are the guest **76** (a) followed by the acyclic complex **41:76** (b), the perched complex **42:76** (c) and finally the acyclic receptor **41** (d). There is a clear H-bonding interaction present indicated by the downfield shifts of the NH protons. The imide NH proton of the guest is shifted significantly from 8.1 – 13.1 ppm. There is very little difference between the spectra of the complexes **41:76** and **42:76** indicating that interpretation of an interlocked structure from ^{1}H NMR alone may be difficult.

2.6 Barbiturate Components Towards Click Chemistry – An alternate route to Interlocked Structures

2.6.1 Click Reaction Components - Towards Stoppering

In order to maximise the scope with which to form interlocked structures from Hamilton receptors and barbiturate derivatives, another approach was proposed by our collaborators in Bordeaux. The concept involved the use of a Huisgen 1,3-dipolar cycloaddition, or 'click' reaction, a reaction used extensively in the field of interlocked

structures.[20] Click reactions, as discussed in the introduction, typically involve the use of a complementary azide/alkyne pair which undergo a copper catalysed cycloaddition to form a triazole moiety. The following scheme involves the formation of a [2]-rotaxane via a stoppering event. The procedure, shown schematically in **Figure 2.15** involved the use of the cyclic receptors which will form a H:G complex with a barbiturate which has been appended with azide groups. The azide groups are attached at the end of propyl tethers attached at the 5 position. The relatively short nature of these linkers should aid with the threading process when compared to the longer analogues already discussed. The alkyne component is attached to the stopper and once the H:G complex is formed, the rotaxane will be formed via the click reaction.

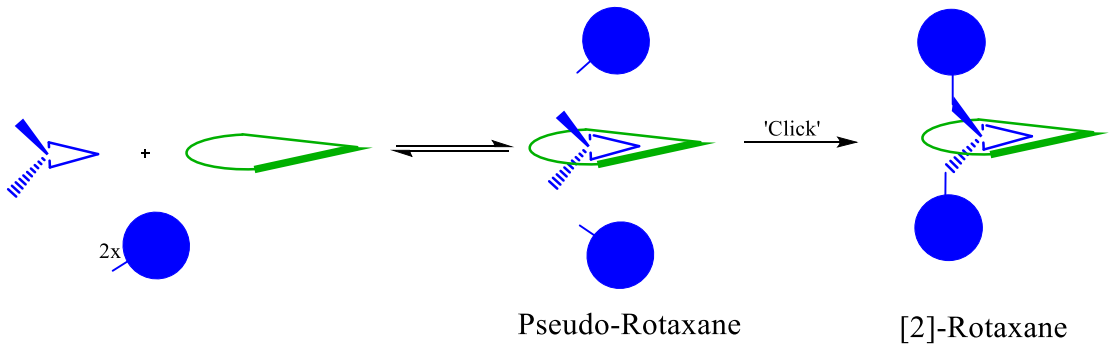

Figure 2.15 – Formation of a [2]-Rotaxane using stoppering via click chemistry

2.6.1.1 Synthesis of Components

The start of the synthesis required the production of the azide linkers. The 1-azido-3-iodopropane, **81**, was synthesised in three steps from 3-bromo-1-propanol, via the tosyl compound, **80**, according to literature procedures and achieved in good yield (**Scheme 2.26**).[21] In the first step, 3-bromo-1-propanol is added to water followed by NaN_3 and the mixture is refluxed overnight. After workup, **79** was isolated and the oil can be used as

obtained with no further purification required. Addition of the tosyl group was achieved by dissolving **79** in DCM and adding 4-toluensulfonyl chloride, with NEt_3 added as a base. The solution was stirred overnight and after work up, a yellow oil is obtained. Addition of ether removed a significant amount of impurity as a white precipitate and the oil obtained from the filtrate was then purified via column chromatography to obtain **80** as a clear oil. In the final step towards the azide tether, the tosyl group was converted to the iodide by dissolving in acetone and adding NaI. The reaction was stirred under reflux overnight and the work up merely consists of filtration of the precipitate formed, and removal of the solvent from the filtrate to obtain **81** as a clear yellow oil. Care was taken when handling these compounds, not only for their volatility due to their relatively low molecular weight, but also because low molecular weight azides have been known to be explosive when under reduced pressure and/or heat.[22]

The iodine terminated azide moiety, **81** was then reacted with diethyl malonate, in the same manner as shown previously and shown in **Scheme 2.26**. The malonate was dissolved in THF, and after the addition of NaH to achieve deprotonation of the malonate, the azide was added in excess and the reaction was stirred under reflux, overnight. After work up and purification via column chromatography the disubstituted product, **82**, was obtained in good yield. The final step in the synthesis of this target barbiturate was cyclisation with urea. The urea was dissolved in DMSO and again NaH was used as a base. The malonate was then added and the solution was stirred overnight. After work up, an oil was obtained from which the impure product crystalised out under high vacuum. The crude solid was separated from the oil and purified via column chromatography to yield the di-azide substituted barbiturate, **83**.

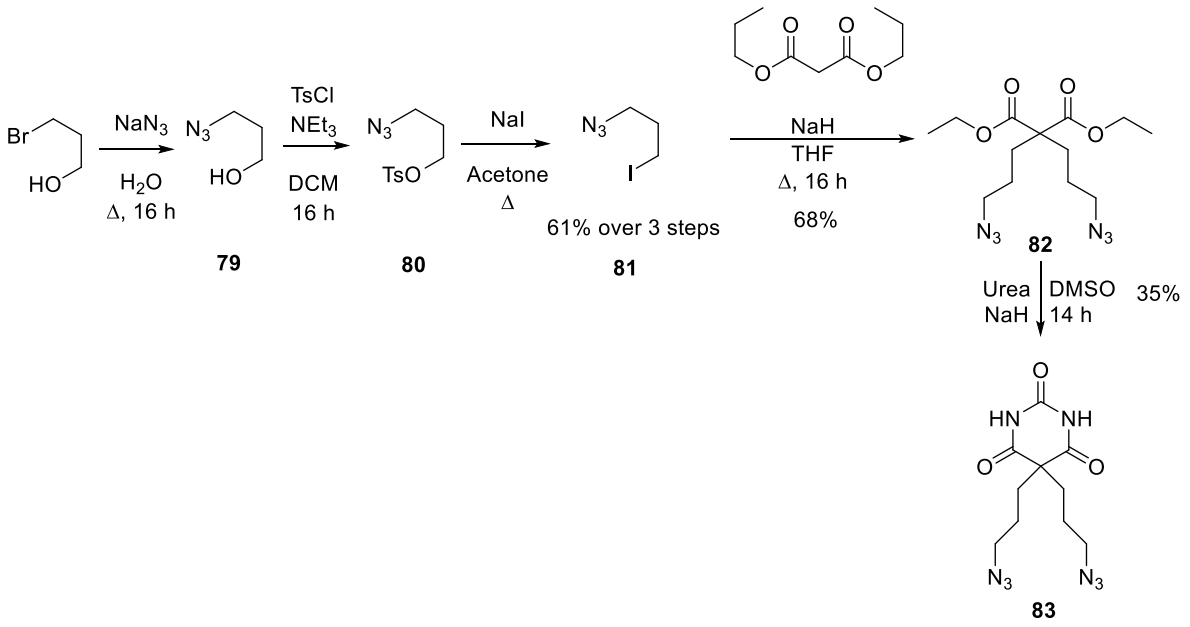

Scheme 2.26 – Synthesis of azide terminated barbiturate thread, **83**.

2.6.1.2 Studies of the Pseudo-Rotaxane 45:83

It was important to establish the nature and strength of binding for these barbiturates so a series of binding studies were carried out regarding the formation of the pseudo-rotaxane.

The job plot in **Figure 2.16** was used to determine the stoichiometry of the binding event between barbiturate **83** and macrocycle **45.** By monitoring the changes in absorbance whilst varying the molar fraction of the system, the job plot was produced, confirming a 1:1 H:G complex, as expected for this Hamilton-Barbiturate motif.

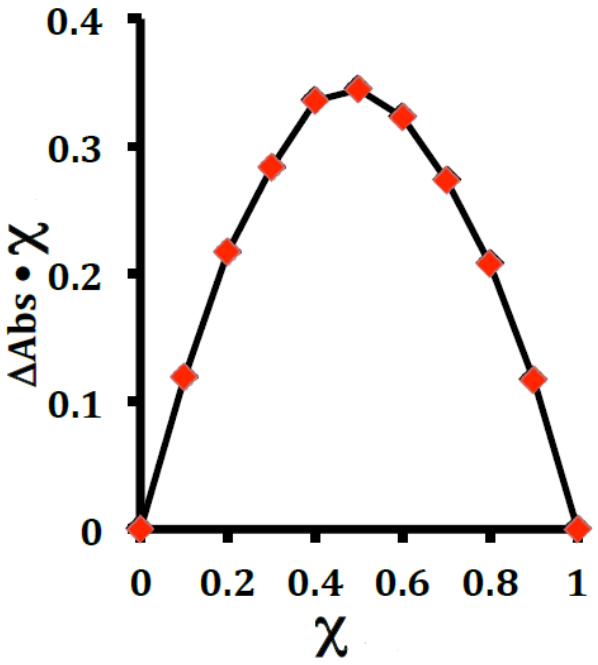

Figure 2.16 - Job plot showing binding-induced absorption changes (310 nm) as a function of molar fraction of azide barbiturate in the binding between receptor **45** and barbiturate **83**. ($[C]_{tot}$ = 50 µM) in $CHCl_3$. ΔAbs = A_{max} - A_{obs}

Formation of this 1:1 complex was confirmed via crystal structure, shown in **Figure 2.17**. The crystals of the Host-Guest complex were obtained via slow diffusion of pentane into a solution of the complex in dichloromethane. From the crystal structure it can be observed that as expected, the barbiturate guest is bound by six complementary H-bonds between the imide and bisamidopyridine units along with a central short contact [C–H---O=C] interaction. The H-bond lengths [N–H---O=C] were found to be 1.9 to 3.2 Å with angles of 164° to 170°. In the complex, the median annular plane of the barbiturate guest formed an average tilt angle of ca. 26° relative to the median plane of receptor, similar to that observed by Hamilton with analogous guest species. Crucially, it is apparent that the two alkyl arms of the guest bonded to the sp^3 carbon protrude from both sides of the

macrocycle cavity forming the desired pseudo-rotaxane, a prerequisite towards the formation of an interlocked structure.

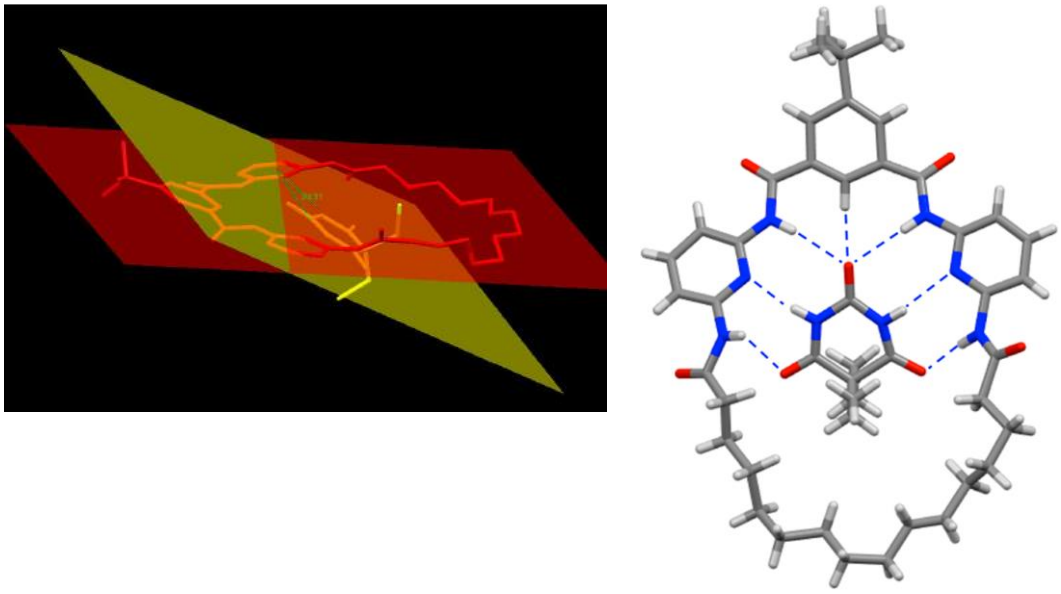

Figure 2.17 - X-Ray crystal structure of the H:G complex formed between **45** and **83**.

The binding constant for this interaction was obtained by analysis of the red-shifting of the pyridine absorption, induced by guest complexation, at 315 nm, as shown in **Figure 2.18**. The value for K_{ass} was found to be 23500 M^{-1}, a logK of 4.37 at 288 K in $CHCl_3$. This value shows a relatively strong interaction when compared with the olefin terminated barbiturates. This is probably a consequence of the guest's ability to interpenetrate the binding cavity when compared to the longer chained moieties.

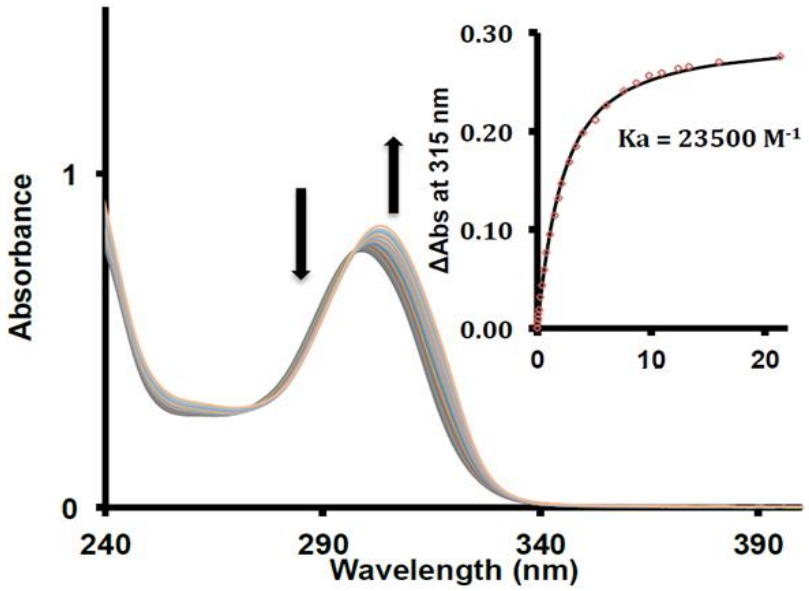

Figure 2.18 - Changes in electronic absorption spectra of receptor **45** in $CHCl_3$ (C = 25 μM) on adding aliquots of **83**. Inset shows absorption changes at 315 nm upon addition of **83** from 0 to 22 equivalents.

The ^1H NMR spectra of **Figure 2.19** shows the shifting of signals upon H:G binding. The H:G spectrum shows similarities with that of **Figure 2.5** where the H_{NH} signals of both the host and guest experience a strong downfield shift (H_{NH}**83**: Δδ = 3.8 ppm, H_{NH}**45**: Δδ = 1.3 and 1.6 ppm, indicative of the binding interaction). As before, a downfield shift of the 'bridge' proton is also observed.

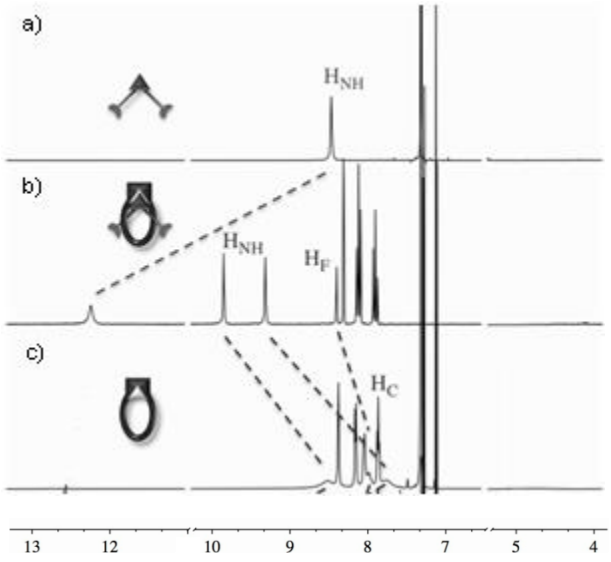

Figure 2.19 – ^1H NMR comparison between **83**, **45**, and a 1:1 mix of **45** and **83** in $CDCl_3$ at 298 K

2.6.1.3 Stopper Synthesis

Both azide and alkyne components are required for the click reaction and the alkyne group was chosen for the stopper due to its ease of synthesis and its prevalence in the literature.[23] The alkyne appended stopper was synthesised in one step from **48**, by reacting with propargyl bromide in DMF, using K_2CO_3 as a base (**Scheme 2.27**). The reaction mixture was stirred at 80^o C overnight and after work up the crude was purified via column chromatography. The product is obtained in an excellent yield of 92%.

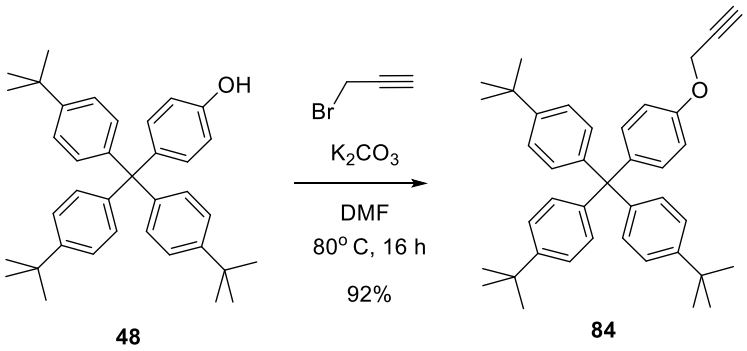

Scheme 2.27 – Synthesis of alkyne functionalised stopper, **84.**

Having shown that the formation of the proposed pseudo-rotaxane is indeed possible, it can be envisaged that following a successful templation/threading event of the barbiturate **83** through a macrocycle, followed by subsequent stoppering with the alkyne stoppers in a click reaction, a [2]-rotaxane will be produced which will be outlined in the following chapter. The method for the synthesis of a [2]-rotaxane is shown in **Figure 2.20**,

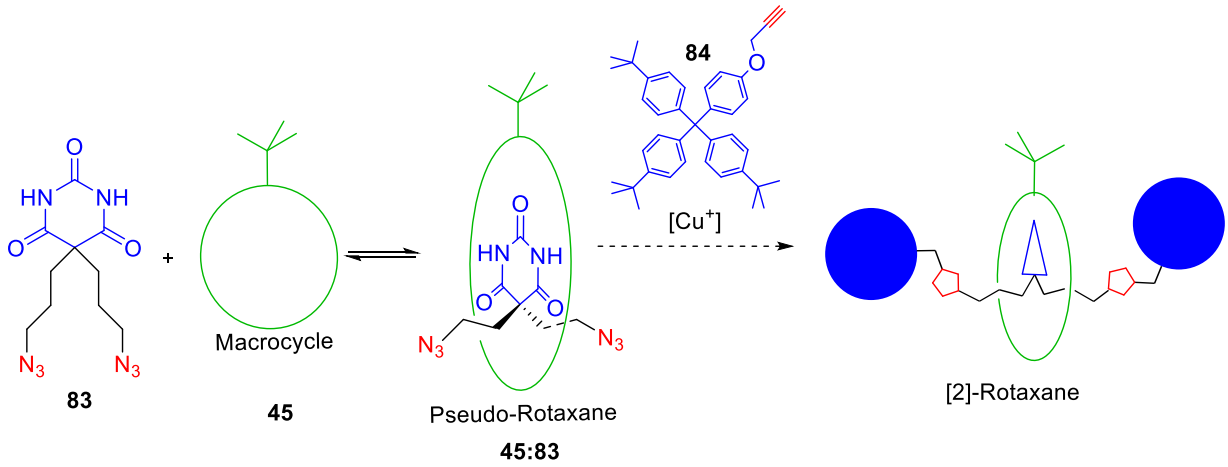

Figure 2.20 – Proposed synthetic strategy towards click-stoppered [2]-rotaxanes.

2.6.1.4 Dumb-bell Synthesis and Binding Study

In order to test the feasibility of the click reaction, a test reaction was carried out between the azide and alkyne substituents in the absence of any form of macrocycle as shown in **Scheme 2.28**. The azide was dissolved in degassed chloroform and the copper catalyst $Cu(MeCN)_4PF_6$ was added, and the solution stirred for one hour. The alkyne stopper was added and the reaction monitored via TLC. After 4 h, the starting materials had been consumed and following work up and purification via column chromatography the barbiturate dumb-bell **85** was obtained in 90% yield.

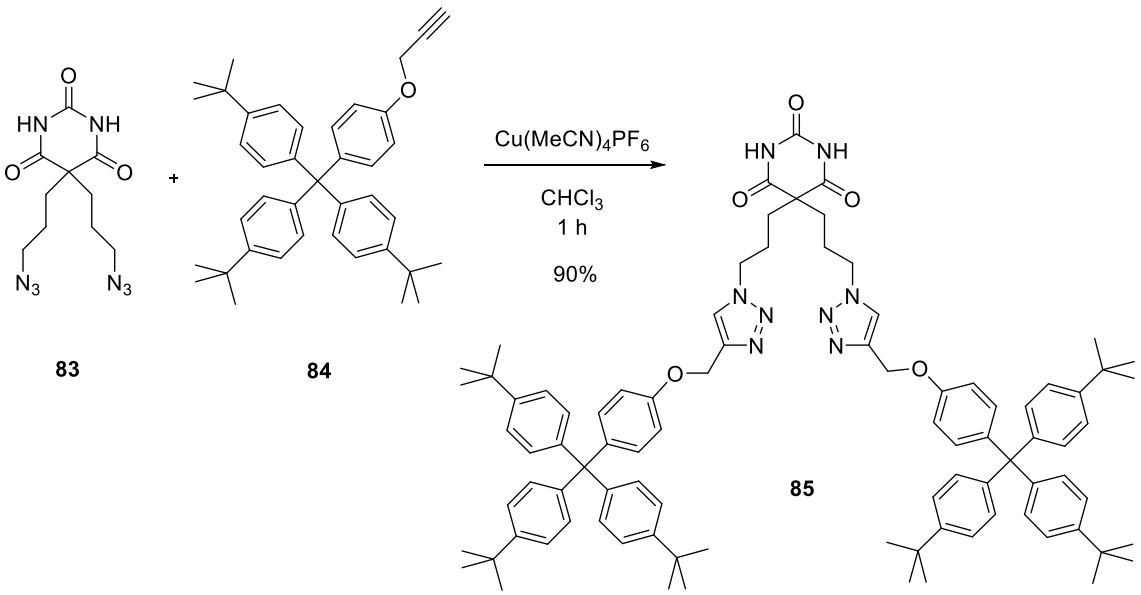

Scheme 2.28 – Synthesis of triazole barbiturate, **85**.

The synthesis of a new dumb-bell shaped barbiturate guest, **85**, has now been accomplished and this can be applied to the synthesis of rotaxanes via a clipping approach with acyclic receptors, which will be outlined in Chapter 4. In order to gauge the level of binding with Hamilton receptors, a binding study was carried out between **85** and **45.**

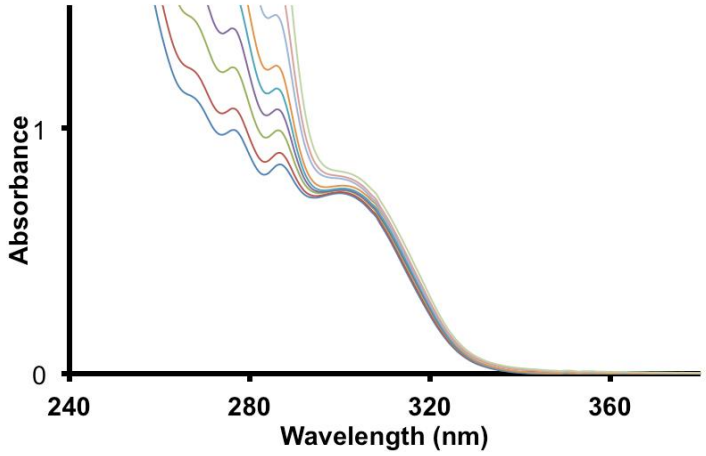

Figure 2.21 - Changes in electronic absorption spectra of receptor **45** in $CHCl_3$ (C = 25 μM) on adding aliquots of **85**. Inset shows absorption changes at 315 nm upon addition of **85** from 0 to 70 equivalents.

Monitoring the change in absorbance upon addition of **85** gave the binding constant and was found to be 4000 M^{-1}, giving a logK of 3.6 at 298 K (**Figure 2.21**). A decrease in binding constant is expected when comparing with the smaller, and threadable guest, **83**. Considering **85**, this is probably because only a perched complex may be formed due to the inability of the dumb-bell to thread through the macrocycle resulting in a less favourable H:G interaction than observed with **83**. This may pose further confirmation towards the perched nature of **53**, due to its similarity in binding constant with **85**.

2.6.2 Click Reaction Components - Active Templation Strategy

The use of click chemistry and active templation regarding the synthesis of interlocked structures has seen many examples over the past decade.[24] For this reason, it seemed acceptable to apply this process towards our series of compounds. Considering **Figure 2.22**, if the Cu^{+} catalyst is able to bind in the active site of the receptor, via the pyridine groups, then an active template situation would arise, whereby two independent azide and alkyne stoppers may click together within the macrocycle. Formation of a rotaxane will then have been achieved without the need for a barbiturate template.

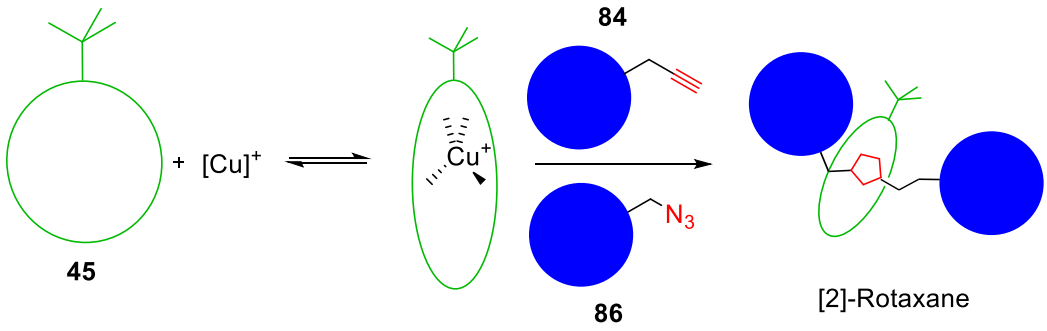

Figure 2.22 - Proposed synthetic strategy towards active template mediated [2]-rotaxanes.

2.6.2.1 – Stopper Synthesis

The synthesis for both the macrocycle, **45**, and alkyne funtionalised stopper, **84**, has already been shown (**Section 2.1.2.2** and **Section 2.6.1.3**). The only component for this approach which needed to be synthesised was the azide functionalised stopper (**Scheme 2.29**). This was achieved starting from the stopper **48**. The azide tosylate, **80**, and **48** were dissolved in butanone. Heating of the mixture results in dissolution and then K_2CO_3 was added. The solution was stirred overnight at 70° C. Once cool, the suspension was filtered and the filtrate was concentrated to give the crude product. Purification via column chromatography afforded the pure, white product **86** in 62% yield.

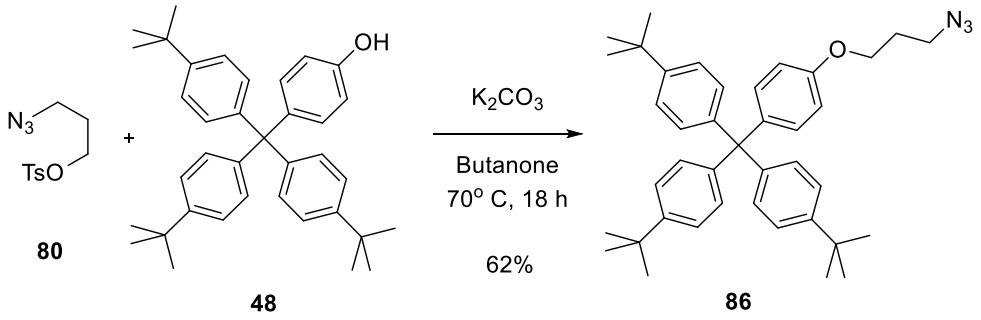

Scheme 2.29 – Synthesis of azide terminated stopper, **86**.

These components were then taken through towards investigating their application towards click chemistry. To test the click reaction itself, in the absence of any receptor species, equimolar equivalents of the azide and alkyne stoppers, and the copper catalyst $Cu(MeCN)_4PF_6$ were dissolved in degassed $CHCl_3$. The reaction was monitored via TLC and all the azide had been consumed after 2.5h. Subsequent work up and purification via column chromatography gave the 'clicked' product in high yield (**Scheme 2.30**) and was analysed via ^1H, ^{13}C and mass spectrometry.

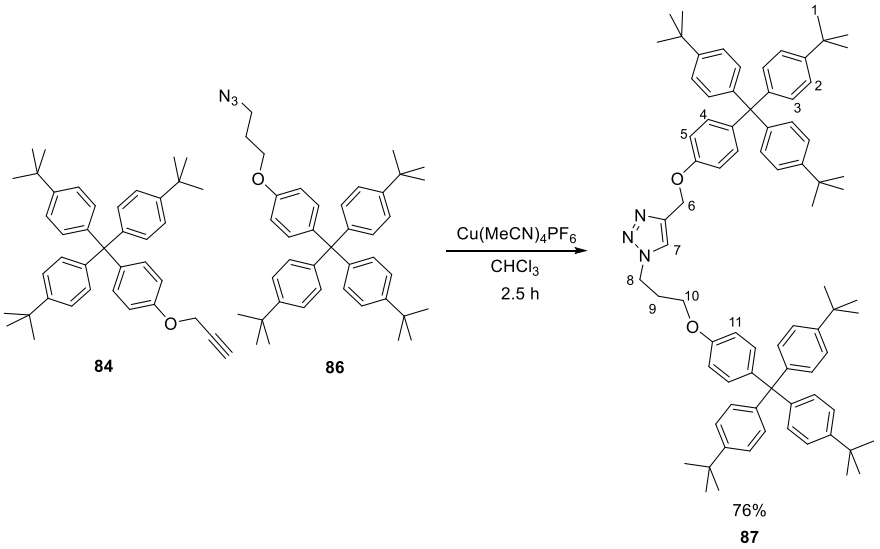

Scheme 2.30 – Synthesis of triazole linked dumbbell.

The ^{1}H nmr spectrum in **Figure 2.23** shows the pure product. The diagnostic peak at 7.7 ppm shows the formation of the triazole ring, confirming the formation of the clicked product.

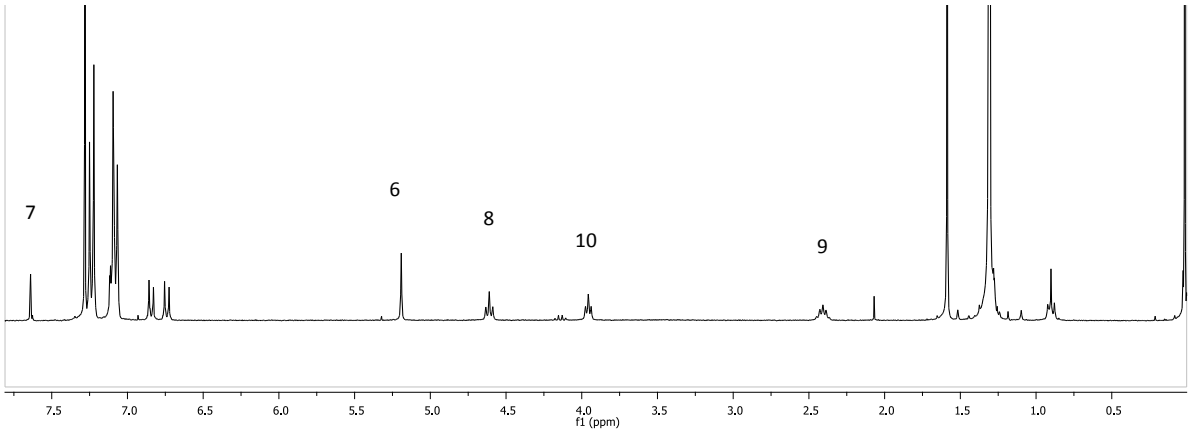

Figure 2.23 – ^{1}H NMR showing the product, **87**, in $CDCl_3$, 298 K.

2.7 Conclusion

In conclusion, a number of host and guest molecules have been synthesised successfully through various strategies.

2.7.1 Receptors

The receptor molecules, both open and closed, have been synthesised with ease and allow different routes towards either catenanes or rotaxanes via clipping and/or stoppering methods. There is also great scope towards further variation in the chain lengths of these compounds to fine tune towards the strongest Host:Guest interaction, as well as reaching a 'goldilocks' point between the ring, guest and stopper size i.e. where the ring size is great enough to cyclise around and/or accommodate the guest and yet, be small enough so as not to slip over the stopper groups.

2.7.2 Guests (Flexible)

Olefin-terminated flexible barbiturates were synthesised in simple steps and as expected, these showed binding to receptor **45**. Stopper-terminated derivatives of these compounds were not synthetically possible via classical methods but triazole analogues were accomplished via 'click' chemistry.

2.7.3 Guests (Rigid)

With regards to the rigid series of compounds, the olefin terminated form initially seemed too problematic and was discontinued due to the low yields and difficult synthesis. The stopper terminated compounds were also abandoned for the same reasons, despite attempts at optimisation using TBDMS stoppers. A protection strategy was attempted regarding the formation of rigid compounds. With the advent of this protection strategy

which utilised DMB-protected barbiturates and lead/boron exchange using protected boronic acids, the synthesis of stoppered, rigid barbiturates was achieved. One aspect of further work would be to reinvestigate the synthesis of previously challenging compounds using this new protection strategy. The hindering problems previously shown for the functional groups required may now be overcome via addition to the guest molecule at a late stage in the synthesis.

2.7.4 Guests (Click compounds)

A series of molecules, including stoppers and guests have been synthesised allowing the application of click chemistry. The guest shows binding with the host receptor and the availability of crystal structures of the H:G interaction look promising towards the formation of an interlocked structure.

2.8 References

1. Chang, S. K.; Van Engen, D.; Fan, E.; Hamilton, A. D., Hydrogen bonding and molecular recognition: synthetic, complexation, and structural studies on barbiturate binding to an artificial receptor. *J. Am. Chem. Soc.* **1991,** *113* (20), 7640-7645.

2. (a) Coquerel, Y.; Brémond, P.; Rodriguez, J., Pd–H from Pd/C and triethylamine: Implications in palladium catalysed reactions involving amines. *J. Organomet. Chem.* **2007,** *692* (22), 4805-4808; (b) Coquerel, Y.; Rodriguez, J., Catalytic properties of the Pd/C-triethylamine system. *Arkivoc* **2008**, 227-237.

3. Ashton, P. R.; Ballardini, R.; Balzani, V.; Bělohradský, M.; Gandolfi, M. T.; Philp, D.; Prodi, L.; Raymo, F. M.; Reddington, M. V.; Spencer, N.; Stoddart, J. F.; Venturi, M.; Williams, D. J., Self-Assembly, Spectroscopic, and Electrochemical Properties of [n]Rotaxanes1. *J. Am. Chem. Soc.* **1996,** *118* (21), 4931-4951.

4. Rocher, M. Towards interlocked structures based on H-bonded barbiturate complexes. University of Birmingham, 2010.

5. Hynes, M. J., EQNMR: A computer program for the calculation of stability constants from nuclear magnetic resonance chemical shift data,. *Dalton Trans.,* **1993**, 311-312.

6. Zhang, C.; Li, S.; Zhang, J.; Zhu, K.; Li, N.; Huang, F., Benzo-21-Crown-7/Secondary Dialkylammonium Salt [2]Pseudorotaxane- and [2]Rotaxane-Type Threaded Structures. *Org. Lett.* **2007,** *9* (26), 5553-5556.

7. Song, H. N.; Lee, H. J.; Kim, H. R.; Ryu, E. K.; Kim, J. N., Friedel-Crafts Type Reactions of Some Activated Cyclic Ketones with Phenol Derivatives. *Synthetic Commun.* **1999,** *29* (19), 3303-3311.

8. Kopinski, R. P., JT. Rowe, BA, The chemistry of aryllead(IV) tricarboxylates. Reaction with derivatives of malonic acid: New routes to aryl carboxylic acids and arylated barbituric acid derivatives. *Aust. J. Chem.* **1984,** *37* (6), 1245-1254.

9. Bell, H. C.; Kalman, J. R.; Pinhey, J. T.; Sternhell, S., The chemistry of aryllead (IV) tricarboxylates. *Tetrahedron Lett.* **1974,** *15* (10), 853-856.

10. Bell, H. C.; Kalman, J. R.; Pinhey, J. T.; Sternhell, S., Synthesis of biaryls by reaction of aryllead (IV) tricarboxylates with aromatic compounds. *Tetrahedron Lett.* **1974,** *15* (10), 857-860.

11. Bell, H. C.; May, G. L.; Pinhey, J. T.; Sternhell, S., Reactions of aryllead(IV) triacetates with phenols. *Tetrahedron Lett.* **1976,** *17* (47), 4303-4306.

12. Pinhey, J. T., *Aust. J. Chem.* **1991,** *44*, 1353.

13. K. A. Kochshkov, E. M. P., *Dokl. Akad. Nauk. SSSR* **1952,** *85*, 1037.

14. Morgan, J.; Pinhey, J. T., Reaction of arylboronic acids and their derivatives with lead tetra-acetate. The generation of aryl-lead triacetates, and meta- and para-phenylenebis(lead triacetate), in situ for electrophilic arylation. *J. Chem. Soc,. Perkin Trans. 1.* **1990,** (3), 715-720.

15. Pinhey, J. T.; Rowe, B. A., The α-arylation of derivatives of malonic acid with aryllead triacetates. New syntheses of ibuprofen and phenobarbital. *Tetrahedron Lett.* **1980,** *21* (10), 965-968.

16. Trost, B.; LaRochelle, R.; Atkins, R., Pentacoordinate Sulfur Compounds as Intermediates in Organic Reactions. *J. Am. Chem. Soc.* **1969,** *91* (8), 2175-2177.

17. Knapp, S.; Hale, J. J.; Bastos, M.; Molina, A.; Chen, K. Y., Synthesis of hypusine and other polyamines using dibenzyltriazones for amino protection. *J. Org. Chem.* **1992,** *57* (23), 6239-6256.

18. Clark-Lewis, J. W. T., M.J. , *J. Am. Chem. Soc.* **1959**, 1628.

19. P., K., *Protecting Groups*. Thieme Verlag: Stuttgart, **2006**; Vol. 3rd Edition.

20. (a) Zhang, H.; Zhou, B.; Li, H.; Qu, D.-H.; Tian, H., A Ferrocene-Functionalized [2]Rotaxane with Two Fluorophores as Stoppers. *J. Org. Chem.* **2012,** *78* (5), 2091-2098; (b) Zhang, H.; Liu, Q.; Li, J.; Qu, D.-H., A Novel Star-Shaped Zinc Porphyrin Cored [5]Rotaxane. *Org. Lett.* **2013,** *15* (2), 338-341; (c) Collin, J.-P.; Frey, J.; Heitz, V.; Sauvage, J.-P.; Tock, C.; Allouche, L., Adjustable Receptor Based on a [3]Rotaxane Whose Two Threaded Rings Are Rigidly Attached to Two Porphyrinic Plates: Synthesis and Complexation Studies. *J. Am. Chem. Soc.* **2009,** *131* (15), 5609-5620.

21. Khoukhi, M.; Vaultier, M.; Carrié, R., The use of ω-iodoazides as primary protected electrophilic reagents. Alkylation of some carbanions derived from active methylene compounds and N,N-dimethylhydrazones. *Tetrahedron Lett.* **1986,** *27* (9), 1031-1034.

22. Bräse, S.; Gil, C.; Knepper, K.; Zimmermann, V., Organic Azides: An Exploding Diversity of a Unique Class of Compounds. *Angew. Chem. Int. Ed.* **2005,** *44* (33), 5188-5240.

23. Aucagne, V.; Hänni, K. D.; Leigh, D. A.; Lusby, P. J.; Walker, D. B., Catalytic "Click" Rotaxanes: A Substoichiometric Metal-Template Pathway to Mechanically Interlocked Architectures. *J. Am. Chem. Soc.* **2006,** *128* (7), 2186-2187.

24. (a) Winn, J.; Pinczewska, A.; Goldup, S. M., Synthesis of a Rotaxane CuI Triazolide under Aqueous Conditions. *J. Am. Chem. Soc.* **2013,** *135* (36), 13318-13321; (b) Aucagne, V.; Berná, J.; Crowley, J. D.; Goldup, S. M.; Hänni, K. D.; Leigh, D. A.; Lusby, P. J.; Ronaldson, V. E.; Slawin, A. M. Z.; Viterisi, A.; Walker, D. B., Catalytic "Active-Metal" Template Synthesis of [2]Rotaxanes, [3]Rotaxanes, and Molecular Shuttles, and Some Observations on the Mechanism of the Cu(I)-Catalyzed Azide−Alkyne 1,3-Cycloaddition. *J. Am. Chem. Soc.* **2007,** *129* (39), 11950-11963; (c) Goldup, S. M.; Leigh, D. A.; McGonigal, P. R.; Ronaldson, V. E.; Slawin, A. M. Z., Two Axles Threaded Using a Single Template Site: Active Metal Template Macrobicyclic [3]Rotaxanes. *J. Am. Chem. Soc.* **2009,** *132* (1), 315-320.

3 Synthesis of non-Photoactive Interlocked Structures

3.1 Chapter Aim and Methodology

This chapter concerns the attempted synthesis of 'non-photoactive' interlocked structures using an array of receptors and guest molecules whose synthesis was detailed in chapter 2. **Table 3.1** summarises the various molecules and methods investigated.

Table 3.1 – Various molecules and methods towards Hamilton-template interlocked structures.

Entry	Methodology	Guest/Guest component	Locking Method	Receptor
1	Guest Threading (catenane)	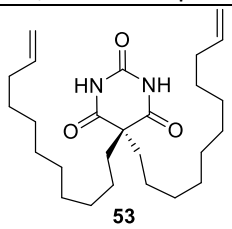 **53**	Grubbs Metathesis	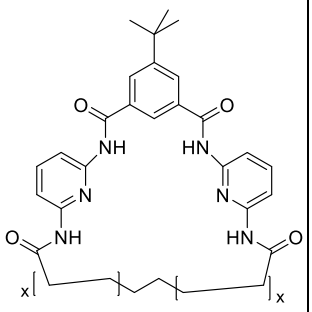 x = 3, **45**
2	Guest Threading (rotaxane)	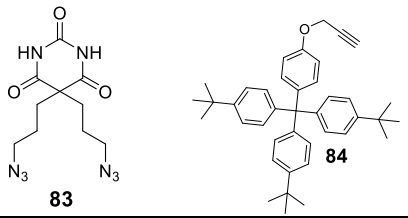 **83** **84**	CuAAC	
3	Active Template (rotaxane)	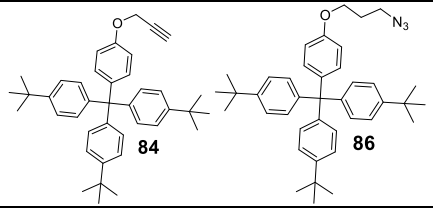 **84** **86**	CuAAC	
4	Receptor Clipping (rotaxane)	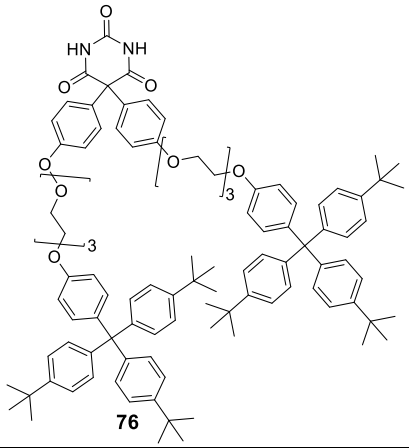 **76**	Grubbs Metathesis	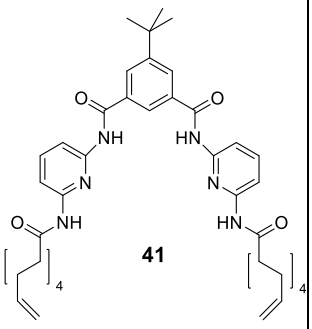 **41**

The 'methodology' column describes the process used by either the guest or receptor to capture the interlocked structure. The next column shows the various guest molecules, with their stoppering counterparts included when required. The 'locking method' column shows the chemical reaction used to attempt the capture of the interlocked structure and the final column shows the complementary receptor required for the system. The active template strategy, entry 3, requires no barbiturate template and instead relies on the complexation of the copper catalyst within the macrocycle.

Contained within this chapter are some studies carried out by our collaborators in Bordeaux. These include a series of stacked ^{1}H NMR spectra of compounds **45**, **83**, **85** and rotaxane **88** and their complexes (**Figure 3.10**) as well as another stacked ^{1}H NMR spectra comparing 'perched' vs 'threaded' components (**Figure 3.11**). A stability study of rotaxane **88** (**Figure 3.12**) was also carried out in Bordeaux.

3.2 Approaches Using Grubbs Metathesis

3.2.1 Using Flexible Barbiturate Guests

The first method to be investigated was the use of Grubbs metathesis as the locking reaction. The first approach was intended to build upon the project of a previous student, Mathias Rocher.[1] This involved the use of the olefin-terminated flexible barbiturate **53**, with the Hamilton-type macrocycle, **45**, (**Scheme 3.1**) the syntheses of which have already been described in Chapter 2 (**Scheme 2.8** and **2.4** respectively).

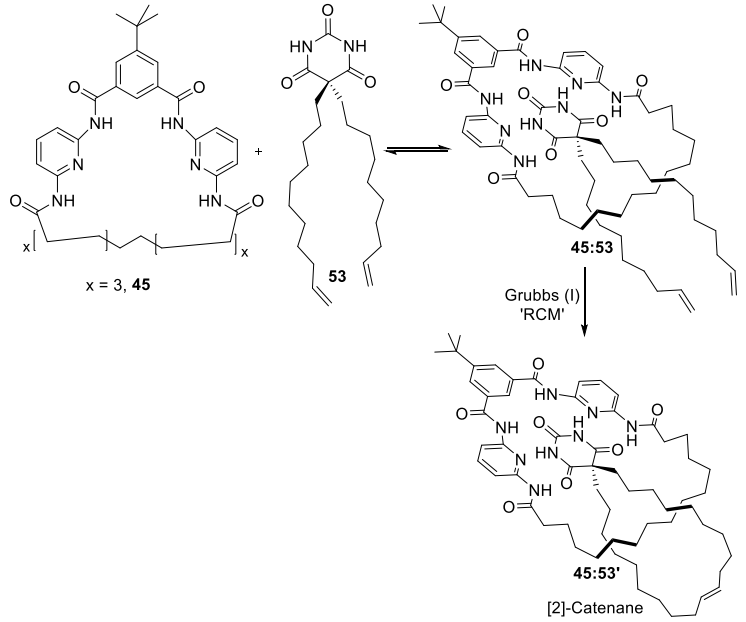

Scheme 3.1 - Scheme showing the proposed H:G interaction of complex **45**:**53** and subsequent clipping to form the desired catenane **45:53'**.

The utility of guest **53** towards the capture of an interlocked structure requires the interpenetration of one pendant arm of **53** through the centre of macrocycle **45** prior to establishing the expected binding motif. Following on from this threading event, promoted by the complementary H:G interaction, subsequent cyclisation of the guest via Grubbs metathesis around **45** would form the desired catenane. Previous unsuccessful attempts had been carried out with a barbiturate linker length of 8-CH_2 groups. Had this produced a catenane, this would have been the smallest ring size for an interlocked structure yet known, where the limit is typically 20-21 atoms.[2] It was for this reason that this approach was reattempted with a longer chain of 9-CH_2 groups.

For the catenation experiment, equimolar amounts of **45** and **53** were dissolved in DCM to achieve a 1:1 H:G complex as proven by ^{1}H NMR spectroscopy (**Figure 2.5**). It was thought that any kinetic barrier to threading would be overcome by gentle heating and so the flask was heated at 40^o C for 2 hours, despite the potential for reduced H:G binding. 10

mol% of Grubbs (I) was then added to the solution and reflux continued for a further 2 hours. Despite not observing complete consumption of the starting guest **53**, the reaction was stopped due to the appearance of numerous spots when analysed by TLC, and so the reaction was cooled and the crude mixture was purified by column chromatography (eluent: DCM/MeOH - 0-4%).

After purification, 28% of the starting barbiturate **53** was recovered. The metathesized guest, **53'**, was isolated from the column in three subsequent fractions in the presence of **45** which could not be isolated as a single fraction. This was evidenced from the presence of signals for both **45** and **53'** (and trace amounts of **53**) in a ^{1}H NMR spectrum of each obtained fraction, which showed strong downfield field shifts of NH signals of both the host and guest. No pure **53'** was able to be isolated. At first glance, this would suggest the formation of a catenane, since non-interlocked structures would be expected to be separated by column chromatography. However, mass spectrometry of this mixture revealed no interlocked structure. Subsequent purification of the mixture gave the separate components confirming the absence of any interlocked structure. It would seem that **45**, **53**, and **53'** are able to move through a column with some degree of complexation, whether the guest is metathesized or not, and possibly in various modes and/or stoichiometries owing to the three distinct fractions isolated. Since no catenane was formed (at least not in any isolatable yield) we can postulate the formation of a 'perched' complex, where **53**, despite binding to **45**, exhibits little or no threading. Despite the sp^3 nature of the carbon at the 5-position of **53**, both arms sit above the plane of the receptor, which is likely due to their length and inherent and required flexibility. In such a situation, ring closing metathesis would then only lead to two non-interlocked macrocycles as shown in **Scheme 3.2**.

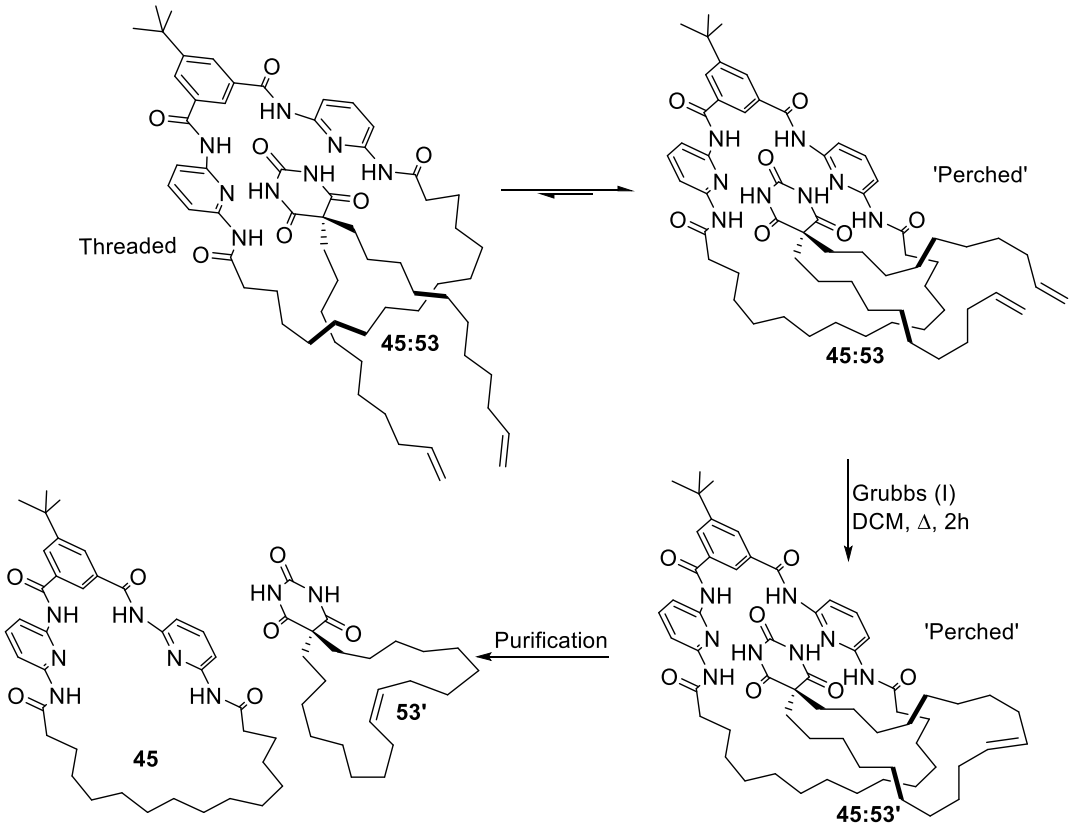

Scheme 3.2 – Modified binding event, followed by a perched clipping resulting in two separable macrocycles.

The primary issue with this synthetic approach seems to be an inability of **53** to interpenetrate **45** prior to cyclisation. Due to this inherent difficulty surrounding the threading of such long, yet necessary tethers, this approach was abandoned in favour of a more directed approach utilising the previously discussed rigid barbiturates.

3.2.2 Rigid Barbiturate Guests

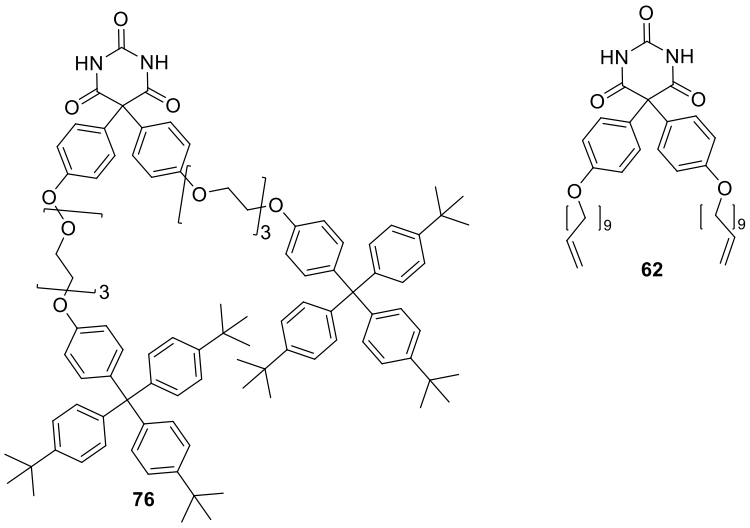

Figure 3.1- 'Rigid' Barbiturate guests **76** and **62**.

As mentioned in the previous chapter, it was anticipated that by introducing greater rigidity into the guest molecule at the sp^3 carbon through the use of a phenyl spacer, then an orientation would be obtained which could be more favourable towards the formation of an interlocked structure. Considering the approach outlined in entry 4 of **Table 3.1**, the rotaxane would be achieved via clipping receptor **41** around the rigid, pre-stoppered thread, **76**, the synthesis of which was outlined in Chapter 2 in **Scheme 2.23** and **2.24**. Owing to the challenging synthesis and subsequent low yields of olefin terminated barbiturate **62**, these were not investigated towards clipping with **41**.

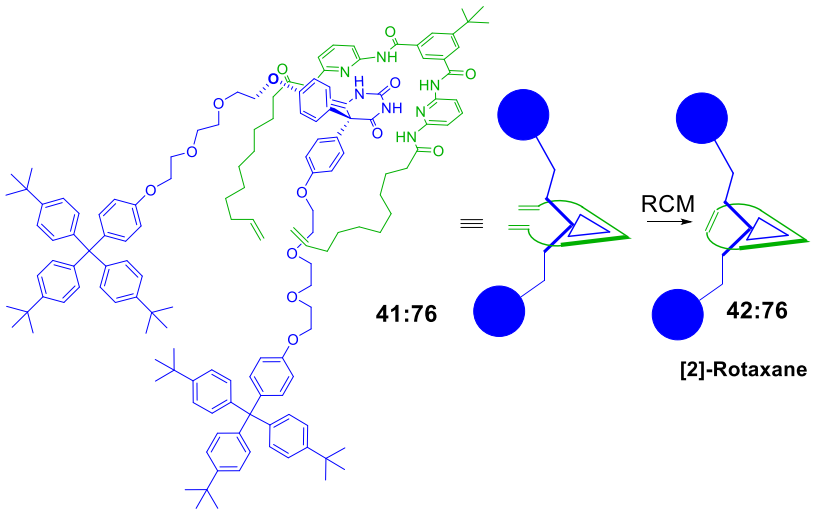

Figure 3.2 – Proposed binding mode of macrocycle **41** with guest **76**, along with schematic representation.

The proposed binding event and subsequent clipping reaction for the molecules **41** and **76** is shown in **Figure 3.2**. To ensure the receptor was fully bound to the guest, an excess of three equivalents of **76** was used for the ring-closing reaction. The solution was heated to 50^{o} C and then 1 mL of a 2.3 mM solution of Grubbs (I) in DCM was added dropwise to the reaction. After 2.5 hours, it was observed via TLC that all of **41** had been consumed and the reaction was stopped.

Interestingly, two extra spots were present which were neither the compounds **42** or **76**, as shown in the TLC, **Figure 3.3**. A ^{1}H NMR spectrum of F2 showed the presence of a complex between **76** and some unknown form of receptor, lacking the C*H*-C*H* signals. Due to the pattern and shifting of observed peaks it can be postulated that this product results from some form of Wacker-Tsuji type oxidation of the double bond, forming an aldehyde. A subsequent TLC of this fraction in fact revealed two spots, and prepTLC resulted in the isolation of **76** and the oxidized receptor compound. A ^{1}H

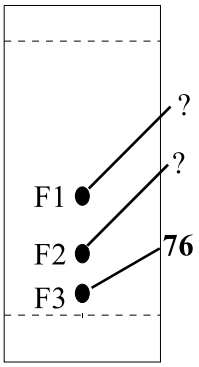

Figure 3.3 – TLC of the crude mixture (eluent: DCM/EtOAc-10 %)

NMR spectrum of the other fraction (F1) revealed this to contain some form of complex between **42** and **76**. This seemed a promising result as a potential candidate for a [2]-rotaxane. However as observed previously, the components have been known to move together on TLC as perched complexes so a series of investigations were carried out, the first being analysis of the sample by mass spectrometry, in which no rotaxane product was detected. Instead, some thread fragmentation of **76** was detected, and only trace amounts of **42** and **76** were observed which meant that the presence of any interlocked structure via mass spectrometry was inconclusive. Interestingly, in order to rule out the detection of H-bonded, perched complexes over their interlocked analogues, a sample was submitted of a premixed, 1:1 solution of the complex **42:76** and analysed by ES^+. What can only be a perched complex was indeed observed and so care should be taken when inferring the interlocked nature of these structures from just a mass spectrum.

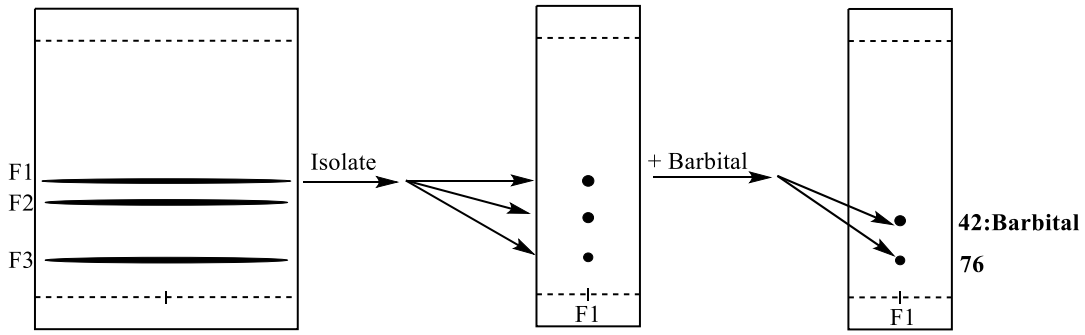

Figure 3.4 – Diagram of prepTLC of the crude reaction mixture followed by TLC of F1, and addition of Barbital to F1

A subsequent TLC of F1, as shown in **Figure 3.4** afforded three further spots indicating that the components of F1 were in equilibrium with the complexes/components within F2 and F3. In an analogous case to that of these receptors with barbital, it would seem that again, there is some form of binding occurring that is not completely disrupted by

the purification process, either on a column or TLC plate. To test this, a TLC was prepared with two spots. The first consisted of a premixed solution of **42** and **76**. The other single spot consisted of independent applications of **42** followed by **76**. The first spot showed the characteristic 3 spots implying a degree of complexation. The second showed only the two spots of the respective components, indicating that the complexation must occur in solution prior to application to the TLC plate. In an attempt to disrupt this complex formation and in turn establish whether any rotaxane had formed, the competitive guest barbital was added to a solution of F1 (**Figure 3.4**). A TLC of this solution showed the disappearance of the **42**:**76** complex (F1) found in the previous mixtures and instead only two component spots were observed. We can assume the barbital now complexes **42**, inhibiting complex formation with **76**. As described previously in chapter 2, when carrying out ring-closing metathesis in the presence of barbital it was observed to form a complex that did not dissociate under the purification conditions and the **42:Barbital** complex was able to be isolated.

These results suggest that for these conditions, the metathesis reaction involving rigid guests is not favourable towards the capture of an interlocked structure. There could be a number of factors inhibiting this process, but the major contributing factors are most probably due to the excess steric bulk added to the guest when two phenyl groups are attached. In the model shown in **Figure 3.5**, constructed in ChemBio3D Ultra, a simpler, rigid guest species has been used to highlight the level of steric interaction in the H:G complex, when cyclised.

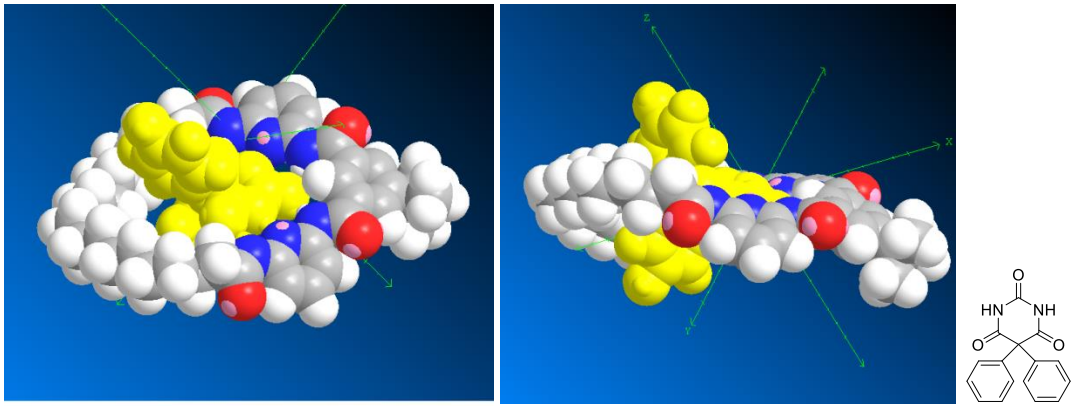

Figure 3.5 – Molecular model constructed in ChemBio3D Ultra between **42** and a simple bi-phenyl guest.

It is evident that there is very little room for the guest molecule in the cyclised receptor which does not sit well in the binding cavity. From this it can be inferred that cyclisation in the presence of the rigid guest may be hindered, which means that cyclisation would only occur in those molecules whose position of equilibrium lies in the dissociated form of the complex i.e. when the guest is absent from the binding site. This is shown schematically in **Scheme 3.3**.

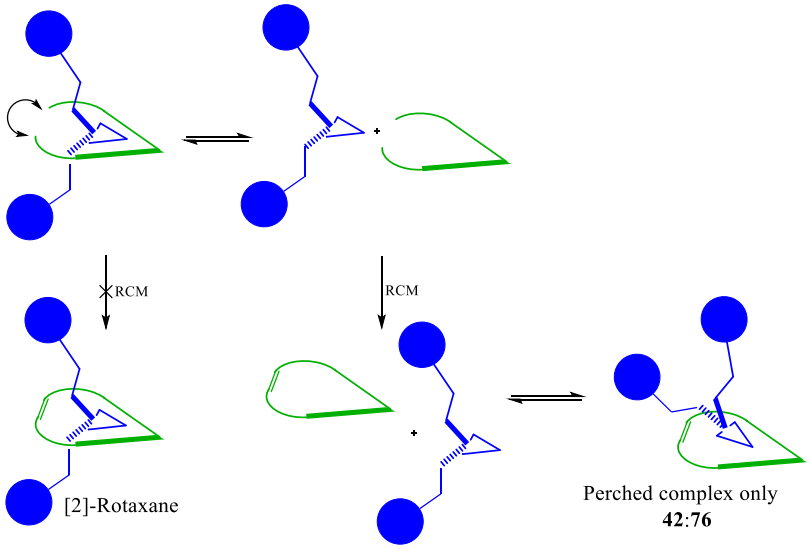

Scheme 3.3 - Proposed reaction pathway towards the formation of a perched complex of **42:76**.

Another issue which was thought to possibly hinder the formation of a rotaxane is that of temperature. Initial binding studies between host and guest were carried out at room temperature; but binding could be less favoured at the 50^{o} C required for the reaction. The series of test reactions at room temperature, discussed in chapter 2, show a diminished, but good yield of cyclisation at room temperature. Therefore, to remove any concerns over diminished complexation at reaction temperatures, the cyclisation with **41** in the presence of **76** was carried out at room temperature.

Three molar equivalents of **76** were used with respect to **41** and the reaction was carried out in DCM at 6.6 mM, using 10 mol% of Grubbs (I) catalyst. Monitoring the reaction via TLC, there was no change observed after 2 hours and therefore stirring was continued overnight. After 16 hours there was still no change and the reaction was then worked up to return only starting materials. From this apparent inhibition of cyclisation at room temperature, it seems that complexation may indeed be an issue with regards to cyclisation. Despite seeing an increase in the yield of cyclisation when using barbital (a considerably smaller guest), the use of bulkier guests required for interlocked structures, hinders cyclisation. The ratio of bound and unbound guest will vary with temperature and at lower temperatures, the guest is favoured in the bound state and appears to inhibit metathesis. At elevated temperatures, there is less binding and so the amount of bound guest decreases, resulting in the observed metathesis. These unsuccessful attempts towards interlocked structures prompted a rethink in the strategy to be used. Since the inherent problem appears to be one of threading, which was not overcome through the use of rigid barbiturates due to their steric hindrance, a different strategy was proposed.

3.3 Approaches via Azide-Alkyne Cycloaddition

3.3.1 Using Barbiturate Guests

Another method for circumventing the problem of threading is to use shorter alkyl chains. If the carbon chain is relatively short, then the directionality imposed by the sp^3 carbon of the barbiturate should be more defined and the alkyl chains are able to sit through the plane of the macrocycle, threading more easily than their longer counterparts. It was thought that if a method could be proposed to stopper these short, threaded molecules, then an interlocked structure could be realised. It would therefore be necessary to consider alternative ways of locking the structure other than clipping the chains of the guest (entry 1, towards a catenane), since the macrocycle formed would be far too small to encompass the chain of the receptor.

Considering entry 2 of **Table 3.1**, this involved the use of short chain barbiturates, in the expectation that threading would occur more easily using shorter appendages. As already discussed in chapter 2, the chosen method for stoppering was the Huisgen 1,3-dipolar cycloaddition (CuAAC, or 'click' reaction), which required using the azide-terminated barbiturate, **83**, as a means towards stoppering, once complexed with **45**, via a coupling with the alkyne-terminated stopper group, **84**. The synthesis of these components (**Figure 3.6**) was previously outlined in **Schemes 2.26** and **2.27**. This method of bond forming has already seen extensive use in the field of interlocked structures owing to its high specificity, high yielding reactions and tolerance of various functional groups.[3] In chapter 2, both the ability to from a threaded complex, **83:45**, as well as the utility of **83** towards a click reaction

with **84** was established. The final step towards an interlocked structure was to combine these aspects and stopper the threaded complex, **45:83**, as described below

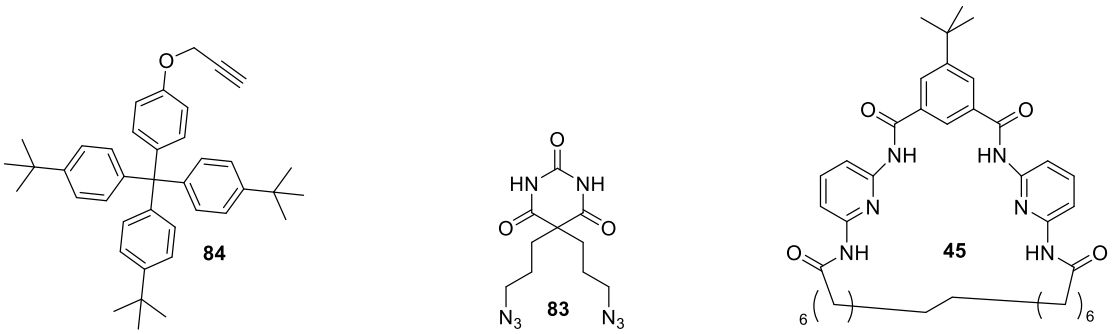

Figure 3.6 – Molecules **84**, **83** and **45** required for the Cu(I)AAC click reaction towards rotaxane formation.

3.3.1.1 Synthesis of a Barbiturate Templated [2]-Rotaxane

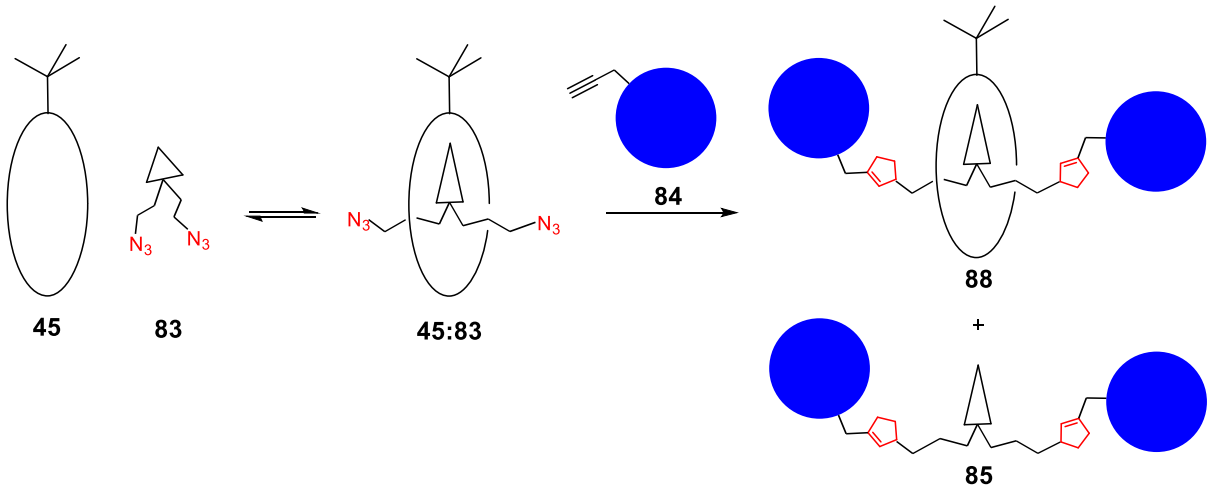

Scheme 3.4 – CuAAC 'click' reaction between **45**, **83** and **84** forming the [2]-Rotaxane **88**, plus free guest **85**.

The click reaction has a wide scope of reaction conditions which may be used, including being carried out at room temperature, in $CDCl_3$. The use of these conditions allows a good degree of certainty that the pseudo-rotaxane will be present in solution. A schematic for the reaction is shown above in **Scheme 3.4**. For the click reaction an equimolar, 56 mM solution of host and guest in $CDCl_3$ was used. Two equivalents of **84** were

added followed by, after a short period of stirring, a catalytic amount of $Cu(MeCN)_4PF_6$ and TBTA. The reaction was stirred at room temperature for 3 days and after removal of the solvent, the crude product was purified via column chromatography to give a 22% yield of rotaxane, **88**, along with a 26% yield of the dumbbell component **85**.

The structure of **88** is shown in **Figure 3.7**, followed by its ^1H NMR spectrum with assignment of peaks and mass spectrum in **Figure 3.8** and **3.9** respectively. **Figure 3.8** clearly shows the presence of a 1:1, H:G complex and the mass spectrum of **Figure 3.9** shows the presence of a H:G complex, however care should be taken when inferring its interlocked nature from this data.

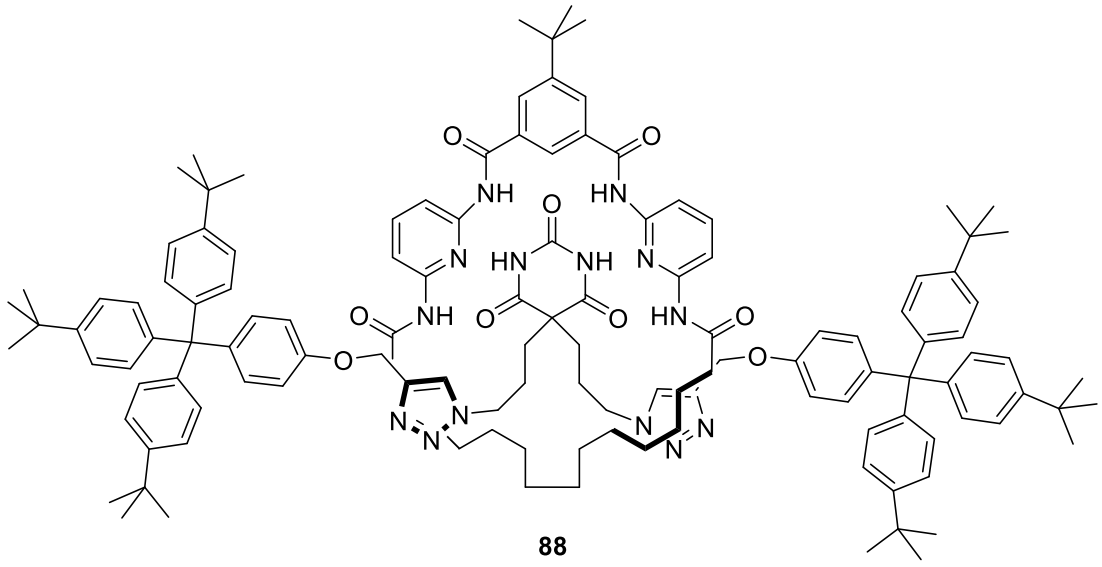

88

Figure 3.7 – Structure of [2]-Rotaxane, **88**.

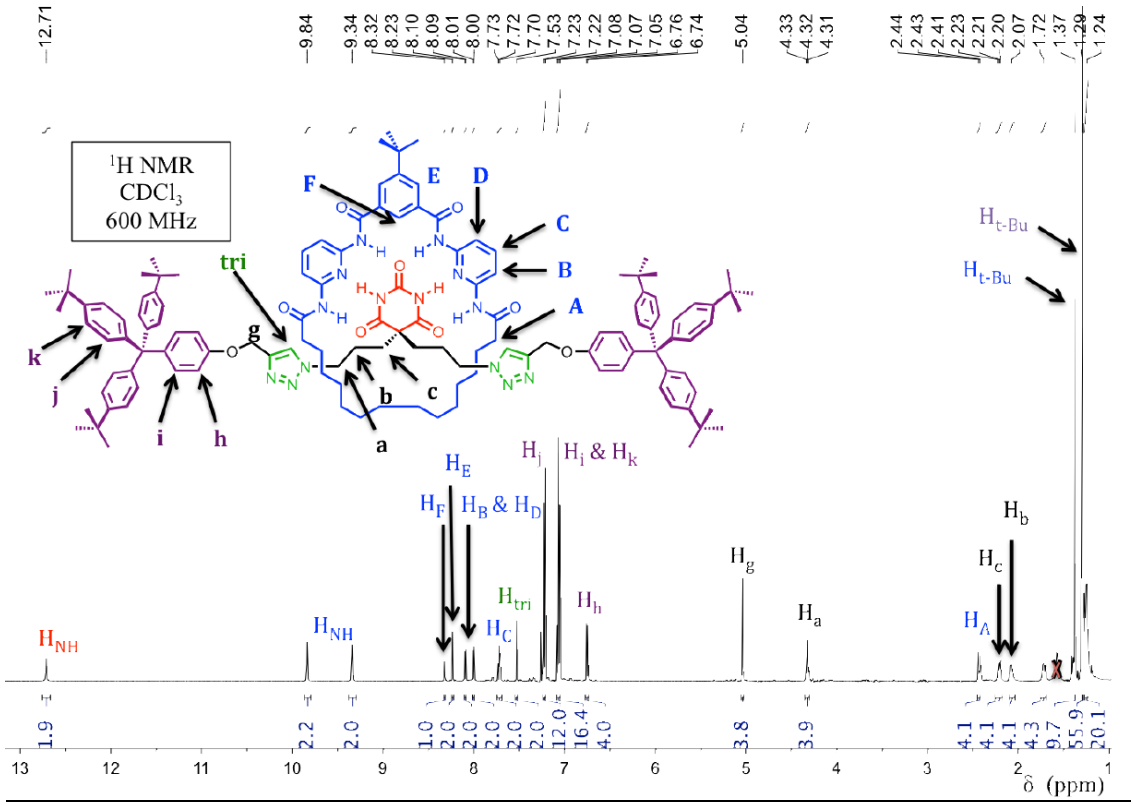

Figure 3.8 – ^{1}H NMR (300 MHz) of [2]-Rotaxane **88** in $CDCl_3$.

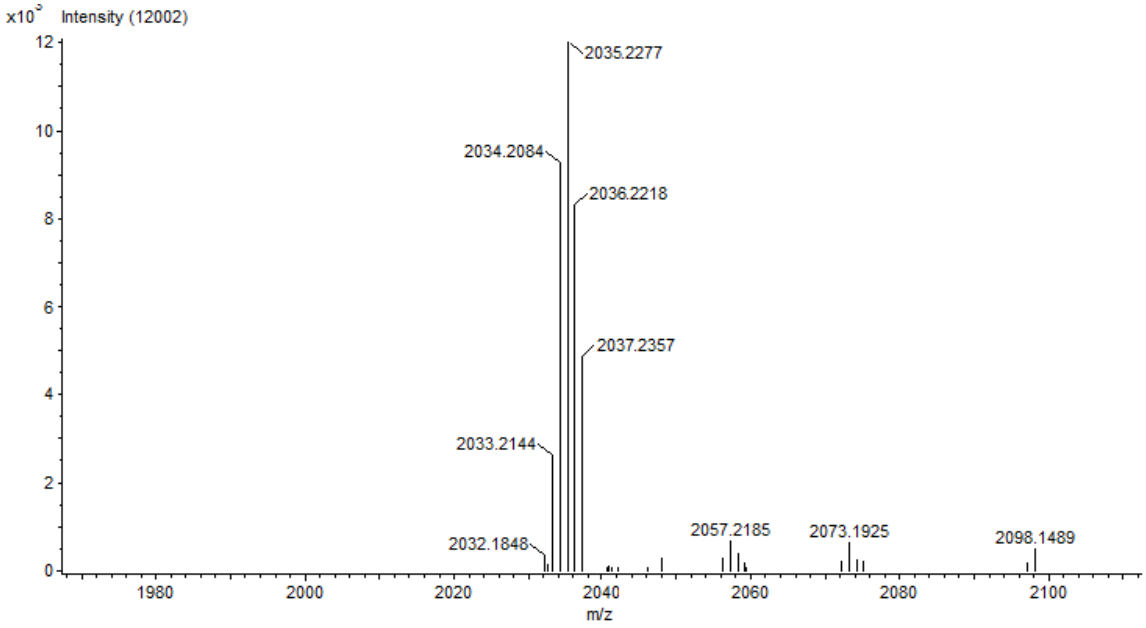

Figure 3.9 – HRMS (ESI) of [2]-Rotaxane, **88**.

3.3.1.2 ^{1}H NMR Studies of [2]-Rotaxane 88

The rotaxane **88** was analysed in detail through a series of ^{1}H NMR experiments. Shown in **Figure 3.10**, the ^{1}H NMR spectra of **88** and dumb-bell component, **85**, have been added to the previous ^{1}H NMR stacked plot of **Figure 2.19**. In comparing the spectra of **45:83**, (b) and **88**, (d), despite minor shifting of the aryl peaks, and a similarity in $H_{N\text{-}H}$ shifts of the amide protons, there is an observable downfield shift in the $H_{N\text{-}H}$ protons of the imide protons of **88** when interlocked. This indicates a stronger binding interaction in the interlocked structure vs the non-interlocked analogue.

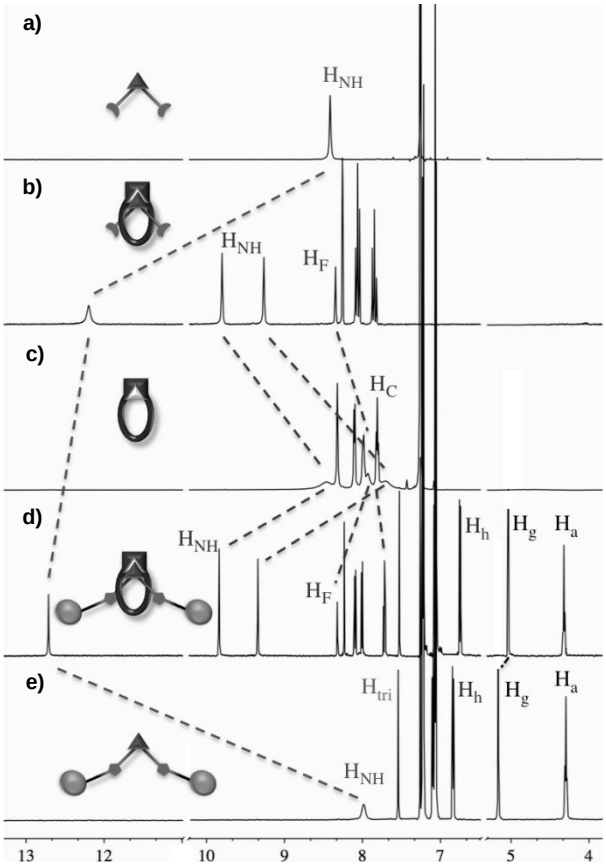

Figure 3.10 - Partial ^{1}H NMR spectra (600 MHz) of barbiturate, **83** (a), pseudo-rotaxane, **45:83** (1:1, 10 mM) (b), receptor **45** (c),[2]-rotaxane **88** (d), and corresponding thread by-product, **85** (e) recorded at room temperature in $CDCl_3$.[4]

Further evidence for the formation of an interlocked structure came from comparing the ^{1}H NMR spectra of each individual rotaxane component, **85** and **45**, the rotaxane, **88** and a solution of non-interlocked host and guest, **45:85** (perched complex) as shown in in **Figure 3.11**. When comparing spectra (a) and (b) ([2]-Rotaxane and perched complex, respectively), one would expect many of the peaks to be almost identical, since almost all protons would be in fairly similar environments, regardless of any interlocked nature. This is mostly what is observed, with one exception; the signal for the NH protons of the guest **85** is significant and shifted downfield by 4.7 ppm (from 8.0 – 12.7 ppm) when present as an interlocked motif.

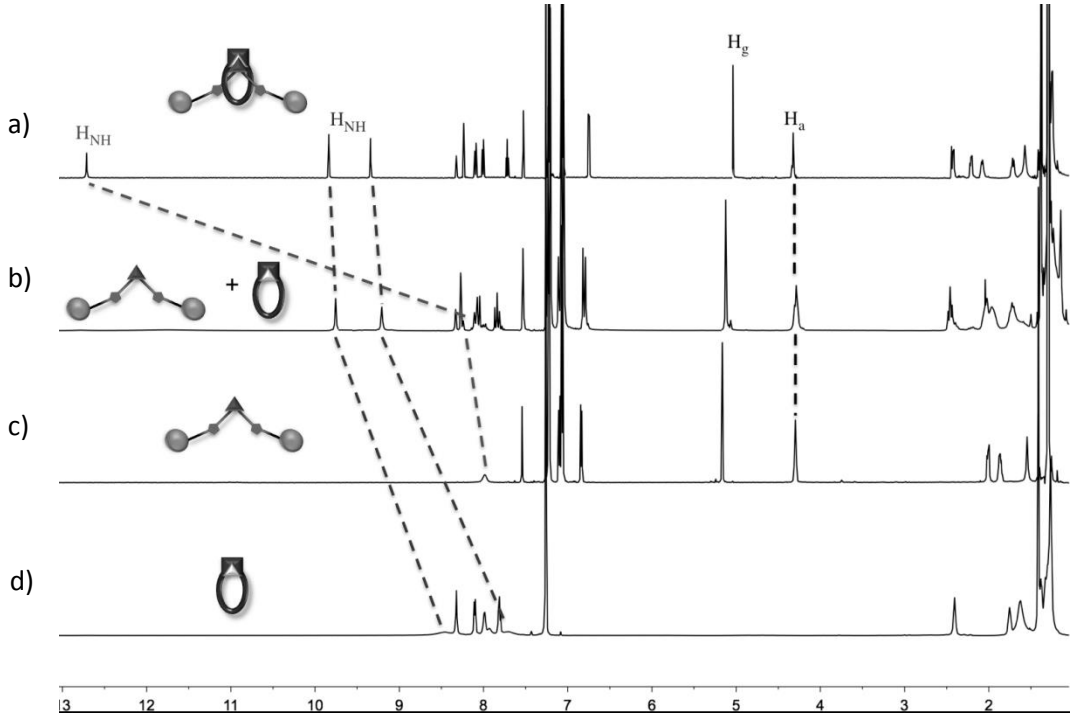

Figure 3.11 - ^{1}H NMR spectra (300 MHz) recorded at room temperature in $CDCl_3$ of the [2]-Rotaxane **88** (10 mM) (a), mixture of barbiturate **85** and receptor **45** (1:1, 10 mM) (b), barbiturate **85** (c) and receptor **45** (d).[4]

To investigate the stability of **88** and to determine whether the rotaxane could be synthesised via a slippage approach, a stability study was carried out. The rotaxane was

dissolved in DMSO-d_6 (10 mM) and subsequently heated at 392 K over a period of several hours to ascertain if any dethreading of **88** from within the macrocycle could occur. The study is shown below in **Figure 3.12.** Due to the nature of the solvent, both **88** and **45** experience a significant effect on their H_{NH} signals. However, molecule:solvent interactions appear somewhat suppressed in the rotaxane, with a distinct upfield shift in the H_{NH} signals. This can be considered further evidence for the strong binding interaction between **45** and **85** when interlocked, due to the removal of the H-bonding solvent from around the vicinity of the binding site. In contrast, the ^{1}H NMR spectrum of the perched complex in DMSO-d_6 shows downfield H_{NH} signals relative to the interlocked analogue, indicating a strong solvent interaction and a weak interaction between the two compounds. From the variable temperature study there is no evidence of any dethreading and the rotaxane can be considered thermally stable. Finally, it is worth noting that the spectrum recorded for the rotaxane in DMSO is almost identical to that in $CDCl_3$, revealing that the H-bonding motif present in the complex is a relatively strong interaction, of the order of the molecule:solvent interactions when using a strong, H-bonding solvent.

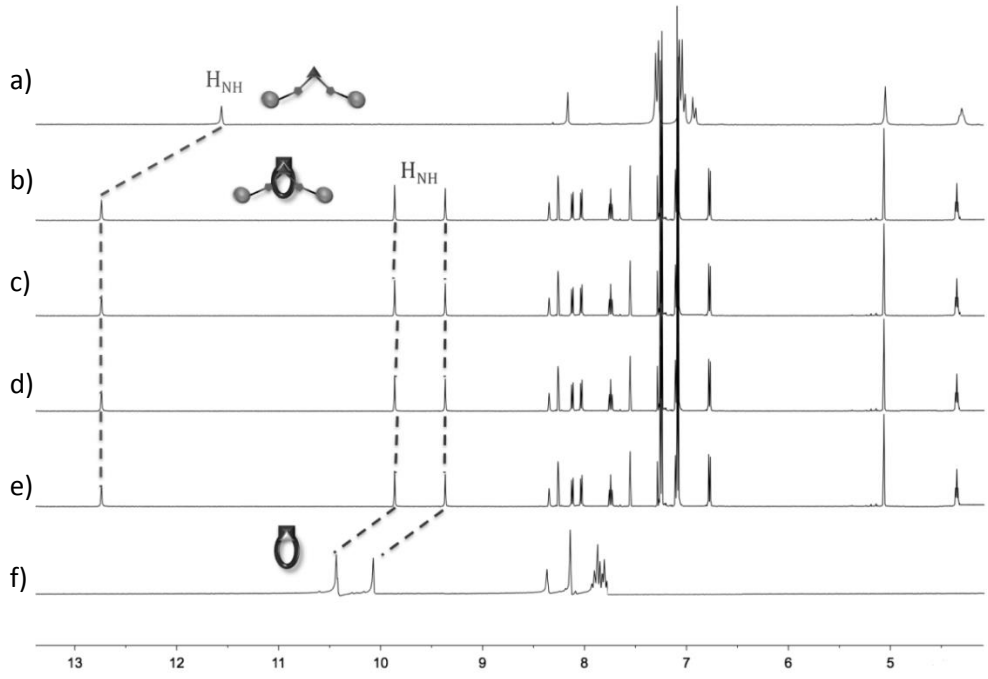

Figure 3.12 - ^{1}H NMR spectra (600 MHz) recorded at room temperature in DMSO-d6 of **85** (a), **88** (10 mM) after heating to 392 K for 0 min (b), 1h (c), 24h (d), 72h (e) and **45** (f).[4]

3.3.2 Active –Template Synthesis of Unsymmetrical Rotaxanes [Cu(I)]

As shown in entry 3 of **Table 3.1**, the approach of using a click reaction was also extended towards the synthesis of interlocked structures through an 'active-template' approach using the Hamilton motif as a Cu(I) binding site. This method of rotaxane formation has no other means of templation other than that of the Cu(I) ion and so this may not be considered as a barbiturate-templated rotaxane, but as a secondary route towards an interlocked structure using the Hamilton binding motif. Such a method to achieve rotaxane synthesis has been carried out previously using various macrocycles.[3b, 5] The synthesis of these components (**Figure 3.13**) was outlined previously in Chapter 2, in **Schemes 2.27** and **2.28.**

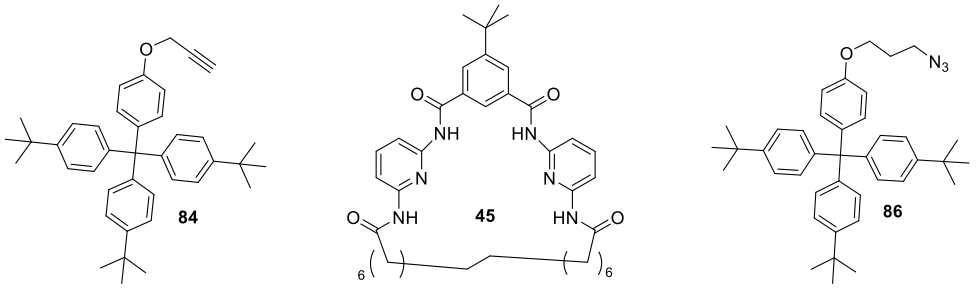

Figure 3.13 - Molecules **84**, **45** and **86** required for the Cu(II)AAC 'click' reaction towards rotaxane formation.

The synthesis of **89** is outlined in **Scheme 3.5.** Receptor **45** was dissolved in chloroform and degassed for 10 minutes. $Cu(MeCN)_4PF_6$ was then added to the solution, forming a suspension which was stirred at room temperature for 1 h, followed by the addition of 1.2 equivalents of both stopper groups, the alkyne, **84**, and azide, **86**. Upon their addition, a solution formed and a colour change to green was observed. After stirring overnight, a suspension had reformed and the workup consisted of adding 10 mL of 0.1 M KCN solution in methanol. There was an immediate formation of a white precipitate and after stirring for 1 h, the solvents were removed and the crude product was purified via column chromatography. No isolated starting materials, **84**/**86**, were obtained from the column, only the non-interlocked dumb-bell, **87**, macrocycle **45** and the [2]-Rotaxane, **89**.

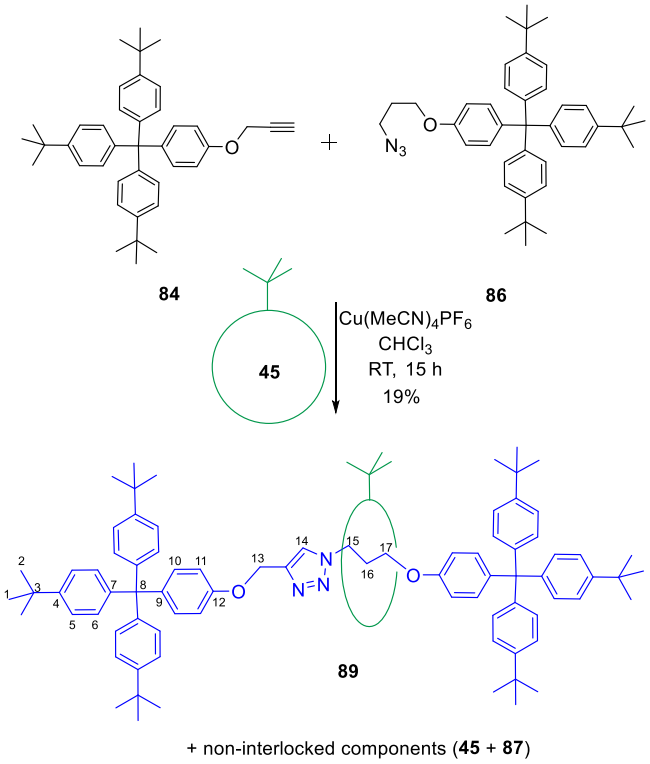

Scheme 3.5 – Reaction scheme for the formation of a Cu(I) templated [2]-Rotaxane **89** using Hamilton-type receptor **45**.

Regarding the bond forming reaction itself, the reaction clearly went to completion. However, it appears that it did not always occur within **45**, leading to the formation of the non-interlocked products **45** and **87**. One useful advantage of this method over previous methods, is the lack of any binding motif between the compounds **87** and **45** and so the problem observed with previous examples regarding possible perched complexation was not observed since any binding interactions present during the process of rotaxane formation do not 'live on' in the interlocked species. The rotaxane could therefore be isolated without any ambiguity over its interlocked nature.

The ^{1}H NMR spectrum of **89** is shown in **Figure 3.14** along with an assignment of the major peaks. This clearly shows the presence of signals for both **45** and **87** in a 1:1 ratio. The mass spectrum of **89** is also shown in **Figure 3.15** and supports the presence of the [2]-

rotaxane via the peak at 1786. A TLC comparison of **45**, **87** and **89** (eluent: Hexane/EtOAc-20%) also gave a clear indication of the formation of an interlocked structure.

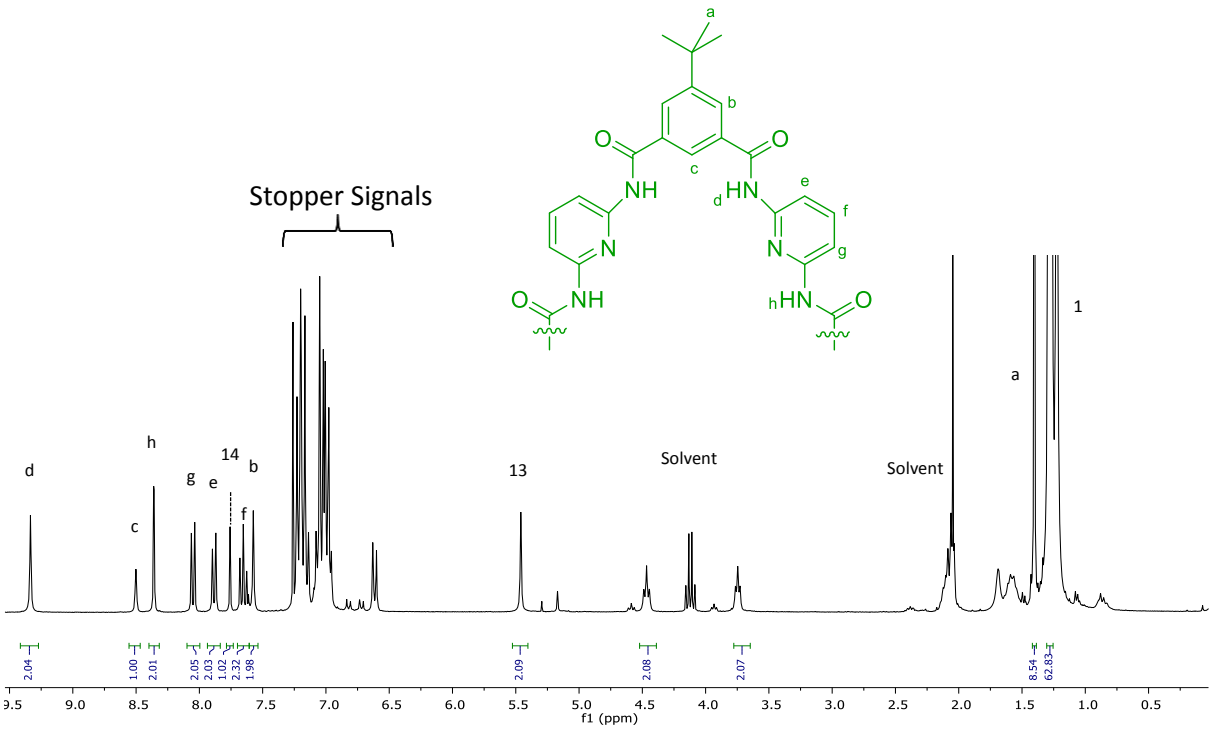

Figure 3.14 – ^{1}H NMR in $CDCl_3$ of [2]-Rotaxane **89** with assignment of peaks. The receptor binding site is shown and labelled for clarity.

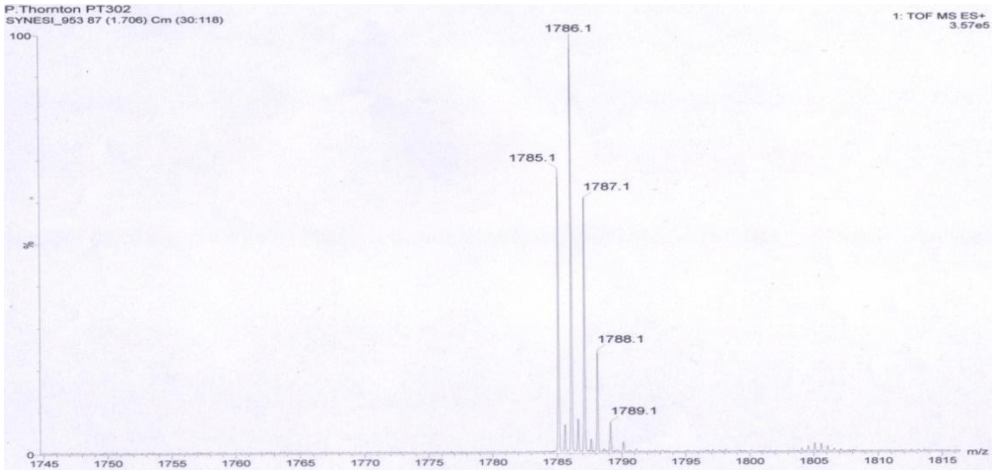

Figure 3.15 - – HRMS (ESI) of [2]-Rotaxane, **89**

3.3.2.1 ^{1}H NMR Studies of [2]-Rotaxane 89

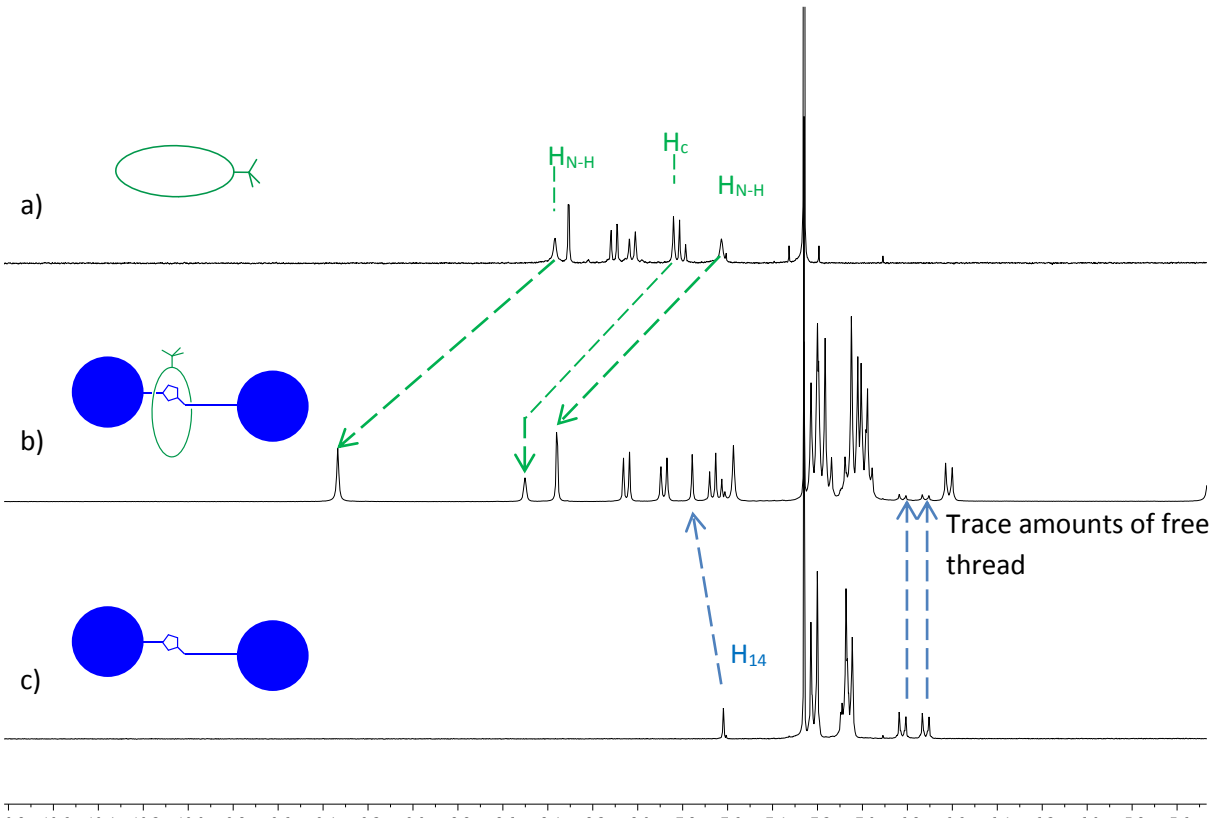

Figure 3.16 – ^{1}H NMR in $CDCl_3$ of receptor **45** (a), [2]-Rotaxane **89** (b) and assymetric dumb-bell **87** (c).

Figure 3.16 shows a series of stacked ^{1}H NMR spectra showing receptor **45** (a), asymmetric rotaxane **89** (b) and the asymmetric dumb-bell **87** (c), respectively. When comparing spectrum (a) with (b), there is a clear downfield shift in the signals for both N-H protons, as well as for the H_c proton of the bridging phenyl group of **86**. There is also a slight downfield shift in the triazole proton signal (H_{14}) of interlocked **87** when comparing spectrum (c) with (b). Despite no specific H:G binding motif present, these downfield shifts are indicative of some level of interaction between the two interlocked components. The aryl region corresponding to the stopper groups has clearly become more complex, which is possibly due to the two stopper groups now residing in slightly different chemical environments. Due to the non-symmetric nature of **89**, one might expect a situation where

45 does not sit perfectly in the centre of the thread, with respect to the stopper groups. From the chemical shifts observed in the ^{1}H NMR spectrum, it appears that **45** is located at or around the triazole group (**Figure 3.17**). This would account for the increase in complexity of the signals relating to the stopper groups.

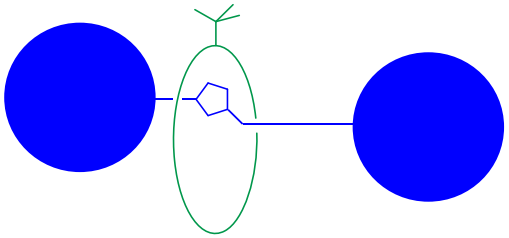

Figure 3.17 – Proposed location of **45**, on the thread of **89**.

Despite the adequate solubility of **89** in $CDCl_3$ for spectral analysis, stacked spectra for probing any differences in perched/threading motifs was not possible due to the non-interlocked component being insoluble. However, as mentioned already, despite some minor interactions observed due to their close proximity in space, there are no intrinsic H:G binding interactions by design, between the thread and macrocycle, as is observed for the barbiturate templates. Therefore it is highly unlikely that any perched complex could form.

3.4 Conclusions and Future Work

3.4.1 Conclusion

A number of approaches, with varying successes, have been implemented towards the capture of an interlocked structure using Hamilton-type receptors, in most cases utilising barbiturate templation. Various methodologies were attempted, including those of threading-clipping, clipping, threading-stoppering and active templation.

In the case of using flexible, olefin terminated guests, despite an observed H:G interaction, no capture of an interlocked structure was possible. This is due to what has been described as formation of 'perched' complexes, resulting in a clipping event producing two independent macrocycles only. Despite the observed H:G binding, it seems that there is not a strong enough driving force to favour the desired threading interaction and subsequently, this method was abandoned in favour of other approaches.

So as to improve the likelihood of threading, attempts were made to increase the directional nature of the pendant arms using phenyl spacers at the sp^3 centre of the barbiturate. Synthetic challenges prevented any attempts of a guest-clipping approach with the olefin-terminated barbiturate **62** and only an investigation involving guest **76** was accomplished. However, once again, despite an observed H:G complex between **76** and **41**, no interlocked structure was isolated using Grubbs metathesis. This has been attributed to a steric effect, introduced by the presence of the phenyl spacers, preventing cyclisation of **41** when present as a H:G complex. It is possible that an increase in the tether length to try to accommodate the increased bulk of the guest would lessen the steric burden. However, with an increase in length, the cyclisation yields could diminish.

Circumventing the problem of threading was a key factor in the synthesis of barbiturate-templated rotaxanes. This was achieved by a move away from a metathesis approach towards one of click chemistry. By appending relatively short pendant arms to the barbiturate, the barrier to threading was overcome and formation of the desired pseudo-rotaxane was achieved and confirmed via a crystal structure of the complex (Chapter 2, **Figure 2.17**). By employing the high yielding CuAAC reaction, an efficient stoppering event

of the threaded **83**:**45** complex was achieved and the synthesis of the first barbiturate-templated rotaxane, using Hamilton-type receptors was realised.

Hamilton receptors were also employed in the synthesis of assymetrical rotaxanes, again employing the CuAAC reaction. The Hamilton receptor was used in an active template approach, via the complexation of the Cu(I) catalyst, thus allowing the click reaction to be performed within the macrocycle, resulting in the formation of a [2]-rotaxane. This method does not require the use of barbiturate templation, but highlights the utility of these Hamilton-type receptors as a scaffold for interlocked structures.

3.4.2 Future Work

The concept of clipping around a pre-stoppered guest, following a H:G binding event (such as the attempts of entry 4 of **Table 3.1**) may see much more synthetic utility in the growing field of interlocked structures than that of a stoppering approach, due to the increased array of novel architectures available. In order to expand and improve upon this method through the use of acyclic receptors, a different approach towards the required rigidity could be investigated. Through the use of different, and less sterically bulky spacer groups, it may be possible to overcome the issues already encountered. One candidate for this steric enhancement may be through the use of barbiturates with alkyne spacers, **Figure 3.18**, which would still provide the desired rigidity and directionality, but are considerably smaller than the phenyl groups already used.

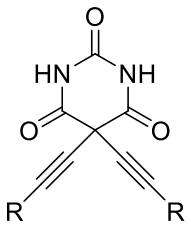

Figure 3.18 – Proposed guest molecule to improve clipping approaches.

Another aspect of future work to be considered is a different method towards the active template approach using a new series of host and guest compounds. This would involve a combination of H-Bonding and active templation. This modified approach, as shown in **Figure 3.19**, involves the use of asymmetrical receptor compounds, which have pendant arms terminated in both azide and alkyne groups. By combining these with barbiturate guests that contain a copper(I) binding site, it may be possible to use the CuAAC reaction to afford rotaxanes in improved yields, provided that long enough linkers are used to alleviate the issues already seen and accommodate the pyridine groups.

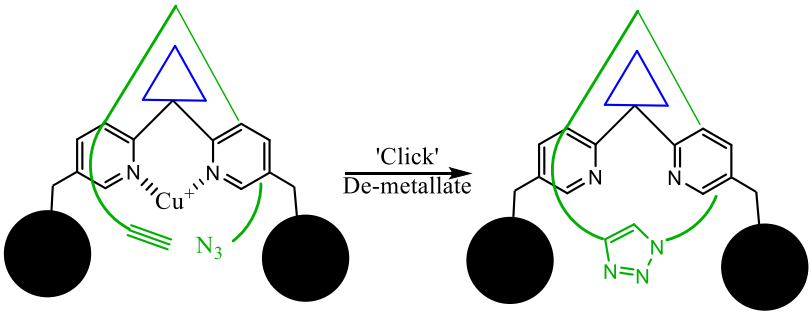

Figure 3.19 – H:G binding event and subsequent 'Click' reaction of a potential route to a new [2]-Rotaxane.

3.5 References

1. Rocher, M. Towards interlocked structures based on H-bonded barbiturate complexes. University of Birmingham, 2010.

2. (a) Frisch, H. L.; Wasserman, E., Chemical Topology1. *J. Am. Chem. Soc.* **1961,** *83* (18), 3789-3795; (b) Schill, G.; Beckmann, W.; Schweickert, N.; Fritz, H., *Chem. Ber.* **1986,** *119* (8), 2647-2655.

3. (a) Aucagne, V.; Berná, J.; Crowley, J. D.; Goldup, S. M.; Hänni, K. D.; Leigh, D. A.; Lusby, P. J.; Ronaldson, V. E.; Slawin, A. M. Z.; Viterisi, A.; Walker, D. B., *J. Am. Chem. Soc.* **2007,** *129* (39), 11950-11963; (b) Aucagne, V.; Hänni, K. D.; Leigh, D. A.; Lusby, P. J.; Walker, D. B., *J. Am. Chem. Soc.* **2006,** *128* (7), 2186-2187; (c) Collin, J.-P.; Durola, F.; Frey, J.; Heitz, V.; Reviriego, F.; Sauvage, J.-P.; Trolez, Y.; Rissanen, K., *J. Am. Chem. Soc.* **2010,** *132* (19), 6840-6850; (d) Dichtel, W. R.; Miljanić, O. Š.; Spruell, J. M.; Heath, J. R.; Stoddart, J. F., *J. Am. Chem. Soc.* **2006,** *128* (32), 10388-10390; (e) Prikhod'ko, A. I.; Sauvage, J.-P., *J. Am. Chem. Soc.* **2009,** *131* (19), 6794-6807.

4. Tron, A.; Thornton, P. J.; Rocher, M.; Jacquot de Rouville, H.-P.; Desvergne, J.-P.; Kauffmann, B.; Buffeteau, T.; Cavagnat, D.; Tucker, J. H. R.; McClenaghan, N. D., *Org. Lett.* **2014,** *16* (5), 1358-1361.

5. (a) Winn, J.; Pinczewska, A.; Goldup, S. M., Synthesis of a Rotaxane CuI Triazolide under Aqueous Conditions. *J. Am. Chem. Soc.* **2013,** *135* (36), 13318-13321; (b) Saito, S.; Takahashi, E.; Nakazono, K., *Org. Lett.* **2006,** *8* (22), 5133-5136.

4 Design and Synthesis of Photoactive Interlocked Structures

4.1 Introduction and Background

4.1.1 Fluorescence and Photochemistry

The following chapter requires a brief outline and general understanding of the concepts of fluorescence and photochemistry and in this particular case, that of anthracene. Photochemistry is the study of chemical reactions that proceed with the absorption of light by atoms or molecules.[1] Photochemistry governs a whole array of synthetic and physical properties and analytical techniques which are beyond the scope of this introduction, but a brief description of the fundamental processes involved is described as follows.

For every molecule, a series of discrete energy levels exist which may be accessed by means of excitation. These energy levels are quantized, and have a specific value for different molecules leading to individual frequencies of radiation for absorption and emission processes. The Stark-Einstein law states that if a species absorbs radiation, then one particle is excited for each quantum of radiation absorbed, which gives us the notion of quantum yield, Φ. Quantum yield is defined as the number of molecules of reactant consumed per photon of light absorbed. This may be specified for a particular process i.e. fluorescence, Φ_f - the ratio of photons absorbed, to those emitted as fluorescence.[2] Considering the absorption of a single photon by a molecule in the ground state, and per the Stark-Einstein law, one molecule is excited for each quantum of radiation absorbed, and provided the incident photon is of sufficient energy, an electronic transition occurs, A, as shown in **Figure 4.1**. If it is of sufficient energy, an electron is promoted from its occupied

orbital to an unoccupied orbital of higher energy. The system is now at a higher energy and is considered an 'excited state'. From here, any number of pathways may be utilised to return to the lower energy ground state through either radiative or non-radiative pathways. The Jabłoński diagram of anthracene, **Figure 4.1**, gives examples of these pathways and shows the singlet ground state, S_0, singlet excited state, S_1 and the triplet excited states, T_1 and T_2 in bold, along with the vibrational levels of each discrete energy level. Radiation processes are shown in straight lines, non-radiative with waved lines.

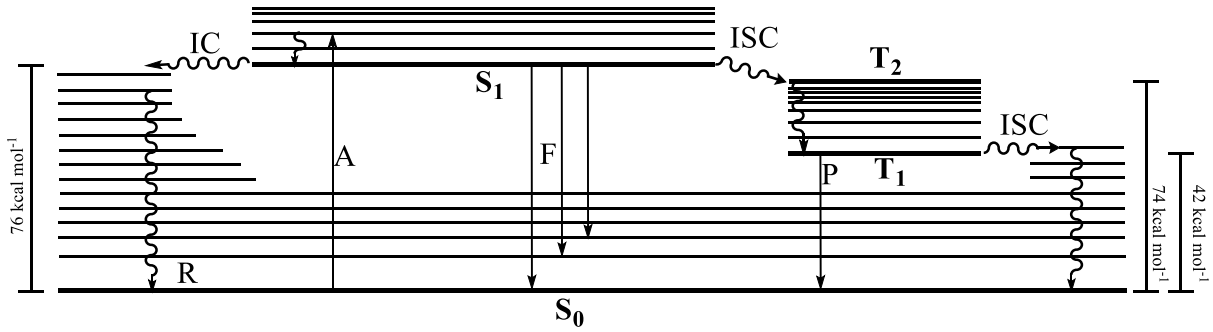

Figure 4.1 - Jabłoński diagram depicting the various electronic states and processes of relaxation for an anthracene molecule. Processes are as follows: A: Absorbance, F: Fluorescence, P: Phosphorescence, IC: Internal Conversion, ISC: Intersystem Crossing, R: Vibronic relaxation, S_n: Singlet State, n = energy level, T_n: Triplet State, n = energy level.

After the initial absorbance of a photon, an electron is excited into a vibrational level of a singlet excited state, depending on the initial energy of the incident photon. A relaxation then occurs to the lowest vibrational energy level of S_1. Every molecule will have its own particular lifetimes associated with each of the processes, and these specific lifetimes and relative energies of the excited states will lead to the favouring of various pathways. If internal conversion, IC, occurs, then the molecule simply relaxes to its original ground state, S_0, with no radiative emission observed. Relaxation from $S_1 \rightarrow S_0$ results in emission of a photon producing fluorescence, F. The third pathway involves intersystem crossing, ISC, to the triplet excited state, T_1, and this is where the spin of the electron is

changed. After relaxation to the lowest vibrational energy, a $T_1 \rightarrow S_0$ transition will result in emission of a photon, known as phosphorescence, P. ISC can also occur from T_1, lowering the energy of the molecule via relaxation with no emission.[2]

There are other, less common ways in which an excited molecule may reduce its energy when in the presence of another molecule. PET, or photo-induced electron transfer can result in the transfer of charge via either intra- or intermolecular electron transfer. This phenomenon is utilised by plants in photosynthesis as well as in non-biological systems such as solar cells. Radiative energy transfer can occur, and involves the emission of a photon, which may be reabsorbed by a nearby molecule. Conversely, non-radiative energy transfer may occur between molecules through dipole-dipole interactions, or collisions. Finally, molecules in the excited state may reach lower energies via chemical reactions, such as dissociation leading to fragmentation, isomerization or reaction, the last of which will be the process of focus for this chapter.

4.1.2 Anthracene and its Photochemical Properties

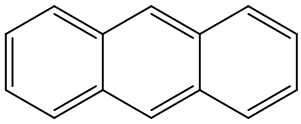

90

Anthracene, **90**, is a small, highly conjugated molecule consisting of three fused benzene rings resulting in a planar structure. It is a colourless compound, emitting blue fluorescence under UV light and is known to have interesting spectral and photochemical properties. The UV-Vis absorption spectrum is shown in **Figure 4.2** with the fine structure of the $S_0 \rightarrow S_1$ band attributed to discrete vibrational transitions between the S_0 and S_1 states.

The energies of the various excited states, relative to S_0 are shown on the diagram in **Figure 4.1**. The $S_1 \rightarrow S_0$ transition has a value of 76 kcal mol^{-1} and the $T_1 \rightarrow S_0$, a value of 42 kcal mol^{-1}. The T_2 is only fractionally lower in energy than S_1, with a value of 74 kcal mol^{-1} and this has significant implications regarding the physical and electronic properties of the molecule. A difference of only 2 kcal mol^{-1} means that ISC from S_1 to T_2 proceeds readily, with a quantum yield of 0.7. The quantum yield of fluorescence has been found to be 0.3 and therefore the sum of quantum yields for ISC and F combine to 1.[3] Therefore, anthracene molecules in S_1 are unlikely to relax via IC, indicating that this process is inhibited.

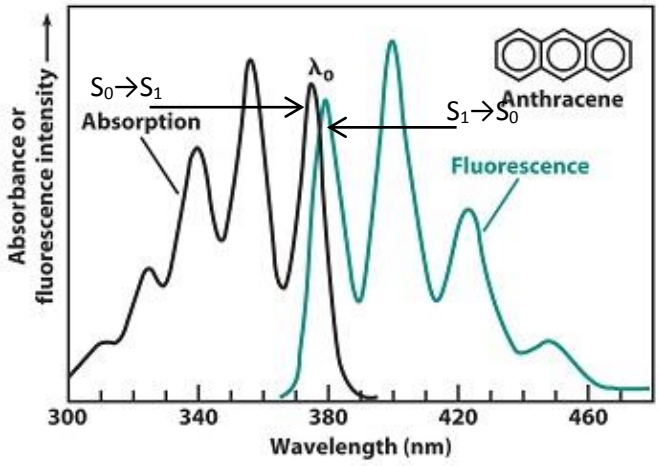

Figure 4.2 - UV-Vis spectrum of anthracene[4] in cyclohexane, showing absorption and emission lines, with the $S_0 \rightarrow S_1$ absorption and $S_1 \rightarrow S_0$ emission highlighted.

In terms of photochemical reactions, a photon of visible light has a similar energy to that of some bond dissociation energies and therefore roughly corresponds to activation energies for various reactions to take place. In other words, the excited state may adopt a conformation and/or electron configuration favourable towards reaction, isomerization, etc. There is also the possibility of excited states having marked differences in acid/base or electrochemical properties. For instance, when an electron is excited it will be more easily removed from the molecule and conversely, the vacancy it leaves behind will be more easily

filled, so an excited molecule will experience a decrease in ionisation energy and an increase in electron affinity. When these excitations are carried out in solution, the close proximity of other molecules, including solvents, has a direct influence on the fate of the excited species and physical quenching may play a more significant role. If the neighbouring molecule is able to react with the excited species, then an intermolecular photochemical reaction can take place. There are numerous photochemical reaction pathways that a molecule may undergo, including isomerizations/rearrangements, inter- and intra-abstractions and photoaddition/cyclisation reactions.[2] The latter is the property of focus for anthracene and is one of the oldest known photochemical reactions, first discovered by Fritzsche in 1867.[5]

When anthracene is present in solution, excimer formation can occur. An excimer, the formation of which was first recognized through the effects of fluorescence on increasing concentrations of solute, is a relatively long-lived dimeric interaction between an excited species and its ground state molecule. The dimerization of anthracene, A, and shown in **Scheme 4.1**, occurs via a singlet (S_1) excimer, which collapses to a photodimer in a 4π+4π pericyclic cycloaddition. The anthracene excimer shows weak fluorescence, so relaxation via emission is supressed and the system therefore reacts efficiently to the dimer, **91**. The process is shown in the following steps, where ^{1}A* is the singlet excited anthracene, ^{1}(A-A)* is the excimer and A-A is the stable photoproduct.[6]

$$A + h\nu \rightarrow {}^1A^* \qquad (1)$$

$$^1A^* + A \rightarrow {}^1(A\text{-}A)^* \qquad (2)$$

$$^1(A\text{-}A)^* \rightarrow A\text{-}A \qquad (3)$$

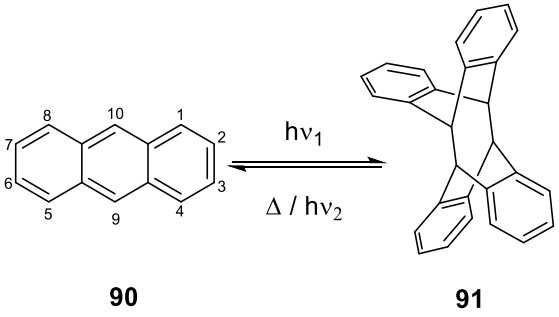

Scheme 4.1 - Dimerization of Anthracene

The case shown above is clearly for free anthracene molecules. However, upon substitution at the 9 position, photodimerization can lead to two different structural isomers, depending upon the orientation of the substituents. The forms can either be head-to-head (hh) or head-to-tail (ht) and are depicted in **Figure 4.3**.[7]

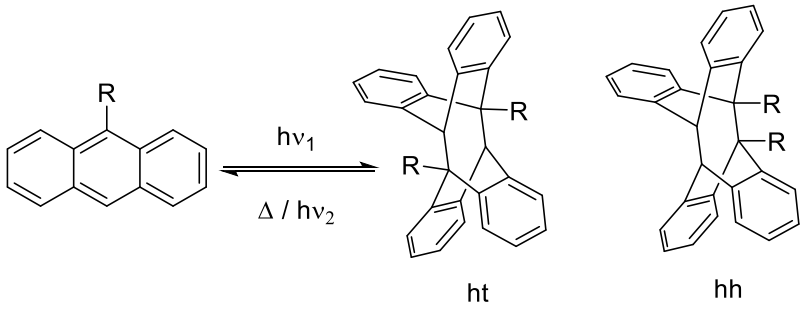

Figure 4.3 – Dimerisation of 9-substituted anthracene forming its two structural isomers, and the reverse reaction reforming the starting material.

In terms of cyclisation reactions, if tethers are implemented between the anthracene units, these molecules can now be considered as bichromophoric systems. For intramolecular reactions, concentrations $<10^{-3}$ M are normally required to avoid any unwanted intermolecular dimerization.[8] Following excitation of one anthracene unit in the system, then an excimer is again formed and dimerization will occur. The reaction can be considered a photocyclomerisation.[9] As shown in **Scheme 4.1**, the photodimerization of

anthracene molecules, whether in a uni- or bimolecular arrangement is by no means a permanent arrangement. The photodimer is able to revert back to the parent molecule/s, either through the application of heat or by irradiation with shortwave UV light, <270 nm. The ease of return depends on the substituents present, and the conformation of the dimer (hh vs ht).[7]

4.1.3 Applications in Supramolecular chemistry

4.1.3.1 Non-interlocked Structures

Owing to their interesting and well-studied optical and electronic properties, coupled with a relatively extensive scope towards synthesis and functionalistion, anthracene has found a broad use in the field of supramolecular chemistry, most notably in the field of chemosensors/devices. Chemosensors typically consist of two regions; a binding site is required, which will usually be tailored for a particular substrate/analyte, and a reporter group is used to signal the presence of the bound substrate. For a supramolecular device to function as such, there must be some variation in the level of observable output of the attached reporter group, be it a gradual increase/reduction in signal, or an on/off switch of the output. An example of an ON/OFF sensor is shown in **Figure 4.4**. The binding site will be tailored towards the complexation of specific analytes and in this particular case a reduction in signal from reporter group R is observed upon the presence of analyte, A, when bound in the binding site, B, thus indicating the presence of the analyte of interest.

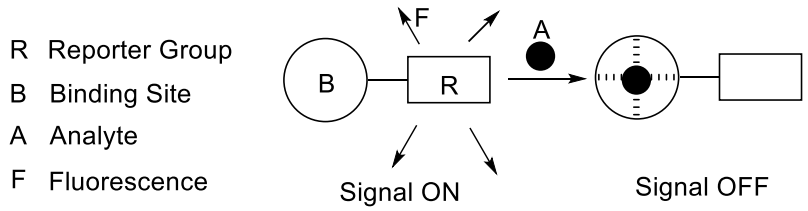

Figure 4.4 – Generic schematic of a signal OFF chemosensor.

This is considered a SIGNAL OFF sensor but in practice it is more beneficial to use the inverse scenario i.e., SIGNAL ON to mitigate ambiguous interpretations. This approach was applied towards the detection of biologically important alkali metal ions by A. P. de Silva and co-workers.[10] The structure and detection process of the ion sensor, **92**, is shown in **Figure 4.5**.

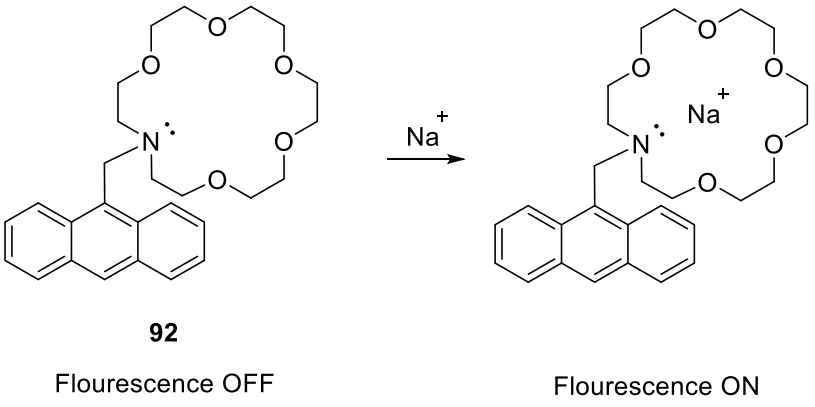

Figure 4.5 – Anthracene based receptor as developed by A. P. de Silva.

In the absence of a metal ion, fluorescence of the anthracene is quenched via photo-induced electron transfer (PET) from the lone pair on the nitrogen of the monoaza crown ether.[11] Upon binding, quenching no longer occurs and fluorescence is observed, indicating the presence of the metal ion.

Another application depicting the use of anthracene in supramolecular chemistry is the work carried out by Tucker et al.[12] This involved utilising the Hamilton-type receptors

towards the photo-switched binding of barbital in chlorinated organic solvents (**Figure 4.6**), (for more detail see **Figure 1.26**) and although this was covered briefly in the introduction, a more thorough discussion of this example follows.

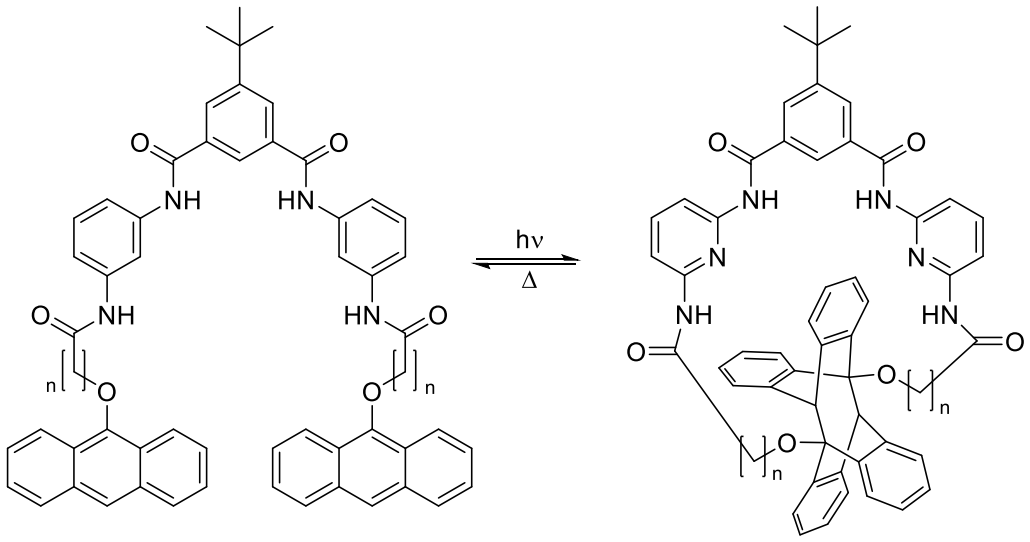

Figure 4.6 – Photodimerization of anthracene terminated Hamilton receptors as demonstrated by Tucker et al.

The acyclic receptors, appended with anthracene molecules, showed high binding constants with barbital. However, after photo-dimerization and formation of the macrocycle, the binding site was disrupted and no longer in an optimal geometry for H:G binding. For shorter linker lengths (n=3), the guest could therefore be expelled from the binding site upon photo-dimerisation. The data obtained regarding the binding constants in the cyclic and acyclic forms of these receptors is shown in **Table 4.1** and clearly shows the differences in binding between the two forms, resulting in the observed photo-switched binding. The crystal structure of the dimerized receptors are shown in **Figure 4.7** and highlights the source of the disturbance towards the binding of barbital where n=3, whereby the xylene units of the photodimer protrude into the binding cavity and release the barbital, evidenced by a three-fold decrease in binding constant. It should be noted that the longer

tether (n=6), despite some distortion in the binding site, experienced reduced changes in geometry and as a result, maintained a relatively good binding constant with barbital as a photodimer.

Table 4.1[12] - Binding constants of bichromophoric hamilton receptors with barbital as determined in [i]CDCl3 at *ca*. 3.5 x 10^{-3} M by NMR spectroscopy, [ii]in $CHCl_2$ at *ca*. 2 x 10^{-6} M by fluorescence spectroscopy and [iii]in $CHCl_2$ at *ca*. 2.5 x 10^{-5} M by UV-Vis spectroscopy.

Tether Length ('C' - cyclised)	Binding Constant
3[ii]	38000
3C[i]	38
6[iii]	71000
6C[iii]	26000

This concept of photo-release of guest molecules upon irradiation offers a new and reversible binding motif, and mode of guest release, into the collection of photo-induced molecular processes.

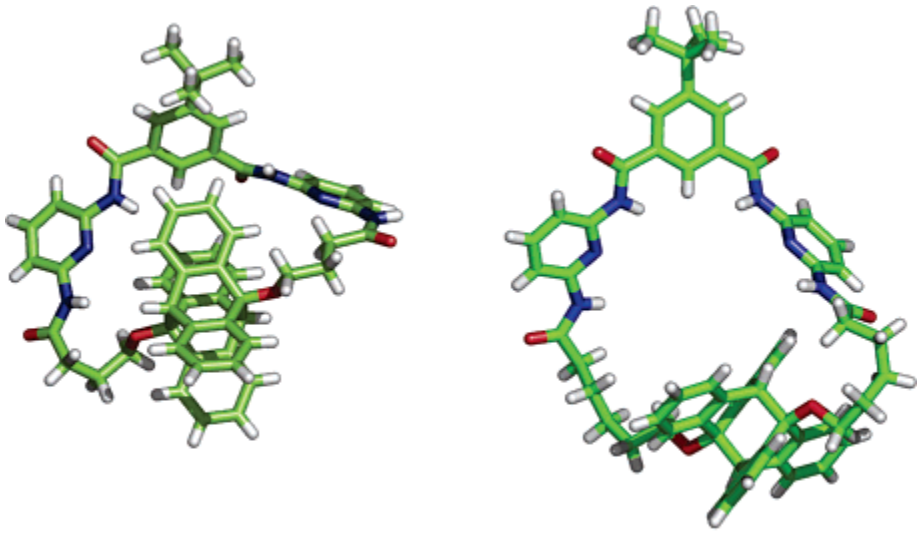

n=3 n=6

Figure 4.7[12] X-Ray crystal structures of dimerised receptors of varying tether lengths.

4.1.3.2 Interlocked Structures

In the field of interlocked structures, the physical, electronic and chemical properties of anthracene have been used. The steric bulk of anthracene has been combined

with its electronic properties and utilised to great effect by the Leigh group.[13] Here, the anthracene molecule was used as a stopper group for an isophthalamide macrocycle as shown in **Figure 4.8**. Originally intended as an 'inactive' model towards studies concerning electron and energy transfer, rotaxane **93** was found to exhibit photo-induced shuttling on a subnanosecond timescale, brought about by a rearrangement in the pattern of hydrogen bonds between thread and macrocycle leading to a shift of the latter from the peptide site toward the anthracene-9-carboxamide stopper which has a greatly enhanced hydrogen bonding affinity in the excited state. In H-bonding solvents, essentially identical absorbance spectra were obtained for the rotaxane and thread components, since the macrocycle is located on the alkyl spacer. However, in non-competitive solvents, the fluorescence of the rotaxane is considerably broader and more intense. This is thought to be due to conformational changes, as proposed by Werner and Rogers in their studies of the fluorescent properties of meso-substituted amidoanthracenes.[14] They explained their observation by assuming that in the excited singlet state, the conformation changes from one in which the planes of the amide group and the anthracene ring are essentially perpendicular to a planar configuration, in which a considerable transfer of charge onto the carbonyl oxygen atom occurs, leading to enhanced hydrogen bonding. The photoinduced motion presented is of particular significance since light is considered an extremely convenient stimulus, when compared to other such photoinduced shuttling phenomena which require the use of external chemical reagents such as photo/redox-active components.[15]

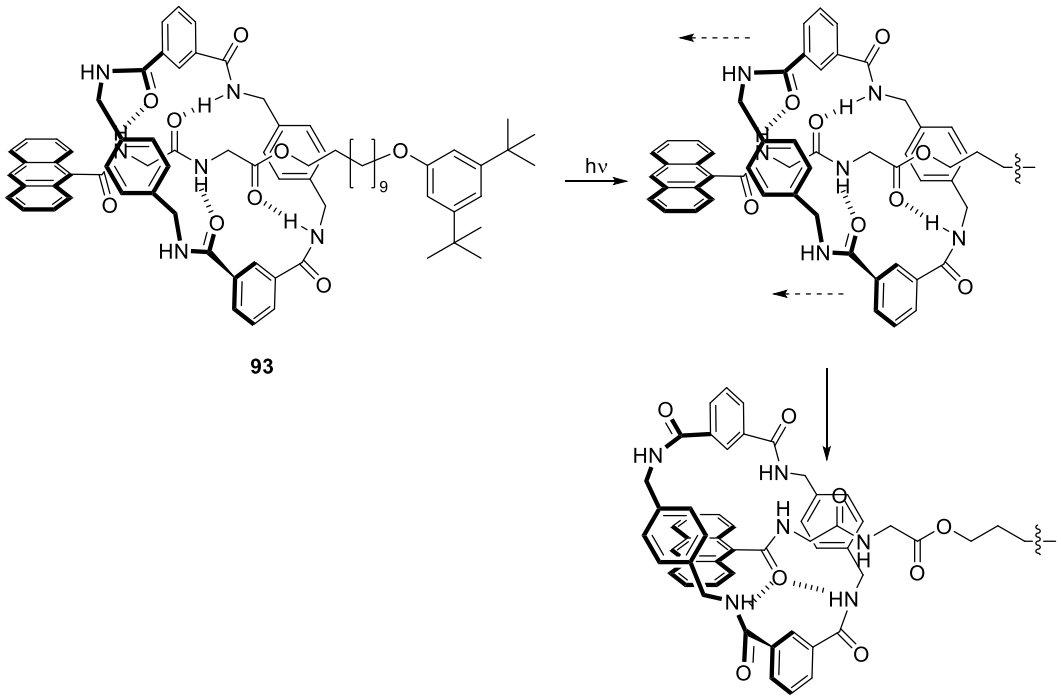

Figure 4.8 – Proposed structures for photo-induced molecular shuttling

Further novel and interesting applications of anthracene related to interlocked structures were achieved through the inclusion of anthracene within the interlocked ring (rather than acting as a stopper group) in the synthesis of the squaraine rotaxane **94** (**Figure 4.9**). When solutions of the rotaxane were irradiated in the presence of oxygen, quantitative formation of the corresponding endoperoxide was observed. These could be stored indefinitely at cool temperatures and upon warming would revert to the parent molecule via chemiluminescent endoperoxide cycloreversion. This process displays possible imaging applications in living subjects due to the molecule's property of near-IR fluorescence.[16]

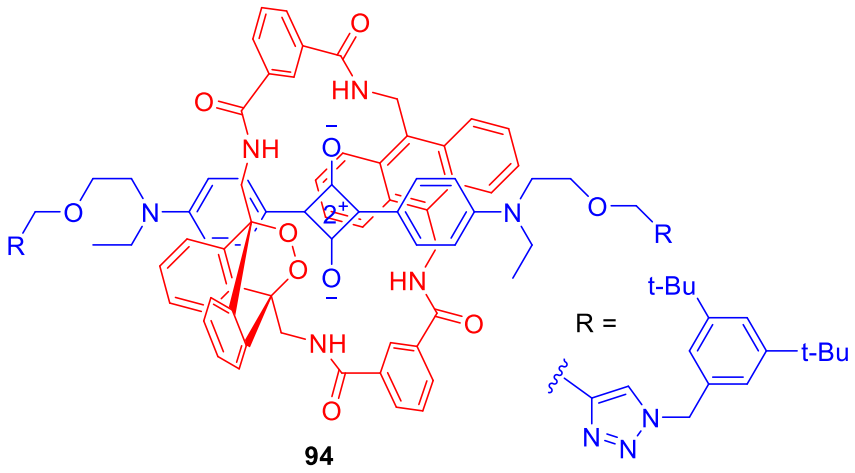

94

Figure 4.9 – Functional, squaraine rotaxane incorporating the use of anthracene**.**

4.1.4 Chapter Aim and methodology

Despite the wide ranging use of anthracene in interlocked structures found in the literature, up until now, its dimerization properties have not yet been attempted to be used in the 'structure forming event' towards the synthesis of such compounds. A photodimerization event of a bis-apended, bichromophoric molecule, as seen in the work of Tucker and others, produces a macrocycle. By utilising the photoactive Hamilton-type receptors and combining with appropriately functionalised barbiturate dumb-bells as shown in **Scheme 4.2**, these compounds are left open to exploitation regarding a clipping event towards an interlocked structure.

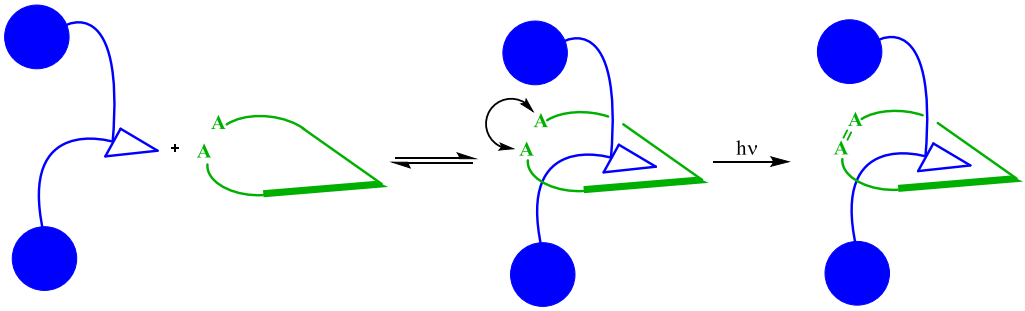

Scheme 4.2 - Proposed scheme towards the clipping of barbiturate dumb-bell molecules via photodimerization of anthracene appended Hamilton receptors.

As already discussed, care should be taken when selecting the appropriate tether length with reference to the ultimate ring size due to variations in binding constants and distortions of the binding site. From crystal structures already produced[12], it was thought that a tether of 3 carbons alone could be too small to incorporate the guest as well as undergo photodimerization, since the guests used would be considerably bulkier than the barbital molecule already investigated. For this reason it was decided to synthesise a series of receptor compounds, containing tethers of length 3, 6 and 9 carbons for a full investigation towards photoactive interlocked structures. Since this method would involve the use of Hamilton-type chromophores, it was clear that only a clipping approach around a barbiturate would be applicable, so the barbiturates chosen to be investigated were the previously synthesised dumbbell shaped guest molecules, **76** and **85**.

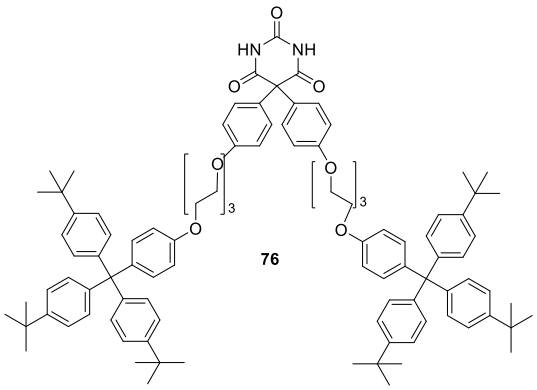

76

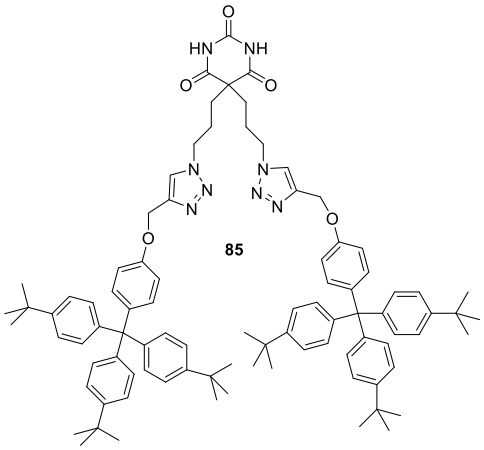

85

Despite the problems already experienced with compound **76**, regarding the failure to cyclise olefin-terminated Hamilton-type receptors via Grubbs Metathesis, it was hoped that this would be overcome in the case of photocyclomerisation since no bulky catalyst would be involved in the cyclisation event, only a single photon.

Contained within this chapter are some studies carried out by our collaborators in Bordeaux. A series of Job plots (**Figure 3.17**) and binding studies (**Figure 3.18 to Figure 3.20**) were conducted between receptor compounds **107**, **108**, and **109** with guest **85**. A fatigue and stability study of rotaxane **113** were carried out (**Figure 3.28 and 3.29**), as well as a ^{1}H NMR comparison between [2]-rotaxane **113** and the non-interlocked complexes of macrocycles **110**, **111**, and **112** with guest **85** (**Figure 3.38**).

4.2 Synthesis and Spectral Analysis of Anthracene-Terminated Receptors and their Complexes

4.2.1 Synthesis

The synthesis of the barbiturate guests, **76** and **85**, has been covered in Chapter 2. The synthesis contained within this section concerns the bi-chromophoric Hamilton-type receptors. Due to insolubility of the precursors, direct functionalization of the binding site motif was not possible and the anthracene terminated receptors were not able to be synthesised using the same approach as shown previously for the acyclic, olefin-terminated receptors. Conversely, for this series of receptors, the synthesis involved formation from the 'appended unit' via functionalization of anthrone with the required tether, followed by construction of the binding site of the receptor. The synthesis was achieved in a total of 5 steps, shown in **Schemes 4.3** and **4.4**. All reactions were conducted in the dark in order to prevent photo-oxidative cleavage of anthracene. Three different chain length receptors, of spacer length 3, 6 and 9 carbons between the receptor amide and terminal anthracene were synthesised as per literature procedures.[12]

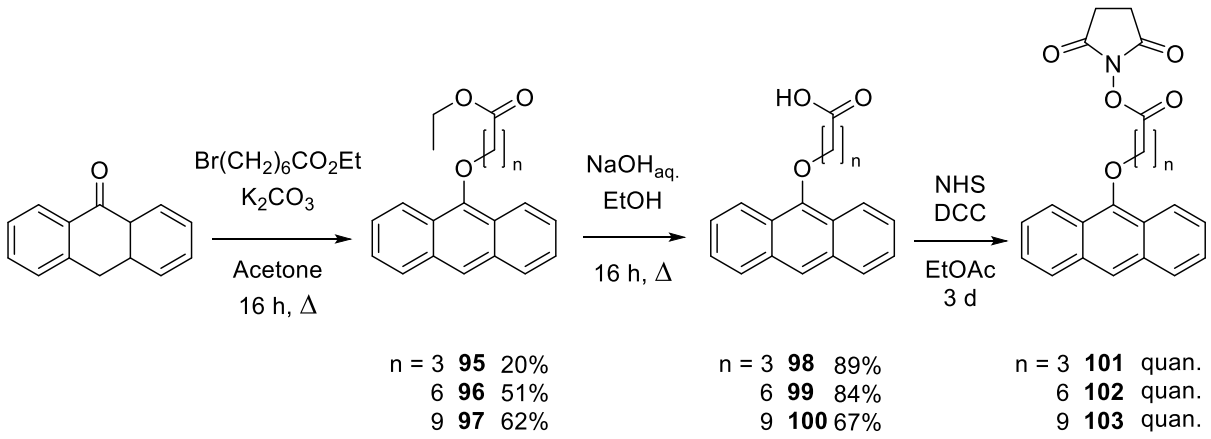

Scheme 4.3 – Synthesis of anthracene terminated receptors up to NHS Ester derivatives.

The first step in the synthesis is the functionalization of anthrone with the desired chain length of bromo-ester. The reagents were dissolved in acetone, K_2CO_3 was added and the mixture refluxed overnight. Purification via column chromatography afforded the ester compounds, **95**-**97**, in varying yields. Formation of the acid followed via hydrolysis of the ester. This was accomplished using NaOH and refluxing overnight. The product was precipitated out of the reaction mixture using the slow addition of conc. HCl and once filtered, the product was used as obtained. Although **98** and **99** were obtained in good yields, this work up became problematic when isolating **100**, since the increased chain length meant that a precipitate was more difficult to obtain. Instead, an extraction was used to isolate **100** from the crude mixture, which was pure enough to be used as obtained. The NHS-activated ester was then formed in excellent yields using dicyclohexyl carbodiimide (DCC) as the coupling reagent. The reaction was refluxed for 3 days and monitored for completion by TLC. Once full conversion of the starting material was observed, the solution obtained after work up was cooled for 4 h on ice to precipitate the products **101**-**103** that required no further purification.

The synthesis was continued as shown in **Scheme 4.4**. The series of NHS-activated compounds were reacted with 2,6-diaminopyridine in DCM and after refluxing for 5 days, the receptor precursors, **104**-**106**, were isolated via column chromatography and obtained in varying yields. The final step was a reaction between *tert*-butyl isophthaloyl chloride, **39**, with 2.2 equivalents of the chosen 2,6-diaminopyridine anthracene compound. Each reaction was carried out in THF under reflux conditions, using NEt_3 as a base. Initially a reflux of 1-2 days was employed and monitored for completion by TLC via the consumption of starting materials. Once complete, and after the subsequent work up, the pure products were isolated via column chromatography to obtain **107** and **108** in acceptable yields to give a series of photo-active, acyclic Hamilton-type receptors. However, in initial attempts to generate the receptor **109**, only a 6% yield was observed after refluxing for three days. No degradation occurred and the starting materials could be recovered. However, the yield greatly improved to 53% by the addition of catalytic DMAP and refluxing for three days. This observation opens up the possibility of increased reaction yields for the other compounds. Throughout the synthesis, the yields varied substantially between the different length chains and, with the exception of the initial step (and the final optimised step forming **109**), a decrease in yield was observed with an increase in chain length.

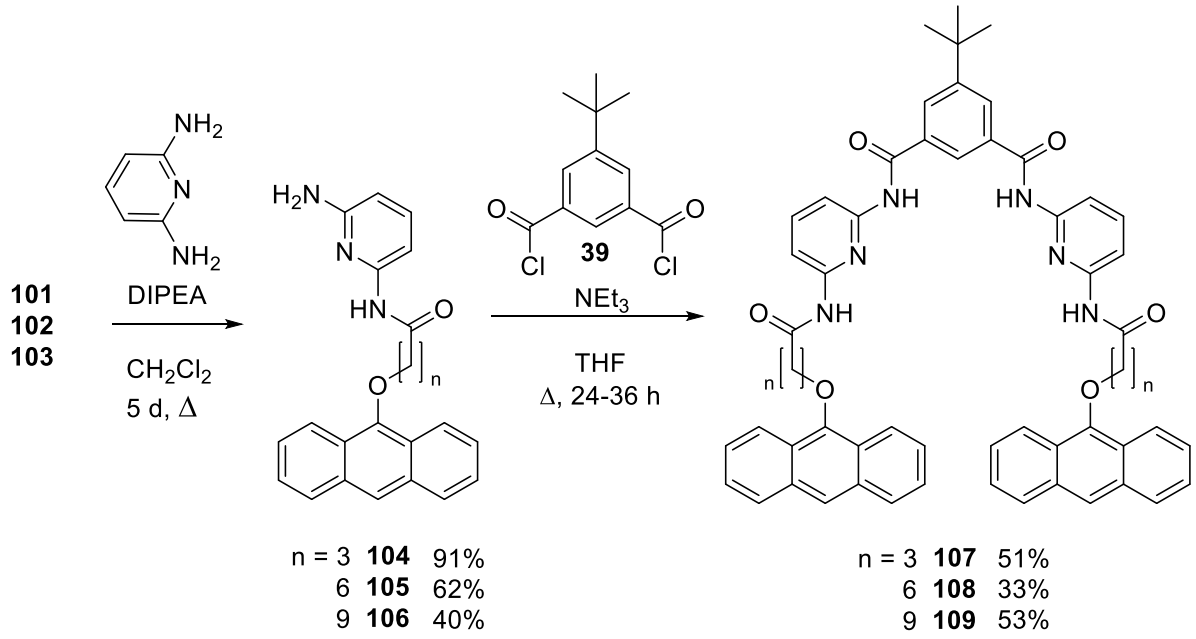

Scheme 4.4 - Synthesis of anthracene terminated receptors, **107**-**109**.

4.2.2 UV-Vis Absorption

The series of receptor compounds, **107**, **108** and **109** were analysed by UV-Vis spectroscopy (DCM at 2.6 x 10^{-5} M). The band between 340-400 nm is the characteristic anthracene band, and the large peak at 270-330 nm is an absorbance of the pyridine rings of the receptor (**Figure 4.10**). The gap in signal at 298-304 nm is instrument error due to the switchover of scanners and the variations in intensity are probably due to operator error, arising from making up solutions and should be repeated before anything is inferred from the relatively large difference observed with **108**. As would be expected, each trace is essentially identical, since the only difference between the three compounds is one of carbon chain length.

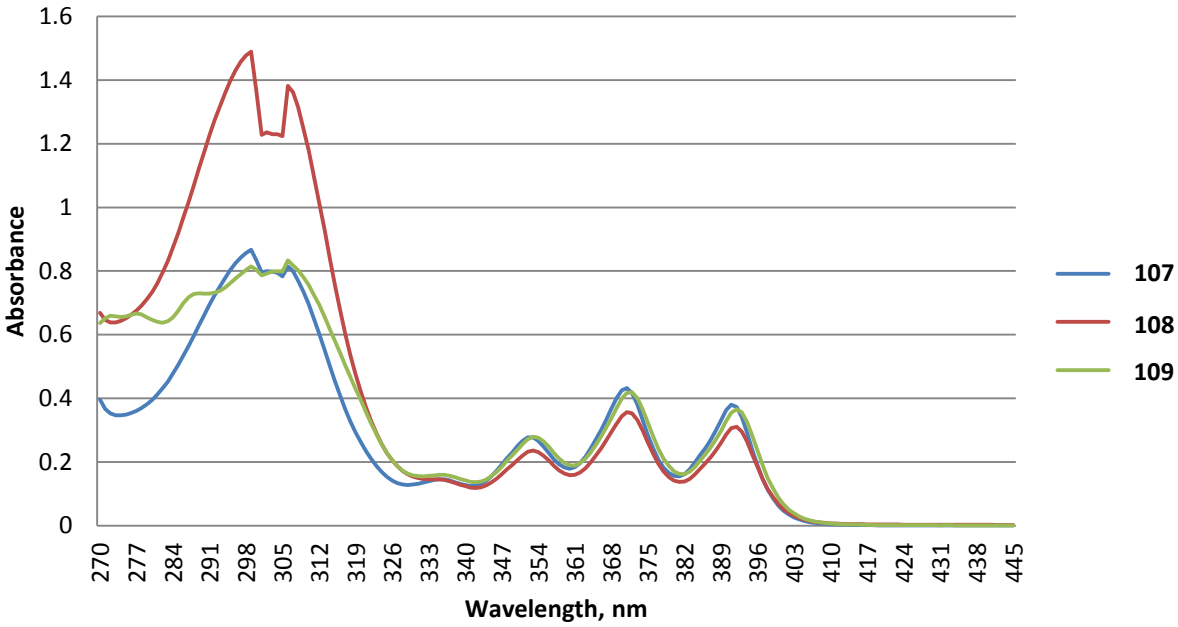

Figure 4.10 – UV-Vis absorption spectrum of **107**, **108** and **109** in DCM at 2.6 x 10^{-5} M and 298 K.

4.2.3 Photo-dimerisation

With the acyclic anthracene-terminated receptors characterised, attempts were then made to cyclise them via photo-dimerisation, **Scheme 4.5**. A solution of each receptor was made up to a concentration of 0.5 mM in DCM. It is imperative to exclude air from these reactions due to an unwanted side reaction of photo-oxidation, which causes cleavage of the anthracene groups, converting them to anthraquinone. The receptor solutions were then subjected to UV radiation using a water-cooled mercury lamp with a bandpass filter at 365 nm.

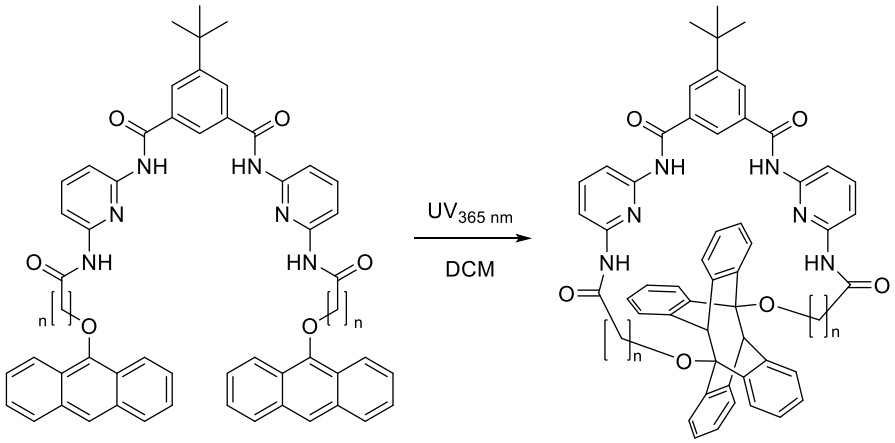

Scheme 4.5 - Cyclisation of acyclic anthracene terminated receptors via photodimerisation.

The dimerization was followed using UV-Vis absorption spectroscopy via the disappearance of the characteristic 3-fingered anthracene absorption band. Shown in **Figures 4.11**-**4.13** are the UV-Vis traces for the dimerization process of compounds **107**-**109**. In all three cases it was not possible to totally exclude oxygen and so degradation of the receptor would increase with time. Therefore, the irradiation was stopped once the signal had been sufficiently reduced to minimise any further degradation which left trace amounts of acyclic receptor still present. The solvent was then removed and in each case, the residue purified via column chromatography to give excellent yields of dimerised receptor. By ^{1}H NMR, only one product was isolated which was thought to be the ht isomer[12] due to the much lower thermal stability of hh photodimers induced by the additional steric and oxygen lone-pair repulsions (absent in a case of ht dimers).

One noticeable difference between traces is the time taken for the dimerization process. Despite the trend being one of decreasing dimerization time with increasing chain length, this is probably not due to any steric or kinetic components of the molecules

themselves, but a physical aspect of the experimental procedure and is due to variations in UV flux from the apparatus between different experiments. This could be confirmed through repetitions of the experiments.

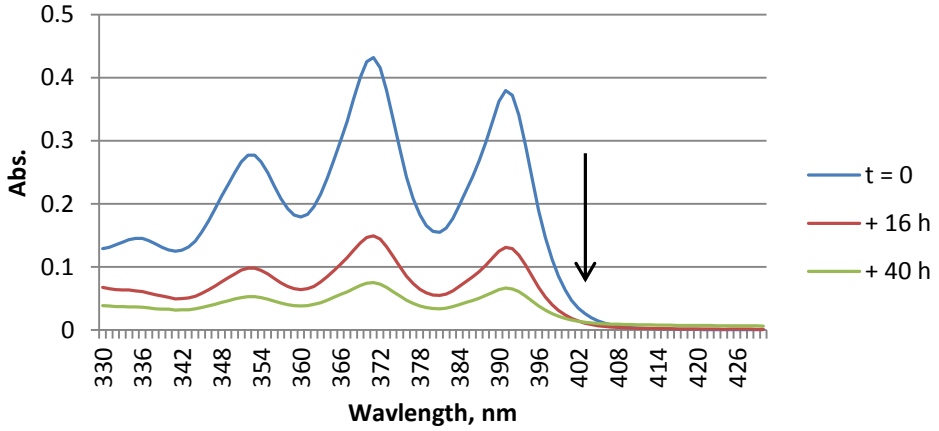

Figure 4.11 - Change in electronic absorption spectra of solution of **107** in DCM over 2 days upon irradiation at 365 nm at 298 K.

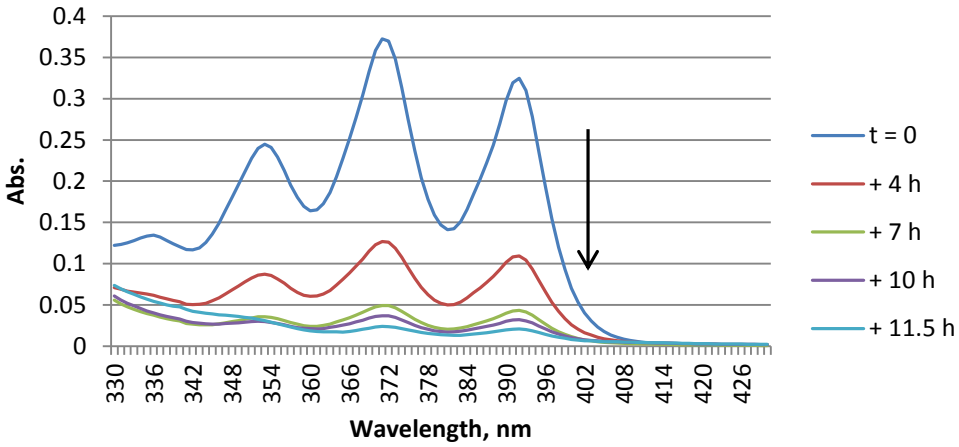

Figure 4.12 - Change in electronic absorption spectra of a solution of **108** in DCM over 11.5 hours upon irradiation at 365 nm at 298 K.

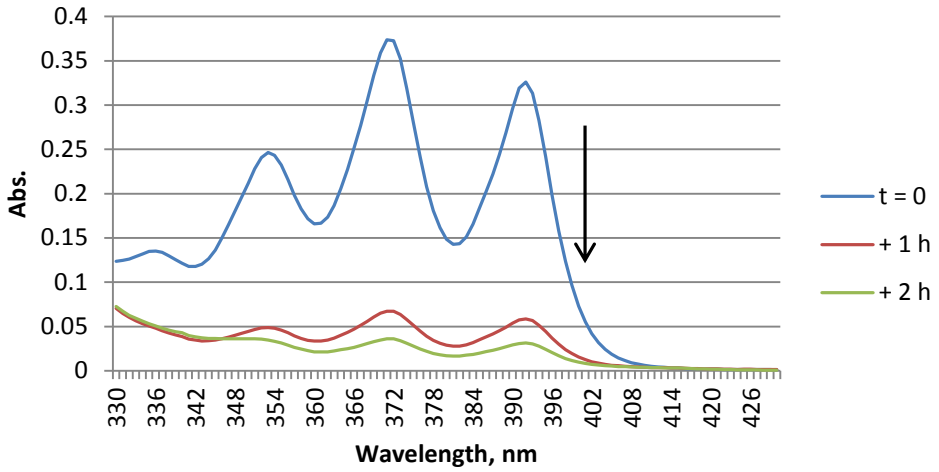

Figure 4.13 - Change in electronic absorption spectra of solution of **109** in DCM over 2 hours upon irradiation at 365 nm at 298 K.

By comparing the ^{1}H NMR spectra of the starting material and product (**Figure 4.14**), the dimerization is clearly observed. The distinctive anthracene signals at 7.41 ppm are completely absent in the product and have been replaced by the xylene signals at 6.69 and 6.92 ppm. Also present in the product is the characteristic bridgehead proton at 4.55 ppm.

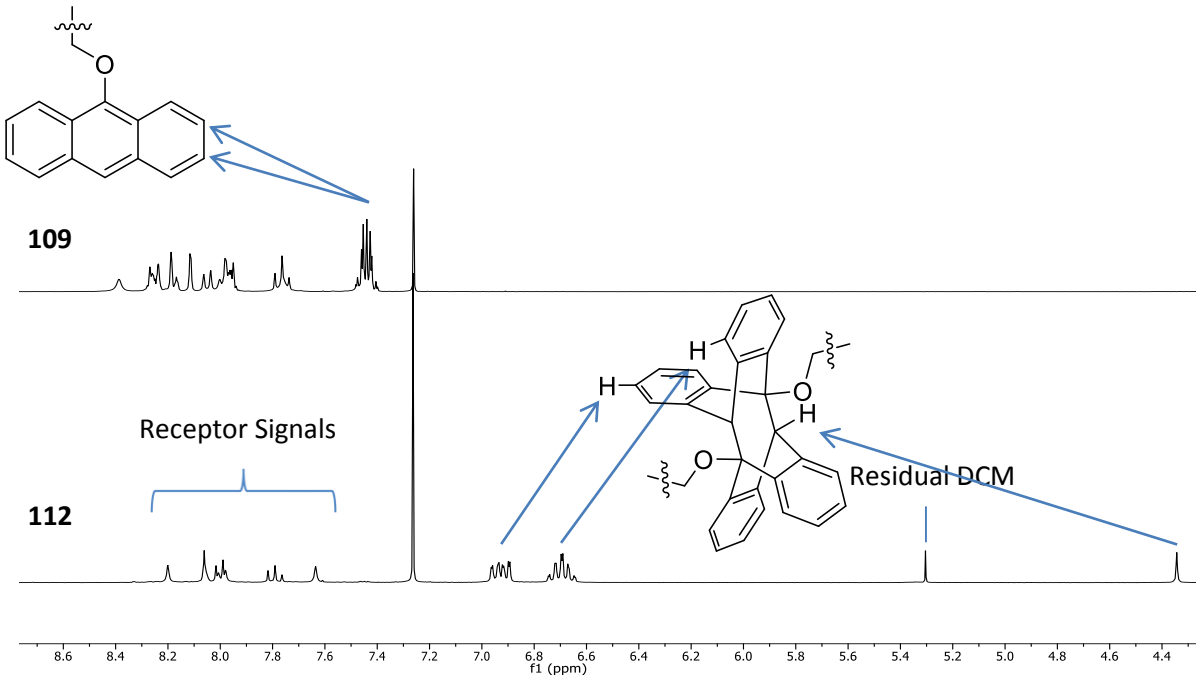

Figure 4.14 – ^{1}H NMR spectra comparing **109** and **112** regarding the signals present before and after photodimerisation.

4.3 Interactions with Guest Molecules

4.3.1 Guest 76

To determine the ability of the macrocycles to act as hosts, a series of ^{1}H NMR spectrometry experiments were conducted to create a stacked spectrum of the receptor, **108**, the rigid barbiturate **76** and a 1:1 mixture of the two components, **108:76** . The interaction is shown in **Scheme 4.6** and the stacked ^{1}H NMR spectra are shown in **Figure 4.15**. From the observed shifting of the NH peaks of **108**, it is clear that an H-bonding interaction is occurring and the complex **108:76** is present in solution.

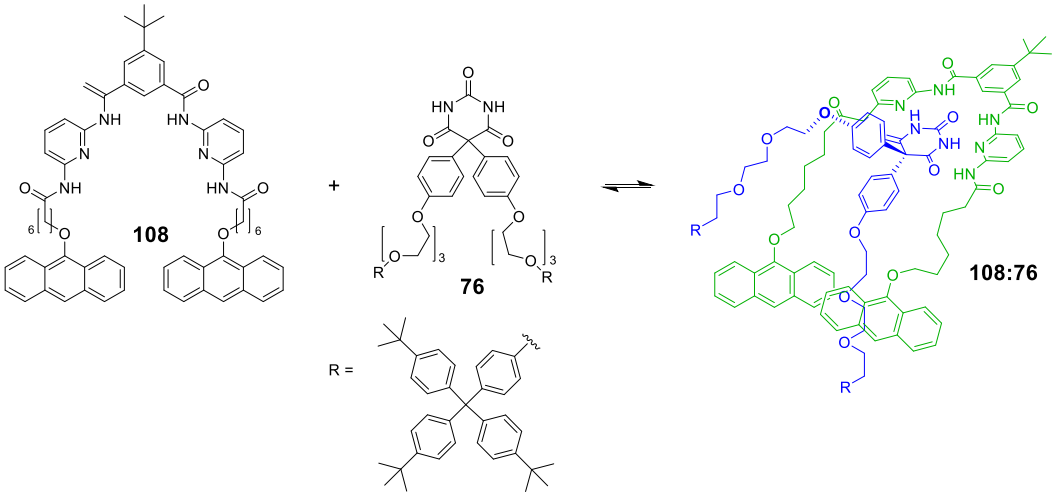

Scheme 4.6 - Host:Guest interaction of receptor **108** with guest **76**.

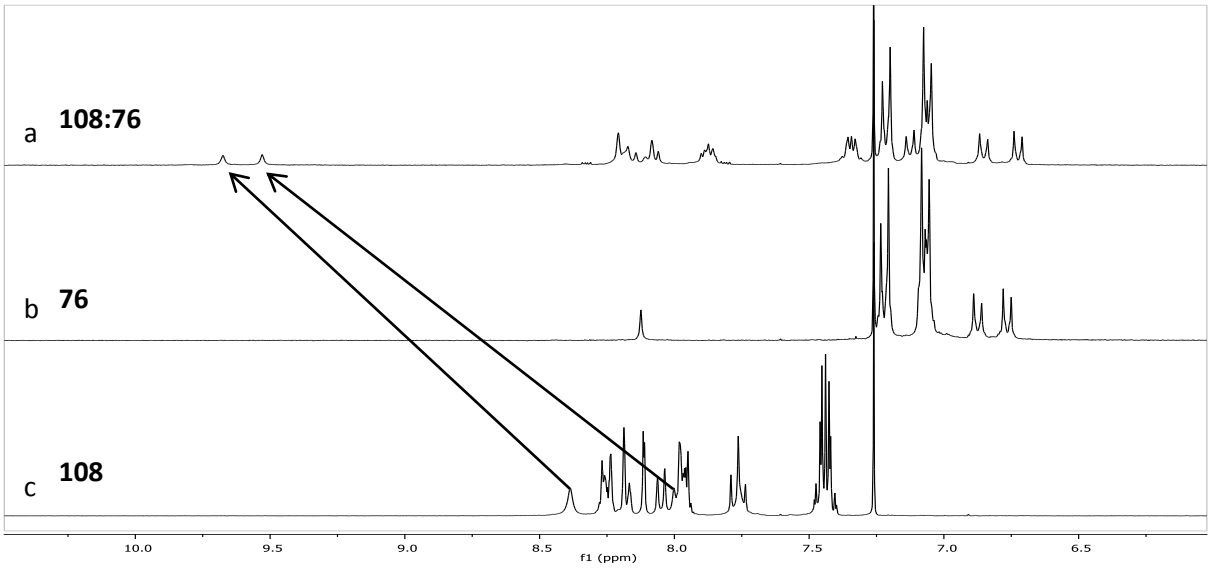

Figure 4.15 – A series of ^{1}H NMR spectra showing the complex **108:76** (a), **76** (b) and **108** (c) in $CDCl_3$ at 5 mM and 298 K.

4.3.2 Guest 85

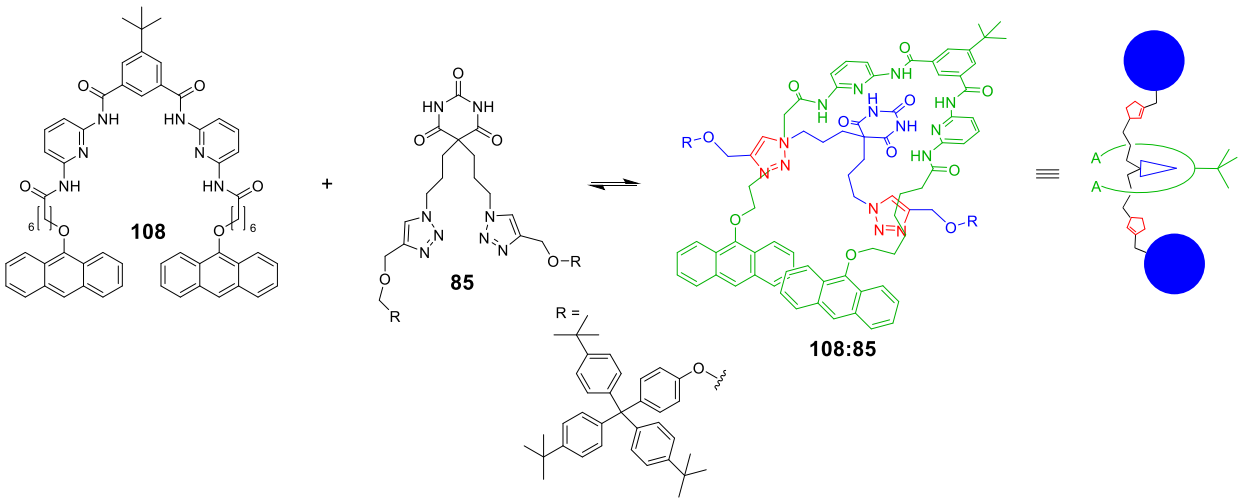

Figure 4.16 – Host:Guest interaction of receptor **108** with guest **85**.

A series of binding studies were carried out to characterise the strength and modes of binding between these receptors and the previously synthesised guest molecule **85**.

4.3.2.1 Job Plot

The first study consisted of a series of Job plots as shown in **Figure 4.17**, plotting the binding induced absorption changes of the pyridine band at 310 nm.

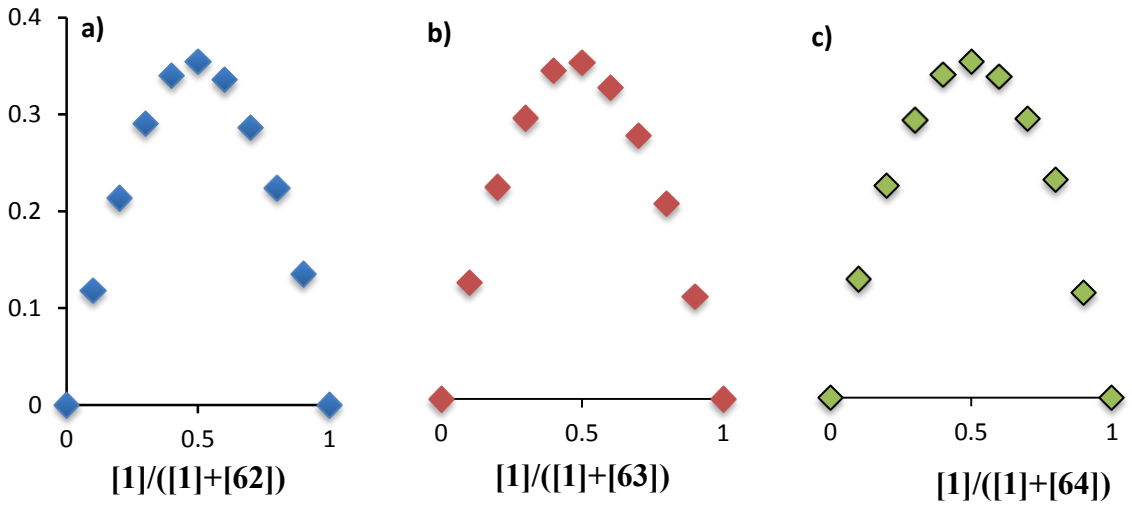

Figure 4.17 - Job plot showing binding induced absorption changes (310 nm) as a function of molar fraction of receptor compounds **107** (a), **108** (b), and **109** (c) in their binding with **85** ($[C]_{tot}$ = 50 uM) in CH_2Cl_2.

As can be seen from the binding curves, a maximum absorbance change occurs at a molar fraction of 0.5, confirming a 1:1 H:G interaction for each of the receptors, as would be expected for this motif.

4.3.2.2 Binding Studies

In order to establish the strength of interaction, titrations with the guest molecule were carried out and monitored via UV-Vis absorption spectroscopy. Shown in **Figures 4.18** - **4.20** are the UV-vis spectra for the titrations for receptors **107**, **108** and **109** with guest **85**.

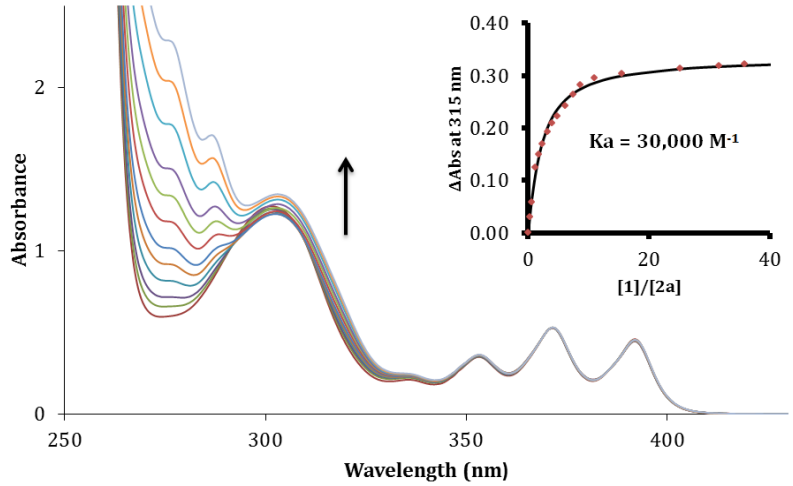

Figure 4.18 – Changes in electronic absorbance of **107** upon addition of **85** up to 40 equivalents in CH_2CL_2 (C = 34 µM), at room temperature. Inset shows the increase in molar absorption coefficient at 315 nm upon addition of **85**.

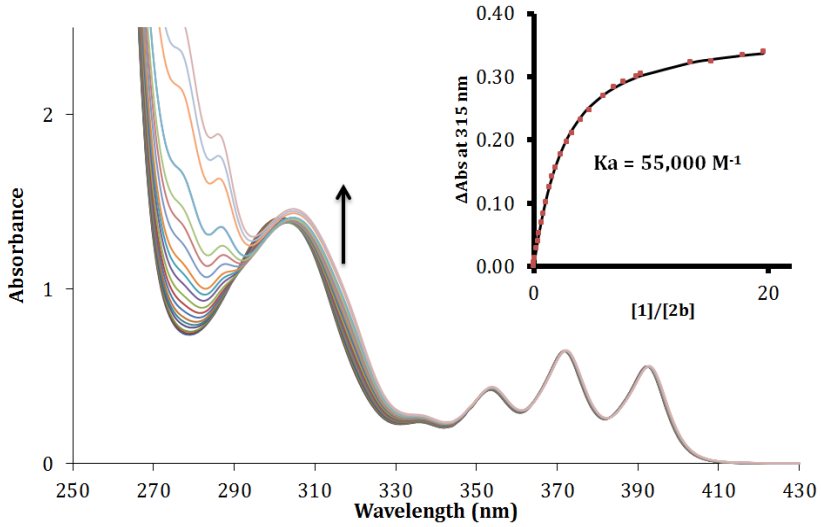

Figure 4.19 - Changes in electronic absorbance of **108** upon addition of **85** up to 20 equivalents in CH_2CL_2 (C = 37 µM), at room temperature. Inset shows the increase in molar absorption coefficient at 315 nm upon addition of **85**.

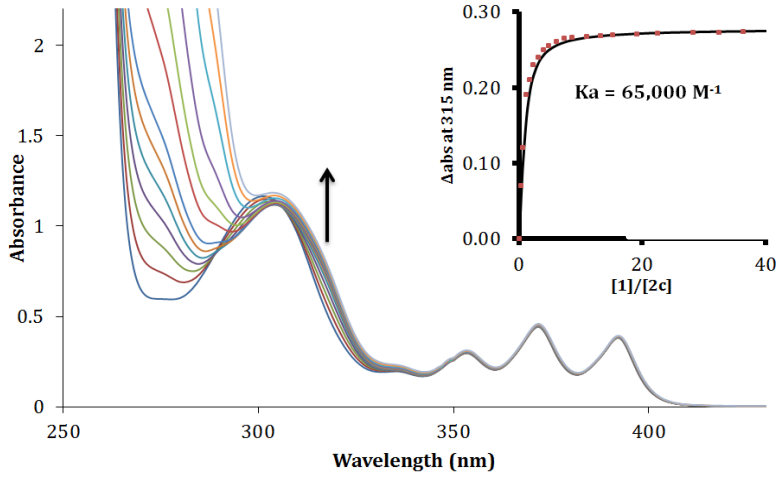

Figure 4.20 - Changes in electronic absorption spectra of receptor **109** in CH_2Cl_2 (concentration = 24 µM) on adding aliquots of barbiturate **85**. Inset shows the increase in the observed molar absorption coefficient at 315 nm upon addition of **85**.

Analysis of the complex-induced red-shifting of the pyridine absorption band of the receptors at 315 nm allowed determination of the binding constants. Summarised in **Table 4.2** are the results of these titrations, and for comparison purposes, the binding constants with barbital have been included.

Table 4.2 – Table displaying the obtained binding constants of receptors **107**, **108** and **109** with guest molecule **85** in DCM, and for comparison purposes, those of barbital (in chlorinated organic solvents) obtained previously.

Receptor	Binding Constant [log(K)] with **Barbital**	Binding Constant [log(K)] (+/-5 %) with **85**
107	4.57	4.47
108	4.85	4.74
109	-	4.81

Comparing the binding constants of the receptors with **85**, and although these values are close to the limit of experimental error, a slight trend appears, where the binding constant is seen to increase with increasing tether length. This is what was observed in the previous studies with barbital[12] and can be explained in terms of sterics. When decreasing the tether length, then the bulky anthracenes are located closer to the binding site and as a result, will have an increased steric effect on the H:G binding interaction. When comparing

between the two guests, a decreased binding constant is observed for guest **85**. This again can be explained in terms of sterics, since despite having the same central binding structure, **85** is considerably more bulky, which would make binding less favourable.

4.4 Attempts Towards Rotaxanes using Receptor 108

4.4.1 Size Constraints

Building upon previous work carried out by the Tucker group,[12] compound **108** was chosen to be investigated first in attempts to form a photo-rotaxane. This length of tether was chosen because of the nature of photo-switched binding and subsequent binding constants exhibited after photodimerization. A linker of 6 carbons as found in **108**, once cyclised, was shown to have the least decrease in binding with respect to a three carbon linker (**Table 4.1**). If the binding with the barbital moiety was still relatively strong in the dimerized form, then one would expect there to be minimal disruption to the binding site upon dimerization, which would provide a cavity of sufficient size to facilitate cyclisation in the presence of the guest. However, it is important not to make the ring too large, otherwise it would be impossible to form an interlocked structure due to slippage of the dumbbell through the macrocycle. The photoproduct of the n=6 linker, compound **111**, gives a ring size of 33 atoms for the *hh* dimer and a ring size of 36 atoms for the more stable *ht* dimer which is thought to form. In fact, 33 atoms is of the order of what is observed with other interlocked systems utilising stopper **48**,[17] and attemps to isolate rotaxanes with higher ring sizes of 41 atoms (i.e. of a similar size to **112**) could not be isolated,[18] even with bulkier biphenyl stopper derivatives. In addition, for longer linker lengths, there would be less of a driving force towards dimerization and the process of polymerisation may be

favoured, or the clipping event may not occur around the axle of the dumbbell, clipping in only a perched conformation due to increased flexibility. For these reasons receptor **108**, was used in the initial investigation.

4.4.2 Dimerization in the Presence of 76

The initial attempt towards rotaxane formation used the bulky guest, **76**. This guest was used since it was hoped that, for the same reasons as applied to the metathesis ring closure (Chapter 3), that the directionality imposed by the phenyl groups would aid the clipping process around the thread and not under it. It was anticipated that the triethylene glycol units would place the stopper groups away from the site of dimerization, so as not to sterically hinder the process.

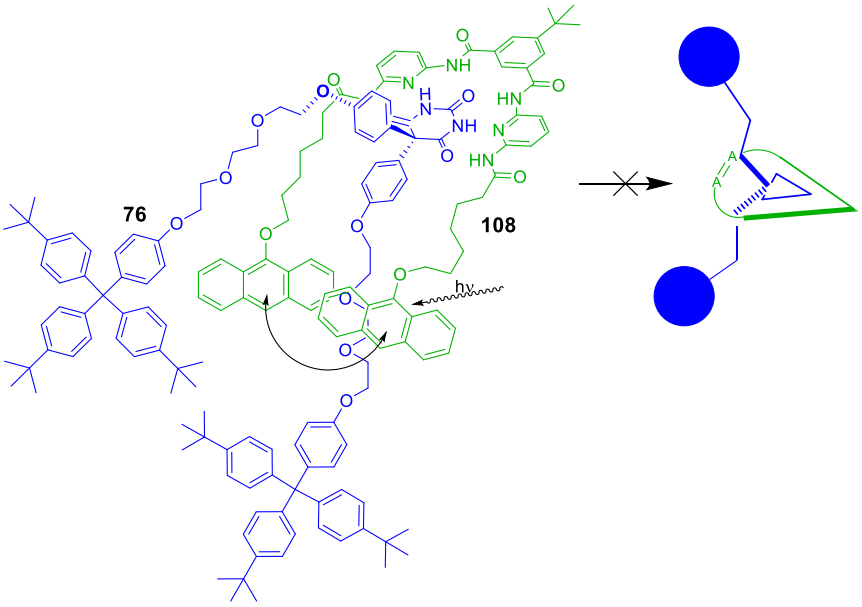

Scheme 4.7 – Proposed process of photodimerization of **108** in the presence of **76**

The planned H:G interaction and subsequent photo-induced clipping event is shown in **Scheme 4.7**. For the dimerization experiment, a receptor solution of 0.5 mM in degassed DCM was made up, followed by the addition of three molar equivalents of the rigid

barbiturate, **76**. The flask was purged with argon and then the solution was irradiated at 365 nm as described before (**Section 4.2.3**). Dimerization was followed via UV-Vis spectroscopy, by monitoring the decrease of the anthracene band over time. The UV-Vis spectrum is shown below in **Figure 4.21**. For the UV-Vis analysis, a 50 µL aliquot of the reaction solution was taken and diluted up to 1 mL to give a concentration 2.53 x 10^{-5} M.

Initially, UV-Vis measurements were taken periodically over a series of hours. However, no substantial reduction in anthracene signal was observed until the reaction had been irradiated overnight. Irradiation was therefore continued over a period of days along with regular monitoring of the system, and eventually the anthracene bands were observed to eventually decrease, as would be expected for a dimerization event.

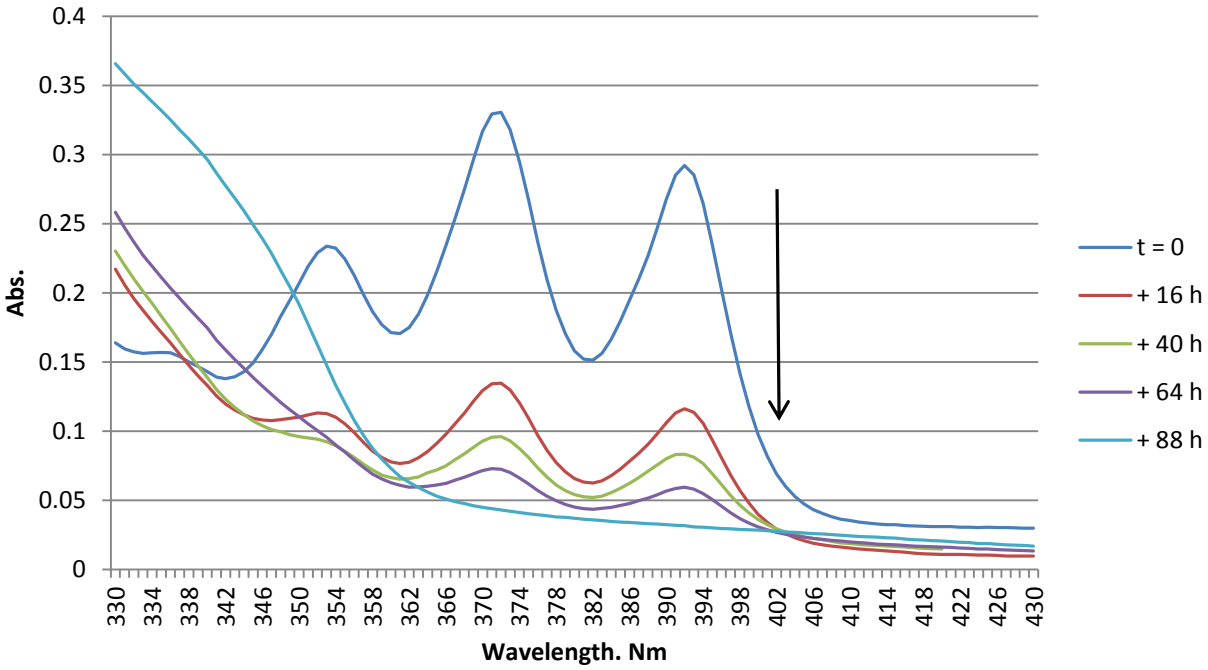

Figure 4.21 – Change in electronic absorbance of **108** in the presence of 3 equivalents of **76** in DCM, upon irradiation at 365 nm over several days

After more than 3 days of continuous irradiation, it appeared that the dimerization was complete. The solvents were removed and the crude mixture analysed by ^{1}H NMR. However, from the spectrum obtained, it was discovered that this decrease in signal was found to be due to degradation of the anthracene, forming anthraquinone, rather than dimerization.

The reason for this lack of photo-dimerization is probably similar to the ring closing metathesis experiment already discussed. Under these conditions the guest is clearly bound at the receptor site; however complexation must inhibit dimerization since it occurs readily in the absence of this guest, over a period of a few hours (**Figure 4.12**). When the macrocycle is dimerised it forms a ring size of 36 atoms (for the ht dimer) and the metathesized receptors form a similar ring size of 35 atoms. So despite the optimism regarding the lack of a bulky catalyst which may have possibly been hindering the cyclisation event, it seems that the ring size may simply be too small to accommodate the bulkier rigid dumbbell barbiturate, **76**. The steric bulk of the guest might prevent the formation of an excimer, which is essential prior to dimerization as shown in **Scheme 4.8**. A secondary consideration is that for the favoured *ht* dimer, the xylene units protrude into the cavity, which would disfavour cyclisation due to the steric bulk of **76**. Therefore it may be the case that the initial *hh* dimer is formed, whose conformation may accommodate the guest, but due to its low thermal stability, it reverts to the open form in situ and is unable to be isolated and the following prolonged and continuous photoexcitation of the anthracene then eventually leads to its degredation. A larger macrocycle would be needed to accommodate the guest, however this increases the probability of slipping and therefore, it

appears that the rigid guest, **76**, is too sterically hindered to function as an appropriate template towards the formation of an interlocked structure.

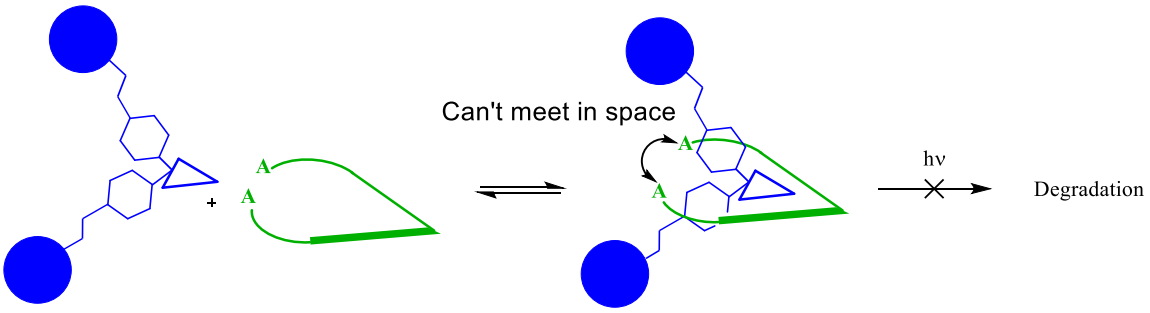

Scheme 4.8 - Process of degradation of **108** when in the presence of **76.**

4.4.3 Attempts toward an Interlocked Structure with Guest 85

Since it has been shown that, at least in terms of its size and inclusion within the binding site, that rotaxane formation is indeed possible with the short-chained triazole linked barbiturate, **85**, (Chapter 3) rotaxane formation through photodimerisation was now attempted with this guest.

4.4.3.1 Dimerization in the presence of 85

The dimerization was carried out at the usual concentration of 0.5 mM for the receptor, in degassed DCM. The anticipated process is shown in **Scheme 4.9**. The dimerization was attempted using receptor **108** and irradiation was carried out at room temperature in the presence of **85**. Three molar equivalents of **85** were used to ensure complete complexation of the guest, to maximise the yield of potential rotaxane. As before, a wavelength of 365 nm was used to achieve the dimerization and the progression of the

reaction was monitored via UV-Vis absorption using diluted aliquots of reaction mixture at a concentration of 2.50 x 10^{-5} M.

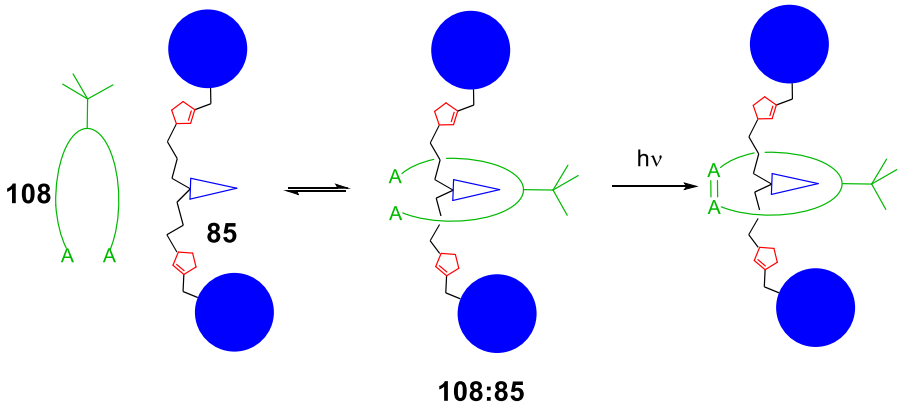

Scheme 4.9 – Proposed complexation and subsequent dimerization event, between **108** and **85**, towards a photo-clipped [2]-Rotaxane.

The UV-Vis spectrum that illustrates the dimerization process is shown in **Figure 4.22**. The dimerization was monitored periodically and after an irradiation time of 5.5 h, there was no further reduction in the anthracene signals and the dimerization was considered complete. Due to the time of completion, it is clear that the photoreaction is considerably more efficient compared to guest **76** and in fact is faster than for **108** alone. Considering that the guest should be completely bound, it is clear that dimerization is by no means hindered with these triazole linked guests and this was a promising result, so long as the guest wasn't so flexible that dimerization could occur in a perched conformation.

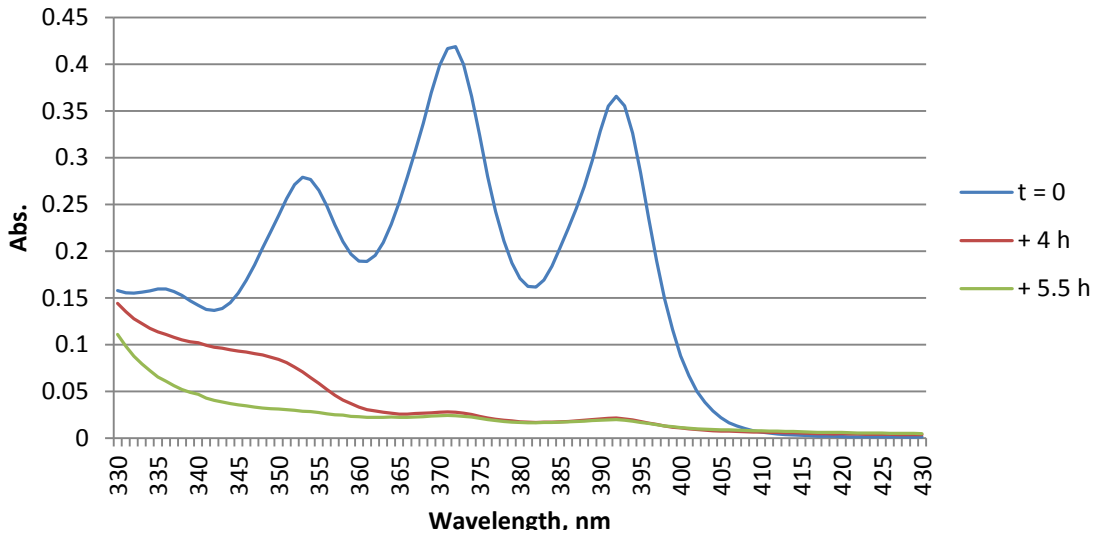

Figure 4.22 - Change in electronic absorbance of **108** in the presence of 3 equivalents of **85** in DCM**,** upon

A TLC of the white solid obtained showed the presence of a small amount of unreacted receptor (R_f = 0.48, eluent: DCM/EtOAc-15%) as well as a new spot at a higher R_f (R_f = 0.66, eluent: DCM/EtOAc-15%). This fraction was isolated by column chromatography (eluent: DCM/EtOAc-5%) and then purified further by prep TLC to afford the reaction product. ^{1}H NMR analysis of the solid revealed the presence of both host and guest compounds, occurring in a 1:1 ratio from their integrations, as would be expected for the formation of a [2]-Rotaxane. This fraction was isolated in 66% yield and the proposed structure of [2]-Rotaxane, **113**, is shown in **Figure 4.23**. It should be noted that no free dimerized receptor, **111**, was isolated from the reaction mixture which is a good indication of the level of binding occurring between the host and guest. It also shows how with sufficient exclusion of air from the reaction mixture, potentially all of macrocycle **108** may be converted to rotaxane **113**.

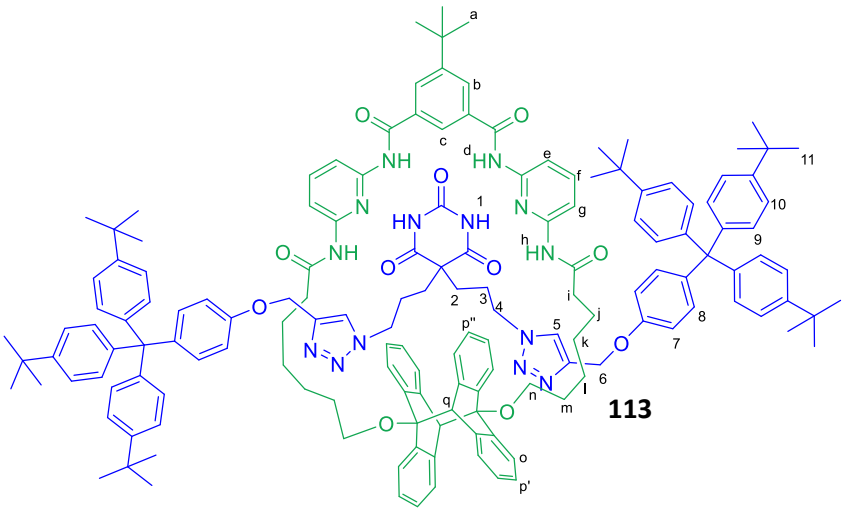

Figure 4.23 – Proposed structure of a photo-clipped [2]-Rotaxane, **113**

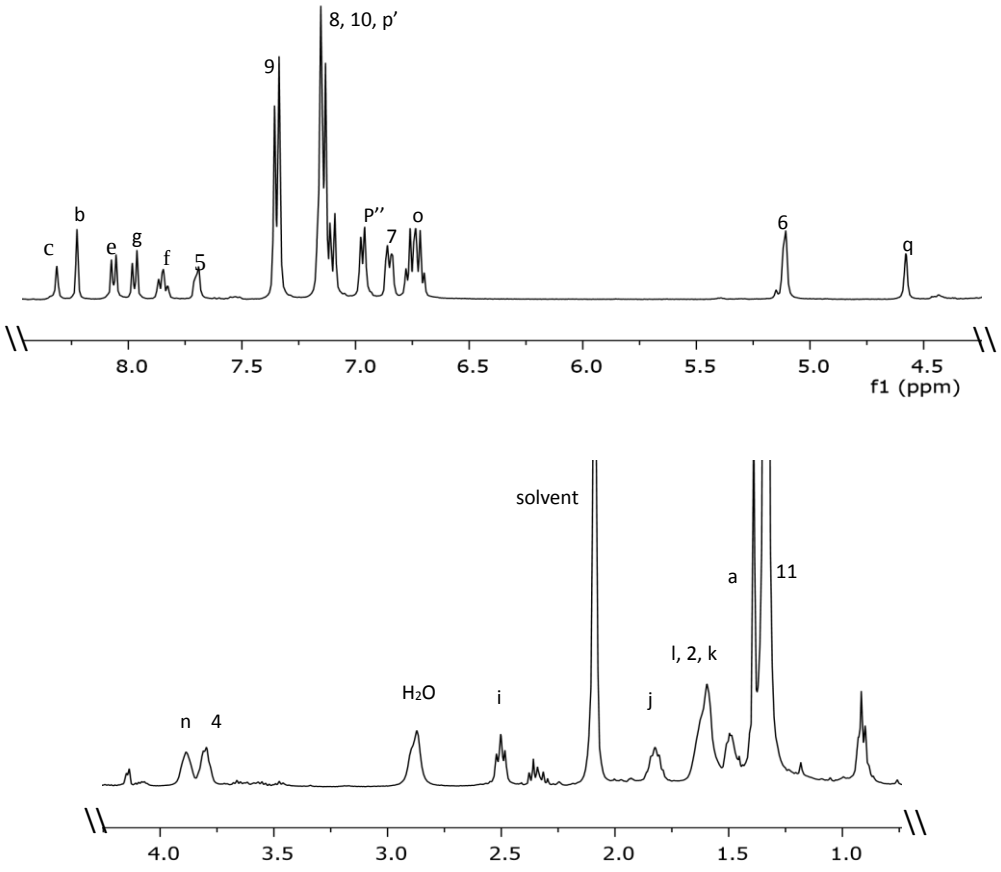

Figure 4.24 - ^{1}H NMR (300 MHz) of **113** in Acetone-d_6 at room temperature

Shown in **Figure 4.24**, is the ^{1}H NMR spectrum in acetone-d_6 of the isolated fraction along with the assignment of peaks. The N-H peaks are shifted downfield, to 9.4 and 9.6 ppm, (the NH of the guest was not observed in acetone-d_6) indicating H-bonding in the complex and are not included in the figure.

As had been observed in some previous attempts, it was possible for the H/G components to move as non-interlocked H:G complexes during purification by column chromatography. To remove any concern over this possibility, a TLC was carried out between the isolated fraction **113** and a premixed solution of components, **111** and **85.** As shown in **Figure 4.25**, when compared to a premixed solution of dimerized host and guest (perched complex) it is clear that the complex **113** is a single, interlocked component whereas the perched complex dissociates.

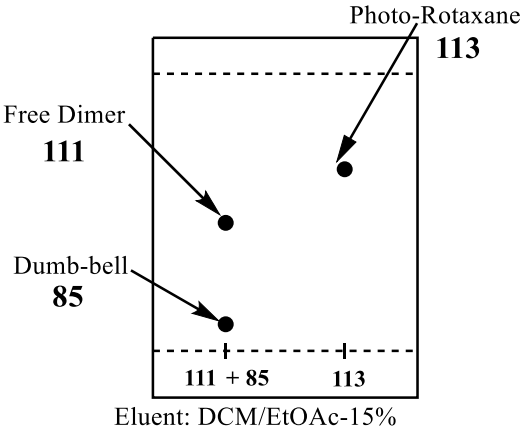

Figure 4.25 – TLC comparing a premixed solution

Further evidence supporting the isolation of an interlocked structure came from the mass spectrum, **Figure 4.26**. Only trace amounts of the molecular ion peak at 2392.3 were observed. However, peaks at 1197.2 and 1197.7 clearly show the presence of a +2 molecular ion peak, with the same analogous pattern of peaks at 798.4 and 798.8 showing the +3 molecular ion peak. Obviously, differences of 0.5 and 0.3/0.4 mass units cannot occur due to singularly charged molecules and must be due to a +2 and +3 molecular ion of the rotaxane, respectively.

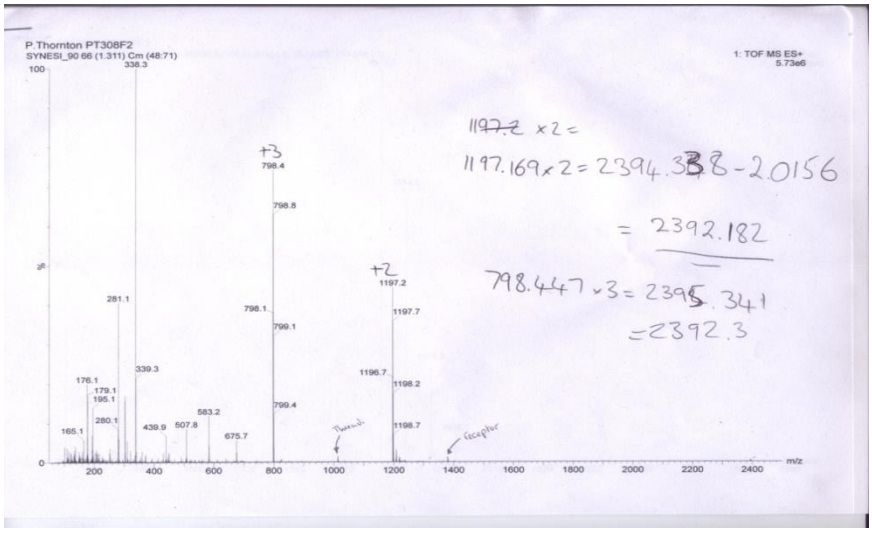

Figure 4.26 – ES^+ Mass Spectrum of isolated product, **113**.

It can be seen from the mass spectrum that there are also small amounts of receptor and dumb-bell present at 1378.0 and 1013.5. It can be assumed that these are due to fragmentation of the rotaxane.

4.4.3.2 Analysis of 113 by ^{1}H NMR Studies

Despite the strong evidence for an interlocked structure from the ^{1}H NMR spectrum, TLC comparisons and mass spectrum, to alleviate any uncertainty over the presence of a perched vs an interlocked compound, a series of ^{1}H NMR spectra were carried out as shown in **Figure 4.27**. Three separate solutions were made up in DCM-d_2; the first solution (a) consisted of a 1:1 mixture of the acyclic host, **108**, and the independent guest, **85**, to allow a comparison of changes before and after dimerization. The second (b) consisted of the proposed photo-clipped rotaxane, **113** (b)**.** The third solution, (c) was a 1:1 mixture of dimerised host, **111**, plus the independent dumb-bell, **85**, which can only form a perched complex. Despite a better resolution of peaks for the rotaxane in acetone-d_6, DCM-

d_2 was used for the comparison due to solubility issues for the non-interlocked **85** in $CDCl_3$ and acetone-d_6.

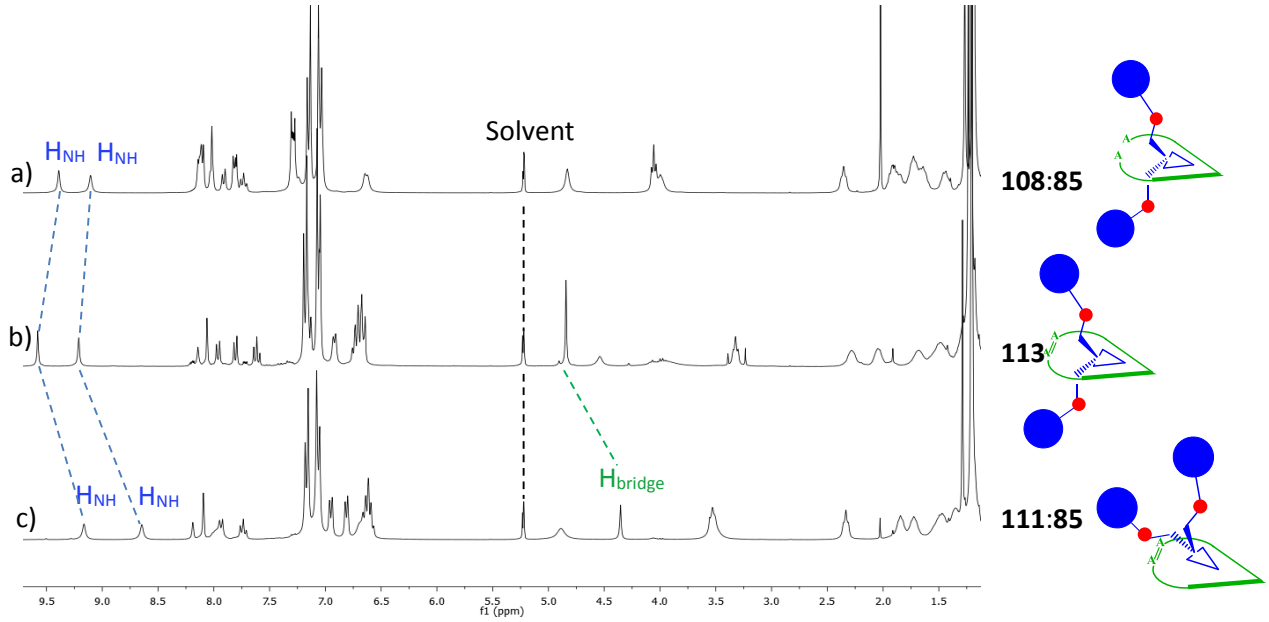

Figure 4.27 – ^{1}H NMR (300 MHz) comparison between the H:G complexes **108**:**85**, **113** and **111**:**85** at a concentration of 5 mM in DCM-d_2 at 298 K, including schematics of the proposed structures present.

The analysis reveals that there is some very minor variation between each spectrum in the alkyl region, with a slight shifting of most peaks observed, but nothing indicative of any specific interaction. Similarly, within the range of 6.5 - 8.3ppm, there are also generally minor changes observed for both the receptor (e.g. the pyridine protons) and the dumbbell. However, the bridgehead proton, H_{bridge}, (q in **Figure 4.23**) formed upon photo-dimerization and present in the spectra b) and c), experiences a small but significant shift of $\Delta\delta$ = 0.3 ppm. This implies a slightly different environment for the binding sites of the perched and threaded forms. Also, it seems as if the symmetry of the structure is maintained, since no extra peaks are observed, which would be expected if the complex became unsymmetrical.

The most prominent change in the comparison of each spectrum concerns the imide NH protons of the receptor (the H_{NH} signal for **85** has been excluded due to its significant shift to ~12 ppm). In all spectra there is a degree of H-bonding present, which is apparent due to the shifts of the H_{NH} peaks relative to the free receptors (*cf* **Figure 4.14**), but each signal is shifted by a different amount depending on the specific H:G interaction. In comparing the shifts of spectra a) and c), the interactions with the acyclic hosts appear significantly stronger, due to the increased downfield shifts of the signals. This fits with what would be expected, since stronger binding should be observed with the acyclic form due to the ability of the guest to be fully inserted into the binding cavity. In contrast with the perched complex, **111**:**85**, formed with cyclised receptors, the barbiturate guest can only sit above the plane of the receptor.

An even greater H_{NH} downfield shift is observed for **113** (**Figure 4.27b**), relative to both **108**:**85** and **111**:**85**. This can be rationalised in the same way in that the guest is internalised into the cavity as part of the rotaxane, with should result in a stronger interaction. This data shows that when in the interlocked form, the macrocycle is still bound through H-bonding to the guest, even with the probable intrusion of the xylene units into the cavity. This is backed up by the downfield shift of the bridgehead proton, which resides close to the binding site and is clearly considerably affected by the structural constraints imposed by the interlocked structure.

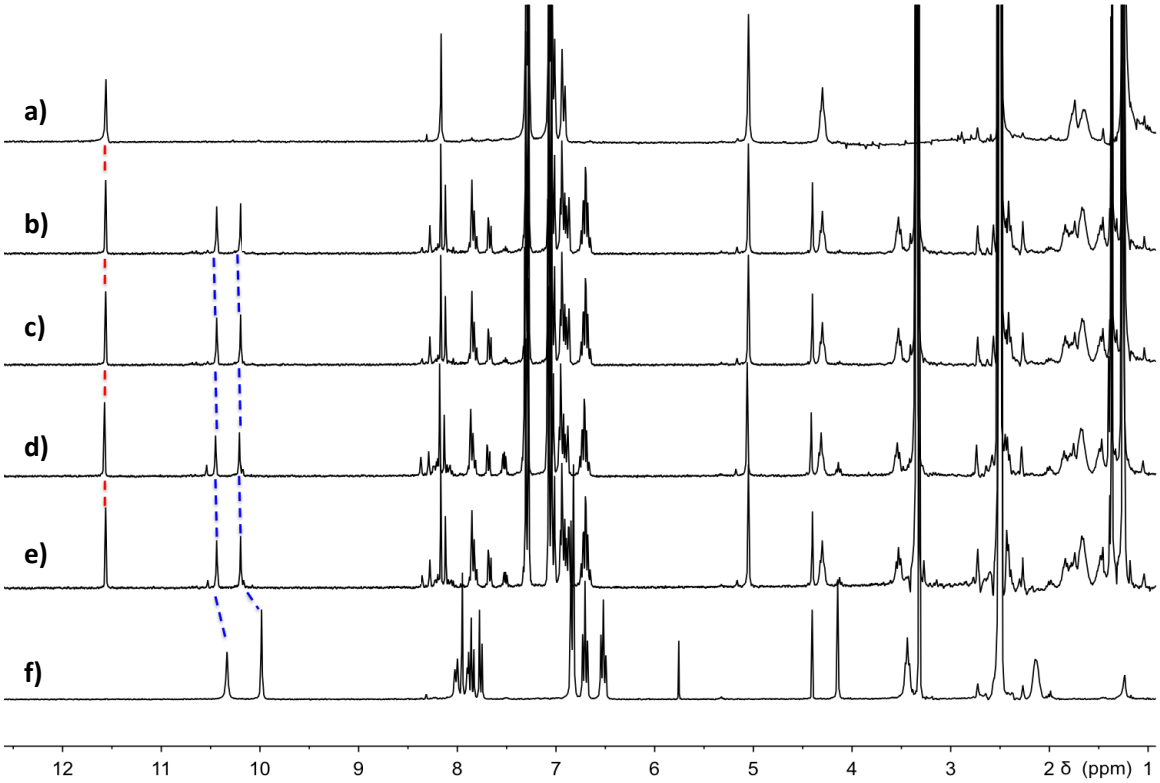

Figure 4.28 – ^{1}H NMR spectra (300 MHz) recorded at room temperature in DMSO of **85** (a), [2]-Rotaxane **113** after heating to 353 K for 0 min (b), 15h (c), 39h (d), 63h (e) and receptor **111** (f).

Shown above in **Figure 4.28** is a temperature study, regarding the [2]-Rotaxane **113** (b)-(e). The molecular components: free guest **85** (a) and free macrocycle **111** (f) are included for comparison purposes. The study was conducted in DMSO and hence a strong downfield shift is observed initially for the NH resonances. Although the NH shift of the guest experiences no difference in shift in DMSO when either free or interlocked, interestingly, the NH peaks of the receptor are shifted further downfield when interlocked as part of the rotaxane, showing a significantly strong interaction when in this conformation. The rotaxane was monitored over a period of 63 h at a temperature of 353 K. The rotaxane shows fairly good stability at this temperature. However, after 38 h, secondary NH peaks appear, which may be the product of either degredation, or cycloreversion. From

the emergence of the multiplet at 7.5 ppm, it can be concluded that the rotaxane is indeed opening up into its constituent acyclic receptor, releasing the guest.

To elaborate upon this thermal opening to the acyclic complex, a fatigue study was conducted. A solution was made up in degassed DCM, consisting of the acyclic receptor **108** and the dumb-bell guest **85** in a ratio of 1:40. The solution was irradiated at 365 nm for 1 h to achieve photodimerization of **108**. The solution was then be heated to 110^{o} C for 14 h to cause the thermal return of the cyclic complex. The results are shown in **Figure 4.29** and indicate that despite a significant amount of degredation the system is able to withstand several cycles.

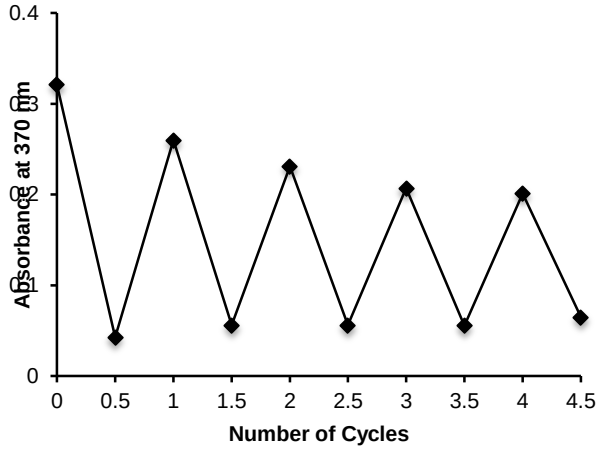

Figure 4.29 – Fatigue study of complex **108:85** (40:1) in degassed CH_2Cl_2 (25 x 10^{-6} M monitored by UV-Vis absorption. Each cycle corresponds to an irradiation at 365 nm (1 h) resulting in photodimerization followed by thermal return (110^{o} C, 14 h).

4.5 DOSY NMR

4.5.1 Background

Diffusion-ordered NMR spectroscopy (DOSY) is based on a pulse-field gradient spin-echo (PGSE) NMR experiment and was first developed by Tanner and Stejskal in 1965.[19] The PGSE sequence is shown in **Figure 4.30**.

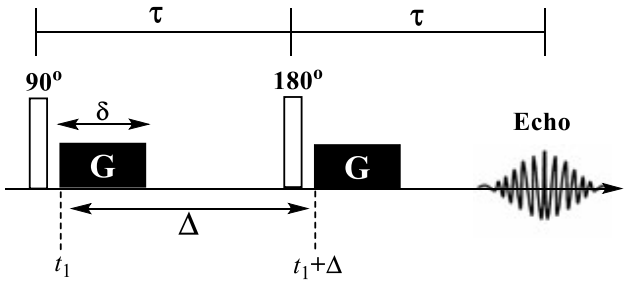

Figure 4.30 - Pulse-gradient spin-echo experiment used for DOSY NMR

The initial net magnetization is orientated along the *z*-axis. What follows is a 90° radio frequency (RF) pulse which rotates the magnetization into the *x*-*y* plane. A pulse gradient of duration δ and magnitude G is then applied at a time point t_1 and each spin experiences a phase shift. A subsequent 180° RF pulse reverses the sign of processing and phase angle, and a second gradient is applied at t_1+Δ which is of equal duration and magnitude to the original pulse. If diffusion has occurred, then the phase shift experienced after the initial τ, will be different to that experienced after the second τ. This is due to each species being located in a different spatial position along the *z*-axis between times t_1 and time t_1+Δ and as a result, each species will experience a different magnetic field, dependent on its relative positions. The phase angle will therefore fan out, refocussing will be poor and a reduced echo signal will be recorded as a direct result of diffusion. Note: if no diffusion occurs, then the spins are refocused after the 180° RF pulse (and subsequent G) and there

will be no attenuation of the signal. In essence a gradient pulse is used to encode the spatial positions of nuclear spins, and a second matched gradient pulse decodes positions.[20]

Relating this to a specific sample, for a given mixture containing different components, each component will have a different translational diffusion coefficient, related to its hydrodynamic radius and molecular weight, a product of Brownian motion. This value relies on any number of factors such as size, shape, mass and charge, as well as external factors such as solvent, temperature, aggregation etc. Essentially, field gradients are used to make the sample experience a different field in different parts of the NMR tube and as molecules diffuse during the acquisition process, they experience a different field depending on their relative motion. The more a molecule moves, the more different the field it experiences and this will decrease the intensity of the signals.[20] Attenuation of the spin-echo and a Fourier transformation of the half echo permits diffusion rates to be associated with individual lines in the NMR spectrum.[20] In terms of mixtures, the signal of each component will decay over time and this rate of decay will vary depending on the factors listed above.

A DOSY spectrum, obtained from the PGSE experiment provides a means for 'virtual separation' of mixtures and displays this diffusion data in a 2D matrix and a two-dimensional spectra is produced, with one dimension being the standard chemical shift and the other displaying that specific molecules diffusion behaviour. In general, it is assumed that the larger the molecule, the slower the diffusion coefficient. For well resolved spectra, the diffusion coefficient is obtained, after suitable experimental and processing methods, with good accuracies of 0.2%.

4.5.2 Applications

One of the more widely used applications of DOSY NMR is the identification of individual species in multi-component solutions, which involves 'separating' spectra with similar or overlapping chemical shifts based on their individual diffusion properties and has been used by Jayawickrama et al. in the identification of polymer additives.[21] This concept of in situ, spectroscopic separation has earned it the nickname 'NMR chromatography'.[20] DOSY has seen many applications including the characterization of reactive intermediates,[22] as well as extensive use in determining accurate molecular weights from mixtures in polymer chemistry,[23] the petrochemical industry[24] and of nanoparticles[25]. The technique can also be used for signal suppression, such as that of water signals in aqueous solutions[26], of course, as long as the molecule in question has a different value of diffusion compared with water.

As well as its use in medicinal,[27] polymer and material science, DOSY NMR has a particular appeal towards supramolecular chemists, and specifically in the field of interlocked structures[28, 28b] where a proof of their interlocked nature is required. Molecular interactions, the essence of supramolecular chemistry, may be probed by any number of spectroscopic techniques and of these; DOSY NMR can prove a powerful tool providing information unavailable by other means. Diffusion coefficients not only give an idea of the presence of H:G systems and interlocked structures, but also their physical properties and interactions, since their diffusion coefficient will also vary due to their shape, size and intermolecular interactions. DOSY also enables chemists, given the right binding modes and conditions, to deduce binding and association constants from diffusion data.

4.5.3 DOSY NMR of [2]-Rotaxane, 113, and its components

In order to gain further insight regarding the interlocked nature of **113**, as well as its physical behaviour in solution, a series of ^{1}H DOSY NMR spectra were recorded for the various components. These consisted of the photo-clipped rotaxane, **113**, the dumb-bell + cyclic receptor (perched) solution, **111**:**85,** as well as solutions of free dumb-bell, **85**, and free cyclic receptor, **111**. The spectra are shown in **Figures 4.31**-**4.34**. The value obtained for each solution gives the linear diffusion coefficient and gives some idea of how the molecules and/or complexes diffuse in solution, with lower values meaning a slower rate of diffusion. It should be noted that solutions of equivalent concentrations are essential, since the diffusion is affected not just by molecular mass, but also by external factors i.e. viscosity. Using solution concentrations of 27 mM and the solvent DCM-d_2 throughout, the first coefficients to be calculated are that of the individual components, **85** and **111**. Shown in the figures below are the DOSY spectra of **85** (**Figure 4.31**) and **111** (**Figure 4.32**). The diffusion coefficients were found to be 0.31 $x10^{-9}$ m^2s^{-1} and 0.65 $x10^{-9}$ m^2s^{-1} for the dumb-bell, **85**, and macrocycle, **111**, respectively. The diffusion coefficients of the solvent, DCM-d_2, in each case were found to be 3.1 $x10^{-9}$ m^2s^{-1} and 3.3 $x10^{-9}$ m^2s^{-1} respectively.

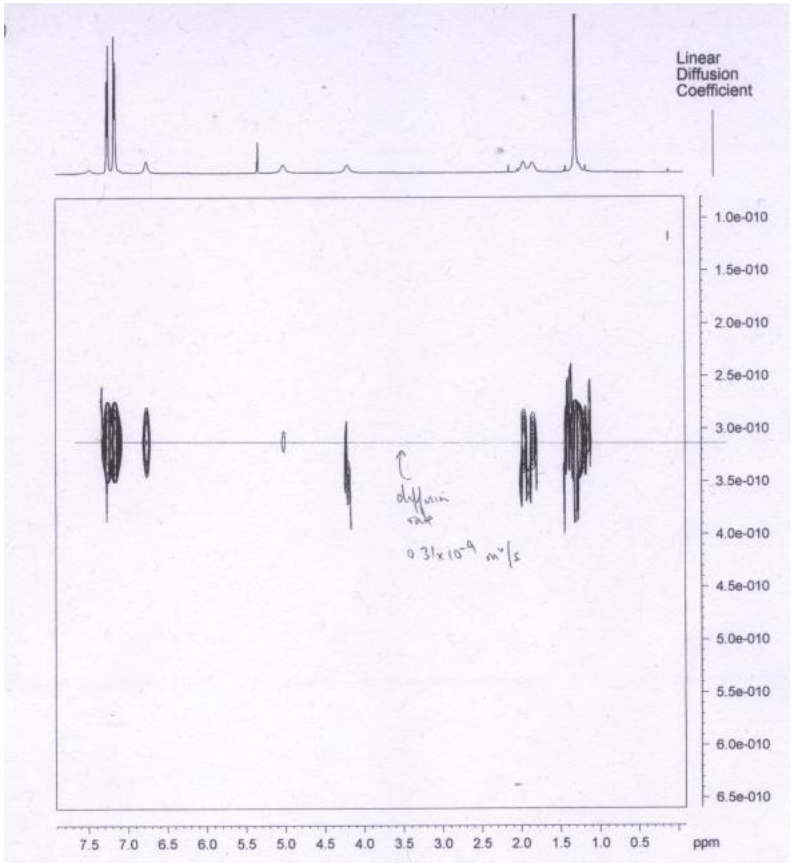

Figure 4.31 - ^{1}H DOSY NMR of **85** at a concentration of 27 mM in DCM-d_2

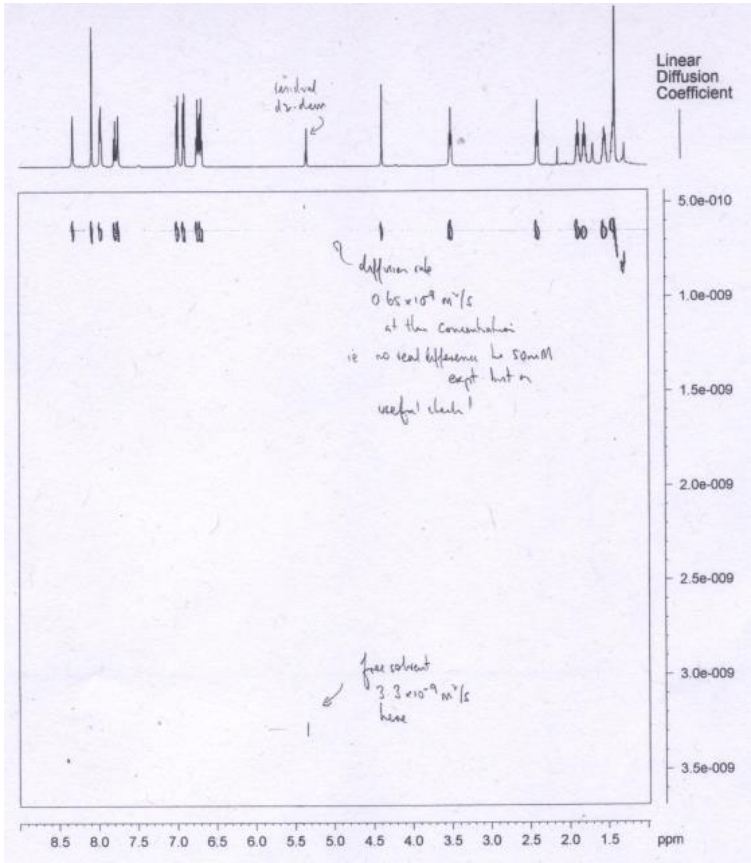

Figure 4.32 - ^{1}H DOSY NMR of **111** at a concentration of 27 mM in DCM-d_2

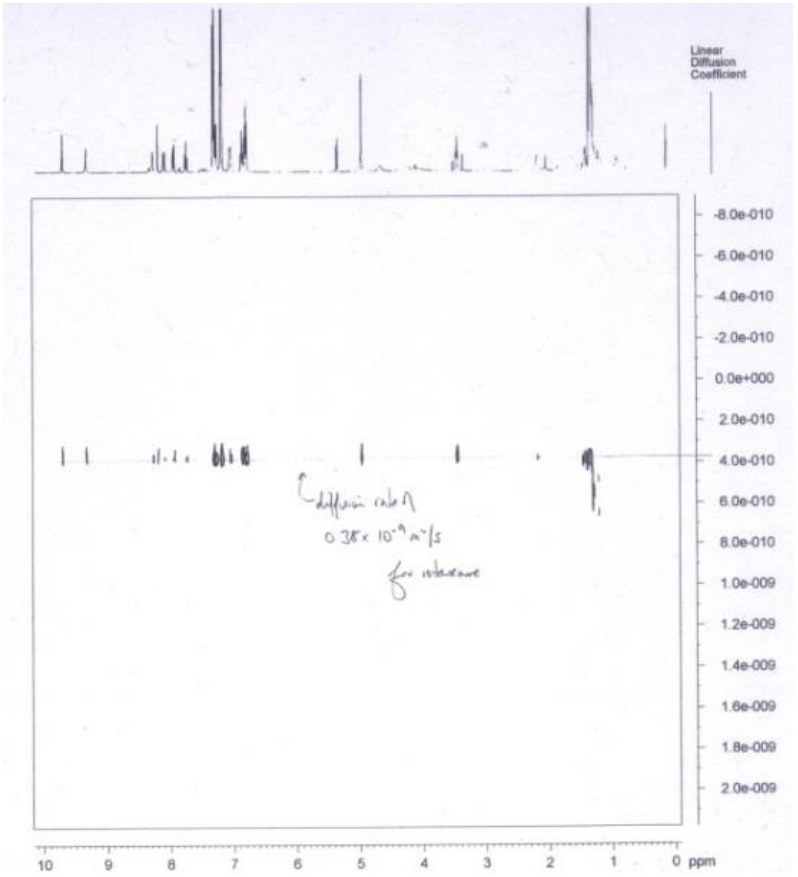

Figure 4.33 - ^{1}H DOSY NMR of **113** at a concentration of 27 mM in DCM-d_2

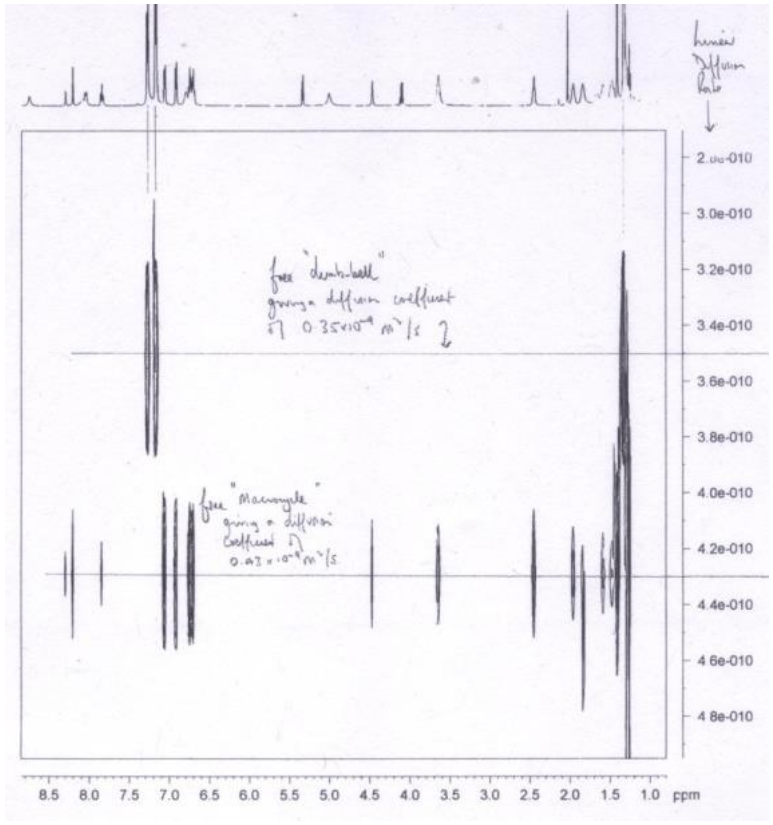

Figure 4.34 - ^{1}H DOSY NMR of **85**:**111** at a concentration of 27 mM in DCM-d_2

The rotaxane, **113**, was then analysed. The spectrum obtained is shown in **Figure 4.33** and the coefficient was found to be 0.38 $x10^{-9}$ m^2s^{-1} with a consistent solvent value found to be 3.2 $x10^{-9}$ m^2s^{-1}. The most important aspect of this result was the fact that a single diffusion coefficient was found for the complex, giving further evidence to support its interlocked nature. The final comparison to be made was a mixture of the guest, **85**, and macrocycle, **111**, to try to distinguish the two molecules based on their independent diffusion rates. This comparison was important due to the fact that two separate diffusion coefficients should be obtained since any complex formed will not be interlocked, and be in a state of equilibrium. The spectrum obtained is shown in **Figure 4.34**. As expected, two separate values were obtained for each component. **85** was found to have a value of 0.35 $x10^{-9}$ m^2s^{-1} and **112**, 0.43 $x10^{-9}$ m^2s^{-1}. Again, a consistent solvent value of 3.1 $x10^{-9}$ m^2s^{-1} was found. The summary of results is shown in **Table 4.3**, below.

Table 4.3 - Various results of diffusion coefficients, obtained via ^{1}H DOSY NMR, of **85**, **111**, **113** and **85**:**111**

	Linear Diffusion Coefficient ($x10^{-9}$ m^2s^{-1})				
Entry	Concentration, mM	Dumb-bell M_r = 1379.9 **85**	Macrocycle M_r = 1011.3 **111**	Rotaxane M_r = 2391.2 **113**	Solvent (DCM-d_2)
1	27	0.31	0.65	0.38	**85** – 3.1 **111** – 3.3 **113** – 3.2
2	27	0.35	0.43	-	**111:85** – 3.1
3	50	-	0.62	-	**111** - 3.2
4	96	0.20	-	-	**85** - 2.6
5	50	-	0.43	-	**111** - 2.5 ($CDCl_3$)

Using the table for comparison, it is now clear to see that the variations in molecular weight and shape alter the diffusion coefficient. When comparing **85** with **111** at 27 mM (entry 1), the larger and considerably more bulky dumbbell diffuses slower than the

macrocycle. At constant concentrations, a consistent diffusion coefficient was found for the solvent.

Highlighting the importance of a consistent concentration, when the concentration of solution was altered, so too did the diffusion coefficient. This is highlighted by entry 4, where a solution of **85** was used at a concentration of 96 mM in DCM-d_2. Comparing with a concentration of 27 mM (entry 1) there is a reduction in diffusion coefficient for both the molecule under consideration and solvent. This is an expected result, since in a more viscous solution, both solute and the solvent will be diffusing slower relative to one another, resulting in a lower diffusion coefficient. A similar argument can be made for varying solvent. When comparing entries 3 and 5, which consist of 50 mM solutions of **111** in DCM-d_2 and $CDCl_3$ respectively, the diffusion coefficient for both solute and solvent are observed to decrease in the case of $CDCl_3$. This can be explained via the known viscosities of the solvents. DCM has a viscosity of 0.41 cP with chloroform having a higher value of 0.54 cP.[29] An inherently more viscous solution will show decreased diffusion coefficients when compared to less viscous samples and this is what was observed.

When comparing the independent diffusion rates of macrocycle, dumb-bell and rotaxane, one would expect a step-wise decrease with increasing molecular weight. However, despite the trend holding when comparing **111** and **113**, in fact a higher value than expected for the rotaxane was found, which diffuses faster than **85**. However, at this point it is important to state that there are many factors, both intrinsic and external, which affect the diffusion coefficient, besides molecular weight. It could be possible that any solvent-solute interactions, due to the polar regions present in the components of the

rotaxane, are reduced and/or occupied in the interlocked form due to the presence of H-bonding, folding of the complex, etc. This concept is supported by the notable presence of H-bonding in the complex, observable via ^{1}H NMR, see **Figure 4.27**. This may be analogous to the situation observed under TLC comparison, **Figure 4.25**, where the rotaxane and non-interlocked H:G complexes would diffuse up the TLC plate faster than the free components. Size may also be a contributing factor, not just the lack of interacting groups and it is feasible that the rotaxane is folded into a smaller shape and conformation when interlocked and therefore diffuses faster than its free components.

Another important comparison to be made is between the free and mixed components, perched complex **85**:**111** (entry 2). As expected, when a mixed solution was analysed, two independent diffusion coefficients were observed, clearly visible on the DOSY NMR in **Figure 4.34**. The values for **85** and **111**, were found to be 0.35 and 0.43 respectively, which differ from the values obtained as independent solutions, despite identical conditions of temperature, solvent and concentration. This can be rationalised due to the occurrence of complexation between the host and guest molecules. This is also evident from the NH shifts of the amide protons in the 'perched' spectra in **Figure 4.27**. The only variable between each sample was the presence of each molecules corresponding H-bonding component. If we consider that some degree of complexation is occurring, it appears as if the faster diffusing **111** is 'held back' by the slower **85** and inversely the slower diffusing **85** is 'sped up' through solution by **111**, due to their H-bonding behaviour. Despite this interesting result, the most important aspect concerning this experiment was the presence of two values for the diffusion of the two independent components. Comparing this DOSY 2D-spectrum to the one obtained for the rotaxane, where a single diffusion coefficient was

obtained and therefore, a single compound is present, it can be concluded that the molecule, **113**, is in fact interlocked and not moving as a complex.

4.6 Attempts Towards Dimerization with Different Length Tethers

In an attempt to expand upon the utility of this photo-clipping method, the n=3 and n=9 linker receptors, **107** and **109**, were investigated to establish their abilities to form photo-rotaxanes. Only guest **85** was used in these attempts, owing to the fact that it has already shown its ability towards the synthesis of interlocked structures.

4.6.1 Attempts with Anthracene Receptor 107 (n=3)

The first receptor investigated was **107** and as before, it was dissolved in degassed DCM to form a 0.5 mM solution. As done previously 3 equivalents of **85** were added and the flask was then irradiated at 365 nm. The dimerization was monitored periodically using UV-Vis spectroscopy. The UV-Vis spectrum is shown in **Figure 4.35.**

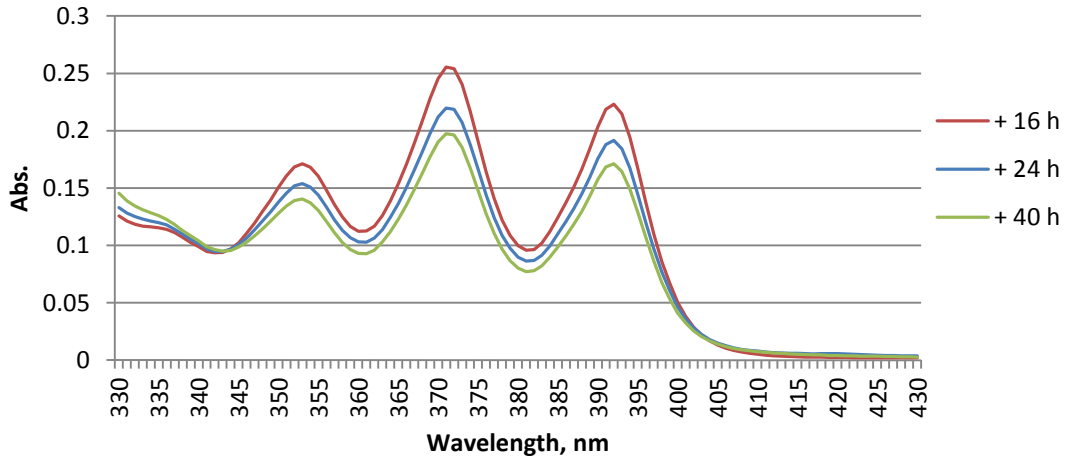

Figure 4.35 - Variation in electronic absorption spectra of **107** in the presence of **85** in DCM upon irradiation at 365 nm.

Based on previous observations, concerning the issues observed during the dimerization of **108** with the rigid barbiturate **76**, for the time taken to obtain such a meagre reduction in signal, it was clear that the dimerization was unable to occur. Further evidence for this lack of dimerization was found from periodic analysis by TLC of the reaction solution. An anthraquinone spot was observed to increase over time, showing increasing degradation of the receptor, and so irradiation was stopped and the solvents were removed. The crude ^{1}H NMR spectrum confirmed the lack of any dimerization whatsoever, and only **107**, **85** and the products of oxidation (accounting for the reduction in signal) were observed. These were separated via column chromatography. Over the period of irradiation, there is very little decrease in anthracene signal and this appears to show a similar trend to that observed with the rigid dumbbell, **76**, **Figure 4.21**. This highlights the relationship between the tether length, which affects the capability of cyclisation. Despite guest **85** showing the capability of forming interlocked structures when dimerizing with a receptor of sufficient tether length (n=6, compound **108**), upon reduction of the length, the guest is now too big for the receptor to cyclise around it as shown in **Scheme 4.10.**

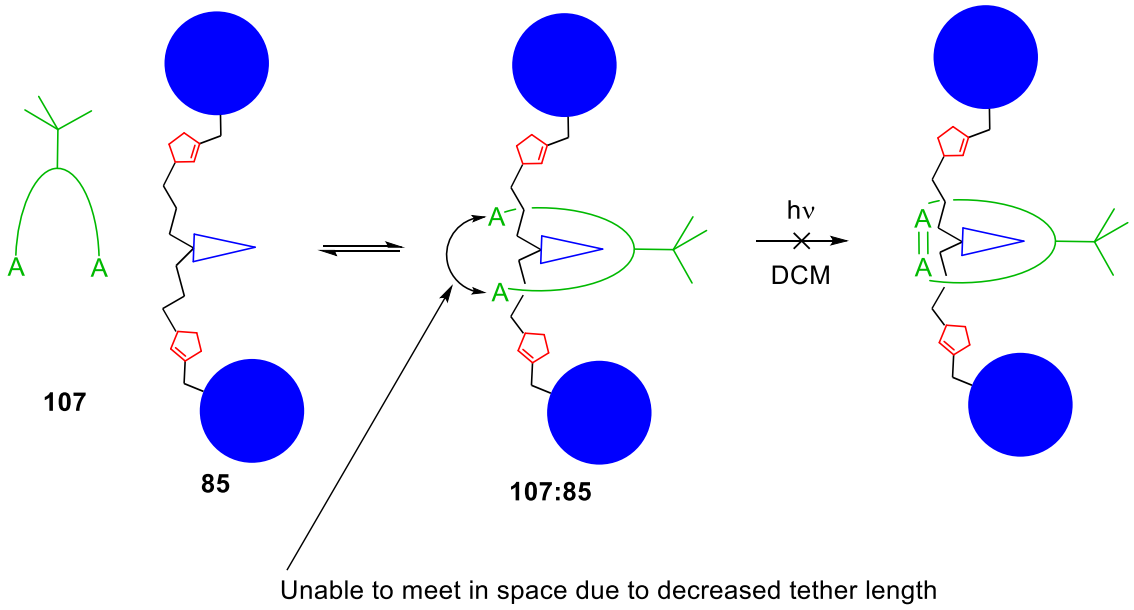

Scheme 4.10 - Proposed scheme for the failed clipping attempt of **107** with **85**.

This result is not unexpected and it has been previously shown by Tucker,[12] that the n=3 linker receptors show photo-switched binding of barbital (a much smaller guest), with the guest released upon cyclisation. Therefore in this case, the guest prevents the anthracene from coming into close enough proximity to cyclise and so the formation of an interlocked structure is not possible with this combination of components. This could however, be considered as guest-mediated, on/off photo-dimerization.

4.6.2 Attempts with Anthracene Receptor 109 (n=9)

It was anticipated that increasing the tether length between amide and anthracene groups to nine carbons would allow a more facile route towards the rotaxane due to minimization of any steric hindrance from the guest. It was also thought that this could promote the situation where the macrocycle would be large enough to no longer favour strong H-bonding with the clipped guest and so move away from the binding site upon

dimerization under certain conditions. This would be advantageous towards applications regarding shuttling or the synthesis of [n]-Rotaxanes, provided the dumb-bell linker groups could accommodate this.

The photo-clipping process was therefore attempted with the n=9 linker, **109**. A 0.5 mM solution of **109**, in degassed DCM was used and after the addition of three molar equivalents of **85** the solution was irradiated at 365 nm and the dimerization monitored via UV-Vis spectroscopy as before. The UV-Vis spectrum obtained for the dimerization is shown in **Figure 4.36**. It is clear that the dimerization is extremely efficient, and faster than observed for the free receptor (**Figure 4.13**), with no further dimerization occurring after 1.5 h.

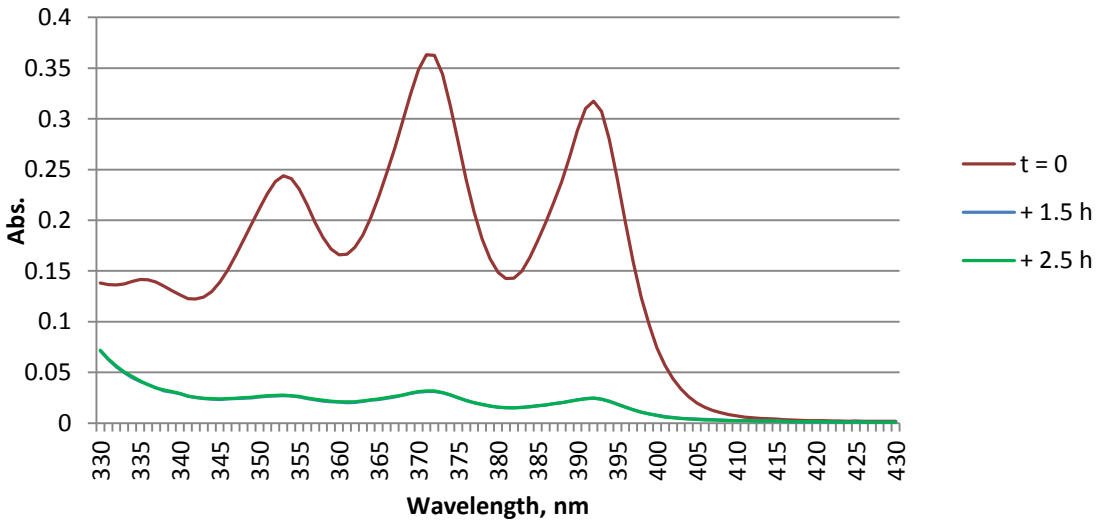

Figure 4.36 - Variation in electronic absorption spectra of **109** in the presence of **85** in DCM upon irradiation at 365 nm.

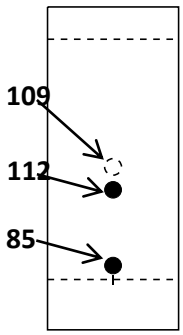

Figure 4.37 - TLC of the reaction mixture

After 2.5 hours of irradiation, the solvents were removed and a TLC of the reaction mixture (eluent: DCM/EtOAc-10%) revealed two major components (**Figure 4.37**). Subsequent column chromatography and ^{1}H NMR revealed these to be the dimerised receptor, **112** and the non-interlocked dumb-bell, **85**. Trace amounts of **109** were isolated and interestingly, this was the only dimerised compound which could be separated from its acyclic isomer due to a different R_f. Despite a successful and highly efficient dimerization, the components were returned, clearly in a non-interlocked fashion. It seems that when using n=9 tethers, an interlocked structure is not possible, at least not with this particular guest and clipping method. In this case, the dimerization was clearly not hindered, so steric factors regarding the guest can be ruled out, and as far as irradiation time was concerned, an increase in efficiency of the system appears to have been achieved, albeit lacking the target rotaxane.

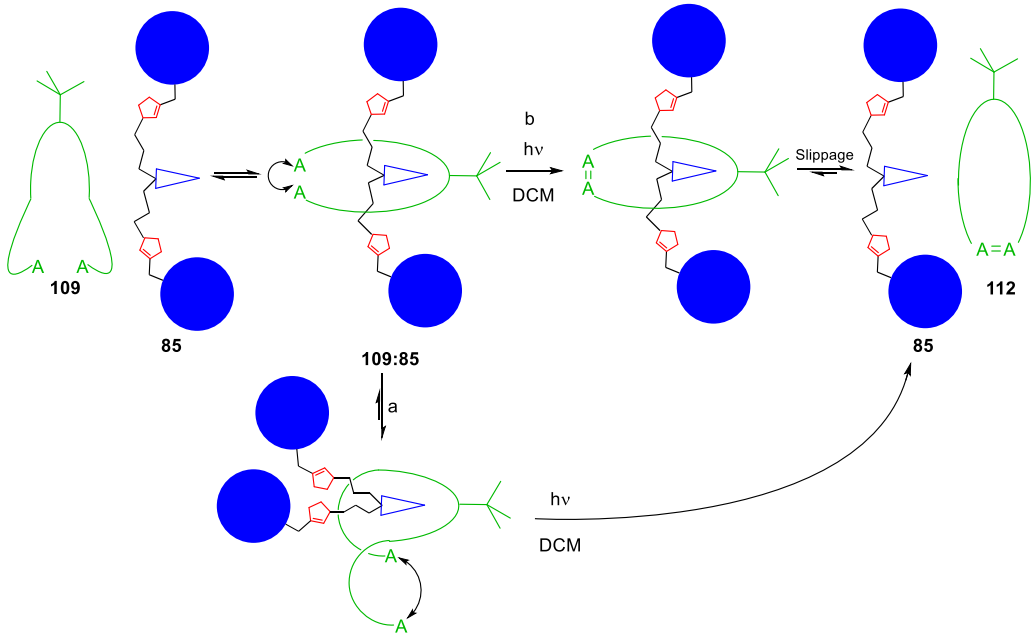

Scheme 4.11 - Proposed scheme for the failed clipping attempt of **109** with **85**.

The simplest explanation for this data is that the macrocycle is too large for the capture of an interlocked structure and may be due to one of two proposed reasons as outlined in **Scheme 4.11**. The first, route a, is the possibility of conformations available which are not favourable for the capture of an interlocked structure. Due to the increased length of tether, it is feasible that the anthracenes may orientate themselves away from the guest and essentially clip together in a perched conformation, resulting in the isolation of separable components. The second potential route, b, is the possibility of slippage of the dumbbell over the macrocycle, a consequence of the increased ring size. The ring size obtained upon cyclisation is approaching the limit regarding this size of stopper group, so the dimerization may occur around the axle of the dumb-bell, but is unable to stay interlocked. If this process is occurring in situ, then it may be worthy of further investigations with these 9-C tethers centred around larger stopper groups since dimerization is clearly not disfavoured by complexation of **85**.

4.6.3 Summary of Perched complexes

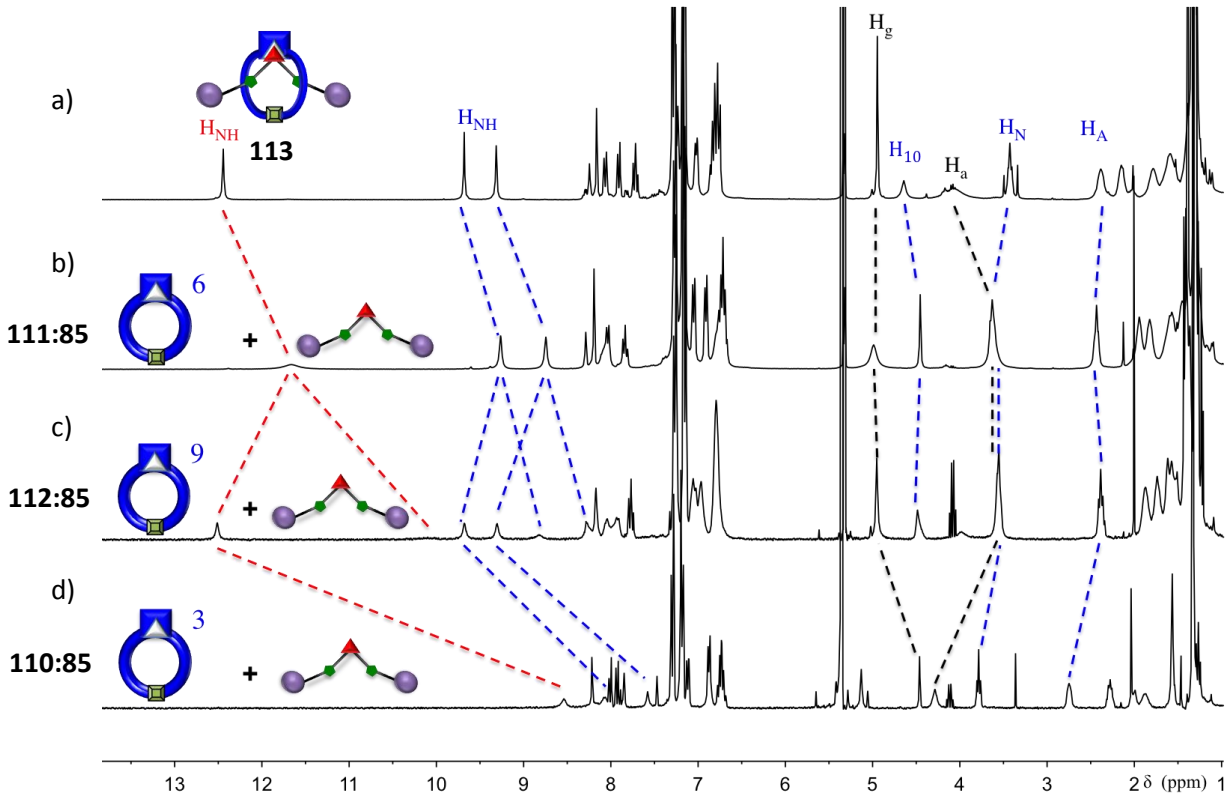

Figure 4.38 – ^{1}H NMR spectra (300 MHz) at room temperature in CD_2Cl_2 of **113** (a) and 1:1 complexes of **111**:**85** (b), **112**:**85** (c) and **110**:**85** (d) at concentrations of 5 mM.

Expanding upon this notion of a slippage event the series of perched complexes were investigated. From the summary of spectra in **Figure 4.38**, comparing rotaxane **113** (n=6) and the formation of perched products, between the three various cyclised receptors and guest **85**, it is clear from the apparent shifts of the receptor NH signals that spectra of **111**:**85** (**Figure 4.38.b**) and **110**:**85** (**Figure 4.38.d**) do indeed show the formation of perched complexes due to their relative differences in spectra, when compared to [2]-Rotaxane **113**. Considering the spectrum of **112**:**85** (**Figure 4.38.c**), however, two independent sets of signals are present for the NH protons (12.49 and 10.05 for the imide NH protons of the guest and 9.70, 8.75 and 9.25, 8.32 for the two NH protons of the receptor) and this denotes the presence of two separate complexes which are forming in situ. One of the sets

of signals correlates to what can be considered a strong interaction analogous to that of a threaded complex. This is potentially the formation of a pseudorotaxane via a slippage event which appears to be unable to be isolated, due to the increase in ring size.

4.7 Conclusion and Future Work

4.7.1 Conclusion

In conclusion, what may be considered the first reported capture of an interlocked structure, via a light-triggered photo-dimerization, has been demonstrated through the use of bichromophoric Hamilton-type receptors and appropriately functionalised barbiturate guest molecules. Proof of the molecules interlocked nature has been shown using ^{1}H NMR spectral analysis, ^{1}H DOSY NMR and mass spectrometry. Minor attempts towards the optimisation of rotaxane formation through variations in ring-size have been attempted; however, these seem to have been hindered via either steric constraints or increased flexibility and it seems that the ideal ring size was found originally, (n=6).

Aside from unsuccessful attempts regarding different receptors, other failed attempts included the use of guest **76**, probably due to increased steric hindrance near the binding site for this guest.

Future work to be carried out on compound **113** should initially consist of fine tuning the ring-size through variation in the tether length, for example, 4, 5 or 7-C linkers and optimisation of the size of the stopper moiety, which may provide higher yielding and more stable products. Possible capture of the proposed slippage product of **112**:**85** could also be considered, however, this would be unstable at room temperature.

Greater understanding of why the other attempts failed may be garnered through further investigations of guests of various sizes and geometries and through the analysis of the specific photochemistry of the molecules and complexes. The determination of the presence of the excimer required for dimerization would also be beneficial.

4.7.2 Future Work

A further concept of exploration would be the synthesis of [n]-Rotaxanes via a multi-dimerization event in order to create interesting topologies of these motifs and provide a route towards multiply functionalised rotaxanes. As shown in **Scheme 4.12**, if the barbiturate dumb-bell is created with a sufficiently long linker between the stopper groups and barbiturate, then there should be space on the axle to accommodate more than one ring. This will depend on many factors, especially whether or not the binding site is occupied more strongly by the first macrocycle than subsequent acyclic receptors. Despite rotaxane **113** showing some degree of H:G binding, there is evidence that this should not necessarily localise at the binding site in the presence of acyclic receptor compounds, since dimerised receptors have been shown to have weaker binding with barbiturate guests when in their cyclised form. In the presence of another guest, or under different solvent conditions, the receptor could slip down onto the axle, leaving a binding site free for a subsequent dimerization event. There is also the mode of addition to consider; this process could feasibly be a one-pot reaction, using a large excess of receptor, or a multi-step process requiring subsequent addition of successive rings after purification of each [n]-rotaxane.

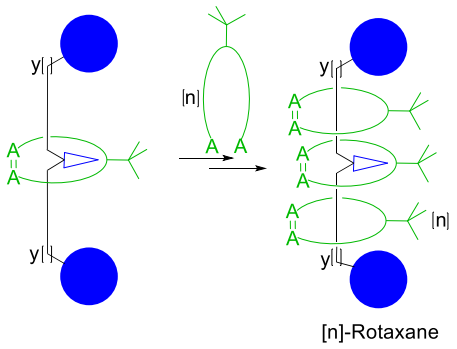

Scheme 4.12 – A potential multidimerisation event producing [n]-rotaxanes

Further, and more in-depth studies may be applied towards these systems using new functionalised guests to impart some functionality into the rotaxane, as well as the possibility of designing new and different receptors and/or guests to create an array of interesting structures. i.e. attachment to a surface, or multi guest and/or receptor compounds as illustrated in **Figure 4.39**.

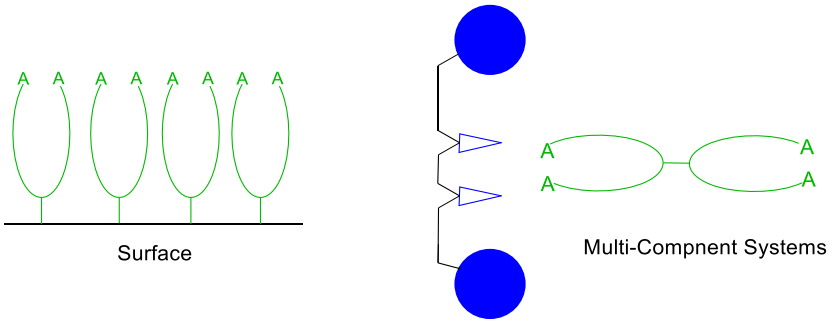

Figure 4.39 – Potential multicomponent systems towards alternate interlocked structures and possible surface applications

Efforts could also be made to use this photo-clipping strategy towards current H:G motifs. Employing the use of considerably more studied systems, such as Beer's anion templates,[30] or Leigh's fumarimide systems,[31] could allow further advancements and functionalizations of these motifs, or towards new topologies of structures not yet obtained.

4.8 References

1. Verhoeven, J. W., Glossary of terms used in photochemistry (IUPAC Recommendations 1996). *Pure Appl. Chem.* **1996,** *68*, 2223.

2. Wayne, C. E.; Wayne, R. P., *Photochemistry*. Oxford University Press: Oxford, 1996.

3. Becker, H. D., Unimolecular photochemistry of anthracenes. *Chem. Rev.* **1993,** *93* (1), 145-172.

4. Byron, C. M.; Werner, T. C., Experiments in synchronous fluorescence spectroscopy for the undergraduate instrumental chemistry course. *J. Chem.Educ.* **1991,** *68* (5), 433.

5. Fritzsche, J., *Bull. Acad. Imper. Sci. St.-Petersbourg* **1866,** *9*, 406-419.

6. McCullough, J. J., Photoadditions of aromatic compounds. *Chem. Rev.* **1987,** *87* (4), 811-860.

7. Bouas-Laurent, H.; Castellan, A.; Desvergne, J.-P.; Lapouyade, R., Photodimerization of anthracenes in fluid solution: structural aspects. *Chem. Soc. Rev.* **2000,** *29* (1), 43-55.

8. Bouas-Laurent, H.; Castellan, A.; Desvergne, J.-P.; Lapouyade, R., Photodimerization of anthracenes in fluid solutions: (part 2) mechanistic aspects of the photocycloaddition and of the photochemical and thermal cleavage. *Chem. Soc. Rev.* **2001,** *30* (4), 248-263.

9. Bouas-Laurent, H. C., A. Desvergne, J-P., From anthracene dimerisation to jaw photochromic materials and photocrowns. *Pure Appl. Chem.* **1980,** *52* (12), 2633.

10. de Silva, A. P.; de Silva, S. A., Fluorescent signalling crown ethers; 'switching on' of fluorescence by alkali metal ion recognition and binding in situ. *J.Chem. Soc.,Chem.Comm* **1986,** (23), 1709-1710.

11. Weller, A., *Pure Appl. Chem.* **1968,** *16* (1), 115.

12. Molard, Y.; Bassani, D. M.; Desvergne, J.-P.; Moran, N.; Tucker, J. H. R., Structural Effects on the Ground and Excited-state Properties of Photoswitchable Hydrogen-Bonding Receptors. *J. Org. Chem.* **2006,** *71* (22), 8523-8531.

13. Wurpel, G. W. H.; Brouwer, A. M.; van Stokkum, I. H. M.; Farran, A.; Leigh, D. A., Enhanced Hydrogen Bonding Induced by Optical Excitation: Unexpected Subnanosecond Photoinduced Dynamics in a Peptide-Based [2]Rotaxane. *J. Am. Chem. Soc.* **2001,** *123* (45), 11327-11328.

14. Werner, T. C.; Rodgers, J., Studies on the fluorescence properties of meso-substituted amidoanthracenes. *J. Photochem.* **1986,** *32* (1), 59-68.

15. (a) Ashton, P. R.; Ballardini, R.; Balzani, V.; Credi, A.; Dress, K. R.; Ishow, E.; Kleverlaan, C. J.; Kocian, O.; Preece, J. A.; Spencer, N.; Stoddart, J. F.; Venturi, M.; Wenger, S., A Photochemically Driven Molecular-Level Abacus. *Chem. Eur. J.* **2000,** *6* (19), 3558-3574; (b) Armaroli, N.; Balzani, V.; Collin, J.-P.; Gaviña, P.; Sauvage, J.-P.; Ventura, B., Rotaxanes Incorporating Two Different Coordinating Units in Their Thread: Synthesis and Electrochemically and Photochemically Induced Molecular Motions. *J. Am. Chem. Soc.* **1999,** *121* (18), 4397-4408.

16. Baumes, J. M. G., J. J.; Giblin, J.; Lee, J. J.; White, A. G.; Culligan, W. J.; Leevy, W. M.; Kuno, M.; Smith, B. D., *Nature Chem.* **2010,** *2*, 1025.

17. (a) Mobian, P.; Collin, J.-P.; Sauvage, J.-P., Efficient synthesis of a labile copper(I)-rotaxane complex using click chemistry. *Tetrahedron Lett.* **2006,** *47* (28), 4907-4909; (b) Crowley, J. D.; Goldup, S. M.; Gowans, N. D.; Leigh, D. A.; Ronaldson, V. E.; Slawin, A. M. Z., An Unusual Nickel−Copper-Mediated Alkyne Homocoupling Reaction for the Active-Template Synthesis of [2]Rotaxanes. *J. Am. Chem. Soc.* **2010,** *132* (17), 6243-6248; (c) MacLachlan, M. J.; Rose, A.; Swager, T. M., A Rotaxane Exciplex. *J. Am. Chem. Soc.* **2001,** *123* (37), 9180-9181.

18. Saito, S.; Takahashi, E.; Wakatsuki, K.; Inoue, K.; Orikasa, T.; Sakai, K.; Yamasaki, R.; Mutoh, Y.; Kasama, T., Synthesis of Large [2]Rotaxanes. The Relationship between the Size of the Blocking Group and the Stability of the Rotaxane. *J. Org. Chem.* **2013,** *78* (8), 3553-3560.

19. Stejskal, E. O.; Tanner, J. E., Spin Diffusion Measurements: Spin Echoes in the Presence of a Time-Dependent Field Gradient. *J. Chem. Phys.* **1965,** *42* (1), 288-292.

20. Cohen, Y.; Avram, L.; Frish, L., Diffusion NMR Spectroscopy in Supramolecular and Combinatorial Chemistry: An Old Parameter—New Insights. *Angew. Chem. Int. Ed.* **2005,** *44* (4), 520-554.

21. Jayawickrama, D. A.; Larive, C. K.; McCord, E. F.; Roe, D. C., Polymer additives mixture analysis using pulsed-field gradient NMR spectroscopy. *Magn. Reson. Chem.* **1998,** *36* (10), 755-760.

22. Li, D.; Keresztes, I.; Hopson, R.; Williard, P. G., Characterization of Reactive Intermediates by Multinuclear Diffusion-Ordered NMR Spectroscopy (DOSY). *Acc. Chem. Res.* **2008,** *42* (2), 270-280.

23. Li, W.; Chung, H.; Daeffler, C.; Johnson, J. A.; Grubbs, R. H., Application of 1H DOSY for Facile Measurement of Polymer Molecular Weights. *Macromolecules* **2012,** *45* (24), 9595-9603.

24. Pekerar, S.; Lehmann, T.; Méndez, B.; Acevedo, S., Mobility of Asphaltene Samples Studied by 13C NMR Spectroscopy. *Energy & Fuels* **1998,** *13* (2), 305-308.

25. Canzi, G.; Mrse, A. A.; Kubiak, C. P., Diffusion-Ordered NMR Spectroscopy as a Reliable Alternative to TEM for Determining the Size of Gold Nanoparticles in Organic Solutions. *J. Phys. Chem. C.* **2011,** *115* (16), 7972-7978.

26. van Zijl, P. C. M.; Moonen, C. T. W., Complete water suppression for solutions of large molecules based on diffusional differences between solute and solvent (DRYCLEAN). *J. Magn. Reson.* **1990,** *87* (1), 18-25.

27. Hoehn-Berlage, M., Diffusion-weighted NMR imaging: Application to experimental focal cerebral ischemia. *NMR Biomed.* **1995,** *8* (7), 345-358.

28. (a) Collin, J.-P.; Frey, J.; Heitz, V.; Sauvage, J.-P.; Tock, C.; Allouche, L., Adjustable Receptor Based on a [3]Rotaxane Whose Two Threaded Rings Are Rigidly Attached to Two Porphyrinic Plates: Synthesis and Complexation Studies. *J. Am. Chem. Soc.* **2009,** *131* (15), 5609-5620; (b) Hori, A.; Kumazawa, K.; Kusukawa, T.; Chand, D. K.; Fujita, M.; Sakamoto, S.; Yamaguchi, K., DOSY Study on

Dynamic Catenation: Self-Assembly of a [3]Catenane as a Meta-Stable Compound from Twelve Simple Components. *Chem. Eur. J.* **2001,** *7* (19), 4142-4149.

29. Lide, D. R., *CRC Handbook of Chemistry and Physics*. 85th Edition ed.; CRC Press Boca Raton, FL., 2004.

30. Wisner, J. A.; Beer, P. D.; Drew, M. G. B.; Sambrook, M. R., Anion-Templated Rotaxane Formation. *J. Am. Chem. Soc.* **2002,** *124* (42), 12469-12476.

31. Gatti, F. G.; Leigh, D. A.; Nepogodiev, S. A.; Slawin, A. M. Z.; Teat, S. J.; Wong, J. K. Y., Stiff, and Sticky in the Right Places: The Dramatic Influence of Preorganizing Guest Binding Sites on the Hydrogen Bond-Directed Assembly of Rotaxanes. *J. Am. Chem. Soc.* **2001,** *123* (25), 5983-5989.

5. Experimental

5.1 General

All starting materials were purchased from Aldrich or Lancaster and solvents from Fischer and VWR. Commercially available solvents and reagents were used without further purification, except for Et_2O, MeOH, THF, MeCN and DCM, which were dried in Pure Solv™ Solvent Purification Systems, and DMSO, which was dried using CaH_2 and stored under argon and in the presence of molecular sieves. Unless otherwise stated, all reactions were carried out under argon atmosphere with the exclusion of moisture, and for reactions containing the anthracene molecules, the reactions were conducted in the absence of light, using tin foil, in degassed solvents. Thin layer chromatography plates were visualised under UV light, or by the stains potassium permanganate or ceric ammonium molydbate (CAM) and flash chromatography was carried out using silica gel (Merck, grade 60) using the eluent stated. ^{1}H NMR spectra were recorded at 300 MHz on a Bruker AVIII300 spectrometer and ^{13}C NMR spectra at 101 MHz on a Bruker AVIII400 NMR spectrometer, at room temperature, unless otherwise stated. Chemical shifts (δ) are in ppm and coupling constants (*J*) are in Hz. Mass spectra were recorded with a Waters/Micromass spectrometer using the method stated. IR spectra were recorded neat on a PerkinElmer Spectrum 100 FT-IR spectrometer.

[WARNING] - When conducting any azide chemistry, as a precaution, a blast shield was used during solvent removal due to the potentially explosive nature of low molecular weight azides.

Photochemistry of the anthracene moieties were conducted by making up solutions of the desired compound to a concentration of 0.5 mM in degassed DCM. The solutions were then irradiated using a Photochemical Reactors Ltd. 125W mercury arc lamp, which was enclosed within a housing with an outlet containing a 365 nm bandpass filter (Edmund Optics 65-615, 12.5 mm diameter, 10 nm bandwidth). The dimerization was monitored at set intervals through UV spectroscopy measuring the decrease in absorbance of the anthracene band at 320-400 nm. UV-Vis spectra were recorded using a Shimadzu 1800 spectrometer using samples at 2.6 x 10^{-5} M.

5.2 Experimental Procedures and Characterisation

(5-*tert*-butyl Isophthaloyl Dichloride), 39

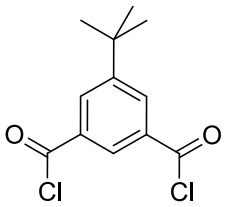

Oxalyl Chloride (5.70 mL, 66.0 mmol) was added to a solution of 5-*tert*-butyl isophthaloic acid (2.52 g, 11.3 mmol) in DCM (40 mL). The mixture was heated to reflux and 1 drop of DMF (approx. 0.05 mL) was then added. After 2 h under reflux the yellow solution was cooled and the solvents removed under vacuum to afford a yellow, oily solid. Unreacted oxalyl chloride was removed under high vacuum to afford 2.81 g of a beige solid in quantitative yield, no purification required. ^{1}H NMR ($CDCl_3$, 300 MHz): δ = 8.72 (s, 1H, Ar), 8.41 (s, 2H, Ar), 1.42 (s, 9H, ^{t}-Bu). Analysis is in agreement with literature data.[1]

(*N,N'*-bis-(6-aminopyridin-2-yl)-5-*tert*-butyl isophthalamide), 40

Isophthaloyl dichloride, **39**, was dissolved in dry THF (80 mL) and added dropwise over 2 h via syringe pump to a solution of 2,6-diamino pyridine (6.25 g, 57.0 mmol) and NEt_3 (1.90 g,

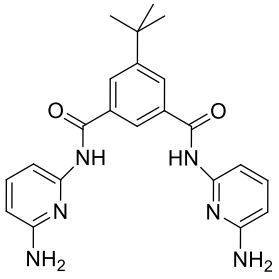

19.0 mmol) in THF (40 mL). The solution was stirred for 16 h. The volatiles were then removed under vacuum. Water (200 mL) was added to the residue and the grey precipitate was filtered and washed with water (50 mL) and then ethanol (20% aq. solution). The crude product was purified *via* flash column chromatography on silica (eluent: DCM/THF 3:1) to give 3.36 g of **40** (8.31 mmol, 75% yield). ^{1}H NMR (300 MHz, $CDCl_3$) δ = 8.36 (s, 2H, NH), 8.20 (t, J = 1.6 Hz, 1H, ArH), 8.13 (d, J = 1.6 Hz, 2H, ArH), 7.74 (dd, J = 7.9, 0.5 Hz, 2H, pyr), 7.55 (t, J = 8.0 Hz, 2H, pyr), 6.33 (dd, J = 8.0, 0.6 Hz, 2H, pyr), 4.38 (s, 4H, NH_2), 1.42 (s, J = 8.0 Hz, 9H, ^{t}Bu). ^{13}C NMR (101 MHz, CDCl3) δ = 164.87 (*C*O), 157.16 (*C*pyr), 149.80 (*C*pyr), 140.21 (CHpyr), 134.95 (C Ar), 128.02 (CH Ar), 122.44 (CH Ar), 104.75 (CH pyr), 103.66 (CH pyr), 31.20 (CH ^{t}Bu), 25.61 (C ^{t}Bu). Analysis is in agreement with literature data.[2]

(5-*tert*-Butyl- *N,N'*-bis-(6-undec-10-enoylamino-pyridin-2-yl)-isophthalamide), 41

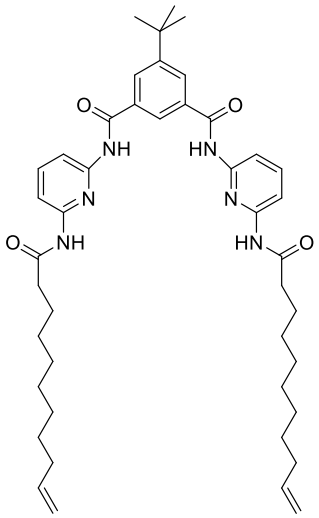

40 (0.40 g, 0.98 mmol) was dissolved in dry THF (100 mL). NEt_3 (0.35 mL, 2.5 mmol) was added and the flask cooled to 0^{o} C. A solution of 10-undecenoyl chloride (0.50 mL, 2.4 mmol) in THF (40 mL) was added via syringe and the reaction was stirred overnight. The solvent was evaporated and the residue diluted in DCM (100 mL). The organic phase was washed with sat. $NaHCO_3$ (4 x 50 mL). The organic phase was separated and dried using $MgSO_4$, filtered, and concentrated under vacuum to afford a yellow oil. Addition of hexane (approx. 10 mL) produced a cream solid which was filtered and washed with hexane to afford 0.48 g of desired product. (0.65 mmol, 65% yield). ^{1}H NMR (300 MHz, $CDCl_3$) δ = 8.41 (s, 2H, NH), 8.23

(s, 1H, ArH), 8.15 (d, J = 1.3 Hz, 2H, ArH), 8.08 (d, J = 8.0 Hz, 2H, CH pyr), 8.00 (d, J = 8.0 Hz, 2H, CH pyr), 7.80 (t, J = 8.1 Hz, 2H, CH pyr), 7.70 (s, 2H, NH), 5.82 (ddt, J = 16.9, 10.2, 6.7 Hz, 2H, C*H*CH_2), 5.11 – 4.87 (m, 4H, CHC*H*$_2$), 2.42 (t, J = 7.5 Hz, 4H, COC*H*$_2$), 2.11 – 1.99 (m, 4H, CH=CH_2C*H*$_2$), 1.74 (dd, J = 14.6, 7.5 Hz, 4H, $COCH_2$C*H*$_2$), 1.44 (s, 9H, ^{t}Bu), 1.42 – 1.26 (m, J = 10.8 Hz, 20H, Alk). ^{13}C NMR (101 MHz, $CDCl_3$) δ = 178.14, 171.75 (CO), 164.90 (CO), 153.38 (C pyr), 149.73, (Cpyr) 149.36 (C Ar), 141.15 (CH pyr), 139.11 (*C*H=CH_2), 134.51 (C Ar), 128.34 (CH Ar), 122.70 (CH Ar), 114.17 (CH=*C*H_2), 110.09 (CH pyr), 109.75 (CH pyr), 37.79 (CO*C*H_2), 34.11 (C ^{t}Bu) 33.76 (CH_2=CH*C*H_2), 31.17 (CH_3), 29.30 (CH_2), 29.19 (CH_2), 29.06 (CH_2), 28.88 (CH_2), 25.33 (CH_2). Mass Spectrum (ES^+): calcd for $C_{44}H_{60}N_6O_4Na$ $[M+Na]^+$ m/z = 759.457, found m/z = 759.457. Analysis is in agreement with literature data [3]

(Z)-4^5-(tert-butyl)-2,6,8,29-tetraaza-1,7(2,6)-dipyridina-4(1,3)-benzenacyclononacosaphan-18-ene-3,5,9,28-tetraone, 42

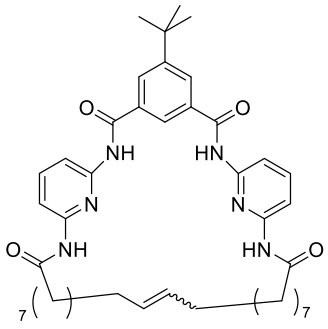

A solution of Grubbs 1st Generation catalyst (27 mg, 0.034 mmol) in DCM (17 mL) was added dropwise to a solution of **41** (0.22 g, 0.28 mmol) in DCM (53 mL). The reaction mixture was heated to reflux and stirred for 2 h. The mixture was cooled and any volatiles removed under vacuum to afford an oily brown solid which was purified using flash column chromatography (eluent: DCM/EtOAc - 0-10%) to afford 150 mg of solid (0.21 mmol, 68% yield). ^{1}H NMR (300 MHz, $CDCl_3$) δ = 8.39 (s, 2H, NH), 8.32 (s, 1H, ArH), 8.29 (s, 2H, ArH), 8.09 (d, J = 7.9 Hz, 2H, pyr), 7.99 – 7.93 (m, 2H, pyr), 7.82 (t, J = 8.1 Hz, 2H, pyr), 7.65 (s, 2H, NH), 5.41 – 5.33 (m, 2H C*H*=C*H*), 2.41 (t, J = 7.5 Hz, 4H, COC*H*$_2$), 2.05 – 1.94 (m, 4H, CH=CHC*H*$_2$), 1.82 – 1.70 (m, 4H, $COCH_2$C*H*$_2$), 1.43 (s, 9H, ^{t}Bu),

1.39 – 1.27 (m, 20H, Alk). ^{13}C NMR (101 MHz, $CDCl_3$) δ = 171.87 (CO), 165.44 (CO), 153.87 (C pyr), 149.77 (C pyr), 149.57 (C Ar), 140.93 (CH pyr), 134.14 (C Ar), 130.46 (*C*H=*C*H trans), 129.94 (*C*H=*C*H cis), 129.72 (CH Ar), 120.67 (CH Ar), 110.03 (CH pyr), 109.79 (CH pyr), 37.83 (CO*C*H_2), 35.21 (C ^{t}Bu), 32.14 (CH_2=CH*C*H_2), 31.02 (CH_3), 29.45 (CH_2), 29.29 (CH_2), 29.14, 29.05 (CH_2), 26.91 (CH_2), 25.50 (CH_2), 25.34 (CH_2). MS (ES^+): calcd for $C_{42}H_{56}N_6O_4Na$ $[M+Na]^+$ *m/z* = 731.9, found m/z = 731.5. Analysis is in agreement with literature data [3]

4^5-(tert-butyl)-2,6,8,29-tetraaza-1,7(2,6)-dipyridina-4(1,3)-benzenacyclononacosaphane-3,5,9,28-tetraone, 43

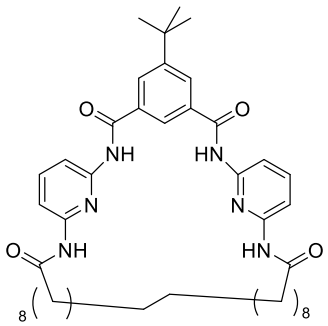

42 (50 mg, 0.07 mmol) was dissolved in EtOAc (3 mL). Pearlman's catalyst (20 mg) was then added followed by NEt_3 (6 drops). An H_2 balloon was then added and the vessel sealed. The mixture was heated to 35^o C and stirred for 16 h. The suspension was filtered through a plug of silica and washed with EtOAc. The filtrate was concentrated under reduced pressure to give 47 mg of pure **43** (0.06 mmol, 86% yield). ^{1}H NMR (300 MHz, $CDCl_3$) δ = 8.30 – 8.18 (m, 3H, NH and ArH), 8.08 (d, J = 8.1 Hz, 2H, pyr), 8.02 (d, J = 7.8 Hz, 2H, pyr), 7.91 (s, 1H, ArH), 7.83 (t, J = 8.1 Hz, 2H, pyr), 7.61 (s, 2H, NH), 2.42 (t, J = 7.4 Hz, 4H, COC*H*$_2$), 1.76 (quint. J = 7.6 Hz, 4H, $COCH_2$C*H*$_2$), 1.44 (s, 9H, CH_3), 1.25-1.33 (m, 28H, Alk). ^{13}C NMR (101 MHz, $CDCl_3$) δ = 171.69 (CO), 165.19 (CO), 153.94 (C pyr), 149.70 (C pyr), 149.41 (C Ar), 141.03 (CH pyr), 134.57 (C Ar), 129.50 (CH Ar), 120.32 (CH Ar), 109.99 (CH pyr), 109.77 (CH pyr), 37.87 (CO*C*H_2), 35.28 (C ^{t}Bu), 31.10 (CH_3), 29.70 (CH_2), 29.08 (2 x CH_2), 29.01 (CH_2), 28.96 (2 x CH_2), 28.82 (CH_2), 25.37 (CH_2). Mass Spectrum (ES^+): cald for $C_{42}H_{58}N_6O_4$ $[M+Na]^+$ *m/z* = 733.4417, found m/z = 733.4446. Elemental Analysis:

found: H, 8.43; C, 71.09; N, 11.91; calculated: H, 8.22; C, 70.95; N, 11.82. mp: decomposition at 250^{o} C. IR (neat, cm^{-1}): 3422, 3314 (NH), 2992, 2851 (CH), 1677, 1585 (CO).

(hexadecane-dioyl chloride), 44

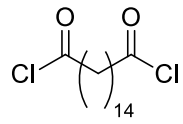

Hexadecane-dioic acid (0.33 g, 1.1 mmol) was dissolved in DCM (60 mL) and 1-2 drops of DMF were added. The solution was cooled to 0^{o} C and oxaloyl chloride (0.47 mL, 5.5 mmol) was added dropwise. The solution was heated to reflux and maintained for 2 h. The volatiles were then removed to afford a yellow oily solid, **44**, in quantitative yield which was used in the next step without further purification.

4^{5}-(tert-butyl)-2,6,8,25-tetraaza-1,7(2,6)-dipyridina-4(1,3)-benzenacyclopentacosaphane-3,5,9,24-tetraone, **45**

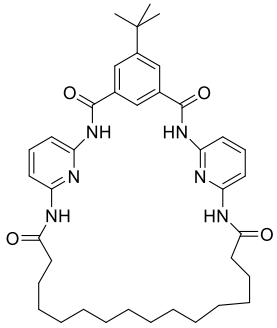

Two solutions of hexadecane-dioyl chloride (0.74 mmol as obtained), in THF (20 mL) and NEt_3 (0.53 mL, 3.8 mmol) and **40** (0.30 g, 0.74 mmol) in THF (20 mL) were added simultaneously, over 2 h, to a round bottom flask containing THF (80 mL) and once the addition was complete the mixture was stirred for a further 16 h. The volatiles were then removed under reduced pressure to produce an oily solid. This was dissolved in DCM (100 mL) and washed with 1 M NaOH (50 mL). The separated organic phase was then washed with 5% $NaHCO_3$ (3 x 50 mL), dried using $MgSO_4$ and filtered. Concentration under vacuum afforded a cream/yellow solid which was purified *via* flash column chromatography (eluent: DCM/EtOAc - 0-10%) to afford 140 mg of solid (0.22 mmol, 30% yield). ^{1}H NMR (300 MHz, $CDCl_3$) δ = 8.33 (s, 1H, ArH), 8.25 (s, 2H, NH), 8.12 (d, J = 7.5 Hz, 2H, CH pyr), 8.04 (d, J =

7.6 Hz, 2H, CH pyr), 7.88 – 7.80 (m, 3H, ArH and CH pyr), 7.63 (s, 2H, NH), 2.42 (t, J = 7.4 Hz, 4H, COC*H*$_2$), 1.83 – 1.73 (m, 4H, COCH$_2$C*H*$_2$), 1.44 (s, 9H, CH$_3$), 1.40 – 1.24 (m, 20H, Alk). ^{13}C NMR (101 MHz, $CDCl_3$) δ = 171.80 (CO), 165.38 (CO), 153.60 (C pyr), 149.76 (C pyr), 149.52 (C Ar), 141.70 (CH pyr), 133.70 (C Ar), 130.27 (CH Ar), 120.82 (CH Ar), 110.53 (CH pyr), 110.16 (CH pyr), 37.74 (CO*C*H$_2$), 35.27 (C ^{t}Bu), 31.12 (CH$_3$), 29.34 (CH$_2$), 29.10 (CH$_2$), 28.67 (CH$_2$), 28.36 (CH$_2$), 25.19 (CH$_2$), 24.81 (CH$_2$). MS (ES$^+$): calcd for $C_{38}H_{50}N_6O_4Na$ $[M+Na]^+$ m/z = 677.3791, found m/z = 677.3784. Analysis is in agreement with literature data [3]

(4-bromo-*tert*-butyl benzene), 46

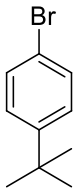

tert-butyl benzene (0.77 ml, 5.0 mmol) was cooled to 0^{o} C. I_2 (0.065 g, 5 mol%) was added and once dissolved, bromine (0.27 mL, 5.0 mmol) was added and stirred for 16 h. The reaction was then washed with sat. $Na_2S_2O_3$ (40 mL), extracted with DCM (60 mL), dried using $MgSO_4$, filtered and concentrated under vacuum to afford a clear oil (quantitative yield) which required no further purification. ^{1}H NMR (300 MHz, $CDCl_3$) δ = 7.46 – 7.41 (m, 2H, ArH), 7.31 – 7.26 (m, 2H, ArH), 1.33 (s, 4H, CH$_3$).

tris(4-(tert-butyl)phenyl)methanol, 47

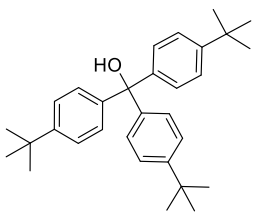

In a 2-neck round bottom flask, Mg turnings (3.00 g, 83.0 mmol) were heated under vacuum with a heat gun and then allowed to cool under argon. The process was repeated two more times to ensure the removal of any moisture. To the flask, a spatula tip of iodine was added followed by dry THF (3 mL). A solution of **46** (8.48 g, 40.0 mmol) in THF (18 mL) was made up and 3 mL was added to the reaction flask. When the reaction was observed to initiate, the remaining

solution was added dropwise over 20 minutes to maintain auto-reflux. Upon full addition the solution was stirred for 2 h. Diethyl carbonate (1.56 mL, 13.4 mmol) in THF (2 mL) was added slowly over 20 minutes and the solution was left to stir for 16 h. The reaction mixture was then acidified to pH 7 with 1 M HCl and water (50 mL) was added. The organic layer was removed and the aqueous layer was washed with DCM (60 mL). The organic phases were combined, dried with $MgSO_4$, filtered and evaporated to give a blue/white crude solid which was purified via crystallisation in hot hexane to give 3.51 g of **47**, as a white solid (8.28 mmol, 62% yield). ^{1}H NMR (300 MHz, $CDCl_3$) δ = 7.37 – 7.30 (m, 6H, ArH), 7.24 – 7.17 (m, 6H, ArH), 1.33 (s, 27H, CH_3). ^{13}C NMR (101 MHz, $CDCl_3$) δ = 149.81 (C Ar), 144.17 (C Ar), 127.54 (CH Ar), 124.70 (CH Ar), 34.45 (C ^{t}Bu), 31.37 (CH_3). HRMS (ES^+). calcd for $C_{31}H_{40}O$ $[M]^+$ m/z = 428.3, found m/z = 428.4. Analysis is in agreement with literature data.[4]

4-(tris(4-(tert-butyl)phenyl)methyl)phenol, **48**

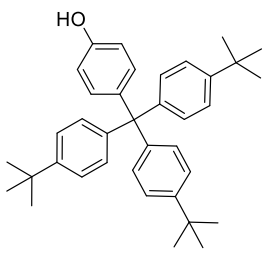

47, (1.64 g, 3.84 mmol) was added to a round bottom flask followed by phenol (6.20 g, 66.0 mmol). The flask was heated to 80^o C and once a solution has formed, HCl (1.15 mL, 1.25 M in MeOH) was added and the reaction stirred vigorously for 2 h. The reaction mixture was partitioned between toluene (50 mL) and 0.5 M NaOH (30 mL). The aqueous phase was extracted with Toluene (3 x 50 mL) and the combined organics were dried using $MgSO_4$, filtered and concentrated to afford a crude solid which was purified *via* flash column chromatography, (eluent DCM/Hexane 1:1) to give 1.03 g of **48** as a white solid (2.04 mmol, 53% yield). ^{1}H NMR (300 MHz, $CDCl_3$) δ = 7.27 – 7.19 (m, 6H, ArH), 7.14 – 6.98 (m, 8H, 2 x ArH), 6.76 – 6.68 (m, 2H, ArH), 4.61 (s, 1H, OH), 1.32 (s, 27H, CH_3). ^{13}C NMR (101 MHz,

$CDCl_3$) δ = 153.24 (C Ar), 148.32 (C Ar), 144.10 (C Ar), 139.80 (C Ar), 132.47 (CH Ar), 130.71 (CH Ar), 124.05 (CH Ar), 113.92 (CH Ar), 34.30 (C ^{t}Bu), 31.39 (CH_3). HRMS (ES^+): calcd for $C_{37}H_{44}O$ $[M]^+$ m/z = 504.3, found m/z = 504.5. Analysis is in agreement with literature data. [4]

4,4',4''-((4-(2-(2-(2-iodoethoxy)ethoxy)ethoxy)phenyl)methanetriyl)tris(tert-butylbenzene), 49

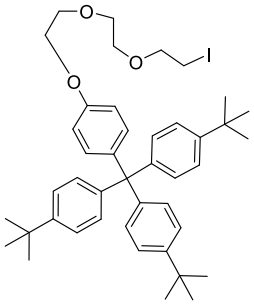

48 (0.20 mg, 0.41 mmol) was dissolved in acetonitrile (30 mL). 1,2-bis(2-iodoethoxy)ethane (1.54 g, 4.10 mmol) was added, followed by K_2CO_3 (0.25 g, 1.8 mmol) and the suspension was refluxed for 16 h. The solvents were removed and the crude mixture was purified *via* flash column chromatography, (eluent: Hexane/EtOAc - 5-10%) to give 0.14 g of **49** as a white solid (0.19 mmol, 46% yield). ^{1}H NMR (300 MHz, $CDCl_3$) δ = 7.26 (d, J = 8.6 Hz, 6H, ArH), 7.11 (d, J = 8.4 Hz, 8H, ArH), 6.81 (d, J = 8.9 Hz, 2H, ArH), 4.18 – 4.11 (m, 2H, AR-OCH_2), 3.91 – 3.87 (m, 2H, Ar-$OCH_2C\mathit{H}_2$), 3.82 – 3.71 (m, 6H, $OC\mathit{H}_2C\mathit{H}_2OC\mathit{H}_2$), 3.28 (t, J = 6.9 Hz, 2H, ICH_2), 1.33 (s, 27H). ^{13}C NMR (101 MHz, $CDCl_3$) δ = 156.55 (C Ar), 148.31 (C Ar), 144.15 (C Ar), 139.80 (C Ar), 132.25 (CH Ar), 130.74 (CH Ar), 124.07 (CH Ar), 113.08 (CH Ar), 70.83 (CH_2 gly), 70.30 (CH_2 gly), 69.90 (CH_2 gly), 67.23 (CH_2 gly), 61.81 (CH_2 gly), 34.31 (C ^{t}Bu), 31.42 (CH_3), 2.97 (ICH_2). HRMS (ES^+): calcd for $C_{43}H_{55}IO_3$ $[M]^+$ m/z = 746.3196, found m/z = 746.3200. Analysis is in agreement with literature data. [5]

(2,2-Bis-dec-9-enyl-malonic acid diethyl ester), 50

Diethyl malonate (0.24 mL, 1.6 mmol) and 10-bromo-1-decene (0.80 mL, 4.0 mmol) were added to a suspension of NaH (160 mg – 60% w/w dispersion in mineral oil, 4.0 mmol) in THF (60 mL). The reaction mixture was stirred under reflux for 2 days and then the volatiles

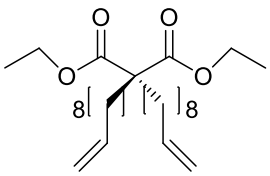

were removed. The residue was dissolved in EtOAc (40 mL) and washed with brine (50 mL) and water (50 mL). The aqueous phase was then extracted with EtOAc (3 x 20mL). The organics were combined and dried using $MgSO_4$. The solution was filtered and concentrated under reduced pressure to afford a crude yellow oil which was purified *via* flash column chromatography (eluent: Hexane/DCM - 0-10%) to give 0.22 g of **50** as a clear oil (0.50 mmol, 31% yield). ^{1}H NMR (300 MHz, $CDCl_3$) δ = 5.82 (ddt, J = 16.9, 10.1, 6.7 Hz, 2H, C*H*=CH_2), 5.08 – 4.88 (m, 4H, CH=C*H*$_2$), 4.19 (q, J = 7.1 Hz, 4H, OCH_2), 2.05 (dd, J = 14.2, 6.8 Hz, 4H, CCH_2), 1.97 – 1.78 (m, 4H, CH=CH_2C*H*$_2$), 1.45 – 1.11 (m, 30H, OCH_2CH_3, 12 x CH_2). ^{13}C NMR (101 MHz, $CDCl_3$) δ = 172.0 (CO), 139.2 (*C*H=CH_2), 114.1 (CH=*C*H_2), 60.9 (OCH_2), 52.4 (C), 38.7 (*C*H_2CH=CH_2), 33.8 (CH_2), 32.1 (CH_2), 29.8 (CH_2), 29.3 (CH_2), 29.1 (CH_2), 28.9 (CH_2), 23.9 (CH_2), 14.1 (OCH_2*C*H_3). Analysis is in agreement with literature data. [3]

(2,2-Bis-undec-10-enyl-malonic acid diethyl ester), 51

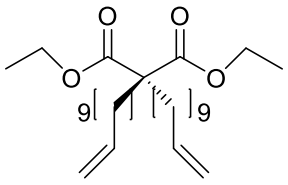

Diethyl malonate (0.30 mL, 2.0 mmol) and 1-bromo decene (1.2 mL, 5.5 mmol) were added to a suspension of NaH (0.22 g – 60% w/w dispersion in mineral oil, 5.5 mmol) in THF (80 mL). The reaction mixture was stirred under reflux for 2 days and then the volatiles were removed. The residue was dissolved in EtOAc (50 mL) and washed with brine (50 mL) and water (50 mL). The aqueous phase was then extracted with EtOAc (3 x 20 mL). The organics were combined and dried using $MgSO_4$. The solution was filtered and concentrated under reduced pressure to afford a crude yellow oil which was purified *via* flash column chromatography (eluent: Hexane/DCM - 0-10%) to give 0.57 g of **51** as a clear oil (1.2 mmol, 62% yield). ^{1}H NMR (300

MHz, $CDCl_3$) δ = 5.83 (ddt, J = 16.9, 10.1, 6.7 Hz, 2H, C*H*=CH_2), 5.07 – 4.87 (m, 4H, CH=C*H*$_2$), 4.19 (q, J = 7.1 Hz, 4H, OCH_2), 2.05 (q, J = 7.0 Hz, 4H, CCH_2), 1.95 – 1.76 (m, 4H), 1.45 – 1.09 (m, 34H, OCH_2CH_3, 14 x CH_2). ^{13}C NMR (101 MHz, $CDCl_3$) δ = 172.03 (CO), 139.21 (*C*H=CH_2), 114.09 (CH=*C*H_2), 60.89 (OCH_2), 57.54 (C), 33.80 (CH_2), 32.09 (CH_2), 29.83 (CH_2), 29.45 (CH_2), 29.32 (CH_2), 29.12 (CH_2), 28.93 (CH_2), 23.89 (CH_2), 14.12 (OCH_2*C*H_3). HRMS (ES^+): calcd for $C_{29}H_{52}O_4Na$ $[M+Na]^+$ m/z = 487.3763, found m/z = 487.3778. IR (neat, cm^{-1}): 2924, 2853 (CH), 1730 (CO), 1068 (COOC).

(5,5-Bis-dec-9-enyl-pyrimidine-2,4,6-trione), 52

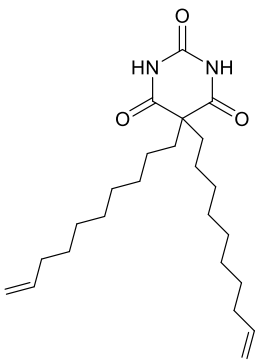

50 (0.25 g, 0.60 mmol) was dissolved in dry DMSO (3 mL). NaH (60 mg – 60% dispersion, 1.5 mmol) was added to the solution followed by urea (76 mg, 1.3 mmol). The mixture was then stirred for 16 h. The mixture was then poured into sat. $NaHCO_3$ solution (60 ml) and the aqueous phase extracted with EtOAc (2 x 50 mL). The solution was dried using $MgSO_4$, concentrated under reduced pressure to afford a yellow oil which partially crystallised. The oil was recrystallised from hexane to afford 32 mg of white crystals of **52** (0.08 mmol, 13% yield). ^{1}H NMR (300 MHz, $CDCl_3$) δ = 7.91 (s, 2H, NH), 5.82 (ddt, J = 16.9, 10.1, 6.7 Hz, 2H, C*H*=CH_2), 5.09 – 4.89 (m, 4H, CH=C*H*$_2$), 2.13 – 1.90 (m, J = 15.5, 6.9 Hz, 8H, $CH=CH_2CH_2$ and CCH_2), 1.41 – 1.13 (m, 24H, 12 x CH_2). ^{13}C NMR (101 MHz, $CDCl_3$) δ = 172.32 (CO), 148.17 (CO), 139.12 (*C*H=CH_2), 114.17 (CH=*C*H_2), 56.73 (C), 39.22 (*C*H_2CH=CH_2), 33.75 (CH_2), 29.38 (CH_2), 29.24 (CH_2), 29.08 (CH_2), 28.97 (CH_2), 28.83 (CH_2), 25.06 (CH_2). HRMS (ES^-): *m/z* = calcd for $C_{24}H_{40}N_2O_3$ $[M]^-$ m/z = 403.2961, found m/z = 403.2946. Analysis is in agreement with literature data. [5]

(5,5-Bis-undec-10-enyl-pyrimidine-2,4,6-trione), 53

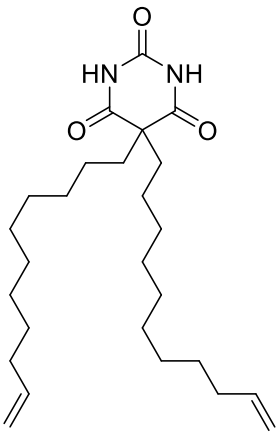

51 (0.50 g, 1.1 mmol) was dissolved in dry DMSO (5 mL). NaH (0.12 g – 60% dispersion, 3.0 mmol) was added to the solution followed by urea (0.13 g, 2.2 mmol). The mixture was then stirred for 16 h. The mixture was then poured onto sat. $NaHCO_3$ solution (130 ml) and the aqueous phase extracted with EtOAc (2 x 100 mL). The solution was dried using $MgSO_4$, concentrated under reduced pressure to afford a yellow oil which partially crystallised. The oil was recrystallised from hexane to afford 92 mg of **53** as white crystals (0.21 mmol, 20% yield). ^{1}H NMR (300 MHz, $CDCl_3$) δ = 7.81 (s, 2H, NH), 6.00 – 5.68 (m, 2H, C*H*=CH_2), 5.10 – 4.82 (m, 4H, CH=C*H*$_2$), 2.14 – 1.87 (m, 8H, CH=CH_2C*H*$_2$ and CCH_2), 1.45 – 1.11 (m, 28H, 7 x CH_2). ^{13}C NMR (101 MHz, $CDCl_3$) δ = 172.40 (CO), 148.31 (CO), 139.18 (*C*H=CH_2), 114.13 (CH=*C*H_2), 56.74 (C), 39.23 (*C*H_2CH=CH_2), 33.78 (CH_2), 29.41 (CH_2), 29.35 (CH_2), 29.13 (CH_2), 29.05 (CH_2), 28.89 (CH_2), 25.08 (CH_2). MS (ES^+): calcd for $C_{26}H_{43}N_2O_3$2Na [M-2H$^+$+2Na] m/z = 477.6, found m/z = 477.4 mp = 82-85^o C. Elemental Analysis: found: H, 10.33; C, 72.17; N, 6.52; calculated: H, 10.25; C, 72.18; N, 6.48. . IR (neat, cm^{-1}): 3203, 3085 (NH), 2912, 2850 (CH), 1691 (CO).

1-(allyloxy)-4-bromobenzene, 57

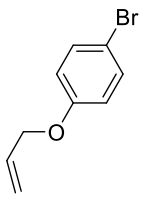

4-Bromophenol (1.73 g, 10.0 mmol) and K_2CO_3 (1.80 g, 13.0 mmol) were dissolved in DMF (3 mL). Allyl bromide (1.04 mL, 12.0 mmol) was added, and the reaction was heated to 60^o C for 50 minutes. Once cooled to room temperature, water (40 mL) was added and the reaction mixture was extracted with diethyl ether (2 x 60 mL). The organic extracts were then combined and washed with brine (60 mL)

and dried using $MgSO_4$, filtered and concentrated to afford a crude yellow oil, which was purified *via* flash column chromatography (eluent: Hexane/EtOAc-10%) to afford 2.01 g of **57** as a clear oil (9.41 mmol, 94% yield). ^{1}H NMR (300 MHz, $CDCl_3$) δ = 7.48 – 7.32 (m, 2H, ArH), 6.89 – 6.74 (m, 2H, ArH), 6.05 (ddt, *J* = 17.2, 10.5, 5.3 Hz, 1H, C*H*=CH_2), 5.48 – 5.24 (m, 2H, CH=C*H*$_2$), 4.53 (dt, *J* = 5.3, 1.5 Hz, 2H, C*H*$_2$CH=CH_2). ^{13}C NMR (101 MHz, $CDCl_3$) δ = 157.68 (C Ar), 132.86 (*C*H=CH_2), 132.23 (CH Ar), 117.90 (CH=*C*H$_2$), 116.56 (CH Ar), 112.99 (C Ar), 69.00 (*C*H$_2$CH=CH_2). HRMS (ES^+): calcd for C_9H_9BrO $[M]^+$ m/z = 211.984, found m/z = 211.983. Analysis is in agreement with literature data. [6]

1-bromo-4-(undec-10-en-1-yloxy)benzene, 58

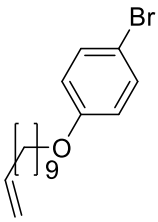

4-Bromophenol (1.11 g, 6.40 mmol) and K_2CO_3 (1.15 g, 8.30 mmol) were dissolved in DMF (3 mL). 10-bromo-undecene (1.50 g, 6.40 mmol) was added, and the reaction was heated to 60^o C for 16 h. Once cooled to room temperature, water (40 mL) was added and the reaction mixture was extracted with diethyl ether (2 x 60 mL). The organic extracts were then combined and washed with brine (60 mL) and dried ($MgSO_4$), filtered and concentrated to afford a crude yellow oil, which was purified *via* flash column chromatography (eluent: Hexane) to afford 1.88 g of **58** as a clear oil (5.80 mmol, 91% yield). ^{1}H NMR (300 MHz, $CDCl_3$) δ = 7.46 – 7.32 (m, 2H, ArH), 6.88 – 6.72 (m, 2H, ArH), 5.84 (ddt, *J* = 16.9, 10.1, 6.7 Hz, 1H, C*H*=CH_2), 5.12 – 4.87 (m, 2H, CH=C*H*$_2$), 3.93 (t, *J* = 6.6 Hz, 2H, OCH_2), 2.07 (dd, *J* = 14.1, 6.8 Hz, 2H, C*H*$_2$CH=CH_2), 1.88 – 1.67 (m, 2H, OCH_2C*H*$_2$), 1.5 – 1.22 (m, 12H, 6 x CH_2). ^{13}C NMR (101 MHz, $CDCl_3$) δ = 158.25 (C Ar), 139.19 (*C*H=CH_2), 132.17 (CH Ar), 116.30 (CH Ar), 114.13 (CH=*C*H$_2$), 112.55 (C Ar), 68.26 (OCH_2), 33.80 (*C*H$_2$CH=CH_2), 29.49 (CH_2), 29.41 (CH_2), 29.35 (CH_2), 29.17

(CH_2), 29.11 (CH_2), 28.93 (CH_2), 25.99 (CH_2). HRMS (ES^+): calcd for $C_{17}H_{25}BrO$ $[M]^+$ m/z = 324.1089, found m/z = 324.1086. Analysis is in agreement with literature data. [7]

(4-(allyloxy)phenyl)boronic acid, 59

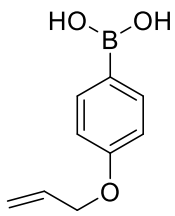

57 (0.57 g, 2.7 mmol) was dissolved in THF (5 mL) and cooled to -78° C. ^{n}BuLi (1.20 mL – 2.5 M in hexane, 2.99 mmol) was then added dropwise over 5 minutes and stirring was then continued for 1 h. $B(OEt)_3$ (0.50 mL, 3.1 mmol) was then added dropwise over 5 minutes and stirring was continued for 90 minutes. The solution was warmed to room temperature and sat. NH_4Cl (2.5 mL) was added, followed by water (15 mL). Diethyl ether (30 mL) was added, the organic phase separated and washed with sat. $NaHCO_3$ (15 mL) and then brine (15 mL). The organic phase was then dried using Na_2SO_4, filtered and evaporated to afford a yellow oil. Recrystallisation from water afforded a white solid which was filtered to give 156 mg of **59** as a white solid (1.61 mmol, 59% yield). ^{1}H NMR (300 MHz, $CDCl_3$) δ = 8.25 – 7.60 (m, 2H, ArH), 7.13 – 6.87 (m, 2H, ArH), 6.10 (ddt, *J* = 16.4, 10.6, 5.3 Hz, 1H, C*H*=CH_2), 5.59 – 5.15 (m, 2H, CH=C*H*$_2$), 4.69 – 4.59 (m, 2H, OCH_2). ^{13}C NMR (101 MHz, $CDCl_3$) δ = 162.21 (C Ar), 137.48 (CH Ar), 135.25 (*C*H=CH_2), 117.93 (CH=*C*H_2), 114.24 (CH Ar), 68.63 (*C*H_2CH=CH_2). HRMS (ES^+): calcd for $C_9H_{11}BO_3$ $[M]^+$ m/z = 178.0801, found m/z = 178.0801.

(4-(undec-10-en-1-yloxy)phenyl)boronic acid, 60

58 (0.98 g, 3.0 mmol) was dissolved in THF (3 mL) and cooled to -78° C. ^{n}BuLi (1.32 mL - 2.5 M in hexane, 3.30 mmol) was then added dropwise over 5 minutes and stirring was then continued for 1 h. $B(OEt)_3$ (0.58 mL, 3.4 mmol) was added dropwise over 5 minutes and stirring was continued for 90 minutes. Repeated warming and cooling was required to

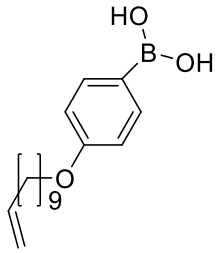

prevent gel formation. The solution was then warmed to room temperature and sat. NH_4Cl (2.5 mL) was added, followed by water (15 mL). Diethyl ether (30 mL) was added, the organic phase separated and washed with sat. $NaHCO_3$ (15 mL) and then brine (15 mL). The organic phase was then dried using Na_2SO_4, filtered and evaporated to afford a crude off-white solid. Purification *via* flash column chromatography (eluent: Hexane-Et_2O 1:1) afforded 58 mg of **60** as a white solid (0.20 mmol, 15% yield). ^{1}H NMR (300 MHz, $CDCl_3$) δ = 8.17 (d, *J* = 8.6 Hz, 2H, ArH), 7.02 (d, *J* = 8.7 Hz, 2H, ArH), 5.85 (ddt, *J* = 16.9, 10.2, 6.7 Hz, 1H¸ C*H*=CH_2), 5.14 – 4.87 (m, 2H¸ CH=C*H*$_2$), 4.06 (t, *J* = 6.5 Hz, 2H¸ OCH_2), 2.07 (dd, *J* = 14.1, 6.8 Hz, 2H¸ C*H*$_2$CH=CH_2), 1.95 – 1.73 (m, 2H¸ OCH_2C*H*$_2$), 1.60 – 1.21 (m, 12H, 6 x CH_2). ^{13}C NMR (101 MHz, $CDCl_3$) δ = 162.79 (C Ar), 139.22 (*C*H=CH_2), 137.46 (CH Ar), 122.01 (C Ar), 114.13 (CH Ar), 114.01 (CH=*C*H_2), 67.88 (OCH_2) , 33.81 (*C*H_2CH=CH_2), 29.52 (CH_2), 29.40 (CH_2), 29.24 (CH_2), 29.13 (CH_2), 28.94 (CH_2), 26.06 (CH_2). HRMS (ES^+): calcd for $C_{17}H_{25}O$ $[M-(BOH)_2]^+$ m/z = 245.3, found m/z = 246.0.

5,5-bis(4-(allyloxy)phenyl)pyrimidine-2,4,6(1H,3H,5H)-trione, 61

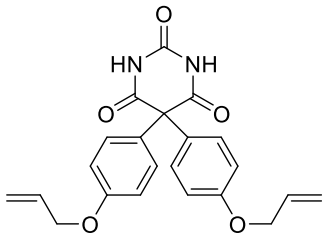

59 (0.14 g, 0.77 mmol) was added slowly over 15 minutes to a solution of $Pb(OAc)_4$ (0.37 g, 0.84 mmol) and $Hg(OAc)_2$ (19 mg, 0.084 mmol) in $CHCl_3$ (1.5 mL) at 40^o C. The mixture was stirred for 1 h. Barbituric acid (0.11 g, 0.85 mmol) and pyridine (0.19 mL, 2.3 mmol) were added and the mixture was stirred for 16 h at room temperature. The yellow suspension was then filtered through celite and washed with $CHCl_3$ (10 mL). The filtrate was then shaken with 3 M H_2SO_4 (8 mL) and the aqueous phase extracted with $CHCl_3$

(2 x 5 mL). The organics were then combined, dried using Na_2SO_4, filtered and concentrated to afford a crude yellow oil which was purified *via* flash column chromatography (eluent: DCM/EtOAc gradient 10-50%) to afford 73 mg of **61** as an off white solid (0.19 mmol, 24 % yield). ^{1}H NMR (300 MHz, $CDCl_3$) δ = 8.84 (s, 2H, NH), 7.19 – 7.05 (m, 4H, ArH), 6.99 – 6.82 (m, 4H, ArH), 6.05 (ddt, *J* = 17.2, 10.5, 5.3 Hz, 2H, C*H*=CH_2), 5.53 – 5.21 (m, 4H, CH=C*H*$_2$), 4.54 (dt, *J* = 5.3, 1.3 Hz, 4H¸ C*H*$_2$CH=CH_2). ^{13}C NMR (101 MHz, $CDCl_3$) δ = 170.40 (CO), 158.78 (C Ar), 148.52 (CO), 132.89 (*C*H=CH_2), 130.17 (CH Ar), 128.81 (C Ar), 117.95 (CH=*C*H_2), 114.90 (CH Ar), 68.87 (*C*H_2CH=CH_2). HRMS (ES^-): calcd for $C_{22}H_{19}N_2O_5$ $[M-H]^-$ m/z = 391.4, found m/z = 391.1. mp: 95-98^o C. IR (neat, cm^{-1}): 3464, 3230 (NH), 2924, 2855 (CH), 1683 (CO), 1607 (C=C).

5,5-bis(4-(undec-10-en-1-yloxy)phenyl)pyrimidine-2,4,6(1H,3H,5H)-trione, 62

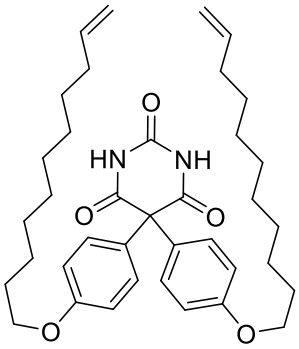

60 (0.68 g, 2.3 mmol) was added slowly over 15 minutes to a solution of $Pb(OAc)_4$ (1.12 g, 2.54 mmol) and $Hg(OAc)_2$ (56 mg, 0.25 mmol) in $CHCl_3$ (4.0 mL) at 40^o C. The mixture was stirred for 1 h. Barbituric acid (0.33 g, 2.6 mmol) and pyridine (0.58 mL, 7.0 mmol) were added and the mixture was stirred for 16 h at room temperature. The yellow suspension was then filtered through celite and washed with $CHCl_3$ (30 mL). The filtrate was then shaken with 3 M H_2SO_4 (25 mL) and the aqueous phase extracted with $CHCl_3$ (2 x 15 mL). The organics were then combined, dried using Na_2SO_4, filtered and concentrated to afford a crude yellow oil which was purified *via* flash column chromatography (eluent: DCM/EtOAc - 10%) to afford 0.28 g of **62** as a white solid (0.47 mmol, 20 % yield). ^{1}H NMR (300 MHz, $CDCl_3$) δ = 8.38 (s, 2H, NH), 7.19 – 7.08 (m, 4H, ArH),

6.97 – 6.81 (m, 4H, ArH), 5.83 (ddt, *J* = 16.9, 10.2, 6.7 Hz, 2H, C*H*=CH_2), 5.14 – 4.83 (m, 4H, CH=C*H*$_2$), 3.96 (t, *J* = 6.5 Hz, 4H, OCH_2), 2.06 (q, *J* = 7.2 Hz, 4H, C*H*$_2$CH=CH_2), 1.86 – 1.71 (m, 4H, OCH_2CH_2), 1.53 – 1.24 (m, 24H). ^{13}C NMR (101 MHz, $CDCl_3$) δ = 170.19 (CO), 159.36 (C Ar), 147.89 (CO), 139.21 (*C*H=CH_2), 130.08 (CH Ar), 128.33 (C Ar), 114.65 (CH Ar), 114.12 (CH=*C*H_2), 68.07 (OCH_2), 33.80 (*C*H_2CH=CH_2), 29.50 (CH_2), 29.41 (CH_2), 29.34 (CH_2), 29.18 (CH_2), 29.11 (CH_2), 28.92 (CH_2), 26.02 (CH_2). HRMS (ES^+): calcd for $C_{38}H_{52}N_2O_5Na$ $[M+Na]^+$ m/z = 639.3774, found m/z = 639.3769. IR (neat, cm^{-1}): 3221, 3079 (NH), 2924, 2853 (CH), 1703 (CO), 1609 (C=C).

4,4',4''-((4-(2-(2-(2-(4-bromophenoxy)ethoxy)ethoxy)ethoxy)phenyl)methanetriyl)tris(tert-butylbenzene), 63

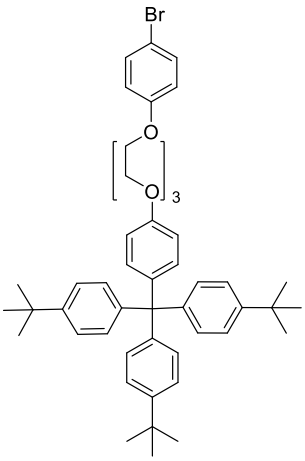

49 (0.43 g, 0.58 mmol), bromophenol (0.12 g, 0.59 mmol) and K_2CO_3 (0.11 g, 0.77 mmol) were dissolved in DMF (4 mL) and heated to 80^o C. The reaction was then stirred for 16 h and cooled to room temperature. Water (10 mL) was added followed by toluene (30 mL) and the organic phase was separated. The aqueous phase was extracted with toluene (20 mL) and the organics were combined, dried using $MgSO_4$, filtered and concentrated to afford a white solid in quantitative yields which was carried through with no further purification. ^{1}H NMR (400 MHz, $CDCl_3$) δ = 7.33 – 7.24 (m, 2H, ArH), 7.22 – 7.10 (m, 6H, ArH)), 7.06 – 6.94 (m, 8H, ArH), 6.78 – 6.65 (m, 4H, ArH), 4.08 (dd, J = 9.4, 3.9 Hz, 4H, CH2-gly), 3.90 – 3.83 (m, 4H, CH2-gly), 3.76 (s, 4H, CH2-gly), 1.23 (s, 27H, CH_3). ^{13}C NMR (101 MHz, $CDCl_3$) δ = 156.49 (C Ar), 148.32 (C Ar), 144.12 (C Ar), 139.87 (C Ar), 132.25 (CH Ar), 130.72 (CH Ar), 124.05 (CH

Ar), 116.48 (CH Ar), 113.08 (CH Ar),), 70.83 (CH_2-gly), 69.84 (CH_2-gly), 69.66 (CH_2-gly), 67.74 (CH_2-gly), 67.44 (CH_2-gly), 67.20 (CH_2-gly), 34.30 (C ^tBu), 31.39 (CH_3). HRMS (ES^+): calcd for $C_{47}H_{55}BrO_3Na$ $[M+Na]^+$ m/z = 769.3, found m/z = 769.3. mp: 138-140^o C. IR (neat, cm^{-1}): 2958, 2932, 2865 (CH), 1244 (COC).

2-(2-(2-(4-bromophenoxy)ethoxy)ethoxy)ethan-1-ol, 64

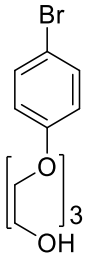

Bromophenol (1.02 g, 5.90 mmol), and K_2CO_3 (1.22 g, 8.85 mmol) were suspended in DMF (2 mL). 2-(2-(2-iodoethoxy)ethoxy)ethan-1-ol (1.50 g, 5.90 mmol) was added to the suspension which was then heated at 60^o C for 16 h. Once cooled to room temperature, water (50 mL) was added and the organics were extracted with diethyl ether (2 x 40 mL). The organics were then combined, dried using $MgSO_4$, filtered and concentrated to give a crude, light-brown oil which was purified *via* flash column chromatography (eluent: Hexane/Acetone 4:1) to afford 1.49 g of **64** as a clear oil (4.88 mmol, 83 % yield). ^1H NMR (300 MHz, $CDCl_3$) δ = 7.49 – 7.33 (m, 2H, ArH), 6.93 – 6.73 (m, 2H, ArH), 4.12 (dd, *J* = 5.5, 4.0 Hz, 2H, CH_2-gly), 3.87 (dd, *J* = 5.4, 4.0 Hz, 2H, CH_2-gly), 3.80 – 3.68 (m, 6H, 3 x CH_2-gly), 3.68 – 3.59 (m, 2H, CH_2-gly). ^{13}C NMR (101 MHz, $CDCl_3$) δ = 157.84 (C Ar), 132.24 (CH Ar), 116.44 (CH Ar), 113.12 (C Ar), 72.45 (CH_2-gly), 70.85 (CH_2-gly), 70.38 (CH_2-gly), 69.64 (CH_2-gly), 67.62 (CH_2-gly), 61.78 (CH_2-gly). HRMS (ES^+): calcd for $C_{12}H_{17}O_4BrNa$ $[M+Na]^+$ m/z = 327.0208, found m/z = 327.0206. Analysis is in agreement with literature data.[8]

12-(4-bromophenoxy)-2,2-dimethyl-3,3-diphenyl-4,7,10-trioxa-3-siladodecane, 65

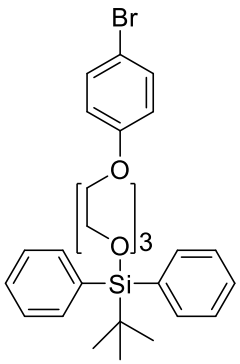

64 (0.53 g, 1.8 mmol) was dissolved in DCM (13 mL). The flask was cooled to 0° C and NEt_3 (0.75 mL, 5.4 mmol) was added followed by *tert*-butyldiphenylsillyl chloride (1.18 mL, 4.52 mmol) and a spatula tip of DMAP. The reaction was left to warm to room temperature and stirred for 16 h. Water (20 mL) was added and the phases were separated. The aqueous layer was extracted with DCM (2 x 30 mL) and the organics were combined, dried using $MgSO_4$ and concentrated to afford a crude, clear oil which was purified *via* flash column chromatography (eluent: Hexane/EtOAc - 5-30%) to afford 0.62 g of **65** as a clear oil (1.1 mmol, 62 % yield). ^{1}H NMR (300 MHz, $CDCl_3$) δ = 7.77 – 7.64 (m, 4H, ArH), 7.48 – 7.31 (m, 8H, ArH), 6.86 – 6.75 (m, 2H, ArH), 4.15 – 4.03 (m, 2H, CH_2-gly), 3.91 – 3.78 (m, 4H, 2 x CH_2-gly), 3.75 – 3.67 (m, 4H, 2 x CH_2-gly), 3.63 (t, *J* = 5.3 Hz, 2H, CH_2-gly), 1.08 (s, 9H, CH_3). ^{13}C NMR (101 MHz, $CDCl_3$) δ = 157.93 (C Ar), 135.63 (CH Ar), 133.69 (C Ar), 132.21 (CH Ar), 129.64 (CH Ar), 127.65 (CH Ar), 116.45 (CH Ar), 113.00 (C Ar), 72.51 (CH_2-gly), 70.95 (CH_2-gly), 70.84 (CH_2-gly), 69.68 (CH_2-gly), 67.69 (CH_2-gly), 63.46 (CH_2-gly), 26.83 (CH_3), 19.22 (C ^{t}Bu). HRMS (ES^+): calcd for $C_{28}H_{36}O_4SiNa$ $[M\text{-}Br+Na]^+$ m/z = 487.2, found m/z = 487.3. IR (neat, cm^{-1}): 3070, 2929, 2857 (CH), 1246, 1111 (COC).

(4-((2,2-dimethyl-3,3-diphenyl-4,7,10-trioxa-3-siladodecan-12-yl)oxy)phenyl)boronic acid, 66

65 (0.61 g, 1.1 mmol) was dissolved in THF (1 mL) and cooled to -78° C. ^{n}BuLi (2.5 M in hexane, 0.50 mL, 1.2 mmol) was added slowly over 5 minutes and stirring was continued for

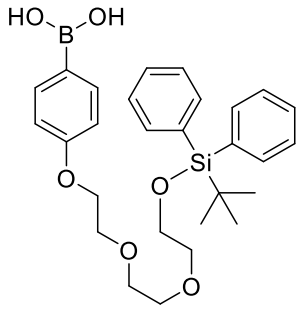

1 h. $B(OEt)_3$ (0.21 mL, 1.2 mmol) was then added and stirring was continued for a further 90 minutes. Sat. NH_4Cl (2 mL) was then added and the reaction was left to warm to room temperature. Water (5 mL) was then added and the reaction mixture extracted with diethyl ether (20 mL). The organic phase was washed with sat. $NaHCO_3$ (10 mL) and then brine (10 mL) and finally dried using Na_2SO_4, filtered and concentrated to afford a yellow viscous oil which was used without further purification, ^1H NMR yield = 65 %. ^1H NMR (300 MHz, $CDCl_3$) δ = 8.17 (d, *J* = 8.6 Hz, 2H, ArH), 7.78 – 7.65 (m, 4H, ArH), 7.48 – 7.30 (m, 6H, ArH), 7.03 (d, *J* = 8.6 Hz, 2H, ArH), 4.26 – 4.18 (m, 2H, CH_2-gly), 3.97 – 3.89 (m, 2H, CH_2-gly), 3.85 (t, *J* = 5.3 Hz, 2H, CH_2-gly), 3.74 (qd, *J* = 5.4, 2.6 Hz, 4H, 2 x CH_2-gly), 3.70 – 3.61 (m, 2H, CH_2-gly), 1.07 (s, 9H, CH_3). HRMS (ES^+): calcd for $C_{28}H_{37}BO_6SiNa$ $[M+Na]^+$ m/z = 531.24, found m/z = 531.4.

1,3-bis(2,4-dimethoxybenzyl)urea, 67

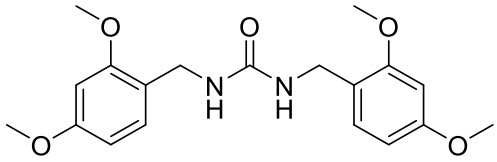

To a round bottom flask, fitted with a drying tube, was added dry DCM (5 mL) followed by benzyl isocyanate (1.00 g, 5.18 mmol). The flask was cooled to below 5° C and then a solution of benzylamine (0.80 mL, 5.2 mmol) in DCM (1 mL) was added slowly over 30 minutes. The precipitate forming hindered stirring so a further 3 mL of DCM was added. After 30 minutes stirring at 0° C, the flask was warmed to room temperature and left stirring for 14 h. The suspension was filtered through a sintered funnel and dried to afford 1.68 g of **67**, as a white solid (4.67 mmol, 91% yield). ^1H NMR (300 MHz, $CDCl_3$) δ = 7.10 (d, *J* = 8.9 Hz, 2H, ArH), 6.39 (dd, *J* = 5.7, 2.2 Hz, 4H, ArH), 4.18 (s, 4H,

NHC*H*$_2$), 3.79 – 3.73 (m, 6H, OCH_3), 3.70 (s, 6H, OCH_3). ^{13}C NMR (101 MHz, $CDCl_3$) δ = 160.25 (CO), 158.85 (C Ar), 158.15 (C Ar), 129.97 (CH Ar), 119.31 (C Ar), 103.96 (CH Ar), 98.36 (CH Ar), 55.32 (OCH_3), 55.12 (OCH_3), 39.44 (NH*C*H$_2$). HRMS (ES^+): calcd for $C_{19}H_{25}N_2O_5$ $[M]^+$ m/z = 361.1763, found m/z = 361.1759. mp: 186-188^o C. IR (neat, cm^{-1}): 3295 (NH), 3002, 2918, 2828 (CH), 1580 (CO).

1,3-bis(2,4-dimethoxybenzyl)pyrimidine-2,4,6(1H,3H,5H)-trione, 68

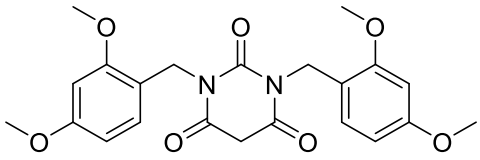

67 (2.99 g, 8.31 mmol) and malonic acid (0.86 g, 8.3 mmol) were added to acetic anhydride (11.8 mL, 0.120 mol) to form a slurry. Once heated to 70^o C a solution formed which was stirred for 16 h. Once cooled to room temperature the acetic anhydride was removed under vacuum and the residue obtained partitioned between 2 M NaOH (40 mL) and diethyl ether (30 mL). The aqueous phase was then acidified to pH 2 with concentrated HCl and the precipitate was dissolved with the addition of $CHCl_3$ (80 mL). The organic phase was washed with water (60 mL), dried using Na_2SO_4, filtered and evaporated to give 3.50 g of **68** as a yellow crystalline solid (8.17 mmol, 98% yield). The solid can be used as obtained, but to gain further purity, decolourising charcoal can be used to obtain a white crystalline solid. ^{1}H NMR (300 MHz, $CDCl_3$) δ = 7.08 (d, *J* = 8.9 Hz, 2H, ArH), 6.47 – 6.40 (m, 4H, ArH), 5.04 (s, 4H, NHC*H*$_2$), 3.85 – 3.68 (m, *J* = 14.5, 8.4 Hz, 14H, 2 x OCH_3, COC*H*$_2$CO). ^{13}C NMR (101 MHz, $CDCl_3$) δ = 164.51 (CO), 160.45 (CO), 158.33 (C Ar), 129.73 (CH Ar), 116.47 (C Ar), 103.95 (CH Ar), 98.51 (CH Ar), 55.41 (OCH_3), 55.38 (OCH_3) 40.65, (COCH_2CO), 39.94 (N*C*H$_2$). HRMS (ES^+): calcd for C22H25N2O7 $[M+Na]^+$ m/z = 429.1662, found m/z = 429.1668. mp: 82-83^o C. IR (neat, cm^{-1}): 2972, 2984 (CH), 1678 (CO).

1,3-bis(4-methoxybenzyl)-5,5-bis(3-methoxyphenyl)pyrimidine-2,4,6(1H,3H,5H)-trione, 69

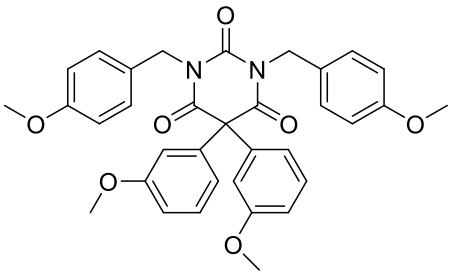

3-methoxyphenylboronic acid (0.28 g, 1.9 mmol) was added slowly over 15 minutes to a solution of $Pb(OAc)_4$ (0.82 g, 1.9 mmol) and $Hg(OAc)_2$ (42 mg, 0.19 mmol) in $CHCl_3$ (2.8 mL) at 40° C. Stirring was then continued for 1 h. *N*-*N*'-PMB-Barbituric acid (0.62 g, 1.7 mmol) and pyridine (0.45 mL, 5.6 mmol) were added and the mixture was stirred for 16 h at room temperature. The yellow suspension was then filtered through celite and washed with $CHCl_3$ (20 mL). The filtrate was then shaken with 3 M H_2SO_4 (16 mL) and the aueous phase extracted with $CHCl_3$ (2 x 10 mL). The organics were then combined, dried using Na_2SO_4, filtered and concentrated to afford a crude, brown solid which was purified *via* flash column chromatography (eluent: DCM) to afford 0.15 mg of **69** as an off white solid (0.26 mmol, 16 % yield). ^{1}H NMR (300 MHz, $CDCl_3$) δ = 7.36 (d, *J* = 8.7 Hz, 4H, ArH(PG)), 7.17 (t, *J* = 8.0 Hz, 2H, ArH), 6.94 – 6.72 (m, 6H, ArH, ArH(PG)), 6.61 – 6.41 (m, 4H, ArH), 5.06 (s, 4H, NHC*H*$_2$), 3.82 (d, *J* = 3.8 Hz, 6H, OCH_3), 3.61 (s, 6H, OCH_3). ^{13}C NMR (101 MHz, $CDCl_3$) δ = 169.22 (CO), 159.53 (C Ar), 159.29 (C Ar), 150.76 (C Ar), 138.17 (C Ar), 130.70 (CH Ar), 129.48 (CH Ar), 128.04 (C Ar), 121.12 (CH Ar), 114.80 (CH Ar), 114.00 (CH Ar), 113.79 (CH Ar), 67.31 (CO*C*CO), 55.27, 55.07, 45.57 (N*C*H$_2$).HRMS (ES$^+$): calcd for $C_{34}H_{33}N_2O_7$ $[M]^+$ m/z = 581.2288, found m/z = 581.2292. mp: 118-120° C. IR (neat, cm^{-1}): 2954, 2837 (CH), 1676 (CO).

5,5-bis(3-methoxyphenyl)pyrimidine-2,4,6(1H,3H,5H)-trione, 70

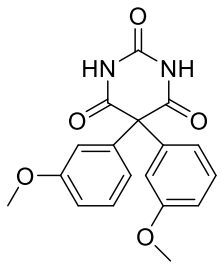

69 (0.10 g, 0.20 mmol) was suspended in a water/CHC_3CN mix (0.5/1.5 mL). Methanol was added slowly until a solution had formed and the reaction was then heated to reflux. CAN (0.51 g, 0.80 mmol) was then added and the solution was stirred for 16 h. The solution was then diluted with DCM (5 mL) and the organic layer separated, washed with water (5 mL), dried using $MgSO_4$, filtered and concentrated to afford a crude yellow solid which was purified *via* flash column chromatography (eluent: DCM/MeOH - 0-5%) to afford 6.5 mg of **70** as a white solid (0.019 mmol, 9% yield). ^{1}H NMR (300 MHz, Acetone) δ = 7.37 – 7.22 (m, 2H, ArH), 6.99 – 6.88 (m, 2H, ArH), 6.88 – 6.79 (m, 4H, ArH), 3.75 (s, 6H, OCH_3). MS (ES^+): calcd for $C_{18}H_{16}N_2O_5Na$ $[M+Na]^+$ m/z = 363.0957, found m/z = 363.0956.

(4-bromophenoxy)(tert-butyl)dimethylsilane, 71

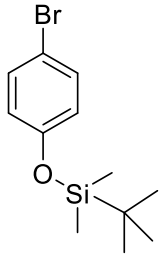

Bromophenol (7.42 g, 42.9 mmol), Imidazole (8.70 g, 127 mmol) and *tert*-butyldimethylsilyl chloride (9.00 g, 59.0 mmol) were dissolved in DMF (100 mL). The reaction was stirred for 16 h. The solution was then poured into water (500 mL) and extracted with ethyl acetate (2 x 200 mL). The organic phase was then washed with water (180 mL) and then brine (180 mL). The organic phase was then dried using Na_2SO_4, filtered and evaporated. The oil was used as obtained with no further purification required. Yield: quantitative. ^{1}H NMR (300 MHz, $CDCl_3$) δ = 7.39 – 7.29 (m, 2H, ArH), 6.82 – 6.66 (m, 2H, ArH), 0.99 (s, 9H, CCH_3), 0.20 (s, 6H, $SiCH_3$). ^{13}C NMR (101 MHz, $CDCl_3$) δ = 154.83 (C Ar), 132.29, (CH Ar), 121.91 (CH Ar), 113.60, (C Ar), 25.63 (CH_3), 18.20 (C ^{t}Bu), -4.49 ($SiCH_3$).

(4-((tert-butyldimethylsilyl)oxy)phenyl)boronic acid, 72

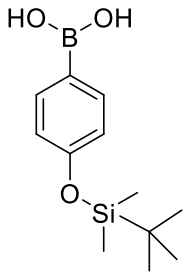

71 (5.44 g, 18.9 mmol) was dissolved in THF (25 mL). The flask was cooled to -78^{o} C and then a solution of n-BuLi (10.4 mL, 2 M in hexane, 20.8 mmol) was added dropwise over 30 minutes. Once addition was complete, the reaction was stirred for a further 30 minutes at -78^{o} C, followed by the dropwise addition of $B(OEt)_3$ (13.1 mL, 56.7 mmol) over 5 minutes. After 30 minutes stirring at -78 ^{o}C, the reaction was warmed to room temperature and acidified with 5% HCl solution. The organic phase was separated, washed with brine (30 mL), dried using Na_2SO_4, filtered and evaporated to form a yellow/white solid. The crude solid was purified *via* flash column chromatography (eluent: Hexane/EtOAc 1:1) to give 2.66 g of **72** (10.6 mmol, 56% yield). ^{1}H NMR (300 MHz, MeOD) δ = 7.73 – 7.49 (m, 2H, ArH), 6.95 – 6.70 (m, 2H, ArH), 1.01 (s, 9H, CH_3), 0.22 (s, 6H, $SiCH_3$). ^{13}C NMR (101 MHz, $CDCl_3$) δ = 159.75 (C Ar), 137.45 (CH Ar), 122.96 (C Ar), 119.78 (CH Ar), 25.69 (CH_3), 18.31 (C ^{t}Bu), -4.31 ($SiCH_3$). Analysis is in agreement with literature data [9]

5,5-bis(4-((tert-butyldimethylsilyl)oxy)phenyl)-1,3-bis(2,4-dimethoxybenzyl)pyrimidine-2,4,6(1H,3H,5H)-trione, 73

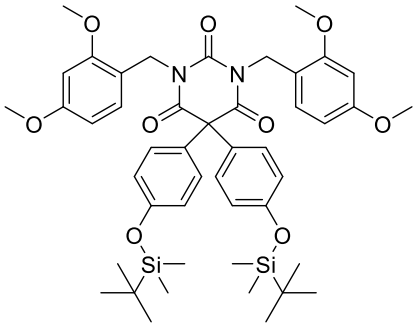

$Pb(OAc)_4$ (2.12 g, 4.78 mmol) and $Hg(OAc)_2$ (0.12 g, 0.38 mmol) were dissolved in dry CH_3Cl (7 mL). Once heated to 40^{o} C, **72** (1.13 g, 4.48 mmol) was added over 15 minutes. After stirring for 30 minutes pyridine (6.4 mL) and **68** (0.71 g, 1.7 mmol) were added and the suspension was stirred for 16 h at room temperature. The suspension was then filtered

through celite and rinsed with CH_3Cl (10 mL). The filtrate was washed with 3 M H_2SO_4 (15 mL) and the organic phase separated, dried with Na_2SO_4, filtered and evaporated to afford a crude red solid which was purified *via* flash column chromatography, eluent (DCM) to give 0.63 g of **73** as a white crystalline solid (0.75 mmol, 45% yield). ^{1}H NMR (300 MHz, $CDCl_3$) δ = 6.96 (d, *J* = 8.3 Hz, 2H, ArH (PG)), 6.87 – 6.76 (m, 4H, ArH), 6.74 – 6.64 (m, 4H, ArH), 6.45 – 6.26 (m, 4H, ArH (PG)), 5.12 (s, 4H, NHC*H*$_2$), 3.80 (s, 6H, OCH_3), 3.61 (s, 6H¸ OCH_3), 1.03 – 0.93 (m, 18H, CH_3), 0.28 – 0.14 (m, 12H, $SiCH_3$). ^{13}C NMR (101 MHz, $CDCl_3$) δ = 169.83 (CO), 160.38 (CO), 158.39 (C Ar), 155.48 (C Ar), 150.35 (C Ar), 130.54 (C Ar), 130.13 (CH Ar), 130.07 (CH Ar), 119.74 (CH Ar), 116.48 (C Ar), 103.74 (CH Ar), 98.31 (CH Ar), 66.31 (CO*C*CO), 55.35 (OCH_3), 55.19 (OCH_3), 41.33 (NCH_2), 25.65 (CH_3), 18.18 (C ^{t}Bu), -4.36 ($SiCH_3$). HRMS (ES^+): calcd for $C_{46}H_{61}N_2O_9Si_2$ $[M]^+$ m/z = 841.3916, found m/z = 841.3917. mp: 58-59 ^{o}C. IR (neat, cm^{-1}): 2975, 2930, 2855 (CH), 1689 (CO), 1257 (COC).

1,3-bis(2,4-dimethoxybenzyl)-5,5-bis(4-hydroxyphenyl)pyrimidine-2,4,6(1H,3H,5H)-trione, 74

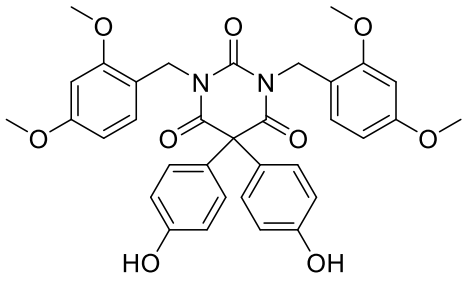

73 (0.10 mg, 0.12 mmol) was dissolved in THF (4 mL). TBAF (0.70 mL, 1 M in THF, 0.70 mmol) was added dropwise. The solution was stirred at room temperature for 2.5 h. The solvent was then removed and the residue taken up in DCM (30 mL). The organic phase was washed with water (20 mL), then brine (20 mL) and dried using Na_2SO_4, filtered and evaporated to afford a crude brown oil which was purified by flash column chromatography (eluent: DCM/MeOH - 4%) to give 72 mg of pure **74** as a white crystalline solid (0.17 mmol, 98% yield). ^{1}H NMR (300 MHz,

$CDCl_3$) δ = 6.99 (d, *J* = 8.2 Hz, 2H, ArH (PG)), 6.87 – 6.76 (m, 4H, ArH), 6.73 – 6.63 (m, 4H, ArH), 6.42 – 6.31 (m, 4H, ArH (PG)), 5.12 (s, 4H, NCH_2), 4.87 (s, 2H, OH), 3.81 (s, 6H, OCH_3), 3.60 (s, 6H, OCH_3). ^{13}C NMR (101 MHz, $CDCl_3$) δ = 170.13 (CO), 160.25 (CO), 158.35 (C Ar), 156.50 (C Ar), 150.30 (C Ar), 130.19 (CH Ar), 130.08 (CH Ar), 128.72 (C Ar), 116.34 (C Ar), 115.20 (CH Ar), 103.76 (CH Ar), 98.20 (CH Ar), 66.43 (CO*C*CO) 55.39 (OCH_3), 55.11 (OCH_3), 41.36 (NCH_2). HRMS (ES^+): calcd for $C_{34}H_{32}N_2O_9Na$ $[M+Na]^+$ m/z = 635.2009, found m/z = 635.1990. mp: 201-203° C. IR (neat, cm^{-1}): 3301 (OH), 3011, 2947, 2839 (CH), 1674 (CO).

1,3-bis(2,4-dimethoxybenzyl)-5,5-bis(4-(2-(2-(2-(4-(tris(4-(tert-butyl)phenyl)methyl)phenoxy)ethoxy)ethoxy)ethoxy)phenyl)pyrimidine-2,4,6(1H,3H,5H)-trione, 75

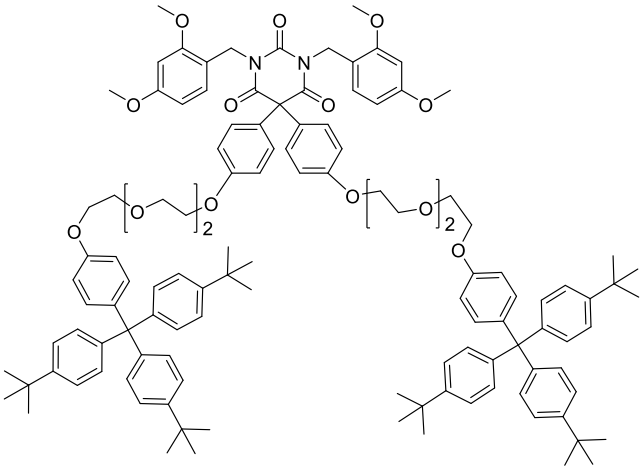

74 (0.23 g, 0.38 mmol), Cs_2CO_3 (0.83 g, 2.6 mmol) and **49** (0.73g, 0.98 mmol) were dissolved in DMF (4 mL) and refluxed for 2 h. The solvent was removed and the residue taken up in DCM (60 mL). The organic phase was then washed with water (40 mL) and then brine (40 mL), dried using Na_2SO_4, filtered and evaporated to afford a crude solid which was purified *via* flash column chromatography (eluent: DCM) to give 0.52 g of **75** as a white solid (0.28 mmol, 78% yield). ^1H NMR (300 MHz, $CDCl_3$) δ = 7.28 – 7.22 (m, 12H, ArH (stopper)), 7.14 – 7.07 (m, 16H, ArH (stopper)), 6.98 (d, *J* = 8.2 Hz, 2H, ArH (barbiturate), 6.91 – 6.72 (m, 12H, ArH (4H-stopper, 8H-barbiturate)), 6.42 – 6.33 (m, 4H, ArH

(barbiturate)), 5.12 (s, 4H, NCH_2), 4.17 – 4.08 (m, 8H, CH_2-gly), 3.91 – 3.83 (m, 8H, CH_2-gly), 3.79 (s, 6H, OCH_3), 3.77 (s, 6H, OCH_3), 3.60 (s, 8H, CH_2-gly), 1.32 (s, 54H, CH_3). ^{13}C NMR (101 MHz, $CDCl_3$) δ = 169.76 (CO), 160.43 (CO), 158.41 (C Ar), 156.53 (C Ar), 156.43 (C Ar), 151.75 (CH Ar), 148.31 (C Ar), 146.01 (C Ar), 144.61 (C Ar), 144.18 (C Ar), 139.86 (C Ar), 132.25 (CH Ar), 131.02 (CH Ar), 130.75 (CH Ar), 130.14 (CH Ar), 125.23 (CH Ar), 124.09 (CH Ar), 116.41 (C Ar), 114.40 (CH Ar), 113.11 (CH Ar), 72.57 (CH_2-gly), 70.89 (CH_2-gly), 69.92 (CH_2-gly), 69.81 (CH_2-gly), 69.76 (CH_2-gly), 67.25 (CH_2-gly), 64.10 (CO*C*CO), 63.16 (C Ar) 55.40 (OCH_3), 55.21 (OCH_3), 41.43 (NCH_2), 34.32 (C ^{t}Bu), 31.42 (CH_3). HRMS (ES^+): calcd for $C_{120}H_{140}N_2O_{15}Na$ $[M+Na]^+$ m/z = 1872.0151, found m/z = 1872.0134. mp: 154-156^o C. IR (neat, cm^{-1}): 2958, 2928, 2867 (CH), 1608 (CO).

5,5-bis(4-(2-(2-(2-(4-(tris(4-(tert-butyl)phenyl)methyl)phenoxy)ethoxy)ethoxy)ethoxy)phenyl)pyrimidine-2,4,6(1H,3H,5H)-trione, 76

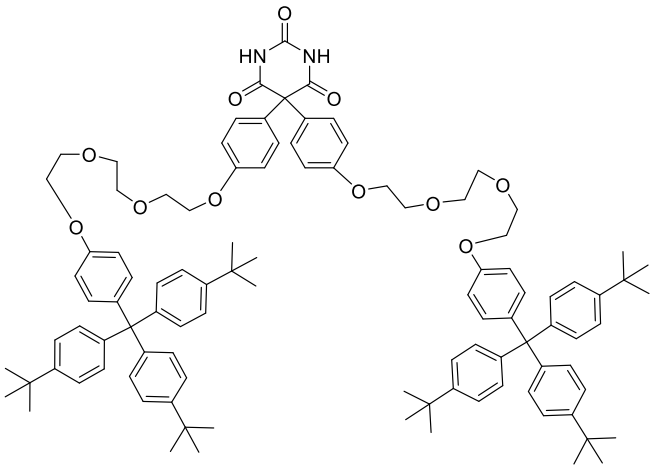

75 (0.47 g, 0.25 mmol) was dissolved in the minimum amount of DCM. Water (1.8 mL) was then added followed by acetone (2 mL). The solution was then heated to 65^o C, followed by the addition of CAN (0.85 g, 1.6 mmol). After stirring for 15 minutes, the solvents were removed and the residue taken up in DCM (10 mL). The organic phase was washed with water (6 mL) and then brine (6 mL). The organic phase was separated , dried

using Na_2SO_4, filtered and evaporated to afford a crude solid which was purified *via* flash column chromatography, eluent (Hexane/EtOAc 1:1) to give 81 mg of **76** (52 µmol, 21% yield). ^{1}H NMR (300 MHz, $CDCl_3$) δ = 7.27 – 7.20 (m, 12H, ArH-stopper), 7.15 – 7.03 (m, 20H, ArH (16H-stopper, 4H-barbiturate), 6.93 – 6.85 (m, 4H, ArH-barbiturate), 6.79 (d, *J* = 8.9 Hz, 4H, ArH-stopper), 4.12 (dd, *J* = 9.4, 3.9 Hz, 8H, CH_2-gly), 3.91 – 3.83 (m, 8H, CH_2-gly), 3.76 (s, 8H, CH_2-gly), 1.31 (s, 54H, CH_3). ^{13}C NMR (101 MHz, $CDCl_3$) δ = 170.14 (CO), 158.92 (CO), 156.52 (C Ar), 148.29 (C Ar), 147.92 (C Ar), 144.13 (C Ar), 139.77 (C Ar), 132.23 (CH Ar), 130.72 (CH Ar), 130.13 (CH Ar), 128.90 (C Ar), 124.04 (CH Ar), 114.76 (CH Ar), 113.07 (CH Ar), 70.83 (2 x CH_2-gly), 69.84 (CH_2-gly), 69.66 (CH_2-gly), 67.44 (CH_2-gly), 67.20 (CH_2-gly), 63.05 (CO*C*CO), 34.30 (C ^{t}Bu), 31.40 (CH_3). HRMS (ES^+): calcd for $C_{102}H_{120}N_2O_{11}Na$ $[M+Na]^+$ /z = 1571.8790, found m/z = 1571.8761. mp: 167-169 ^{o}C. IR (neat, cm^{-1}): 2973, 2942 (CH), 1740, 1703 (CO).

diethyl 2,2-bis(4-methoxyphenyl)malonate, 77

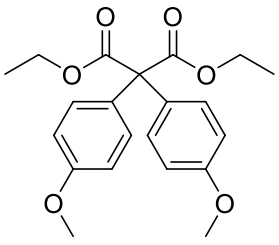

Anisole (4.40 mL, 40.4 mmol) was dissolved in acetic acid (20 mL, 0.21 mol). Diethyl ketomalonate (3.10 mL, 20.2 mmol) was added and the solution heated to 50^o C. H_2SO_4 (2.3 mL, 42 mmol) was added and the reaction was stirred at 80^o C for 2 h and then at room temperature for 16 h. Water (40 mL) was added to the reaction and the diluted reaction solution was poured into 4.75 M NaOH solution (100 mL). The solution was neutralised to pH 7 with acetic acid and then extracted with ethyl acetate (3 x 60 mL), dried using $MgSO_4$, filtered and concentrated to afford a crude viscous oil which was purified *via* flash column chromatography (eluent: Hexane/EtOAc - 10%) to give 0.73 g of **77** (2.0 mmol, 10% yield). ^{1}H

NMR (300 MHz, $CDCl_3$) δ = 7.39 – 7.28 (m, 4H, ArH), 6.98 – 6.79 (m, 4H, ArH), 4.27 (q, *J* = 7.1 Hz, 4H, OCH_2), 3.81 (d, *J* = 4.9 Hz, 6H, OCH_3), 1.25 (t, *J* = 7.1 Hz, 6H, OCH_2CH_3). ^{13}C NMR (101 MHz, $CDCl_3$) δ = 170.24 (CO), 158.78 (C Ar), 130.88 (C Ar), 130.71 (CH Ar), 113.25 (CH Ar), 67.08, (CO*C*CO), 61.73 (OCH_2), 55.21 (OCH_3), 13.94 OCH_2CH_3). HRMS (ES^+): calcd for $C_{21}H_{25}O_6Na$ $[M+Na]^+$ m/z = 373.1651, found m/z = 373.1645. mp: 60-62° C. IR (neat, cm^{-1}): 3003, 2985, 2937, 2838 (C-H), 1718 (CO).

2,2-bis(4-methoxyphenyl)malonic acid, 78

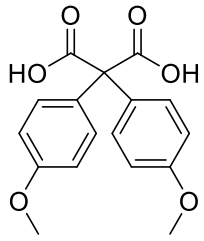

77 (0.30 g, 0.80 mmol) was dissolved in a water/EtOH mix (4 mL, 1:1 v:v). KOH (0.56 g, 10 mmol) was added and the reaction was refluxed for 4 h and then stirred at room temperature for 16 h. The solvents were removed and the residue dissolved in water (20 mL). This was extracted with diethyl ether (2 x 15 mL). The aqueous phase was then acidified to pH 0 with conc. HCl. This was then extracted with diethyl ether (2 x 20 mL), dried with $MgSO_4$, filtered and concentrated to afford 0.32 g of **78** (1.06 mmol, 80% yield). ^1H NMR (300 MHz, $CDCl_3$) δ = 7.36 – 7.18 (m, 4H, ArH), 6.97 – 6.80 (m, 4H, ArH), 3.81 (s, 6H, OCH_3). ^{13}C NMR (101 MHz, $CDCl_3$) δ = 178.98 (CO), 158.85 (C Ar), 130.37 (C Ar), 129.67 (CH Ar), 114.04 (CH Ar), 55.29 (OCH_3). MS (ES^+): calcd for $C_{17}H_{17}O_6$ $[M+H]^+$ m/z = 317.3, found m/z = 317.1. mp: 104-106° C. IR (neat, cm^{-1}): 3596 (OH), 3005, 2984, 2939 (C-H), 1701 (CO), 1506 (COC).

3-azidopropyl 4-methylbenzenesulfonate, 80

3-bromo-propanol (7.69 g, 56.0 mmol) was dissolved in water (120 mL). NaN_3 (9.86 g, 150 mmol) was then added and the suspension was stirred at 80° C for 16 h. The reaction

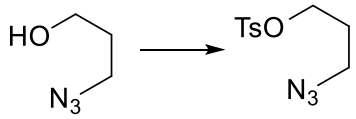

79 **80**

mixture was cooled and then extracted with EtOAc (5 x 90 mL) and the organics were combined and washed with brine (100 mL). The organic layer was then dried using $MgSO_4$, filtered and concentrated to afford 3.66 g of **79** (36.2 mmol, 71% yield) which was used as obtained. **79** (1.09 g, 10.8 mmol) and Et_3N (3.04 mL, 21.6 mmol) were dissolved in DCM (100 mL) and cooled to 0^o C. 4-Toluenesulfonyl chloride (2.17 g, 11.4 mmol) was then added and the solution was allowed to warm to room temperature and stirred for 16 h. The reaction was quenched with water (50 mL) and the organic layer was separated and dried using $MgSO_4$, filtered and evaporated to afford an oily solid which was purified *via* flash column chromatography (eluent: DCM/Pet. Ether 1:9) to give 1.27 g of **80** as a slightly yellow oil (5.00 mmol, 46% yield). ^{1}H NMR (300 MHz, $CDCl_3$) δ 7.82 (d, *J* = 8.3 Hz, 2H, ArH), 7.39 (d, *J* = 8.0 Hz, 2H, ArH), 4.12 (t, *J* = 5.9 Hz, 2H, OCH_2), 3.40 (t, *J* = 6.5 Hz, 2H, N_3CH_2), 2.48 (s, *J* = 12.8 Hz, 3H, CH_3), 1.98 – 1.79 (m, 2H, $OCH_2C\mathit{H}_2$). Analysis is in agreement with literature data.[10]

1-azido-3-iodopropane, 81

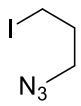

80 (2.00 g, 7.84 mmol), was then dissolved in acetone (20 mL) and NaI (1.77 g, 11.8 mmol) was added. The suspension was refluxed for 16 h. The white suspension was filtered off and washed with acetone (20 mL). Ether was added to the filtrate (60 mL) and this was then washed with water (2 x 20 mL). The organic layer was separated and dried using $MgSO_4$, filtered and concentrated to afford 1.50 g (7.14 mmol, 95% yield) of **81** which was used as obtained with no further purification necessary. ^{1}H NMR (300 MHz, $CDCl_3$) δ 3.46 (t, *J* = 6.3 Hz, 2H), 3.27 (t, *J* = 6.6 Hz, 2H), 2.06 (p, *J* = 6.5 Hz, 2H). Analysis is in agreement with literature data.[11]

diethyl 2,2-bis(3-azidopropyl)malonate, 82

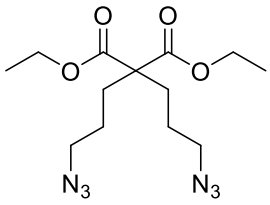

Diethyl malonate (1.44 mL, 9.48 mmol) was dissolved in THF (130 mL). NaH (0.60 g, 23.7 mmol) was added and the solution was refluxed for 1 h. **81** (5.00 g, 23.7 mmol) was then added and the reaction was held at reflux for 16 h. The solvents were then removed and the crude residue purified *via* flash column chromatography (eluent: Pet. Ether/EtOAc 9:1) to give 2.10 g of **82** (6.40 mmol, 68 % yield). ^{1}H NMR (300 MHz, $CDCl_3$) δ = 4.22 (q, *J* = 7.1 Hz, 4H, $COCH_2$), 3.32 (t, *J* = 6.6 Hz, 4H, N_3CH_2), 2.02 – 1.91 (m, 4H, CCH_2), 1.58 – 1.44 (m, 4H, $N_3CH_2CH_2$), 1.28 (t, *J* = 7.1 Hz, 6H, OCH_2CH_3). ^{13}C NMR (101 MHz, $CDCl_3$) δ = 171.05 (CO), 61.45 (OCH_2), 56.77 (C), 51.29 (N_3CH_2), 29.90 (CCH_2), 23.78 ($N_3CH_2CH_2$), 14.06 (OCH_2CH_3). HRMS (ES^+): calcd for $C_{13}H_{22}N_6O_4Na$ $[M+Na]^+$ m/z = 349.2, found m/z = 349.2. Analysis is in agreement with literature data.[12]

5,5-bis(3-azidopropyl)pyrimidine-2,4,6(1H,3H,5H)-trione, 83

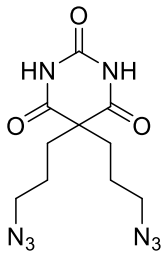

82 (1.80 g, 5.50 mmol) and urea (1.65 g, 27.5 mmol) were dissolved in DMSO (80 mL). NaH (0.66 g, 27 mmol) was added to the solution which was then stirred for 16 h. Sat. $NaHCO_3$ (160 mL) was then added and the mixture was extracted with EtOAc (2 x 200 mL). The combined organic extracts were dried using $MgSO_4$, filtered and concentrated to afford a clear oil. Addition of water precipitates the product, which was filtered, redissolved in EtOAc, dried using $MgSO_4$, filtered and concentrated to afford 0.52 g of **83** as a yellow solid (1.8 mmol, 32% yield)**.** ^{1}H NMR (300 MHz, $CDCl_3$) δ = 8.19 (s, 2H, NH), 3.31 (t, *J* = 6.6 Hz, 4H, N_3CH_2), 2.13 – 2.02 (m, 4H, CCH_2), 1.59 – 1.47 (m, 4H, $N_3CH_2CH_2$). ^{13}C NMR (101 MHz, $CDCl_3$) δ = 172.37 (CO), 149.58

(CO), 55.24 (C), 50.76 (N_3CH_2), 35.51 (CCH_2), 24.43 ($N_3CH_2CH_2$). HRMS (ES^+): calcd for $C_{10}H_{14}N_8O_3Na$ $[M+Na]^+$ m/z = 317.1087, found m/z = 317.1077. Analysis is in agreement with literature data.[12]

4,4',4''-((4-(prop-2-yn-1-yloxy)phenyl)methanetriyl)tris(tert-butylbenzene), 84

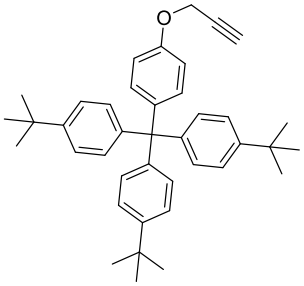

48 (0.40g, 0.79 mmol) was dissolved in DMF (8 mL). K_2CO_3 (0.52 g, 3.8 mmol) was added and the mixture was stirred at 80° C for 30 minutes. Propargyl bromide (0.12 mL, 80% in toluene, 1.3 mmol) was added and stirring continued at 80° C for 16 h. The solvent was removed and the residue taken up in water (20 mL) and EtOAc (30 mL). The aqueous phase was separated, extracted with EtOAc (2 x 30 mL) and the combined organics were dried using $MgSO_4$, filtered and concentrated to afford a white crude solid which was purified *via* flash column chromatography (eluent: Hexane/DCM 8:2) to give 0.40 g of **84** as a white solid (0.73 mmol, 92% yield). ^1H NMR (400 MHz, $CDCl_3$) δ = 7.28 – 7.23 (m, 6H, ArH), 7.15 – 7.08 (m, 8H, ArH), 6.89 – 6.85 (m, 2H, ArH), 4.69 (d, *J* = 2.4 Hz, 2H, OCH_2), 2.54 (t, *J* = 2.4 Hz, 1H, CCH), 1.33 (s, 27H, CH_3). ^{13}C NMR (101 MHz, $CDCl_3$) δ = 155.47 (C Ar), 148.35 (C Ar), 144.02 (C Ar), 140.49 (C Ar), 132.28 (CH Ar), 130.73 (CH Ar), 124.06 (CH Ar), 113.30 (CH Ar), 78.81 (OCH_2C), 75.38 (CCH) 55.77 (OCH_2), 34.31 (C ^{t}Bu), 31.39 (CH_3). HRMS (ES^+): calcd for $C_{40}H_{46}O$ $[M]^+$ m/z = 542.8, found m/z = 542.3. Analysis is in agreement with literature data.[12]

5,5-bis(3-(4-((4-(tris(4-(tert-butyl)phenyl)methyl)phenoxy)methyl)-1H-1,2,3-triazol-1-yl)propyl)pyrimidine-2,4,6(1H,3H,5H)-trione, 85

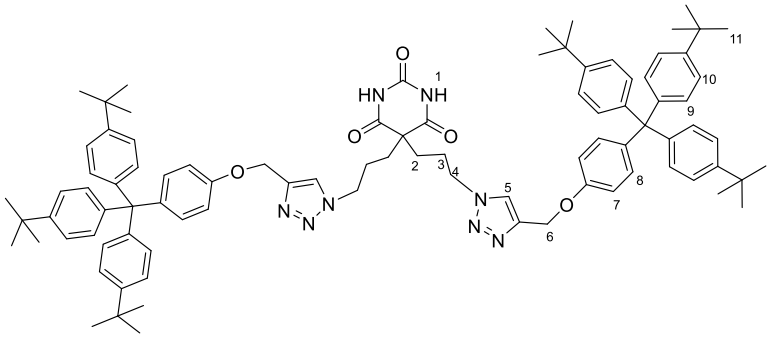

83 (16 mg, 0.054 mmol,), and **84** (62 mg, 0.114 mmol,) were dissolved in dry, degassed chloroform (1 mL). A catalytic amount of $Cu(MeCN)_4PF_6$ and TBTA were added, and the reaction mixture was stirred at room temperature, under argon for 3 days. After solvent removal, the crude product was purified by flash column chromatography (eluent: cyclohexane/EtOAc 7:3) to give 31 mg of **85** as a white solid (22 µmol, 26 % yield). ^{1}H NMR (300 MHz, $CDCl_3$) δ = 8.37 (s, 2H, NH), 7.62 (d, *J* = 6.6 Hz, 2H, CH_{tria}), 7.26 – 7.20 (m, 12H, ArH), 7.14 – 7.04 (m, 16H, ArH), 6.83 (d, *J* = 8.8 Hz, 4H, ArH), 5.18 (s, 4H, OCH_2), 4.39 – 4.24 (m, 4H, NCH_2), 2.06 – 1.97 (m, 4H, CCH_2), 1.97 – 1.83 (m, 4H, $NCH_2C\mathit{H}_2$), 1.31 (s, 54H, CH_3). ^{13}C NMR (101 MHz, CD_2Cl_2) δ = 171.70 (CO), 156.02 (C Ar), 148.39 (C Ar), 144.39 (C Ar), 140.36 (C Ar), 131.95 (CH Ar), 130.37 (CH Ar), 124.32 (CH Ar), 113.27 (CH Ar), 63.10 (C), 61.48 (OCH_2), 55.05 (CO*C*CO), 49.73 (NCH_2), 34.80 ($C\mathit{C}H_2$), 34.18 (C ^{t}Bu), 31.11 (CH_3), 25.35 ($NCH_2\mathit{C}H_2$). HRMS (ES^+): calcd for $C_{90}H_{106}N_8O_5Na$ $[M+Na]^+$ m/z = 1401.8, found m/z = 1401.6. Analysis is in agreement with literature data.[12]

4,4',4''-((4-(3-azidopropoxy)phenyl)methanetriyl)tris(tert-butylbenzene), 86

48 (1.04 g, 2.06 mmol) and **80** (0.53 g, 2.1 mmol) were suspended in butanone. Once heated to 50^o C a solution forms. K_2CO_3 (1.42 g, 10.3 mmol) is then added and the mixture is heated

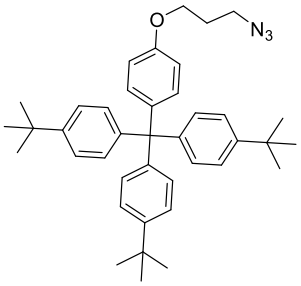

at 70° C for 16 h. The suspension was then filtered through a sintered funnel and washed with acetone. The filtrate was concentrated to give a crude white solid which was purified *via* flash column chromatography (eluent: Pet. Ether/DCM 7:3) to give 0.75 g of **86** (1.3 mmol, 62 % yield). ^{1}H NMR (300 MHz, $CDCl_3$) δ = 7.28 – 7.21 (m, 6H, ArH), 7.15 – 7.05 (m, 8H, ArH), 6.83 – 6.74 (m, 2H, ArH), 4.04 (t, *J* = 5.9 Hz, 2H, N_3CH_2), 3.54 (t, *J* = 6.7 Hz, 2H, OCH_2), 2.06 (p, *J* = 6.3 Hz, 2H, $N_3CH_2C\mathit{H}_2$), 1.32 (s, 27H, CH_3). ^{13}C NMR (101 MHz, $CDCl_3$) δ = 156.44 (C Ar), 148.31 (C Ar), 144.10 (C Ar), 139.86 (C Ar), 132.29 (CH Ar), 130.71 (CH Ar), 124.05 (CH Ar), 112.93 (CH Ar), 64.29 (N_3CH_2), 61.45 (C), 48.31, OCH_2), 34.30 (C ^{t}Bu), 31.39 (CH_3), 28.85 ($N_3CH_2\mathit{C}H_2$). Analysis is in agreement with literature data.[10]

4-((4-(tris(4-(tert-butyl)phenyl)methyl)phenoxy)methyl)-1-(3-(4-(tris(4-(tert-butyl)phenyl)methyl)phenoxy)propyl)-1H-1,2,3-triazole, 87

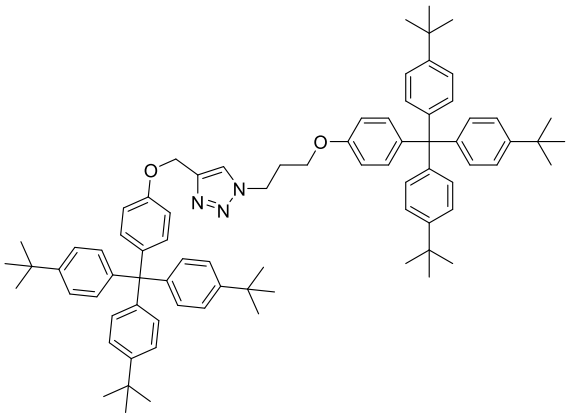

84 (81 mg, 0.15 mmol) and **86** (88 mg, 0.15 mmol) were dissolved in degassed $CHCl_3$ (6.5 mL). A catalytic amount of $Cu(MeCN)_4PF_6$ was then added and the reaction was left to stir for 16 h. The solvents were removed and the residue dissolved in DCM (15 mL) and washed with water (10 mL). The organic phase was then dried using $MgSO_4$, filtered and concentrated to afford a crude white solid which was purified *via* flash column chromatography (eluent: Hexane/EtOAc 8:2) to give 0.13 g of **87** (0.14 mmol, 76 % yield)**.** ^{1}H NMR (300 MHz, $CDCl_3$) δ = 7.64 (s, *J* = 3.9 Hz, 1H, CH_{tria}), 7.24 (d, *J* = 8.6 Hz, 12H, ArH), 7.13 –

7.05 (m, 14H, ArH), 6.84 (d, *J* = 9.0 Hz, 2H, ArH), 6.74 (d, *J* = 8.9 Hz, 2H, ArH), 5.19 (s, 2H, OCH_2C), 4.61 (t, *J* = 6.9 Hz, 2H, NCH_2), 3.96 (t, *J* = 5.6 Hz, 2H, OCH_2CH_2), 2.48 – 2.36 (m, 2H, OCH_2CH_2), 1.29 (d, *J* = 8.4 Hz, 54H). ^{13}C NMR (101 MHz, $CDCl_3$) δ = 156.2 (C Ar), 148.3 (C Ar), 144.1 (C Ar), 132.3 (CH Ar), 130.6 (CH Ar), 124.3 and 124.1 (CH Ar), 119.5 (CH_{tria}), 113.3 and 113.0 (CH Ar), 63.9 ($OCH_2C=C$), 47.5 (NCH_2), 34.3 (C ^{t}Bu), 31.3 (CH_3) HRMS (ES^+): calcd for $C_{80}H_{96}N_3O_2$ $[M]^+$ m/z = 1130.7503, found m/z = 1130.7496. mp: 330-334^{o} C. IR (neat, cm^{-1}): 2957, 2942, 2853 (C-H), 1503 (COC).

5-(tert-butyl)-N1-(6-dodecanamidopyridin-2-yl)-N3-(6-propionamidopyridin-2-yl)isophthalamide compound with 5-(3-(1H-1,2,3-triazol-1-yl)propyl)-5-(3-(4-((4-(tris(4-(tert-butyl)phenyl)methyl)phenoxy)methyl)-1H-1,2,3-triazol-1-yl)propyl)pyrimidine-2,4,6(1H,3H,5H)-trione and 4,4',4''-((4-ethoxyphenyl)methanetriyl)tris(tert-butylbenzene) (1:1), 88

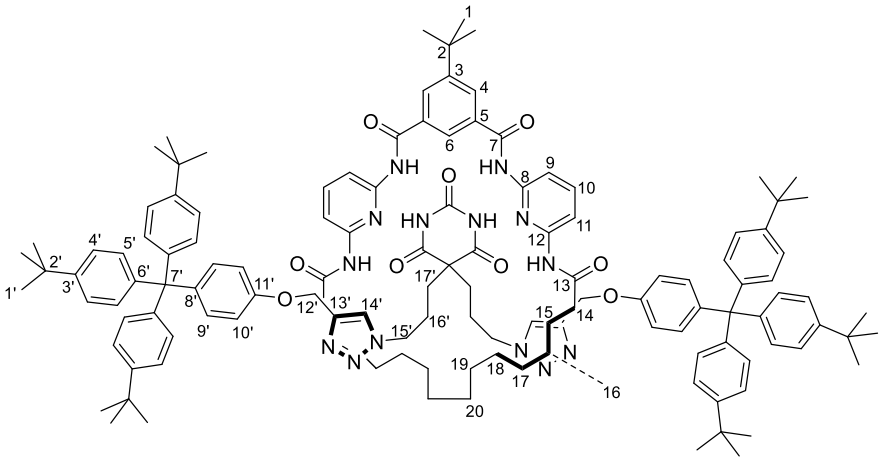

45 (37 mg, 0.056 mmol), **83** (16 mg, 0.054 mmol) and **84** (62 mg, 0.11 mmol) were dissolved in $CHCl_3$ (1 mL). The solution was stirred for 1 h and catalytic amounts of $Cu(MeCN)_4PF_6$ and TBTA were then added. The suspension was stirred for 16 h. The solvents were then removed and the residue purified *via* flash column chromatography (eluent: DCM/MeOH - 2-4%) to afford 6 mg of **88** (2.95 µmol, 5%

yield). ^{1}H NMR (300 MHz, $CDCl_3$) δ 12.72 (s, 2H, NH), 9.84 (s, 2H, NH), 9.34 (s, 2H, NH), 8.32 (s, 1H, 6), 8.22 (s, 2H, 4), 8.09 (d, *J* = 1.4 Hz, 2H, 11), 8.00 (d, *J* = 8.0 Hz, 2H, 9), 7.73 (t, *J* = 7.7 Hz, 2H, 10), 7.52 (s, 2H, 14'), 7.22 (m, 12 H, 5'), 7.08 - 7.06 (m, 12H, 9' and 4'), 6.75 (d, *J* = 8.9 Hz, 4H, 10'), 5.04 (s, 4H, 12'), 4.34 (t, *J* = 6.0Hz, 4H, 15'), 2.44 (m, 4H, 14), 2.21 (m, 4H, 17'), 2.05 (m, 4H, 16'), 1.71 (m, 4H, 15), 1.36 (s, 9H, 1), 1.29 (s, 54H, 1'), 1.24 (m, 20H, alk). ^{13}C NMR (101 MHz, $CDCl_3$) δ 173.951 (CO), 172.72 (CO), 167.28 (CO), 156.17 (C Ar), 152.84 (C Ar), 152.15 (CH Ar), 150.93 (C pyr), 150.29 (C pyr), 148.44 (C Ar), 145.48 (C tria), 144.28 (C Ar), 141.52 (CH pyr), 140.65 (C Ar), 134.37 (CO), 132.54 (CH Ar), 130.85 (CH Ar), 130.15 (CH Ar), 124.49 (CH Ar), 124.26 (CH tria), 122.73 (CH Ar), 113.21 (CH Ar), 112.34 (CH pyr), 111.42 (CH pyr), 63.23 (C Ar), 62.06 (OCH_2), 55.38 (CO*C*CO), 49.65 (NCH_2), 37.77 (CO*C*H_2), 35.94 ($NCH_2CH_2CH_2$), 35.46 (C ^{t}Bu), 34.55 (C ^{t}Bu), 31.58 (CH_3), 31.37 (CH_3), 30.14 (alk), 29.98 (alk), 29.87 (alk), 26.05 (alk), 25.46 (NCH_2*C*H2). HRMS (ES^+): calcd for $C_{128}H_{155}N_{14}O_9Na$ $[M+Na]^+$ m/z = 2055.9, found m/z = 2055.2. Analysis is in agreement with literature data.[12]

[4]5-(tert-butyl)-2,6,8,25-tetraaza-1,7(2,6)-dipyridina-4(1,3)-benzenacyclopentacosaphane-3,5,9,24-tetraone compound with 4-((4-(tris(4-(tert-butyl)phenyl)methyl)phenoxy)methyl)-1-(3-(4-(tris(4-(tert-butyl)phenyl)methyl)phenoxy)propyl)-1H-1,2,3-triazole (1:1:1), 89

45 (73 mg, 0.11 mmol) was dissolved in $CHCl_3$. $Cu(MeCN)_4PF_6$ (42 mg, 0.11 mmol) was added and the reaction was stirred for 1 h. **84** (71 mg, 0.13 mmol) and **86** (77 mg, 0.13 mmol) were then added and the reaction was stirred for 16 h. A solution of KCN (70 mg) in MeOH (10 mL) was added and the white suspension was stirred for 1 h. The solvents were then removed and the residue dissolved in DCM (15 mL) and washed with water (10 mL). The

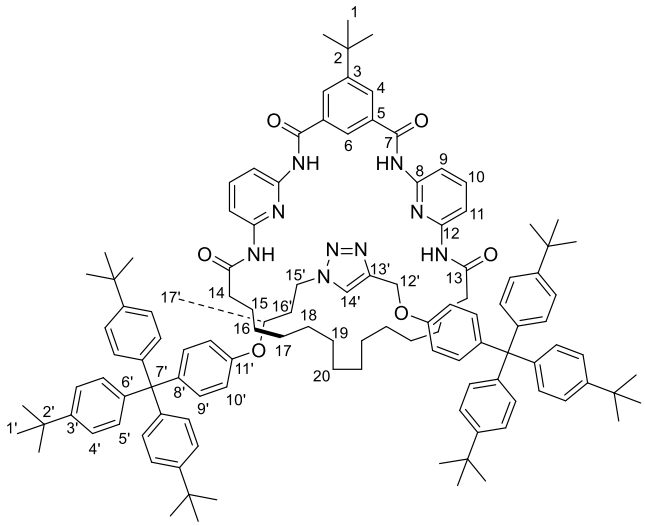

organic phase was then dried using $MgSO_4$, filtered and concentrated to afford a crude white solid which was purified *via* flash column chromatography (eluent: Hexane/EtOAc 8:2) to give 45 mg of **89** (25 μmol, 19% yield). ^{1}H NMR (300 MHz, $CDCl_3$) δ 9.35 (s, 2H, NH), 8.52 (s, 1H, 6), 8.38 (s, *J* = 12.0 Hz, 2H, 4), 8.07 (d, *J* = 8.0 Hz, 2H, 9), 7.90 (d, *J* = 8.0 Hz, 2H, 11), 7.78 (s, 1H, 15'), 7.67 (t, *J* = 8.1 Hz, 2H, 10), 7.59 (s, 2H, NH), 7.28 – 7.13 (m, 14H, 5', 10' [nearest triazole]), 7.13 – 6.95 (m, 16H, 4', 9'), 6.64 (d, *J* = 8.9 Hz, 2H, 10'), 5.48 (s, 2H, 12'), 4.48 (t, *J* = 6.7 Hz, 2H, 17'), 3.77 (t, *J* = 5.4 Hz, 2H, 15'), 2.17 – 2.02 (m, 6H, 16', 14), 1.70 – 1.50 (m, 4H, 15), 1.42 (s, *J* = 3.7 Hz, 9H, 1), 1.30 (d, *J* = 5.4 Hz, 54H, 1'), 1.26 (d, *J* = 5.6 Hz, 20H, alk). ^{13}C NMR (126 MHz, $CDCl_3$) δ 171.64 (CO), 165.24 (CO), 155.93 (C Ar), 155.84 (C Ar), 153.41 (C Ar), 149.94 (C pyr), 149.38 (CH Ar), 148.50 (C Ar), 148.35, 144.79 (C tria), 143.98 (C Ar), 143.69 (C pyr), 141.68 (CH pyr), 140.68 (C Ar), 140.40, 133.83 (CH Ar), 132.69, (CH Ar) 132.37 (CH Ar), 130.66 (CH Ar), 130.57 (CH Ar), 124.16 (CH tria), 124.08 (CH Ar), 118.20, 113.65, 110.00 (CH pyr), 109.62 (CH pyr), 47.70 (NCH_2), 37.57 ($COCH_2$), 35.29 ($NCH_2CH_2CH_2$), 34.29 (C ^{t}Bu), 31.39 (CH_3), 30.04 (CH_3), 29.70 (alk), 29.36 (alk), 28.51 (alk), 28.29 (alk), 28.06 (alk), 25.03 (NCH_2CH2). HRMS (ES^+): calcd for $C_{118}H_{146}N_9O_6$ $[M+H]^+$ m/z = 1785.1396, found m/z = 1785.1267. mp: 143-146° C. IR (neat, cm^{-1}): 3587 (NH), 2963, 2927, 2858 (C-H), 1704 (CO), 1506 (COC).

5.3 Synthesis of Anthracene terminated compounds

General Procedure A for the Synthesis of Ethyl-9-anthryloxyenoate Derivatives:

Acetone (200 mL) was added to a round bottom flask and degassed for 30 minutes. To this was added anthrone and K_2CO_3. After stirring for 10 minutes the flask was heated to reflux at which point the appropriate bromo-ester was added. The solution was left at reflux for 24 h. The contents were then filtered and the solvent removed. The residue was dissolved in DCM (100 mL) and washed with water (50 mL). The organic phase was then dried using $MgSO_4$, filtered and evaporated. The resulting orange oil was purified *via* flash column chromatography, to give a yellow solid.

ethyl 4-(anthracen-9-yloxy)butanoate, 95

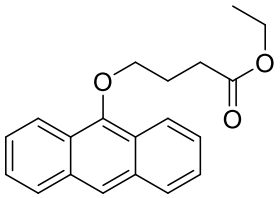

General Procedure A using anthrone (4.00g, 20.1 mmol), K_2CO_3 (2.78 g, 20.1 mmol) and ethyl 4-bromobutyrate (2.90 mL, 20.1 mmol) in acetone (200 mL) gave **95** (1.48 g, 20% yield). Chromatography on silica (eluent: DCM/Hexane 9:1). ^{1}H NMR (300 MHz, $CDCl_3$) δ = 8.36 – 8.16 (m, 3H, Ar), 8.11 – 7.91 (m, 2H, ArH), 7.58 – 7.39 (m, 4H, ArH), 4.31 – 4.18 (m, 4H, OCH_2CH_2 and $COOCH_2CH_3$), 2.82 (t, *J* = 7.4 Hz, 2H, $OCH_2CH_2CH_2$), 2.49 – 2.35 (m, 2H, OCH_2CH_2), 1.33 (t, *J* = 7.1 Hz, 3H¸ $COOCH_2CH_3$). ^{13}C NMR (101 MHz, $CDCl_3$) δ = 173.28 (CO), 151.03 (C Ar), 132.41 (C Ar), 128.46 (CH Ar), 125.47 (CH Ar), 125.20 (CH Ar), 124.64 (C Ar), 122.24 (CH Ar), 74.55 (OCH_2), 60.56 ($COOCH_2CH_3$), 31.19 ($OCH_2CH_2CH_2$), 26.05 (OCH_2CH_2), 14.31 ($COOCH_2CH_3$). MS (ES^+): calcd for $C_{20}H_{20}O_3$ [M^++MeO^-] m/z = 338.15, found m/z = 338.3. Analysis is in agreement with literature data.[13]

ethyl 7-(anthracen-9-yloxy)heptanoate, 96

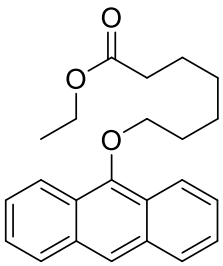

General Procedure A using anthrone (4.00g, 20.1 mmol), K_2CO_3 (2.78 g, 20.1 mmol) and ethyl 7-bromoheptanoate (3.64 mL, 20.1 mmol) in acetone (200 mL) gave **96** (3.59 g, 51% yield). Chromatography on silica (eluent: DCM/Hexane 9:1). ^{1}H NMR (300 MHz, $CDCl_3$) δ = 8.38 – 8.18 (m, 3H, ArH), 8.09 – 7.95 (m, 2H, ArH), 7.56 – 7.41 (m, 4H, ArH), 4.28 – 4.12 (m, 4H, OC*H*$_2$CH$_2$ and COOC*H*$_2$CH$_3$), 2.39 (t, *J* = 7.5 Hz, 2H, COCH$_2$), 2.15 – 2.00 (m, 2H, OCH$_2$C*H*$_2$), 1.84 – 1.69 (m, 4H, Alk), 1.58 – 1.47 (m, 2H, Alk), 1.32 – 1.27 (m, 3H, COOCH$_2$C*H*$_3$). ^{13}C NMR (101 MHz, $CDCl_3$) δ = 173.79 (CO), 151.44 (C Ar), 132.44 (C Ar), 128.43 (CH Ar), 125.45 (CH Ar), 125.07 (CH Ar), 124.72 (C Ar), 122.42 (CH Ar), 121.99 (CH Ar), 75.99 (OCH$_2$), 60.25 (COO*C*H$_2$CH$_3$), 34.35 (CO*C*H$_2$CH$_2$), 30.54 (OCH$_2$*C*H$_2$), 29.15 (C Alk), 26.00 (C Alk), 24.98 (C Alk), 14.29 (COOCH$_2$*C*H$_3$). HRMS (ES$^+$): calcd for $C_{23}H_{26}O_3$ [M]$^+$ m/z = 350.2, found m/z = 350.3. Analysis is in agreement with literature data.[13]

ethyl 10-(anthracen-9-yloxy)decanoate, 97

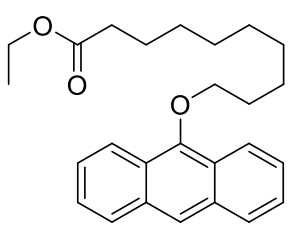

General Procedure A using anthrone (2.79 g, 14.4 mmol), K_2CO_3 (1.99 g, 14.4 mmol) and ethyl 7-bromodecanoate (4.00 mL, 14.4 mmol) in acetone (200 mL) gave **97** (3.54 g, 62% yield). Chromatography on silica (eluent: DCM/Hexane 7:3). ^{1}H NMR (300 MHz, $CDCl_3$) δ = 8.30 – 8.15 (m, 2H, ArH), 8.14 (s, 1H, ArH), 8.01 – 7.83 (m, 2H, ArH), 7.53 – 7.25 (m, 4H, ArH), 4.31 – 3.85 (m, 4H, COOCH$_2$ and OCH$_2$), 2.23 (t, *J* = 7.5 Hz, 2H, COCH$_2$), 1.98 (dd, *J* = 8.4, 6.8 Hz, 2H, OCH$_2$C*H*$_2$), 1.68 – 1.48 (m, 4H, OCH$_2$CH$_2$C*H*$_2$ and COCH$_2$C*H*$_2$), 1.43 – 1.21 (m, 8H, Alk), 1.18 (t, *J* = 7.1 Hz, 3H, COOCH$_2$C*H*$_3$). ^{13}C NMR (101 MHz, $CDCl_3$) δ =

173.92 (CO), 151.52 (C Ar), 132.44 (C Ar), 128.41 (CH Ar), 125.43 (CH Ar), 125.02 (CH Ar), 124.74 (C Ar), 122.45 (CH Ar), 121.93 (CH Ar), 76.17 (OCH_2), 60.18 ($COOCH_2CH_3$), 34.41 ($COCH_2CH_2$), 30.69 (OCH_2CH_2), 29.55 (alk), 29.46 (alk), 29.27 (alk), 29.16 (alk), 26.24 (alk), 25.00 (alk), 14.28 ($COOCH_2CH_3$). HRMS (ES^+): calcd for $C_{12}H_{24}O_3Na$ (loss of anthracene) m/z = 239.16, found m/z = 239.2. IR (neat): 3077 (CH) 2928 (CH) 2855 (CH) 1678 (CO).

General Procedure B for the Synthesis of Carboxylic Derivatives:

The ester compound was dissolved in a round bottom flask containing degassed ethanol (100 mL). 10% NaOH solution (100 mL) was then added and the mixture was heated under reflux for 14 h. Once cooled to room temperature, the ethanol was removed under vacuum to afford a solid which was then dissolved in water (400 mL). To this solution, conc. HCl was added dropwise with stirring until pH 6 at which point a cream precipitate forms. The precipitate was filtered, and dried to give a cream precipitate.

4-(anthracen-9-yloxy)butanoic acid, 98

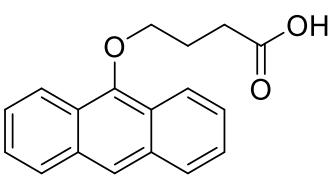

General procedure B using ester **95** (3.45 mmol) gave **98** (0.86 g, 89%). ^1H NMR (300 MHz, $CDCl_3$) δ = 8.32 – 8.20 (m, 3H, ArH), 8.07 – 7.96 (m, 2H, ArH), 7.58 – 7.40 (m, 4H, ArH), 4.27 (t, *J* = 6.2 Hz, 2H, OCH_2), 2.90 (t, *J* = 7.4 Hz, 2H, $COCH_2$), 2.41 (dd, *J* = 13.6, 6.9 Hz, 2H, OCH_2CH_2). ^{13}C NMR (101 MHz, $CDCl_3$) δ = 176.38 (CO), 150.93 (C Ar), 134.18 (CH Ar), 132.37 (C Ar), 128.42 (CH Ar), 125.44 (CH Ar), 125.20 (CH Ar), 124.59 (C Ar), 122.17 (CH Ar), 74.63 (OCH_2), 30.93 ($COCH_2$), 25.93 (OCH_2CH_2). HRMS (ES^+): calcd for $C_{18}H_{16}O_3Na$ $[M+Na]^+$ m/z = 303.0997, found m/z = 303.1003. Analysis is in agreement with literature data.[13]

7-(anthracen-9-yloxy)heptanoic acid, 99

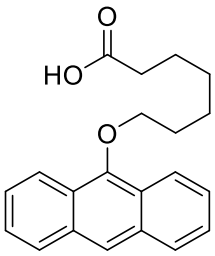

General procedure B using ester **95** (1.03 mmol) gave **99** (2.79 g, 84%). ^{1}H NMR (300 MHz, $CDCl_3$) δ 8.37 – 8.18 (m, 3H, ArH), 8.07 – 7.95 (m, 2H, ArH), 7.55 – 7.41 (m, 4H, ArH), 4.21 (t, *J* = 6.6 Hz, 2H, OC*H*$_2$CH$_2$), 2.45 (t, *J* = 7.4 Hz, 2H¸ COCH$_2$), 2.16 – 2.02 (m, 2H, OCH$_2$C*H*$_2$), 1.84 – 1.67 (m, 4H, OCH$_2$CH$_2$C*H*$_2$ and COCH$_2$C*H*$_2$), 1.61 – 1.49 (m, 2H, COCH$_2$CH$_2$C*H*$_2$). ^{13}C NMR (101 MHz, $CDCl_3$) δ = 179.1 (CO), 151.4 (C Ar), 132.4 (CH Ar), 128.4 (CH Ar), 125.5 (CH Ar), 125.1 (CH Ar), 124.7 (C Ar), 122.4 (CH Ar), 122.0 (CH Ar), 76.0 (OCH$_2$), 33.8 (CO*C*H$_2$), 30.6 (OCH$_2$*C*H$_2$), 29.1 (COCH$_2$CH$_2$*C*H$_2$), 26.1 (OCH$_2$CH$_2$*C*H$_2$), 24.7 (COCH$_2$*C*H$_2$). HRMS (ES$^+$): calcd for $C_{21}H_{21}O_3$ [M-H]$^-$ m/z = 321.1 found m/z = 321.3. Analysis is in agreement with literature data.[13]

10-(anthracen-9-yloxy)decanoic acid, 100

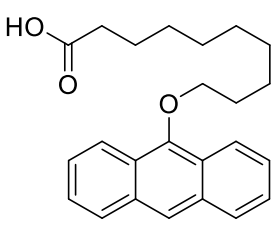

General procedure B using ester **97** (8.90 mmol) gave **100** (2.19 g, 67%). ^{1}H NMR (300 MHz, $CDCl_3$) δ 8.27 – 8.14 (m, 2H, ArH), 8.12 (s, 1H, ArH), 7.90 (m, 2H, ArH), 7.49 – 7.25 (m, 4H, ArH), 4.10 (t, *J* = 6.6 Hz, 2H, OC*H*$_2$CH$_2$), 2.28 (t, *J* = 7.4 Hz, 2H, COCH$_2$), 1.95 (dt, *J* = 12.8, 5.4 Hz, 2H, OCH$_2$C*H*$_2$), 1.68 – 1.44 (m, 4H, OCH$_2$CH$_2$C*H*$_2$ and COCH$_2$C*H*$_2$), 1.46 – 1.21 (m, 8H, Alk). ^{13}C NMR (101 MHz, $CDCl_3$) δ = 179.64 (CO), 151.50 (C Ar), 132.44 (C Ar), 128.41 (CH Ar), 125.44 (CH Ar), 125.03 (CH Ar), 124.74 (C Ar), 122.46 (CH Ar), 121.95 (CH Ar), 76.17 (OCH$_2$), 34.18 (CO*C*H$_2$CH$_2$), 30.68 30.69 (OCH$_2$*C*H$_2$), 29.55 (alk), 29.45 (alk), 29.26 (alk), 29.10 (alk), 26.23 (alk), 24.76 (alk). HRMS (ES$^+$): calcd for $C_{24}H_{29}O_3$ [M]$^+$ m/z = 365.2117, found m/z = 365.2179. mp: 208-210^o C. IR (neat): 3243 (OH) 2913 (CH) 2849 (CH) 1675 (CO).

General Procedure C for the Synthesis of Activated Ester Derivatives:

The carboxylic acid and N-Hydroxysuccinimide were dissolved in dry EtOAc in a round bottom flask. A solution of N,N'-Dicyclohexylcarbodiimide in EtOAc was then added dropwise via syringe over 15 minutes and the resulting solution was stirred at room temperature for 48 h. The suspension formed was filtered through a sintered funnel and the filtrate was then concentrated under reduced pressure to form an orange oil. The flask was then cooled on ice for 4 h to form the pure compound as a yellow crystalline solid. Crude **103** was purified *via* flash column chromatography.

2,5-dioxopyrrolidin-1-yl 4-(anthracen-9-yloxy)butanoate, 101

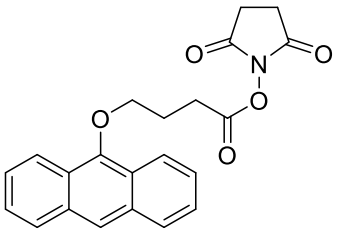

General Procedure C using carboxylic acid **98** (0.82 g, 2.9 mmol), N-Hydroxysuccinimide (0.34 g, 2.9 mmol) in EtOAc (30 mL) and N,N'-Dicyclohexylcarbodiimide (0.66 g, 2.9 mmol) in EtOAc (15 mL) gave **101** (1.08 g, 98%). ^{1}H NMR (300 MHz, $CDCl_3$) δ 8.29 – 8.22 (m, 3H, ArH), 8.01 (dt, *J* = 7.5, 3.7 Hz, 2H, ArH), 7.58 – 7.42 (m, 4H, ArH), 4.30 (t, *J* = 6.1 Hz, 2H, OCH_2), 3.20 (t, *J* = 7.4 Hz, 2H, $COCH_2$), 2.90 (s, *J* = 2.1 Hz, 4H, CH_2-NHS), 2.59 – 2.44 (m, 2H, OCH_2CH_2). ^{13}C NMR (101 MHz, $CDCl_3$) δ 169.09 (CO), 168.43 (CO), 150.66 (C Ar), 132.38 (C Ar), 128.48 (CH Ar), 125.52 (CH Ar), 125.42 (CH Ar), 124.56 (C Ar), 122.41 (CH Ar), 122.09 (CH Ar), 73.44 (OCH_2), 49.30 (CH_2-NHS) 33.82 ($COCH_2$), 27.88 (OCH_2CH_2). HRMS (ES^+): calcd for $C_{22}H_{19}O_5Na$ $[M+Na]^+$ m/z = 400.1161, found m/z = 400.1171. Analysis is in agreement with literature data.[13]

2,5-dioxopyrrolidin-1-yl 7-(anthracen-9-yloxy)heptanoate, 102

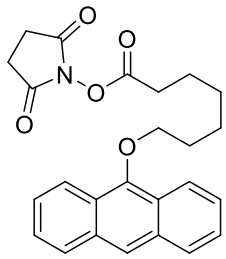

General Procedure C using carboxylic acid **99** (2.60 g, 8.07 mmol), N-Hydroxysuccinimide (1.02 g, 8.88 mmol) in EtOAc (80 mL) and N,N'-Dicyclohexylcarbodiimide (1.83 g, 8.88 mmol) in EtOAc (40 mL) gave **102** (3.21 g, 96%).[1]H NMR (300 MHz, $CDCl_3$) δ = 8.34 – 8.15 (m, 3H, ArH), 8.07 – 7.93 (m, 2H, ArH), 7.59 – 7.39 (m, 4H, ArH), 4.22 (t, *J* = 6.6 Hz, 2H, OCH_2CH_2) 2.85 (s, *J* = 4.7 Hz, 4H, CH_2-NHS), 2.70 (t, *J* = 7.4 Hz, 2H, $COCH_2$), 2.16 – 2.00 (m, 2H, OCH_2CH_2), 1.89 (dt, *J* = 15.1, 7.4 Hz, 2H, $OCH_2CH_2CH_2$), 1.83 – 1.69 (m, 2H, $COCH_2CH_2$), 1.70 – 1.54 (m, 2H, $COCH_2CH_2CH_2$. Analysis is in agreement with literature data.[13]

2,5-dioxopyrrolidin-1-yl 10-(anthracen-9-yloxy)decanoate, 103

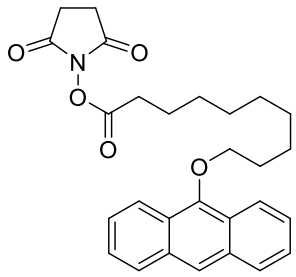

General Procedure C using carboxylic acid **100** (0.99 g, 2.7 mmol), N-Hydroxysuccinimide (0.31 g, 2.7 mmol) in EtOAc (25 mL) and N,N'-Dicyclohexylcarbodiimide (0.61 g, 2.7 mmol) in EtOAc (15 mL) gave **103** (1.21 g, 97%). Chromatography on silica (eluent: DCM/EtOAc 8:2). ^{1}H NMR (300 MHz, $CDCl_3$) δ = 8.27 – 8.17 (m, 2H, ArH), 8.13 (s, 1H, ArH), 7.97 – 7.85 (m, 2H, ArH), 7.45 – 7.34 (m, 4H, ArH), 4.11 (t, *J* = 6.6 Hz, 2H, OCH_2CH_2), 2.81 – 2.63 (m, 4H, CH_2-NHS), 2.54 (t, *J* = 7.5 Hz, 2H, $COCH_2$), 2.05 – 1.89 (quin, *J* = 8.0 Hz, 2H, OCH_2CH_2), 1.69 (quin, *J* = 7.9 Hz, 2H, $COCH_2CH_2$), 1.64 – 1.51 (quin, *J* = 6.8 Hz, 2H, $OCH_2CH_2CH_2$), 1.44 – 1.22 (m, 8H, Alk). ^{13}C NMR (101 MHz, $CDCl_3$) δ = 169.19 (CO), 168.70 (CO), 151.53 (C Ar), 132.44 (C Ar), 128.41 (CH Ar), 125.45 (CH Ar), 125.04 (CH Ar), 124.75 (C Ar), 122.48 (CH Ar), 121.93 (CH Ar), 76.18 (OCH_2), 30.97 ($COCH_2$), 30.68 (OCH_2CH_2), 29.48

(alk), 29.34 (alk), 29.07 (alk), 28.77 (alk), 26.21 ($OCH_2CH_2\mathit{C}H_2$), 25.59 (CH_2-NHS), 24.60 ($COCH_2\mathit{C}H_2$). HRMS (ES^+): calcd for $C_{28}H_{32}N_2O_5$ $[M]^+$ m/z = 462.2280, found m/z = 462.2276. mp: 88-90^o C. IR (neat): 2924 (CH) 2849 (CH) 1778 (CO) 1731 (CO).

General Procedure D for the Synthesis of Diaminopyridine Derivatives:

Diisopropylethylamine and an excess of 2,6-diaminopyridine were suspended in dry DCM (180 mL). A solution of the activated-(NHS) ester in DCM (50 mL) was then added dropwise over 10 minutes with stirring. The mixture was then heated to reflux and maintained for 5 days. Once cooled to room temperature, the suspension was filtered and the filtrate washed with water (3 x 300 mL). The organic phase was then dried using $MgSO_4$, filtered and evaporated. The crude oil obtained was then purified *via* flash column chromatography to give an amber solid.

N-(6-aminopyridin-2-yl)-4-(anthracen-9-yloxy)butanamide, 104

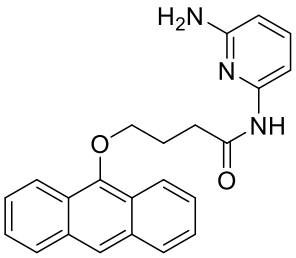

General Procedure D using Diisopropylamine (0.70 mL, 4.0 mmol) and 2,6-diaminopyridine (2.89 g, 26.5 mmol) in DCM (55 mL) and **101** (1.00 g, 2.65 mmol) in DCM (18 mL) gave **104** (0.90 g, 91 %). Chromatography on silica (eluent: DCM/EtOAc 8:2). ^{1}H NMR (300 MHz, $CDCl_3$) δ = 8.30 – 8.21 (m, 3H, ArH), 8.17 (s, 1H, NH), 8.05 – 7.95 (m, 2H, ArH), 7.62 (d, *J* = 7.7 Hz, 1H, pyr), 7.53 – 7.42 (m, 5H, ArH (1H-pyr and 4H-Ar_{anth}), 6.26 (d, *J* = 7.9 Hz, 1H, pyr), 4.37 (s, *J* = 37.7 Hz, 2H, NH_2), 4.26 (t, *J* = 6.2 Hz, 2H, OCH_2), 2.84 (t, *J* = 7.4 Hz, 2H, $COCH_2$), 2.52 – 2.39 (m, 2H, $OCH_2C\mathit{H}_2$). ^{13}C NMR (101 MHz, $CDCl_3$) δ = 170.84 (CO), 157.03 (C pyr), 150.98 (C Ar), 149.75 (C pyr), 140.29 (CH pyr), 132.39 (C Ar), 128.47 (CH Ar), 125.49 (CH

Ar), 125.28 (CH Ar), 124.61 (C Ar), 122.22 (CH Ar), 104.34 (CH pyr), 103.36 (CH pyr), 74.55 (OCH_2), 34.13 ($CO\mathit{C}H_2$), 26.22 ($OCH_2\mathit{C}H_2$). HRMS (ES^+): calcd for $C_{23}H_{22}N_3O_2$ $[M]^+$ m/z = 372.1712, found m/z = 372.1721. Analysis is in agreement with literature data.[13]

N-(6-aminopyridin-2-yl)-7-(anthracen-9-yloxy)heptanamide, 105

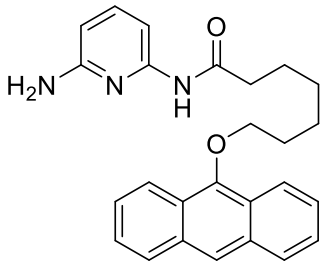

General Procedure D using Diisopropylamine (2.29 mL, 13.2 mmol) and 2,6-diaminopyridine (9.60 g, 88 mmol) in DCM (180 mL) and **102** (3.69 g, 8.80 mmol) in DCM (50 mL) gave **105** (2.21 g, 62 %). Chromatography on silica (eluent: DCM/EtOAc 8:2). ^{1}H NMR (300 MHz, $CDCl_3$) δ = 8.36 – 8.18 (m, 3H, ArH), 8.08 – 7.95 (m, 2H, ArH), 7.78 – 7.65 (m, 1H, NH), 7.61 – 7.54 (m, 1H, pyr), 7.52 – 7.40 (m, 5H ArH (4H-anth and 1H-pyr)), 6.33 – 6.25 (d, *J* = 7.9 Hz, 1H, pyr), 4.42 – 4.26 (m, 2H, NH_2), 4.21 (t, *J* = 6.6 Hz, 2H, $OC\mathit{H}_2CH_2$), 2.46 – 2.37 (m, 2H, $COCH_2$), 2.14 – 2.02 (m, 2H, $OCH_2C\mathit{H}_2$), 1.90 – 1.80 (m, 2H, $COCH_2C\mathit{H}_2$), 1.78 – 1.66 (m, 2H¸ $OCH_2CH_2C\mathit{H}_2$), 1.62 – 1.50 (m, 2H, $COCH_2CH_2C\mathit{H}_2$). Analysis is in agreement with literature data.[13]

N-(6-aminopyridin-2-yl)-10-(anthracen-9-yloxy)decanamide, 106

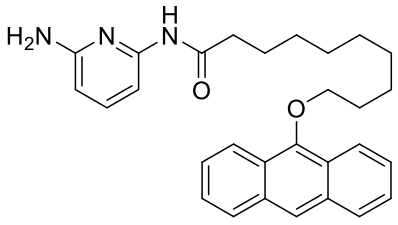

General Procedure D using Diisopropylamine (0.70 mL, 4.0 mmol) and 2,6-diaminopyridine (2.89 g, 26.5 mmol) in DCM (55 mL) and **103** (1.22 g, 2.65 mmol) in DCM (18 mL) gave **106** (0.48 g, 40 %). Chromatography on silica (eluent: DCM/EtOAc 9:1). ^{1}H NMR (300 MHz, $CDCl_3$) δ = 8.27 – 8.16 (m, 2H, ArH), 8.12 (s, 1H, ArH), 7.95 – 7.84 (m, 2H, ArH), 7.68 (s, 1H, NH), 7.47 (d, *J* = 7.9 Hz, 1H, pyr), 7.43 – 7.31 (m, 5H, ArH (4H-ArH_{anth} and 1H-pyr), 6.14

(d, *J* = 8.7 Hz, 1H, pyr), 4.29 – 4.17 (m, 2H, NH_2), 4.10 (t, *J* = 6.6 Hz, 2H, OCH_2), 2.25 (t, *J* = 7.5 Hz, 2H, $COCH_2$), 2.02 – 1.89 (m, 2H, OCH_2CH_2), 1.72 – 1.48 (m, 4H, $OCH_2CH_2CH_2$ and $COCH_2CH_2$), 1.38 – 1.23 (m, 8H, Alk). ^{13}C NMR (101 MHz, $CDCl_3$) δ = 171.59 (CO), 156.87 (C pyr), 151.52 (C Ar), 149.69 (C pyr), 140.33 (CH pyr), 132.44 (C Ar), 128.41 (CH Ar), 125.44 (CH Ar), 125.03 (CH Ar), 124.75 (C Ar), 122.48 (CH Ar), 121.93 (CH Ar), 104.17 (CH pyr), 103.25 (CH pyr), 76.19 (OCH_2), 37.86 $COCH_2$), 30.69 (OCH_2CH_2), 29.55 (alk), 29.45 (alk), 29.34 (alk), 29.20 (alk), 26.23 ($OCH_2CH_2CH_2$), 25.41 ($COCH_2CH_2$). HRMS (ES^+): calcd for $C_{29}H_{34}N_3O_2$ $[M]^+$ m/z = 456.2651, found m/z = 456.2643. mp: 63-65^o C. IR (neat): 3336 (N-H) 2926 (C-H) 2853 (C-H) 1676 (CO) 1617 (CO).

General Procedure E for the synthesis of Acyclic Receptors 107-109

In a round bottom flask, the amine terminated compound and NEt_3 were dissolved in THF. A solution of **39** in THF was added dropwise at room temperature. The reaction mixture was left stirring for 48 h. When using compound **109** catalytic DMAP was added. Once complete, the suspension was filtered, and the solvent removed under reduced pressure. The crude product was then purified *via* flash column chromatography to afford a yellow crystalline solid.

N^1,N^3-bis(6-(4-(anthracen-9-yloxy)butanamido)pyridin-2-yl)-5-(tert-butyl)isophthalamide, 107

General Procedure E using **39** (0.08 g, 0.30 mmol) in THF (20 mL) and **104** (0.25 g, 0.67 mmol), NEt_3 (0.10 mL, 0.72 mmol) in THF (40 mL) gave **107** (0.14 g, 51 %). Chromatography on silica (eluent: DCM/EtOAc - 15%). ^1H NMR (300 MHz, $CDCl_3$) δ = 8.48 (s, 2H, NH), 8.28 –

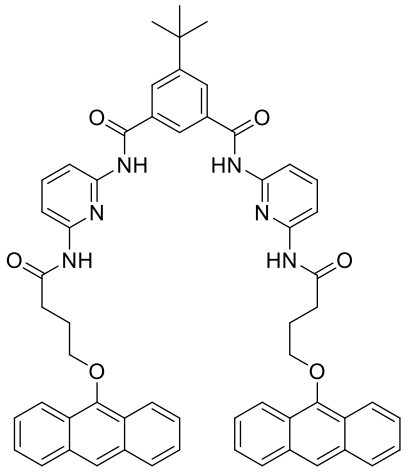

7.89 (m, 19H, (2H-NH, 4H-pyr, 3H Ar, 10H Ar_{anth})), 7.78 (t, *J* = 8.0 Hz, 2H, pyr), 7.47 – 7.35 (m, 8H, Ar_{anth}), 4.24 (t, *J* = 6.0 Hz, 4H, OCH_2), 2.85 (t, *J* = 7.1 Hz, 4H $COCH_2$), 2.50 – 2.36 (m, 4H, $COCH_2CH_2$), 1.39 (s, 9H, CH_3). ^{13}C NMR (101 MHz, $CDCl_3$) δ = 171.20 (CO), 165.03 (CO), 153.35 (C pyr), 150.77 (C Ar_{anth}), 149.68 (C pyr), 149.49 (C Ar), 140.93 (CH pyr), 134.28 (C Ar), 132.31 (C Ar_{anth}), 128.60 (CH Ar_{anth}), 128.49 (CH Ar), 125.43 (CH Ar_{anth}), 125.25 (CH Ar_{anth}), 124.50 (C Ar_{anth}), 122.35 (CH Ar_{anth}), 122.02 (CH Ar_{anth}), 110.14 (CH pyr), 109.88 (CH pyr), 74.38 (OCH_2), 35.16 (C ^{t}Bu), 34.02 ($COCH_2$), 31.07 (CH_3), 26.04 (OCH_2CH_2). HRMS (ES^+): calcd for $C_{58}H_{53}N_6O_6$ $[M]^+$ m/z = 929.4027, found m/z = 929.4016. Analysis is in agreement with literature data.[13]

N^1,N^3-bis(6-(7-(anthracen-9-yloxy)heptanamido)pyridin-2-yl)-5-(tert-butyl)isophthalamide, 108

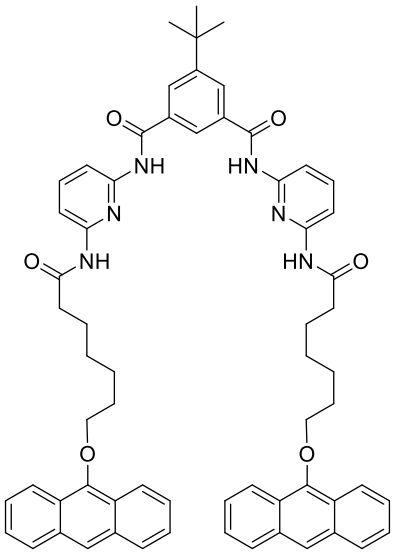

General Procedure E using **39** (0.28 g, 1.1 mmol) in THF (70 mL) and **105** (1.00 g, 2.42 mmol), NEt_3 (0.36 mL, 2.59 mmol) in THF (140 mL) gave **108** (0.37 g, 33 %). Chromatography on silica (eluent: DCM/ EtOAc - 5%). ^1H NMR (300 MHz, $CDCl_3$) δ = 8.41 (s, 2H, NH), 8.31 – 8.24 (m, 4H, ArH_{anth}), 8.21 (s, 2H, ArH_{anth}), 8.19 (s, 1H, ArH), 8.14 (s, *J* = 1.5 Hz, 2H, ArH), 8.07 (d, *J* = 8.0 Hz, 2H, pyr), 8.04 – 7.94 (m, 6H, ArH (4H-anth and 2H pyr), 7.85 – 7.72 (m, 4H, NH and pyr), 7.52 – 7.40 (m, 8H, ArH_{anth}) 4.17 (t, *J* = 6.5 Hz, 4H, OCH_2CH_2), 2.43 (t, *J* = 7.4 Hz, 4H, $COCH_2$), 2.09

– 1.99 (m, 4H, OCH_2CH_2), 1.88 – 1.77 (m, 4H, $COCH_2CH_2$), 1.71 (dt, *J* = 15.3, 7.6 Hz, 4H, $OCH_2CH_2CH_2$), 1.58 – 1.48 (m, 4H, $COCH_2CH_2CH_2$), 1.37 (s, 9H, CH_3). ^{13}C NMR (101 MHz, $CDCl_3$) δ = 171.83 (CO), 165.09 (CO), 153.33 (C pyr), 151.34 (C Ar_{anth}), 149.80 (C pyr), 149.39 (C Ar), 140.95 (CH pyr), 134.38 (C Ar), 132.41 (C Ar_{anth}), 128.45 (CH Ar_{anth}), 125.44 (CH Ar_{anth}), 125.09 (CH Ar_{anth}), 124.68 (C Ar_{anth}), 122.76 (CH Ar), 122.34 (CH Ar_{anth}), 122.04 (CH Ar_{anth}), 110.11 (CH pyr), 109.71 (CH pyr), 75.91 (OCH_2), 37.55 ($COCH_2$), 35.22 (C ^{t}Bu), 31.14 (CH_3), 30.50 (OCH_2CH_2), 29.16 ($COCH_2CH_2CH_2$), 26.07 ($OCH_2CH_2CH_2$), 24.93 ($COCH_2CH_2$). HRMS (ES^+): calcd for $C_{66}H_{68}N_4O_6Na$ $[M+2H+Na]^+$ m/z = 1035.5, found m/z = 1035.6. Analysis is in agreement with literature data.[13]

N^1,N^3-bis(6-(10-(anthracen-9-yloxy)decanamido)pyridin-2-yl)-5-(tert-butyl)isophthalamide, 109

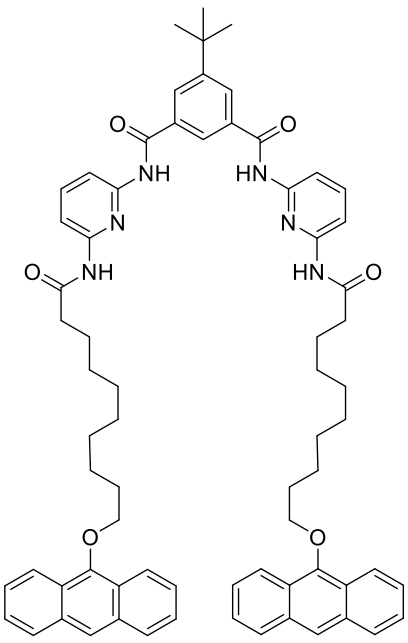

General Procedure E using **39** (0.10 g, 0.39 mmol) in THF (25 mL) and **106** (0.39 g, 0.86 mmol), NEt_3 (0.13 mL, 0.93 mmol) in THF (50 mL) gave **109** (0.23 g, 53 %). Chromatography on silica (eluent: DCM/ EtOAc - 15%). ^{1}H NMR (300 MHz, $CDCl_3$) δ = 8.54 (s, NH), 8.22 – 8.14 (m, 4H, ArH_{anth}), 8.09 (m, 3H, ArH (2H-anth and 1H-Ar), 8.01 (s, 2H, ArH), 7.95 – 7.82 (m, 10H, (8H-pyr, 4H-anth, 2NH)), 7.62 (t, J = 8.1 Hz, 2H, pyr), 7.41 – 7.28 (m, 8H, ArH_{anth}), 4.07 (t, J = 6.7 Hz, 4H, OCH_2), 2.28 (t, J = 7.5 Hz, 4H, $COCH_2$), 1.93 (p, J = 6.8 Hz, 4H, OCH_2CH_2), 1.57 (dq, J = 29.4, 7.2 Hz, 8H, $OCH_2CH_2CH_2$ and $COCH_2CH_2CH_2$), 1.31 – 1.26 (m, 16H, Alk), 1.25 (s, 9H, CH_3). ^{13}C NMR (101 MHz, $CDCl_3$) δ = 172.04 (CO), 165.00

(CO), 153.31 (C pyr), 151.45 (C Ar_{Anth}), 149.86 (C pyr), 149.47 (C Ar), 140.86 (CH pyr), 134.31 (C Ar), 132.42 (C Ar_{anth}), 128.53 (CH Ar), 128.42 (CH Ar_{anth}), 125.44 (CH Ar_{anth}), 125.04 (CH Ar_{anth}), 124.71 (C Ar_{anth}), 122.65 (CH Ar), 122.42(CH Ar_{anth}), 121.95 (CH Ar_{anth}), 110.07 (CH pyr), 109.69 (CH pyr), 76.14 (OCH_2), 37.68 ($COCH_2$), 35.20 (C ^tBu), 31.14 (CH_3), 30.68 (OCH_2CH_2), 29.56 (alk), 29.47 (alk), 29.38 (alk), 29.24 (alk), 26.23 ($COCH_2CH_2CH_2$), 25.36 ($COCH_2CH_2$). HRMS (ES^+): calcd for $C_{70}H_{77}N_6O_6$ $[M]^+$ m/z = 1097.5905, found m/z = 1097.5913. mp: 99-101° C. IR (neat): 3283 (N-H) 3054 (N-H) 2926 (C-H) 2854 (C-H) 1678 (CO) 1584 (CO).

General Procedure F for the synthesis of Cyclic Receptors 110-112

A solution of acyclic receptor in degassed DCM (25 mL) at $c = 5x10^{-4}$ M was irradiated with a UV lamp using a bandpass filter at 365 nm. The dimerization was monitored using UV-Vis absorption to observe the decrease in anthracene signal and once complete the solvent was removed and the obtained crude product was purified *via* flash column chromatography to afford a yellow solid.

(14^5S,14^6R,$14^{11}R$,$14^{12}S$)-45-(tert-butyl)-14^5,14^6,14^{11},14^{12}-tetrahydro-13,15-dioxa-2,6,8,20-tetraaza-1,7(2,6)-dipyridina-14(5,11)-5,12:6,11-bis([1,2]benzeno)dibenzo[a,e][8]annulena-4(1,3)-benzenacycloicosaphane-3,5,9,19-tetraone, 110

Chromatography on silica (eluent: DCM/EtOAc - 10%). Yield: quantitative. ^1H NMR (300 MHz, $CDCl_3$) δ 8.54 (s, 2H, NH), 8.18 (s, 2H, ArH), 8.14 – 8.01 (m, 4H, (2H-pyr and 2H-NH)), 7.95 – 7.80 (m, 5H, (1H-ArH, 4H-pyr)), 7.08 (d, *J* = 7.3 Hz, 4H, ArH-xyl), 6.87 (d, *J* = 7.0 Hz, 4H, ArH-xyl), 6.71 (dt, *J* = 22.0, 7.0 Hz, 8H, ArH-xyl), 4.42 (s, 2H, $CH_{bridgehead}$), 3.75 (t, *J* = 6.0 Hz,

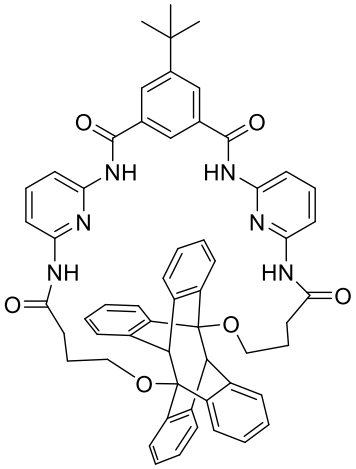

4H, OCH_2), 2.82 – 2.60 (m, 4H, $COCH_2$), 2.34 – 2.19 (m, 4H, $COCH_2CH_2$), 1.42 (s, 9H, CH_3). Analysis is in agreement with literature data.[13]

(17^{5}S,17^{6}R,17^{11}R,17^{12}S)-45-(tert-butyl)-17^5,17^6,17^{11},17^{12}-tetrahydro-16,18-dioxa-2,6,8,26-tetraaza-1,7(2,6)-dipyridina-17(5,11)-5,12:6,11-bis([1,2]benzeno)dibenzo[a,e][8]annulena-4(1,3)-benzenacyclohexacosaphane-3,5,9,25-tetraone, 111

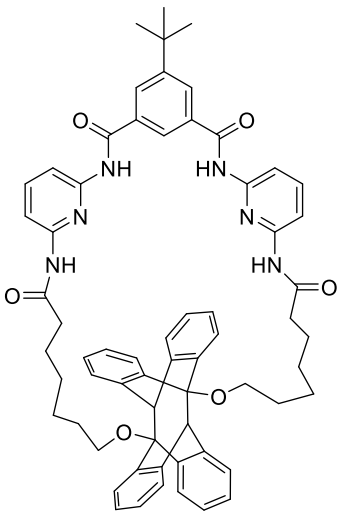

Chromatography on silica (eluent: DCM/EtOAc - 15%). Yield: quantitative. ^{1}H NMR (300 MHz, $CDCl_3$) δ 8.22 (s, 2H, NH), 8.08 (s, 3H, ArH), 8.03 (d, *J* = 2.8 Hz, 2H, pyr), 8.00 (d, *J* = 2.9 Hz, 2H, pyr), 7.81 (t, *J* = 8.1 Hz, 2H, pyr), 7.65 (s, 2H, NH), 7.01 – 6.88 (m, 8H, ArH), 6.78 – 6.64 (m, 8H, ArH), 4.36 (s, 2H, $CH_{bridgehead}$), 3.47 (t, *J* = 6.9 Hz, 4H, OCH_2), 2.41 (t, *J* = 7.1 Hz, 4H, $COCH_2$), 1.89 – 1.77 (m, 12H, Alk), 1.53 (dd, *J* = 14.0, 6.6 Hz, 4H, $COCH_2CH_2CH_2$), 1.41 (s, 9H, CH_3). MS (ES$^+$): calcd for $C_{64}H_{64}N_6O_6$ $[M+H]^+$ 1013.3, found m/z = 1013.5. Analysis is in agreement with literature data.[13]

(20^{5}S,20^{6}R,20^{11}R,20^{12}S)-45-(tert-butyl)-20^5,20^6,20^{11},20^{12}-tetrahydro-19,21-dioxa-2,6,8,32-tetraaza-1,7(2,6)-dipyridina-20(5,11)-5,12:6,11-bis([1,2]benzeno)dibenzo[a,e][8]annulena-4(1,3)-benzenacyclodotriacontaphane-3,5,9,31-tetraone, 112:

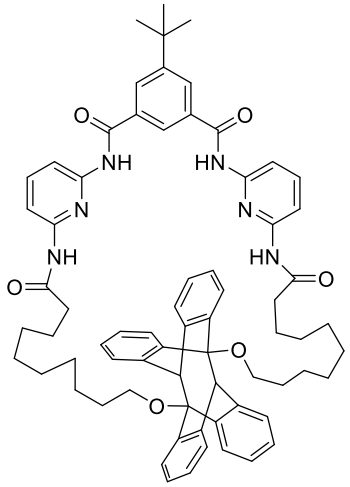

Chromatography on silica (eluent: DCM/EtOAc - 10%). Yield: quantitative. ^{1}H NMR (300 MHz, $CDCl_3$) δ 8.31 (s, 2H, NH), 8.21 (s, 1H, ArH), 8.11 (s, 2H, ArH), 8.07 – 7.94 (m, 4H, pyr), 7.75 (t, *J* = 8.0 Hz, 2H, pyr), 7.64 (s, 2H, NH), 7.10 – 6.88 (m, 8H, ArH), 6.88 – 6.69 (m, 8H, ArH), 4.42 (s, 2H, $CH_{bridgehead}$), 3.50 (t, *J* = 6.7 Hz, 4H, OCH_2), 2.48 – 2.32 (m, 4H, $COCH_2$), 1.94 – 1.70 (m, 8H, OCH_2CH_2 and $OCH_2CH_2CH_2$), 1.44 (s, *J* = 8.2 Hz, 9H, CH_3), 1.38 (s, *J* = 23.4 Hz, 16H, Alk). HRMS (ES^+): calcd for $C_{70}H_{77}N_6O_6$ $[M]^+$ m/z = 1097.5905, found m/z = 1097.5957. mp: 125-128^{o} C.

4^{5}-(tert-butyl)-179,1710-dihydro-16,18-dioxa-2,6,8,26-tetraaza-1,7(2,6)-dipyridina-17(9,)-anthracena-4(1,3)-benzenacyclohexacosaphane-3,5,9,25-tetraone compound with 5,5-bis(3-(4-((4-(tris(4-(tert-butyl)phenyl)methyl)phenoxy)methyl)-1H-1,2,3-triazol-1-yl)propyl)pyrimidine-2,4,6(1H,3H,5H)-trione (1:1), 113

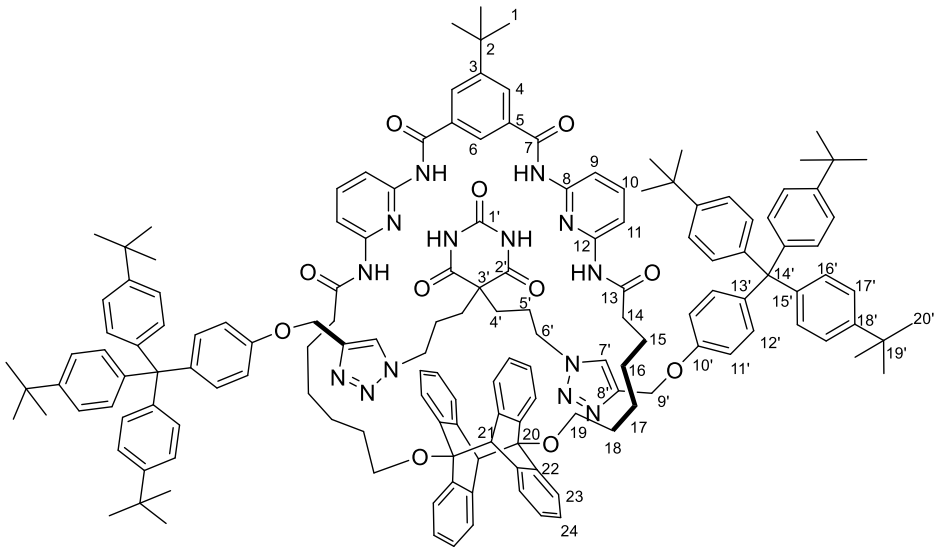

A solution of **108** in degassed DCM (25 mL) at *c* = 5x10^{-4} M, containing **85** (3 equivalents) was irradiated with a UV lamp using a band pass filter at 365 nm. The dimerization was monitored using UV-Vis absorption to observe the decrease in anthracene signal and once complete, the solvent was removed and the white solid obtained was purified *via* flash column chromatography, eluent (DCM/EtOAc – 10%) to give the 20 mg of **113** (8.4 µmol, 58% yield). ^{1}H NMR (300 MHz, Acetone) δ 9.46 (d, *J* = 8.9 Hz, 2H, NH), 8.29 (s, 1H, 6), 8.20 (s, *J* = 1.5 Hz, 2H, 4), 8.04 (d, *J* = 8.0 Hz, 2H, 9), 7.95 (d, *J* = 8.1 Hz, 2H, 11), 7.83 (t, *J* = 8.1 Hz, 2H, 10), 7.69 (s, 2H, 7'), 7.32 (d, *J* = 8.7 Hz, 12H, 16'), 7.19 – 7.01 (m, 20H, 12', 17', 24a), 6.94 (dd, *J* = 6.9, 1.3 Hz, 4H, 24b), 6.83 (d, *J* = 8.9 Hz, 4H, 11'), 6.78 – 6.64 (m, 8H, 23), 5.09 (s, 4H, 9'), 4.54 (s, 2H, 21), 3.94 – 3.71 (m, 8H, 19, 6'), 2.56 – 2.41 (m, 4H, 14), 2.13 – 2.04 (m, 8H, 18, 5'), 1.86 – 1.71 (m, 4H, 15), 1.66 – 1.40 (m, 12H, 4', 16, 17), 1.36 (s, *J* = 6.2 Hz, 9H, 2), 1.31 (s, 54H, 20'). ^{13}C NMR (126 MHz, Acetone-d_6) δ 174.22 (CO), 172.50 (CO'), 166.37 (CO), 157.26 (C Ar'), 153.26 (C pyr), 151.82 (C Ar), 151.65 (C pyr), 151.12 (C Ar), 151.04 (C Ar'), 149.16 (C Ar'), 145.15, 144.38 (C Ar'), 144.23(C_{tria}), 141.44 (CH pyr), 140.67 (C Ar'), 135.46 (CH Ar'), 132.79 (C Ar), 131.42 (CH Ar'), 129.78 (CH Ar'), 128.04 (CH Ar), 126.86 (CH_{tria}), 126.17 (CH Ar), 125.76 (CH Ar), 125.04 (C Ar), 124.27 (CH Ar'), 123.61 (CH Ar), 114.19, 111.30 (CH pyr), 110.55 (CH pyr), 66.28 (OCH_2), 63.89 (C'), 62.62 (C'), 62.40 (OCH_2'), 55.59 (CO*C*CO'), 49.79 (NCH_2'), 37.65 ($COCH_2$), 35.98 (C ^{t}Bu), 34.86 (CCH_2'), 34.32 (C ^{t}Bu), 31.38 (CH_3), 31.08 (CH_3'), 30.04 (OCH_2CH_2), 29.94 (alk), 29.46 (alk), 27.05 (alk), 25.76 (NCH_2CH_2'). HRMS (ESI^{+}) cald for $C_{154}H_{172}N_{14}O_{11}$ $[M + 2H]^{2+}$ m/z = 1197.2, found m/z = 1197.3. Melting Point: 156-158 ^{o}C.

5.4 References

1. Heim, C.; Affeld, A.; Nieger, M.; Vögtle, F., Size Complementarity of Macrocyclic Cavities and Stoppers in Amide-Rotaxanes. *Helv. Chim. Acta* **1999,** *82* (5), 746-759.

2. Al-Sayah, Mohammad H.; McDonald, R.; Branda, Neil R., Structural Studies on Hydrogen-Bonding Receptors for Barbiturate Guests That Use Metal Ions as Allosteric Inhibitors. *Eur. J. Org. Chem.* **2004,** *2004* (1), 173-182.

3. Rocher, M. Towards Interlocked Structures based on H-bonded barbiturate complexes. University of Birmingham, Birmingham, 2010.

4. Ashton, P. R.; Ballardini, R.; Balzani, V.; Bělohradský, M.; Gandolfi, M. T.; Philp, D.; Prodi, L.; Raymo, F. M.; Reddington, M. V.; Spencer, N.; Stoddart, J. F.; Venturi, M.; Williams, D. J., Self-Assembly, Spectroscopic, and Electrochemical Properties of [n]Rotaxanes. *J. Am. Chem. Soc.* **1996,** *118* (21), 4931-4951.

5. Durola, F.; Lux, J.; Sauvage, J.-P., A Fast-Moving Copper-Based Molecular Shuttle: Synthesis and Dynamic Properties. *Chem. Eur. J.* **2009,** *15* (16), 4124-4134.

6. Bauld, N. L.; Aplin, J. T.; Yueh, W.; Endo, S.; Loving, A., Convenient criterion for the distinction between electrophilic and electron transfer reactions of electron-rich alkenes. *J. Phys. Org. Chem.* **1998,** *11* (1), 15-24.

7. Song, Q.; Bogner, A.; Giesselmann, F.; Lemieux, R. P., Tuning 'de Vries-like' properties in binary mixtures of liquid crystals with different molecular lengths. *Chem. Commun.* **2013,** *49* (74), 8202-8204.

8. Abraham, W.; Wlosnewski, A.; Buck, K.; Jacob, S., Photoswitchable rotaxanes using the photolysis of alkoxyacridanes. *Org. Biomol. Chem.* **2009,** *7* (1), 142-154.

9. Hajduk, P. J.; Sheppard, G.; Nettesheim, D. G.; Olejniczak, E. T.; Shuker, S. B.; Meadows, R. P.; Steinman, D. H.; Carrera, G. M.; Marcotte, P. A.; Severin, J.; Walter, K.; Smith, H.; Gubbins, E.; Simmer, R.; Holzman, T. F.; Morgan, D. W.; Davidsen, S. K.; Summers, J. B.; Fesik, S. W., Discovery of Potent Nonpeptide Inhibitors of Stromelysin Using SAR by NMR. *J. Am. Chem. Soc.* **1997,** *119* (25), 5818-5827.

10. Aucagne, V.; Hänni, K. D.; Leigh, D. A.; Lusby, P. J.; Walker, D. B., Catalytic “Click” Rotaxanes: A Substoichiometric Metal-Template Pathway to Mechanically Interlocked Architectures. *J. Am. Chem. Soc.* **2006,** *128* (7), 2186-2187.

11. Yao, L.; Smith, B. T.; Aubé, J., Base-Promoted Reactions of Bridged Ketones and 1,3- and 1,4-Haloalkyl Azides: Competitive Alkylation vs Azidation Reactions of Ketone Enolates. *J. Org. Chem.* **2004,** *69* (5), 1720-1722.

12. Tron, A.; Thornton, P. J.; Rocher, M.; Jacquot de Rouville, H.-P.; Desvergne, J.-P.; Kauffmann, B.; Buffeteau, T.; Cavagnat, D.; Tucker, J. H. R.; McClenaghan, N. D., Formation of a Hydrogen-Bonded Barbiturate [2]-Rotaxane. *Org. Lett.* **2014,** *16* (5), 1358-1361.

13. Molard, Y.; Bassani, D. M.; Desvergne, J.-P.; Moran, N.; Tucker, J. H. R., Structural Effects on the Ground and Excited-state Properties of Photoswitchable Hydrogen-Bonding Receptors. *J. Org. Chem.* **2006,** *71* (22), 8523-8531.